

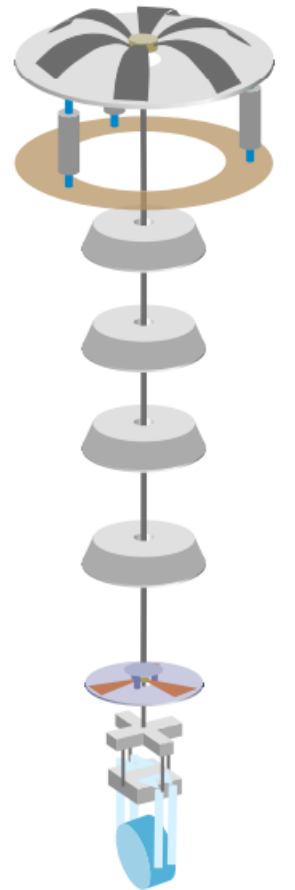
Fast localization of coalescing binaries  
with gravitational wave detectors

and

Low frequency vibration isolation for KAGRA

Yoshinori Fujii

U. of Tokyo, NAOJ



# Abstract

1. Expected fast localization performance by current network with a hierarchical approach using existing low-latency infrastructure
  - \* In heterogeneous HLV-, HLK- and HLVK-network
  - \* If  $V$  (K) sensitivity  $> 0.2$  (0.28) of LIGO, the hierarchical approach improves the localization performance, in the heterogeneous network using existing low-latency pipeline.
2. Local control system for KAGRA full Type-A suspension  
aiming more robust interferometer operation
  - \* I've confirmed the control system satisfied the requirements for acquiring interferometer lock.
  - \* This is the first time to control the KAGRA full Type-A suspension.

# Thesis contents

My main research

1. Introduction

2. Benefit of adding detectors to the observation network

3. Low frequency vibration isolation

4. KAGRA seismic attenuation system

5. Suspension control design

6. Performance test of local control for KAGRA Type-A suspension

7. Summary

→ **Fast localization simulation with current network**

→ **Type-A suspension controls toward lock acquisition**

# Introduction for my research topic:

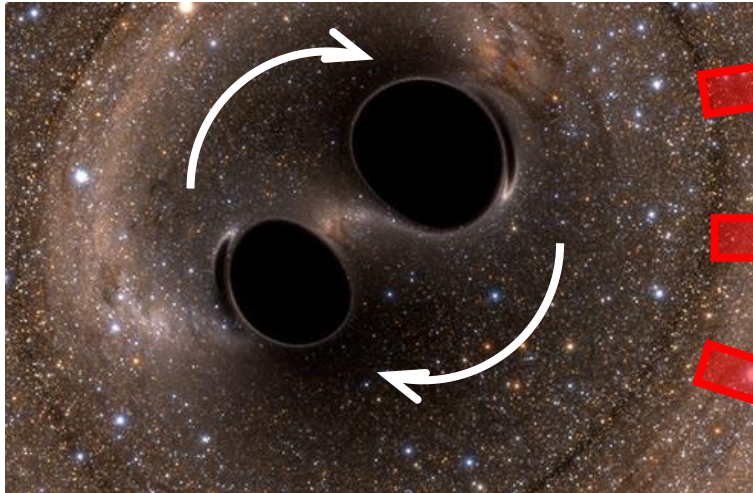
*Gravitational waves*

*The sources*

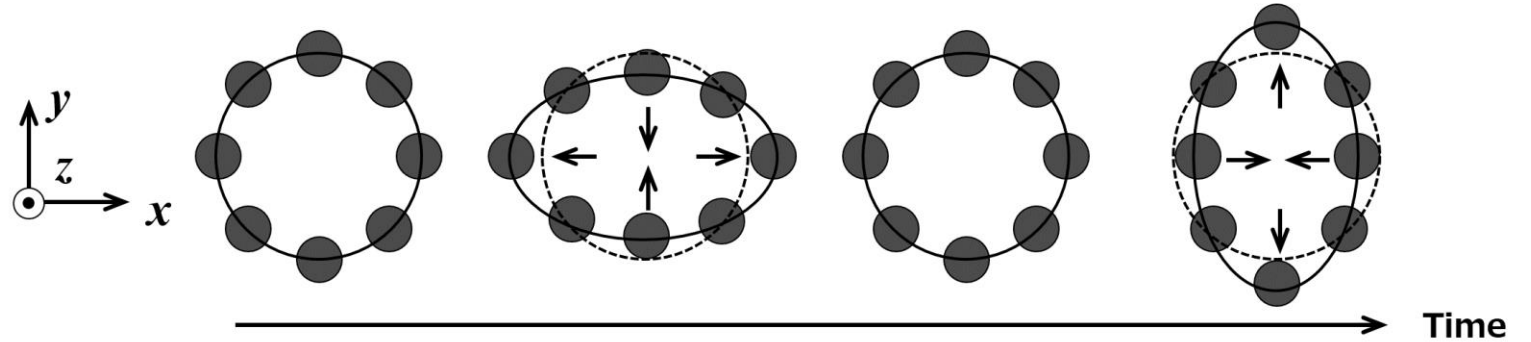
*Detector, detection and source localization*



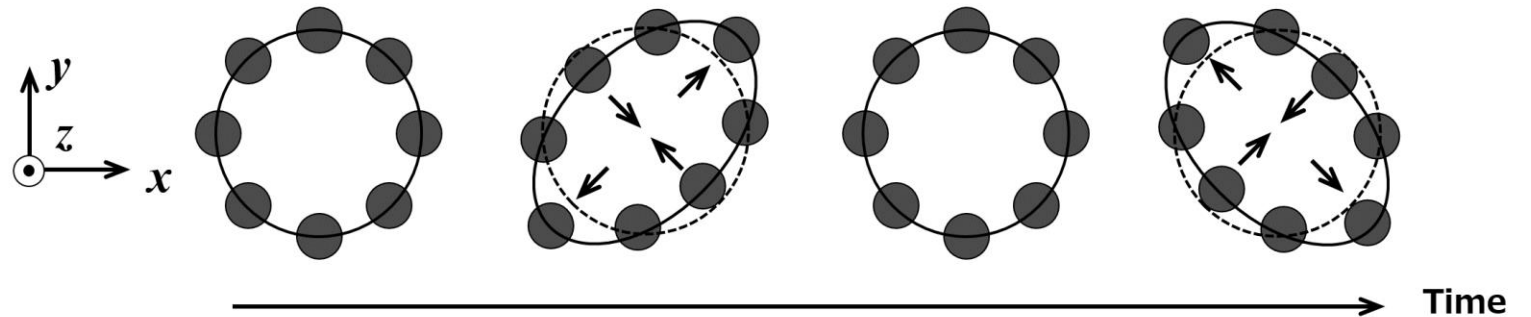
# Gravitational wave (GW):



## Plus mode



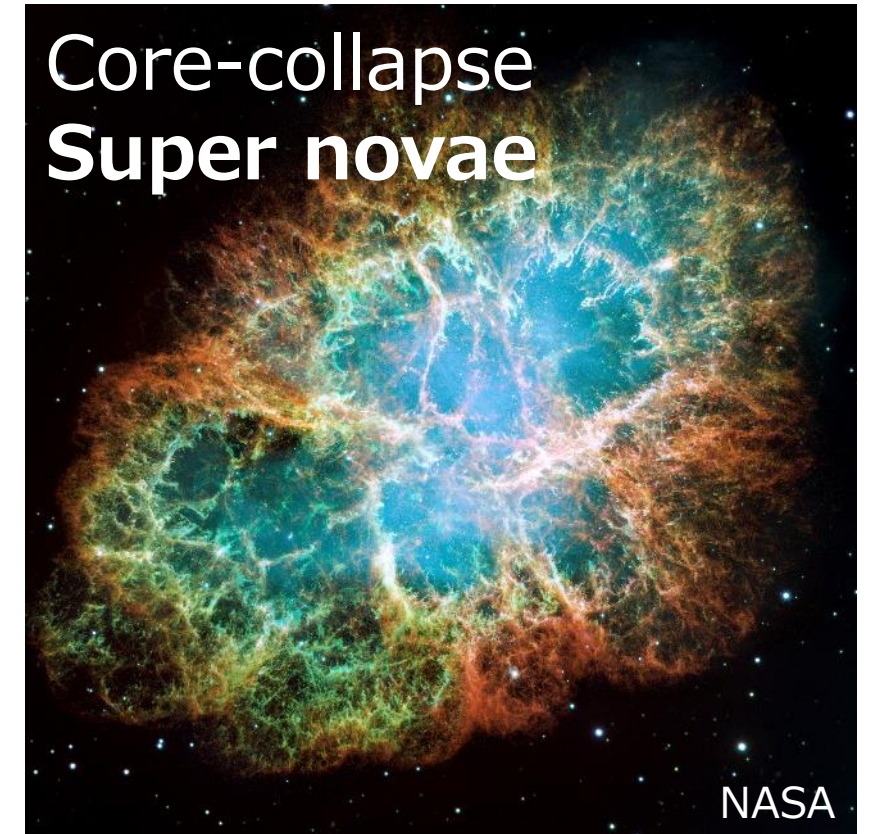
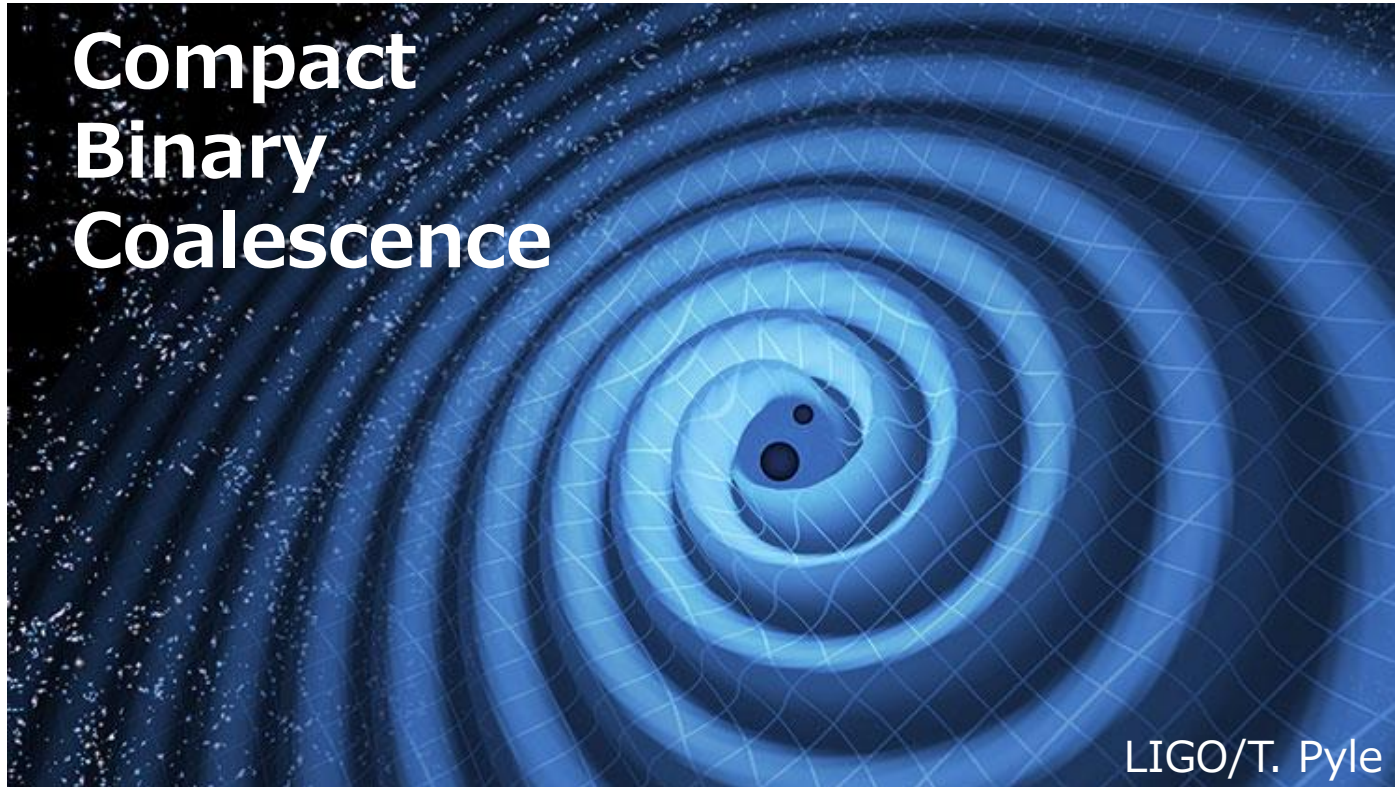
## Cross mode



Accelerated objects generate GWs.

2 polarizations

# Promising sources of GW:

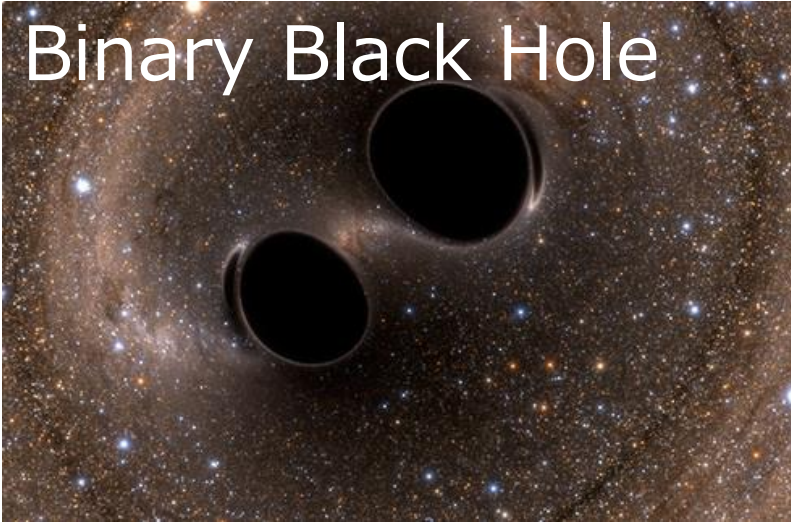


(And more..)



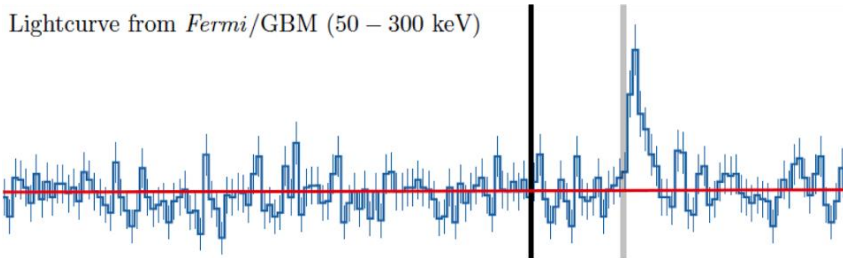
# From CBC, GWs are detected:

Binary Black Hole

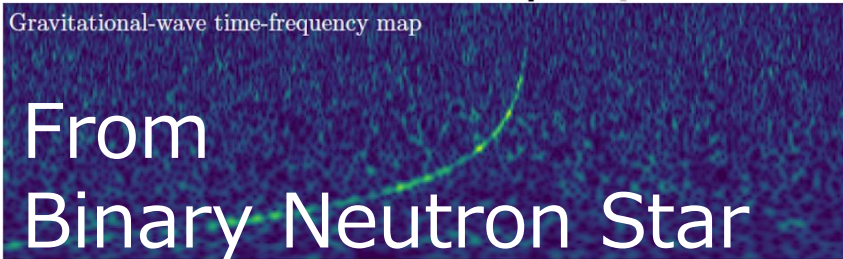


- \* First BBH detection (2015)
- **New field of astrophysics**

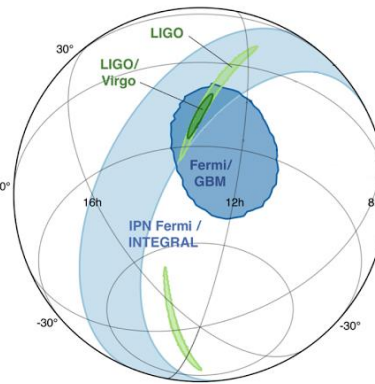
Lightcurve from *Fermi*/GBM (50 – 300 keV)



Gravitational-wave time-frequency map



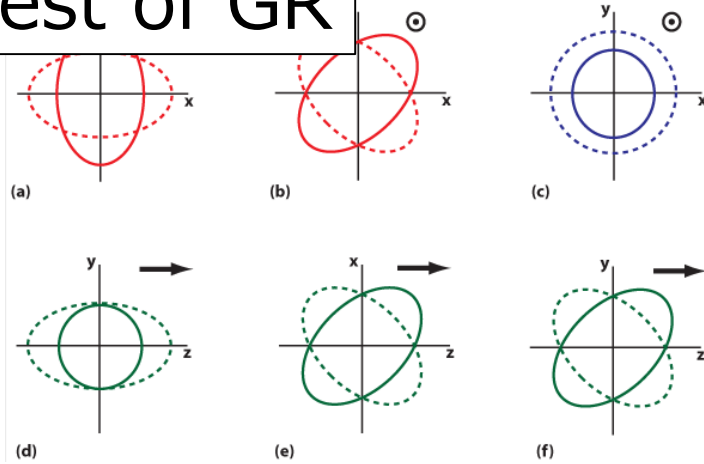
From  
Binary Neutron Star



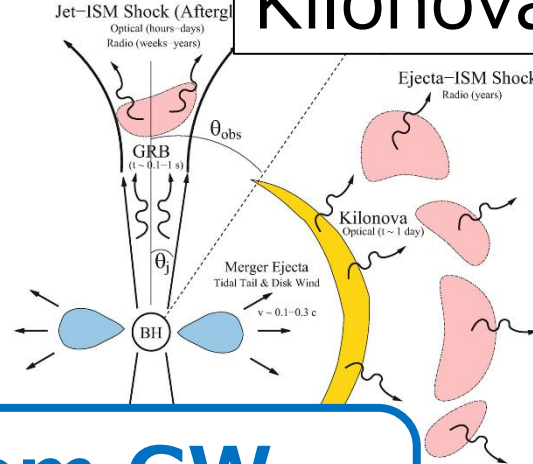
- \* First BNS detection & EM-follow up (2017)
- **Era of Multi-messenger astronomy**

# Astrophysical motivation:

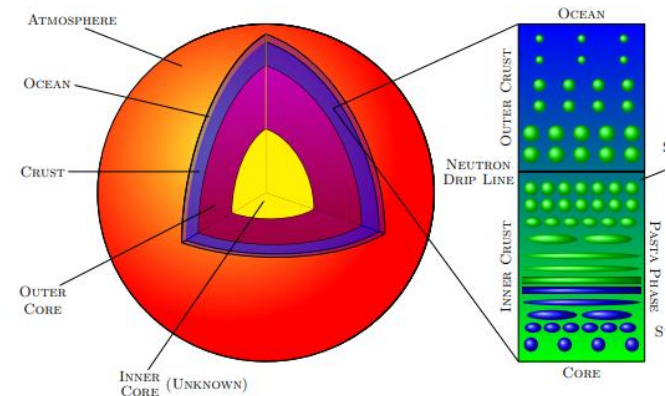
## Test of GR



## Kilonovae

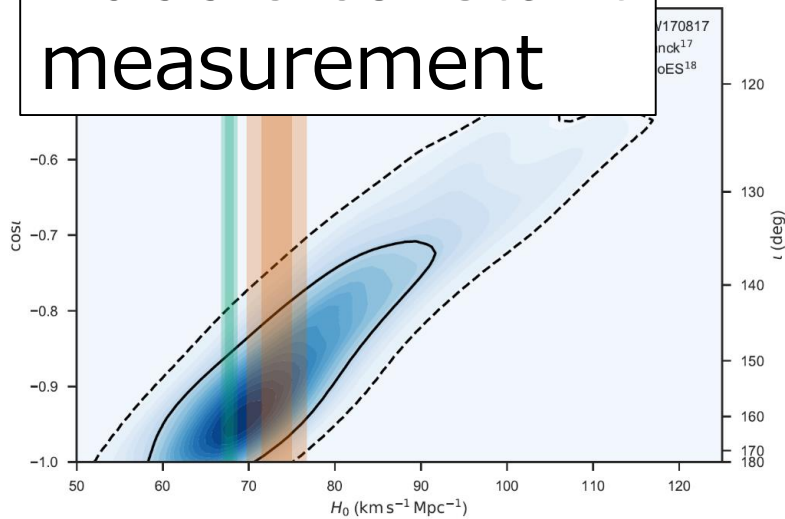


## Neutron Star interior

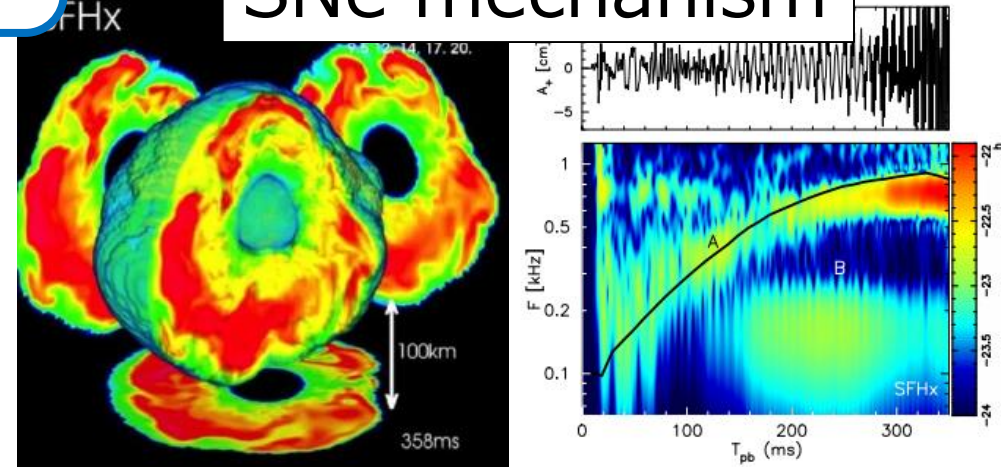


## From GW observation

## Hubble constant measurement

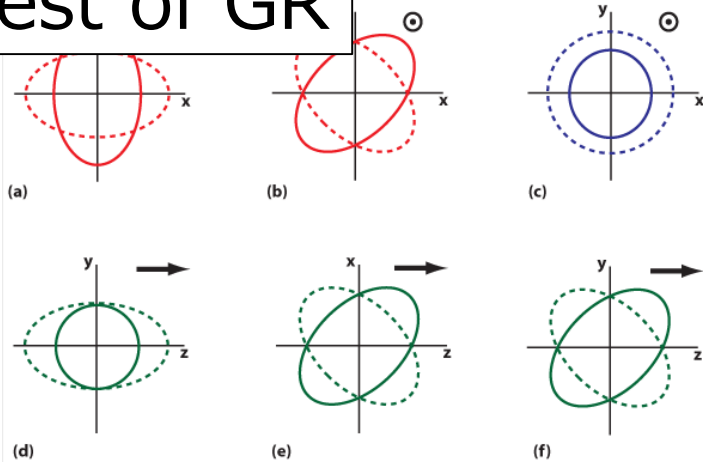


## SNe mechanism

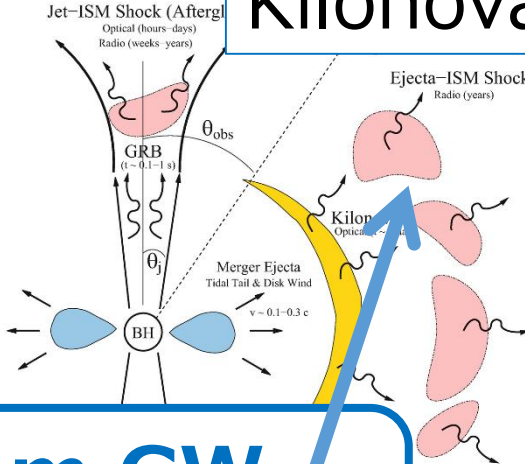


# Astrophysical motivation:

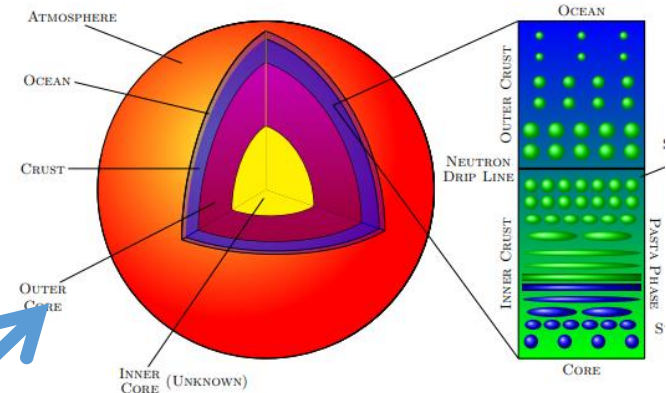
Test of GR



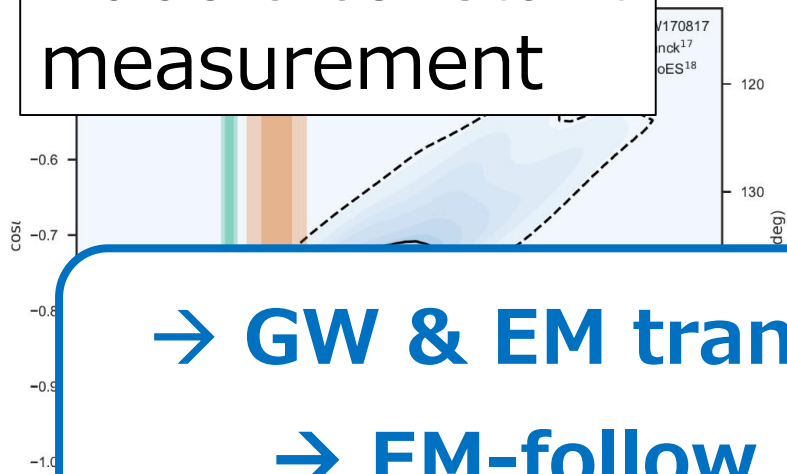
Kilonovae



Neutron Star interior

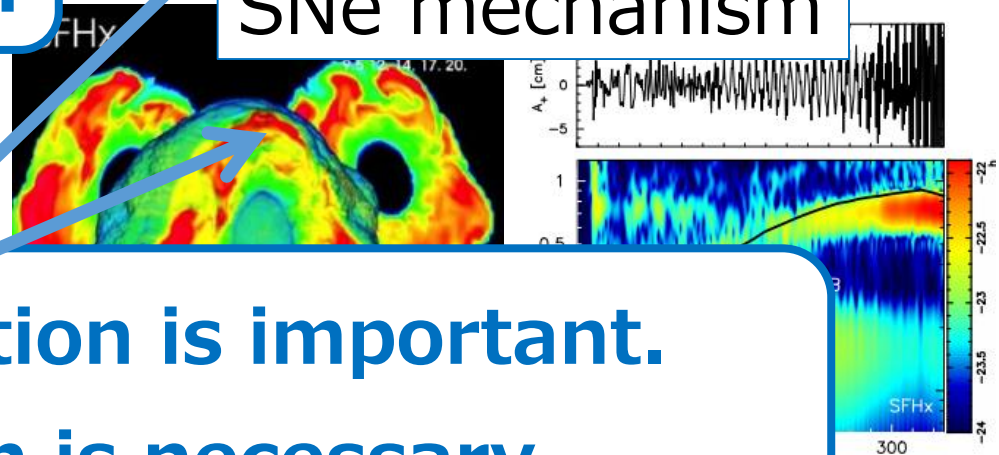


Hubble constant measurement



From GW observation

SNe mechanism

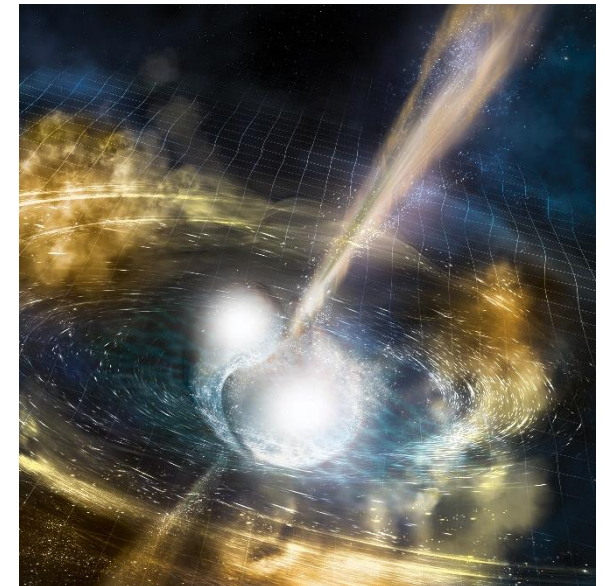
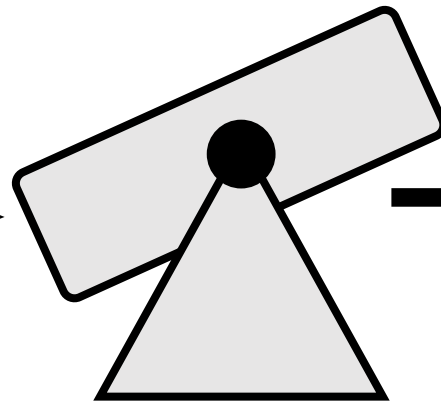
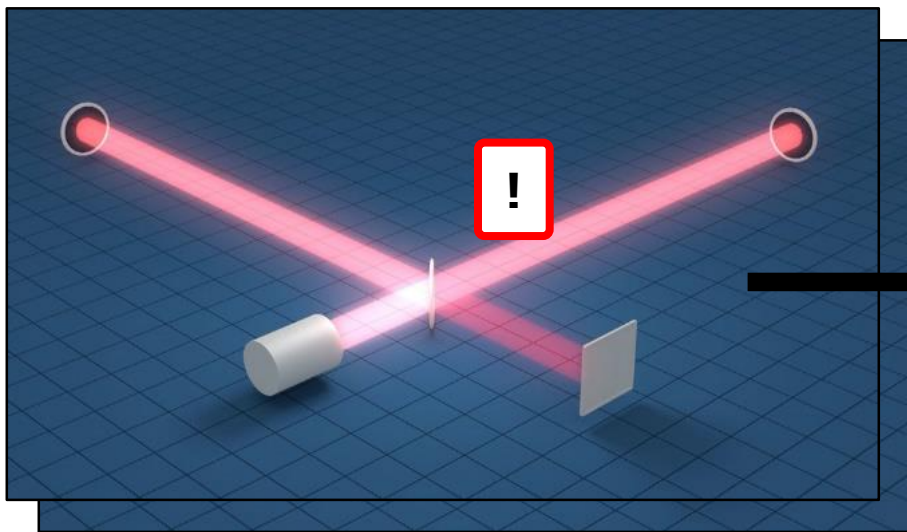


→ GW & EM transient observation is important.  
→ EM-follow up observation is necessary.



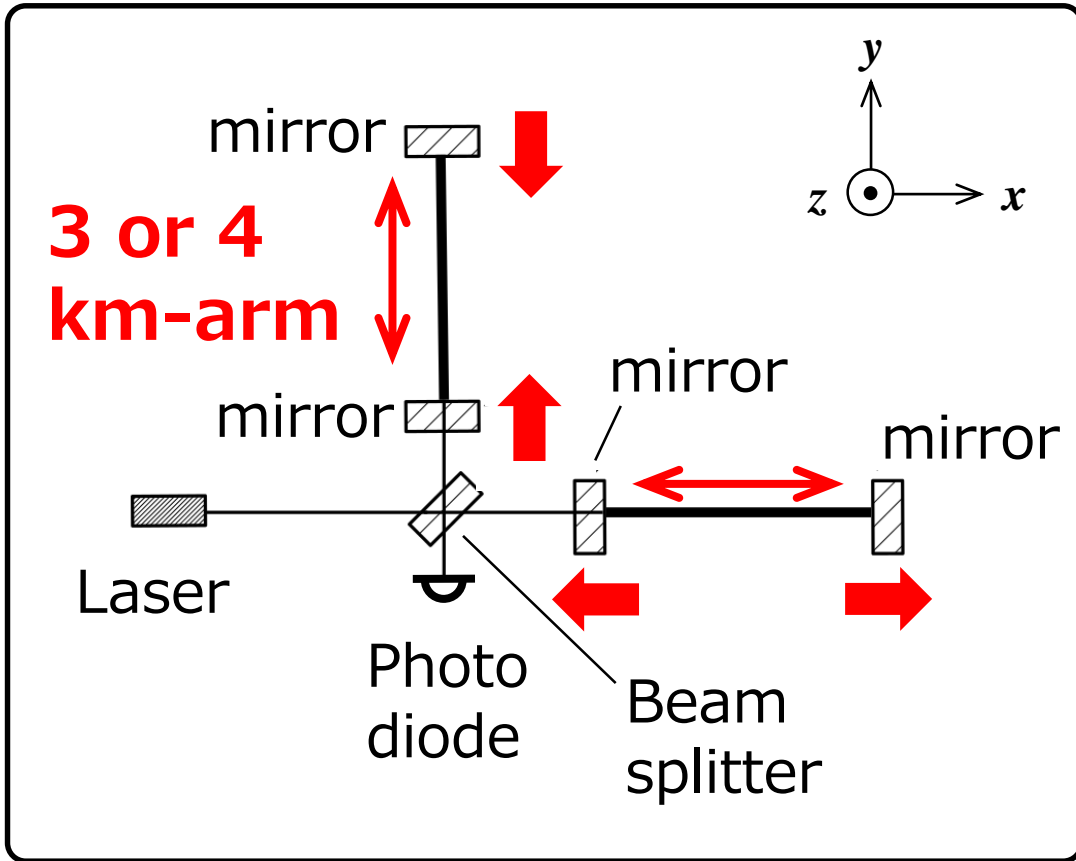
For effective EM-follow up observation

→ **Fast source localization**

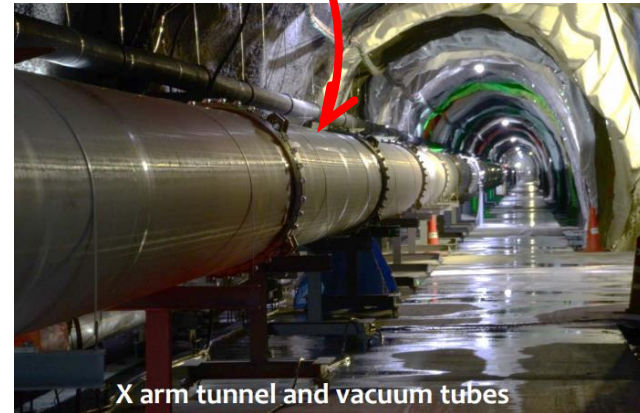


→ **Topic for 1st part**

# GW detectors:



- 1) Based on Michelson interferometer
- 2) Optical cavities (Fabry-Perot cavities)
- 3) 3 or 4 km-arm



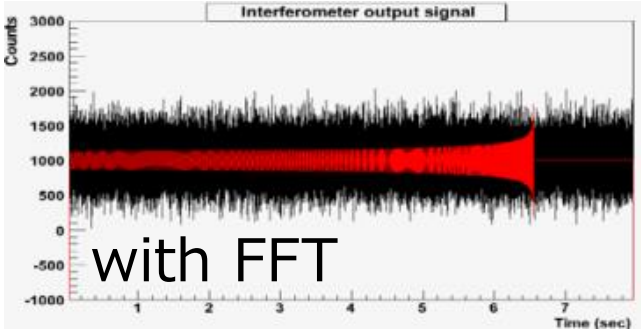
- 4) Suspended core optics
- **Topic for 2nd part**

# Analysis for GW signals:

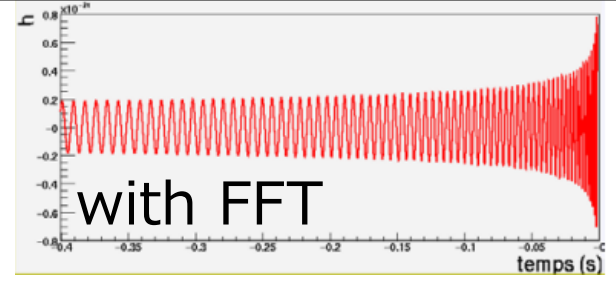
→ Matched filtering, for



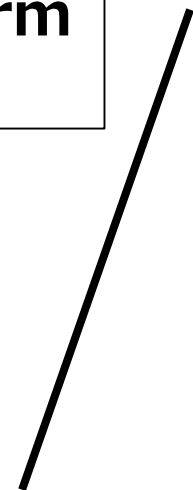
Detector output



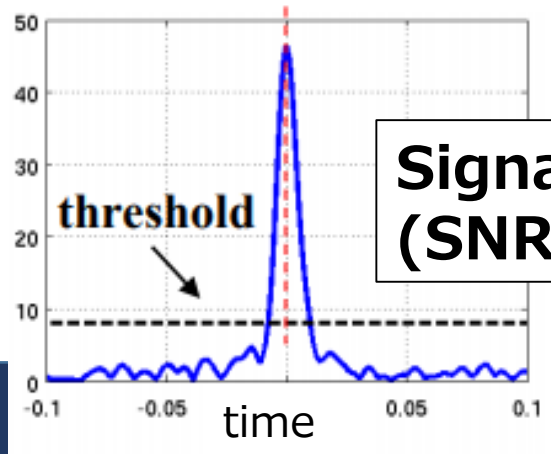
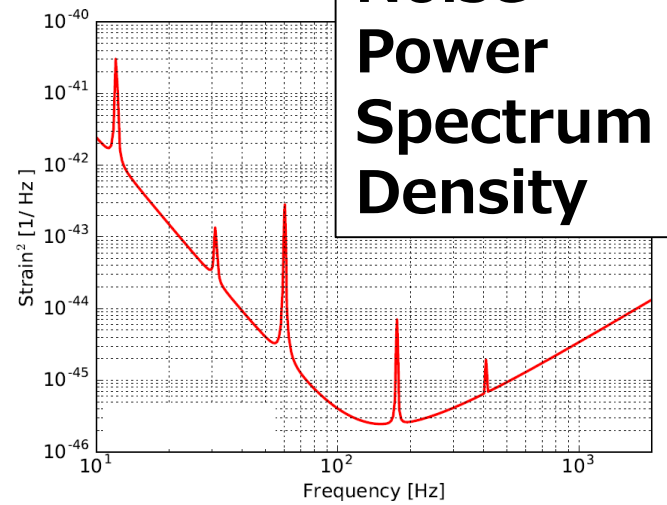
\*Theoretical waveform (Template)



×



Noise Power Spectrum Density

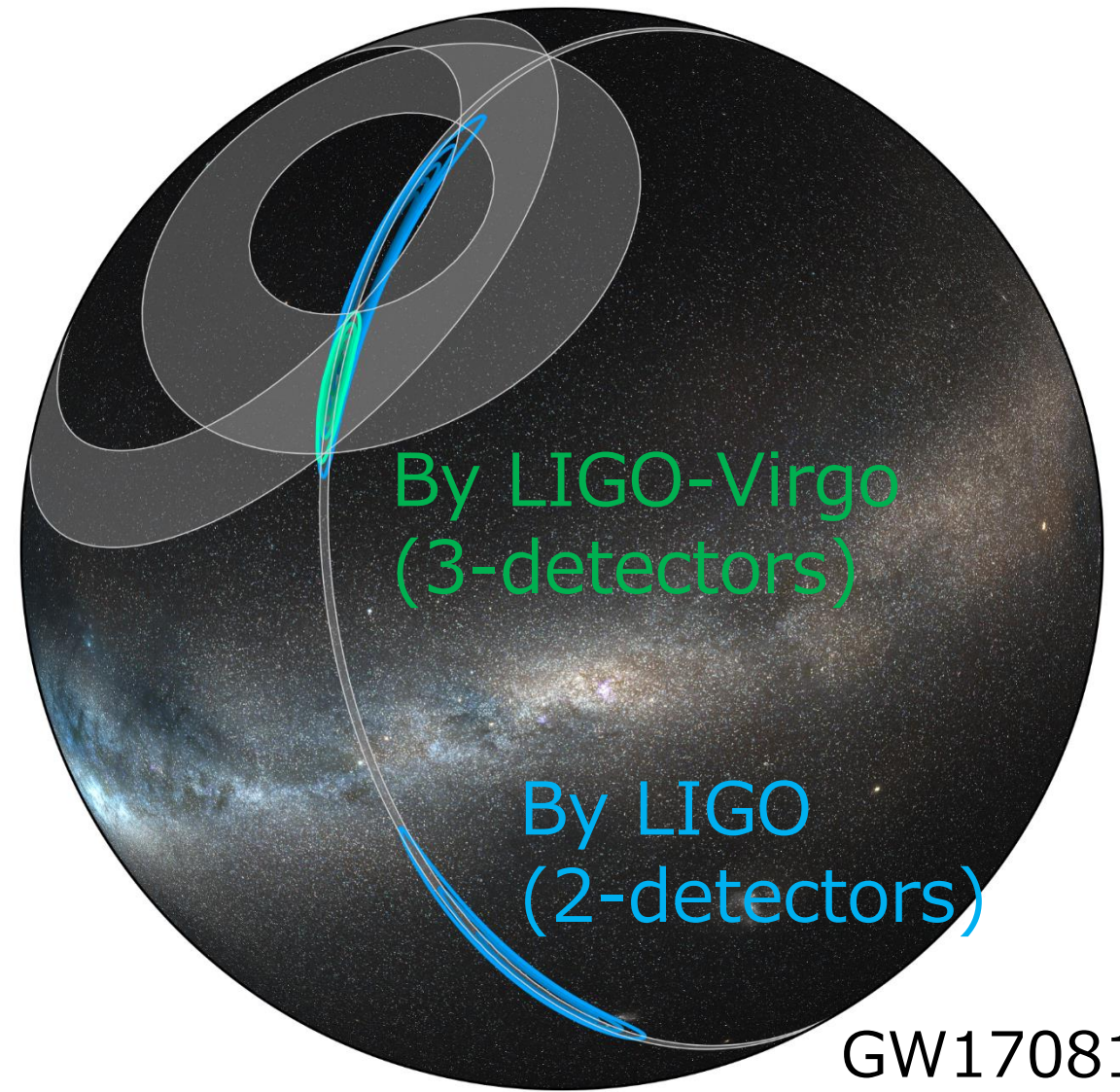
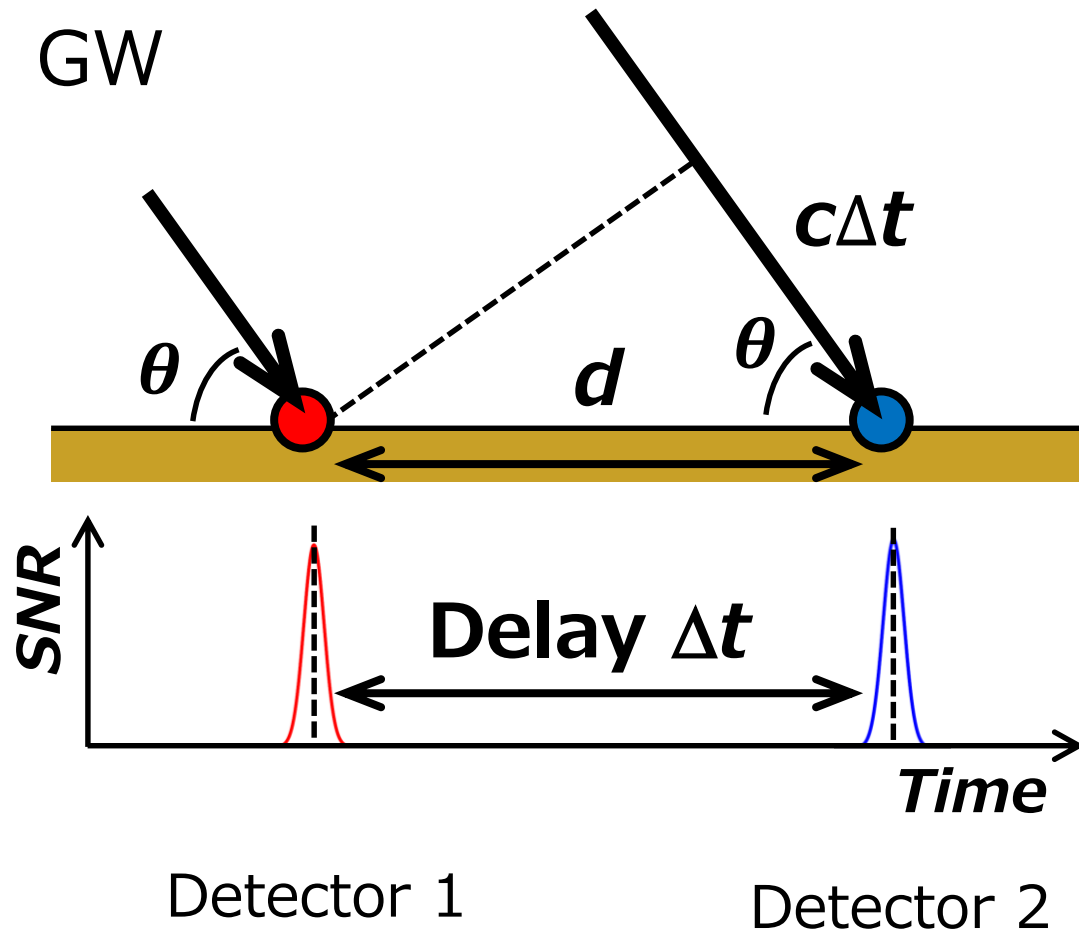


Signal-to-Noise ratio (SNR)



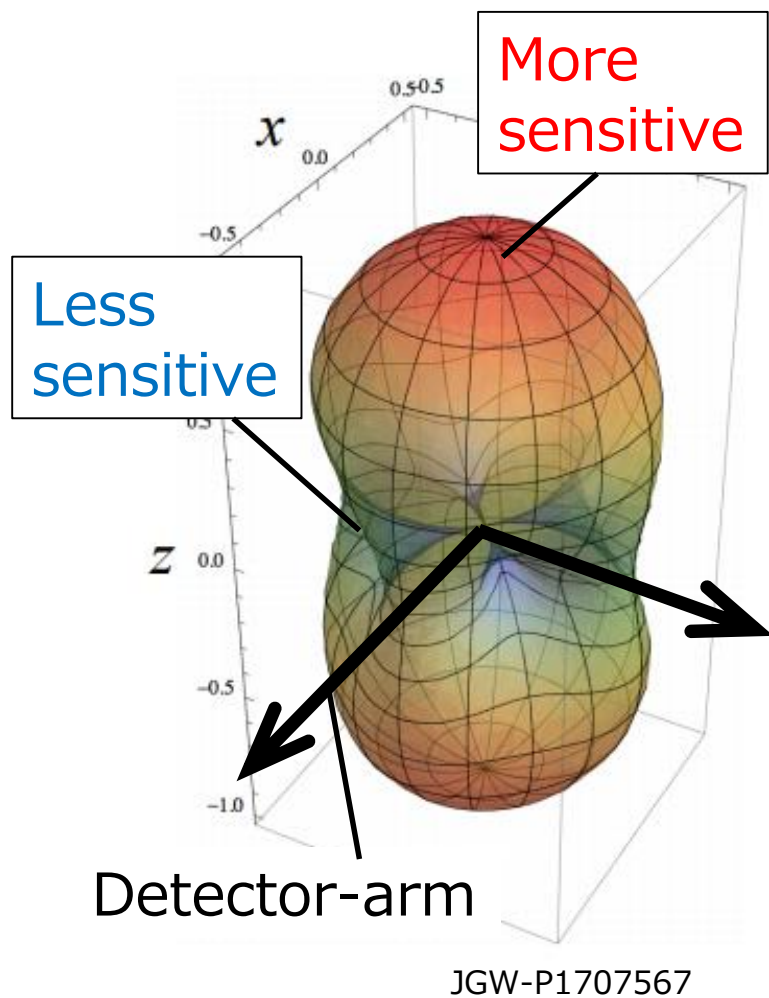
# Source localization:

By 3-detector network :

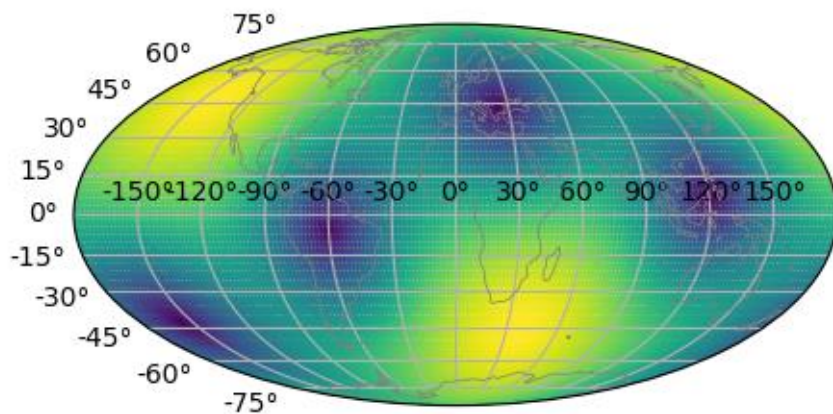


Credit: LIGO/Virgo/NASA/Leo Singer (Milky Way image: Axel Mellinger)

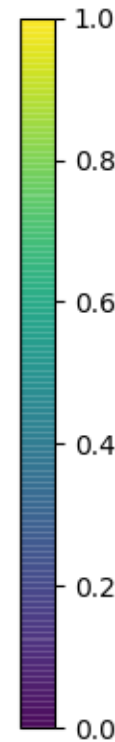
# Antenna pattern of GW detector:



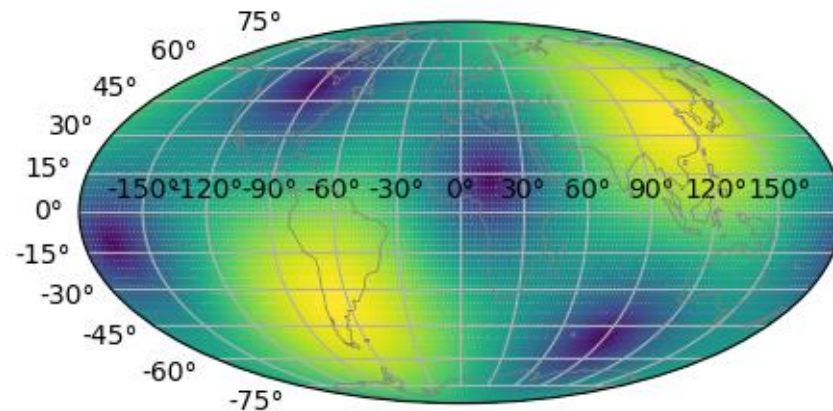
## Detector at Hanford



More sensitive



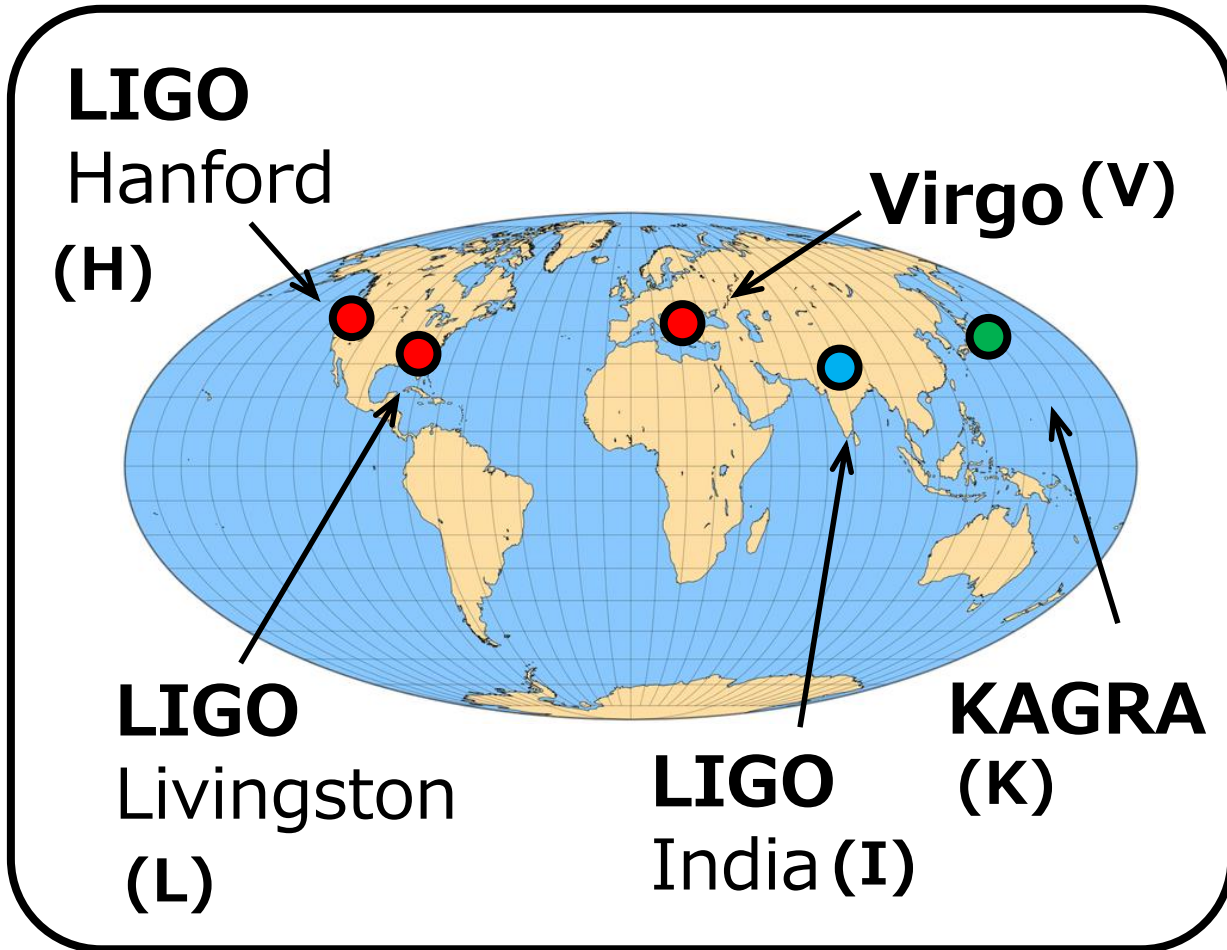
## Detector at Kamioka



Less sensitive

# Network by multiple GW detectors:

→ We are now building the network.



## Multiple detectors will help:

- \* Better sky coverage
- \* More precise localization
- \* Higher network duty cycle



# Thesis contents

My main research

1. Introduction

→ 2. Benefit of adding detectors to the observation network

3. Low frequency vibration isolation

4. KAGRA seismic attenuation system

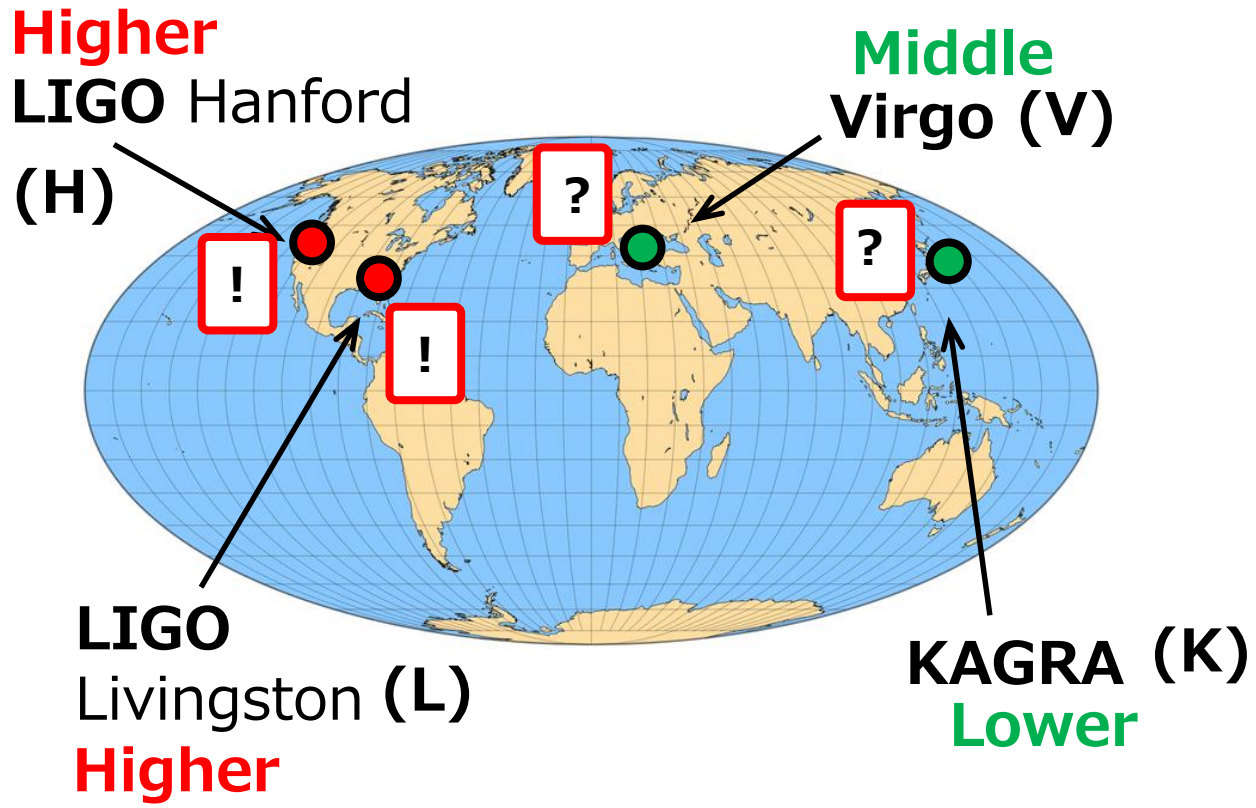
5. Suspension control design

6. Performance test of local control for KAGRA Type-A suspension

7. Summary

# In heterogeneous network:

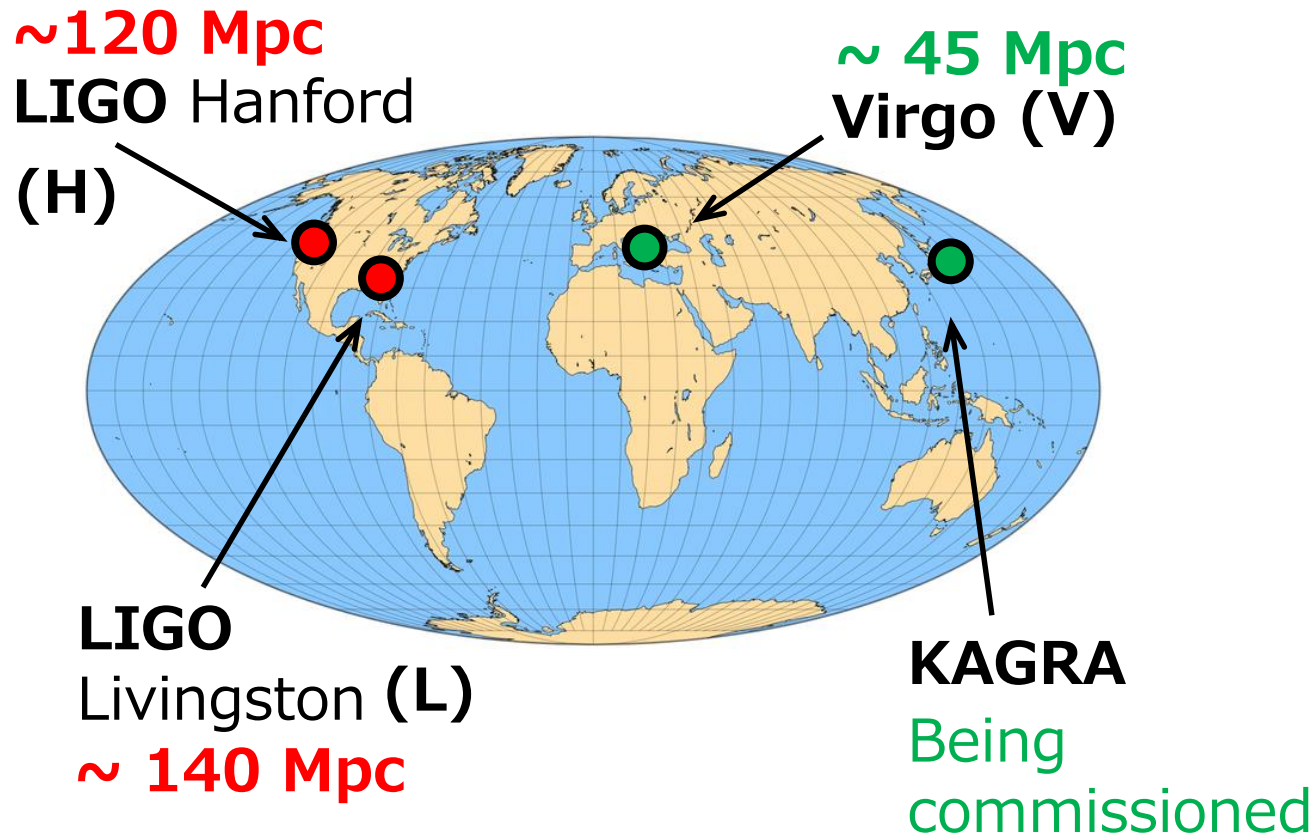
Ex.)  $SNR > SNR_{th} \rightarrow$  detection



(At the beginning)

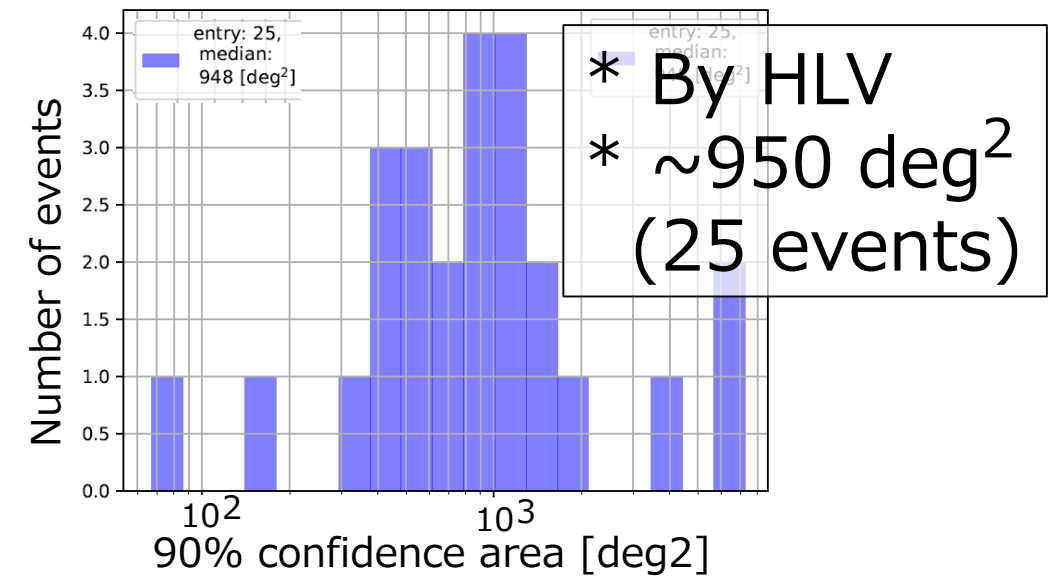
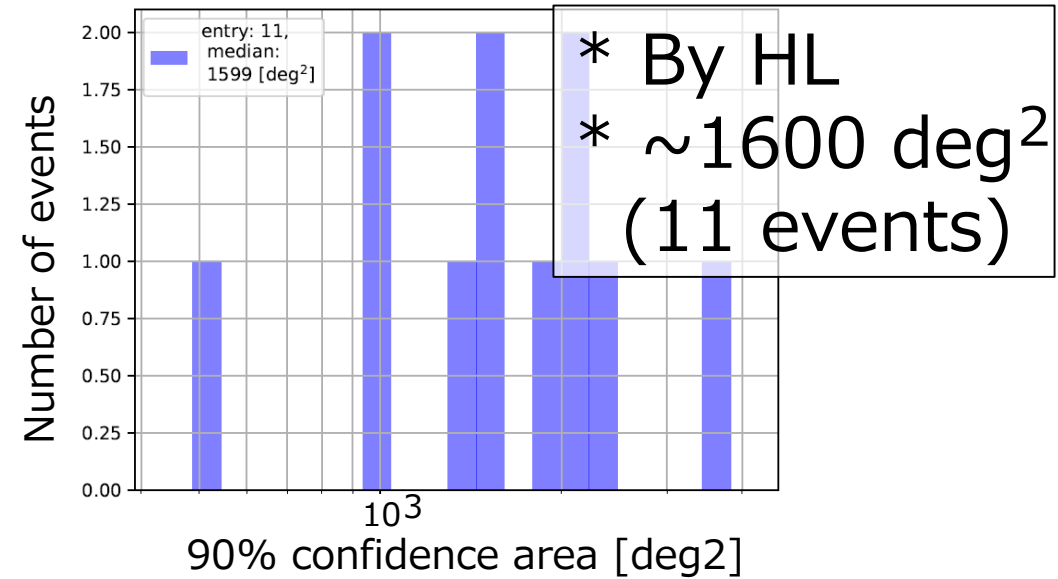
- Triple (or more) coincidences  
→ Hardly happens
- Not good for EM-follow up

# Indeed, the real alert during O3:



[ref] <https://summary.ligo.org/~detchar/summary/O3a/>

## Size of localized area



[ref] <https://gracedb.ligo.org/superevents/public/O3/>

# Demanded for EM-follow up:

As an example:

\* For kilonova search with BlackGEM

→ **2.7 deg<sup>2</sup> / 5 min**  
(for 23rd Magnitude)

[ref] [https://link.springer.com/chapter/10.1007/978-3-319-10488-1\\_5](https://link.springer.com/chapter/10.1007/978-3-319-10488-1_5)

For 1600 deg<sup>2</sup>, it will take ~50 hrs.



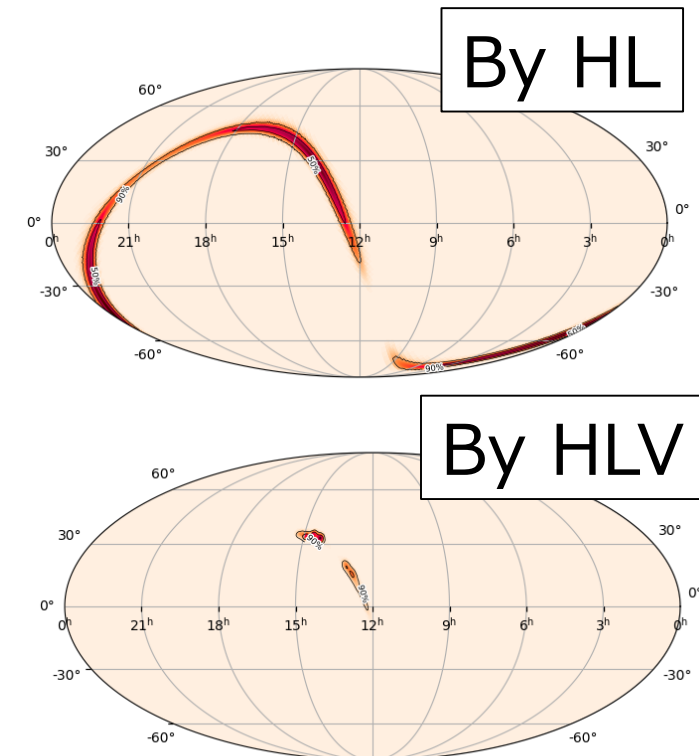
To complete < 9 hrs (one night)

→ < 300 deg<sup>2</sup>

→ More than 3 detectors necessary.

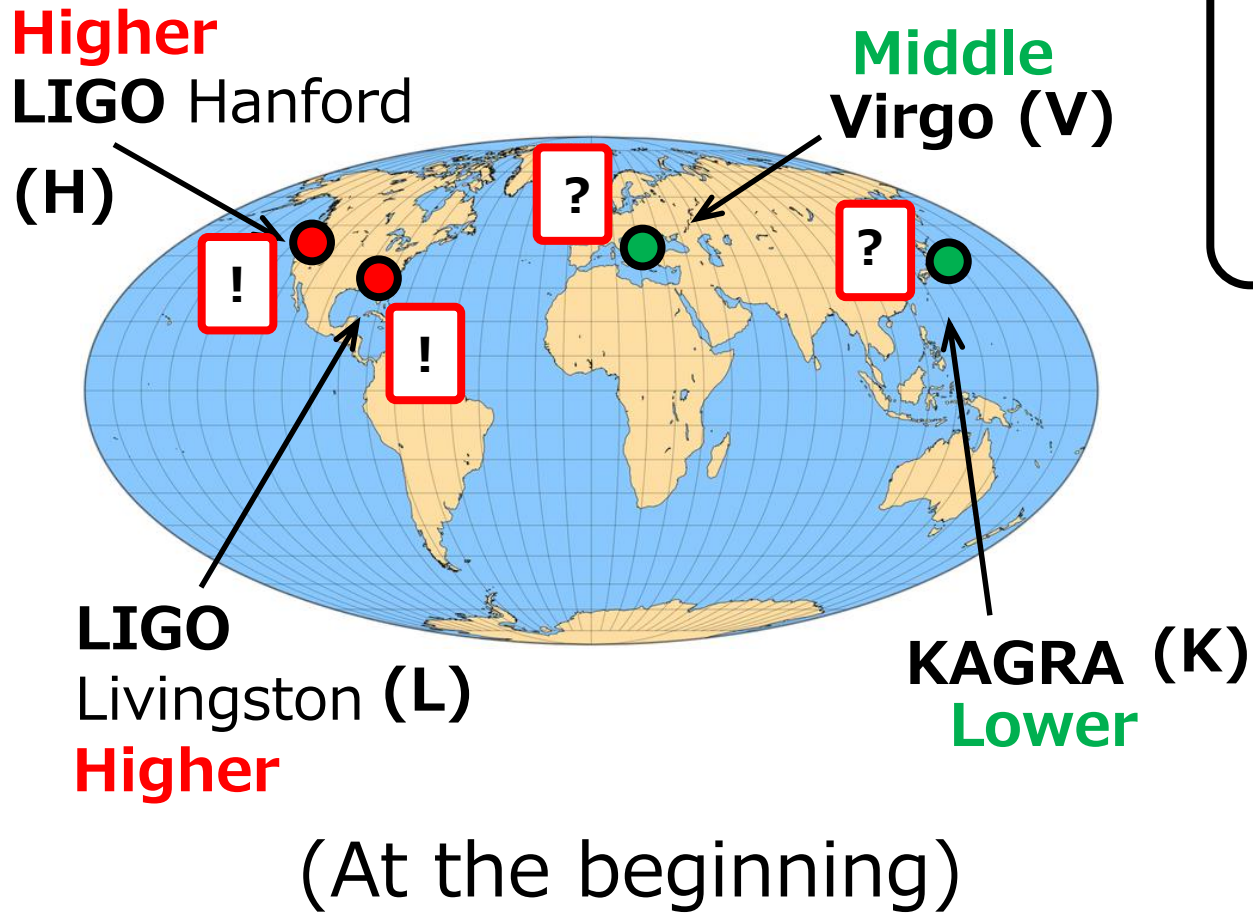


<https://astro.ru.nl/blackgem/>



[ref] <https://gracedb.ligo.org/superevents/public/O3/>

# In heterogeneous network:



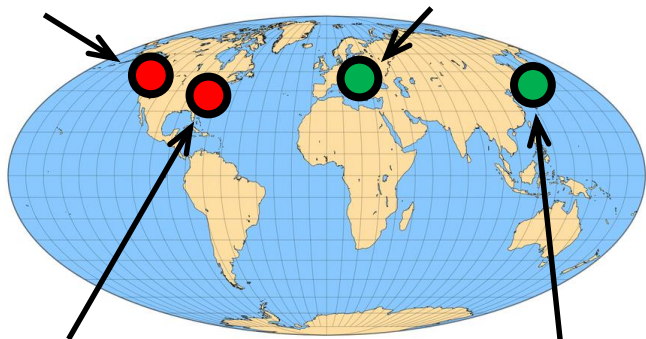
Ex.)  $SNR > SNR_{th} \rightarrow$  detection:  
  
 $\rightarrow$  Not good for EM-follow up

- Target:**
- \* Set a lower threshold,
  - &
  - \* Avoid not too many background triggers.



# Hierarchical approach

Higher sensitivity  
LIGO Hanford (H)    Middle sensitivity  
Virgo (V)



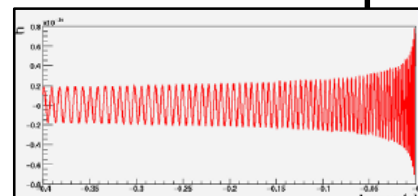
Higher sensitivity  
LIGO Livingston (L)    Lower sensitivity  
KAGRA (K)

(At the beginning)

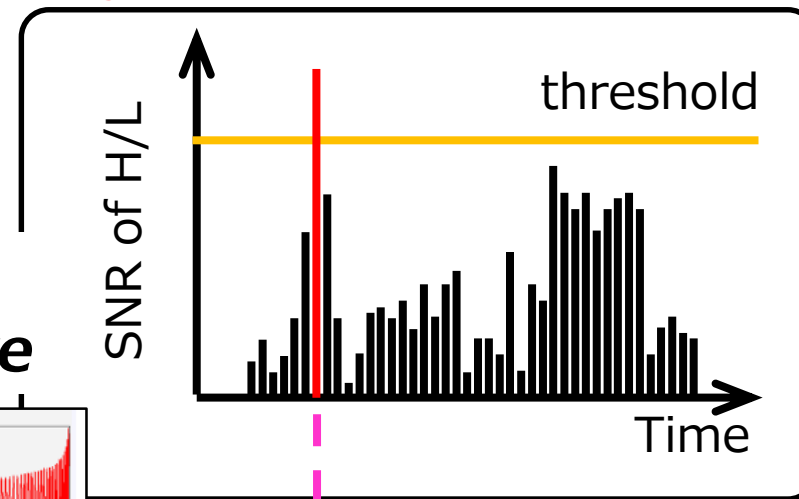
Sub network by higher sensitive detectors find candidate event.



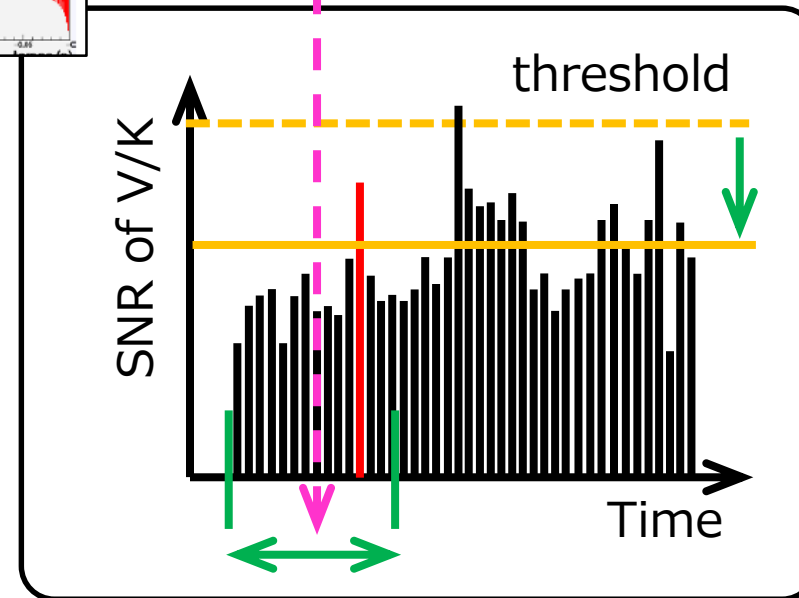
Less sensitive detectors are added into network with  
**1. lower SNR threshold,**  
**2. same template,**  
**3. a small window around time of double coincidences.**



Higher sensitive detector



One template



Lower sensitive detector

# Hierarchical approach in fast localization

With LIGO-Virgo / LIGO-KAGRA / LIGO-Virgo-KAGRA network:

→ **Expected performance?**

→ **Required detector sensitivity?**

→ **Optimal SNR threshold?**

# Hierarchical approach in fast localization

With LIGO-Virgo / LIGO-KAGRA / LIGO-Virgo-KAGRA network:

***Unique***

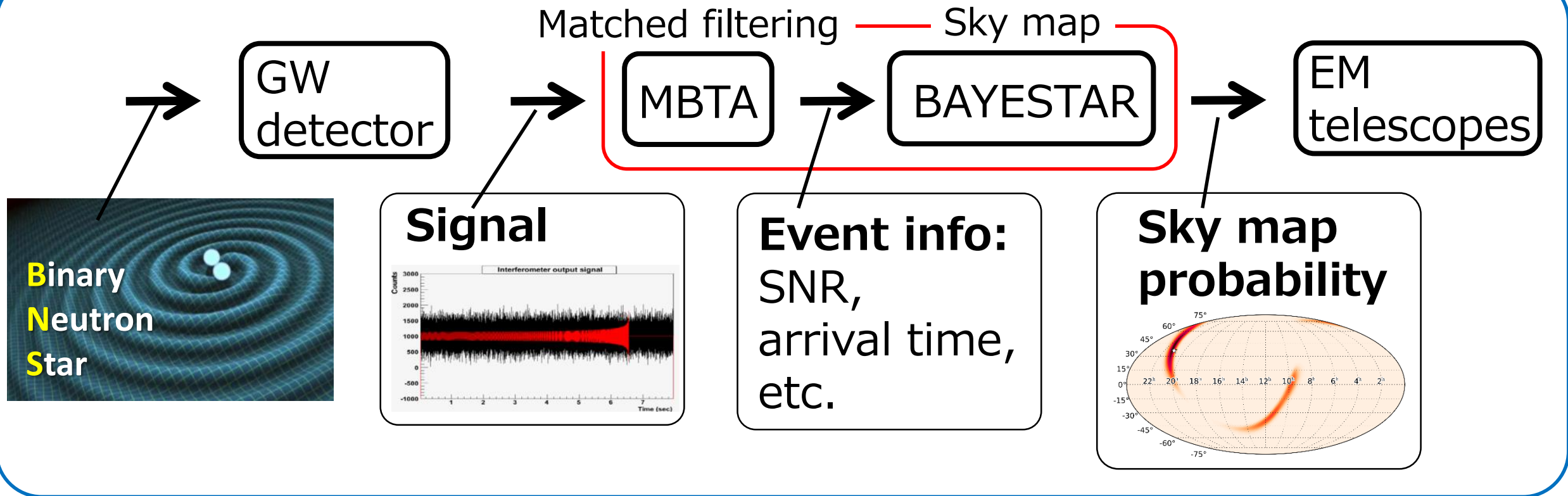
**Hierarchical search  
with heterogeneous network**

Performance by LIGO-Virgo network

→ Published at *Astroparticle Physics*, **Y. Fujii** et. al. (2019)

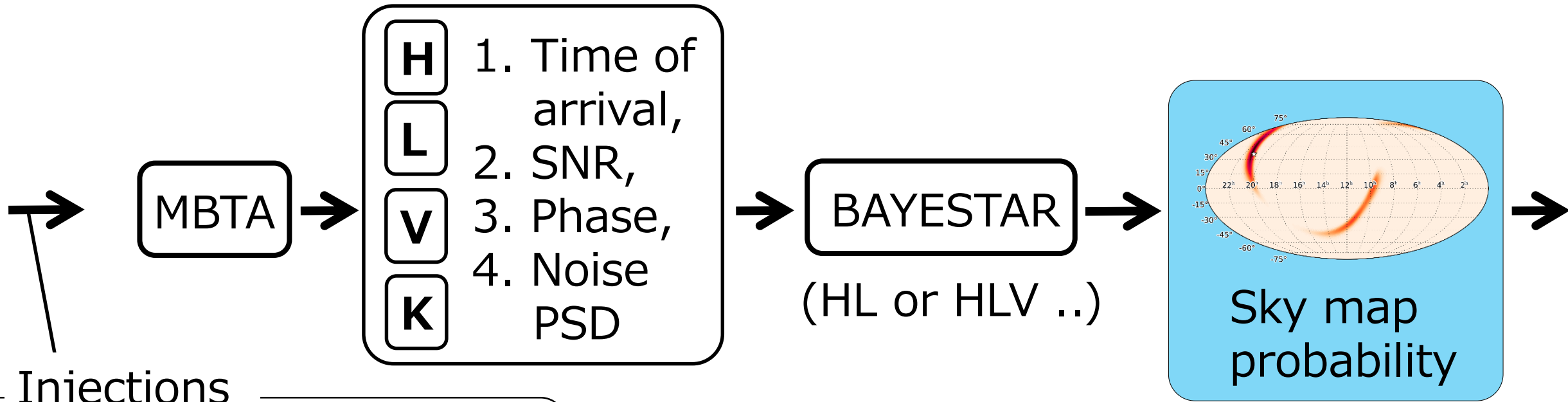
# Calculation set up:

1. GW-EM pipeline (for GWs from BNS)

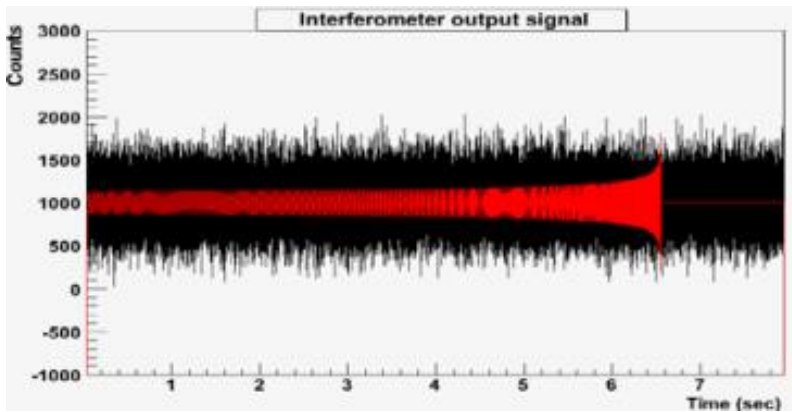


2. Two LIGOs (54 Mpc-BNS range), Virgo, KAGRA ( $< 54$  Mpc)  
→ Relative sensitivities is important.

# Main flow:

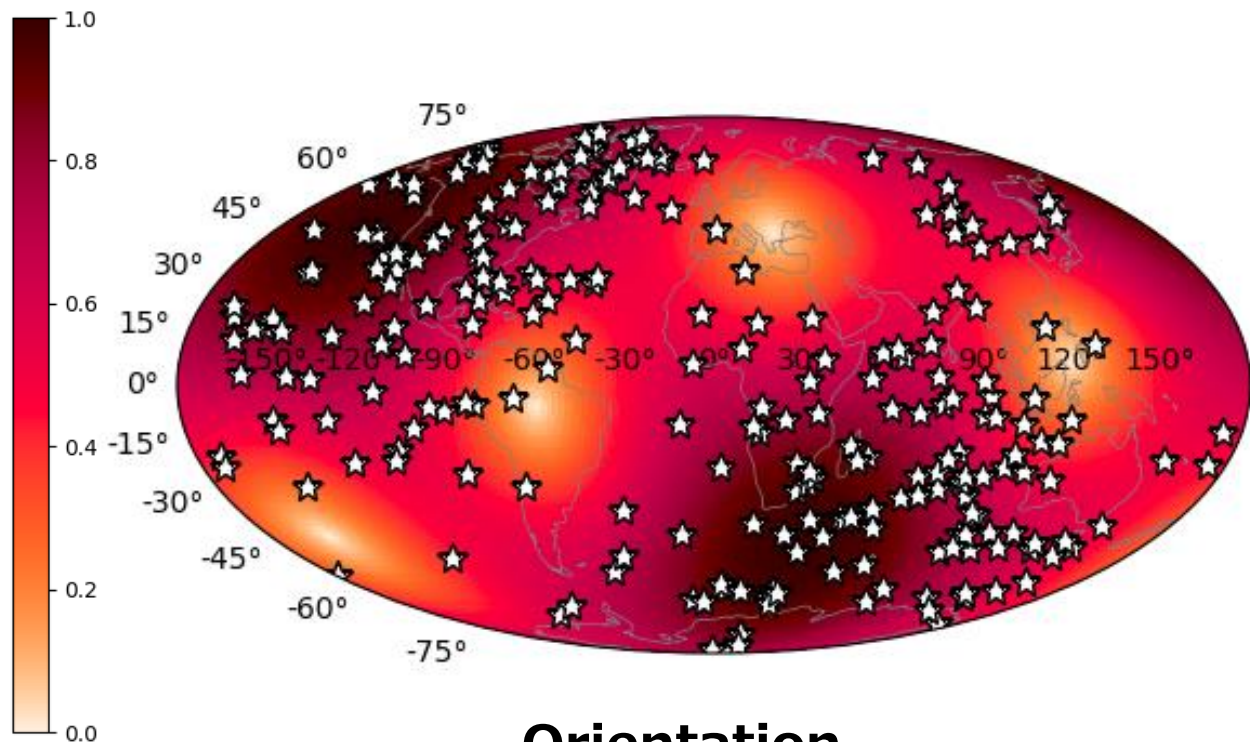


Injections

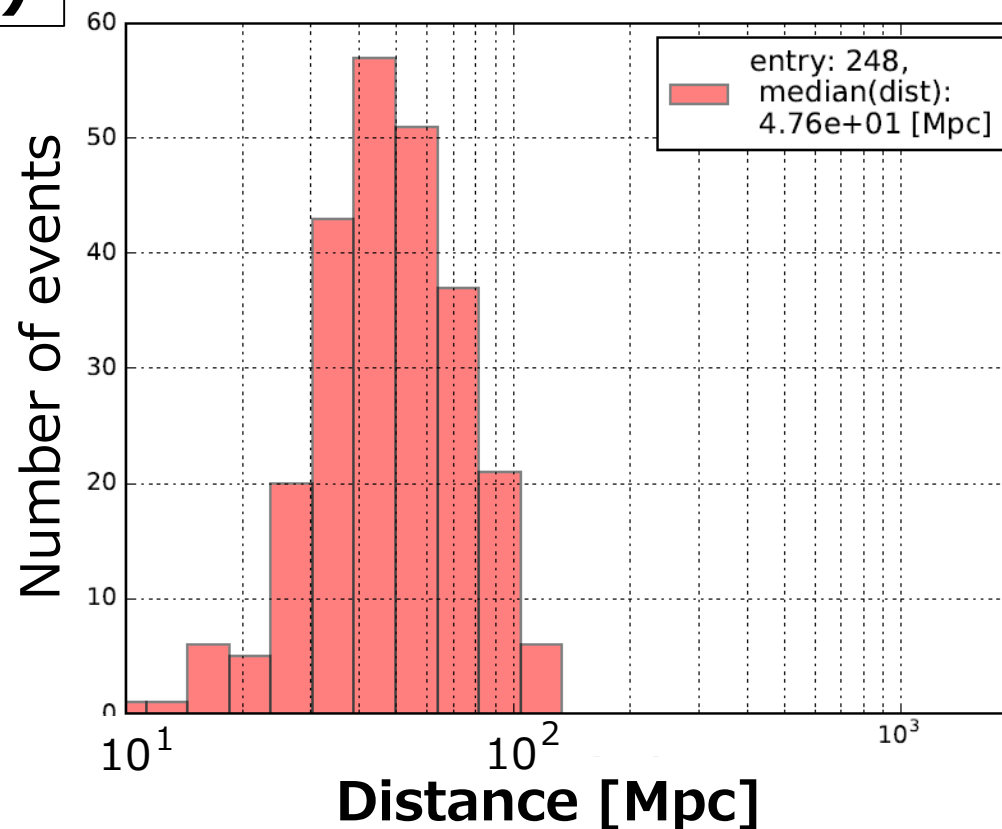


# Main flow:

Injections (number of events: 248)

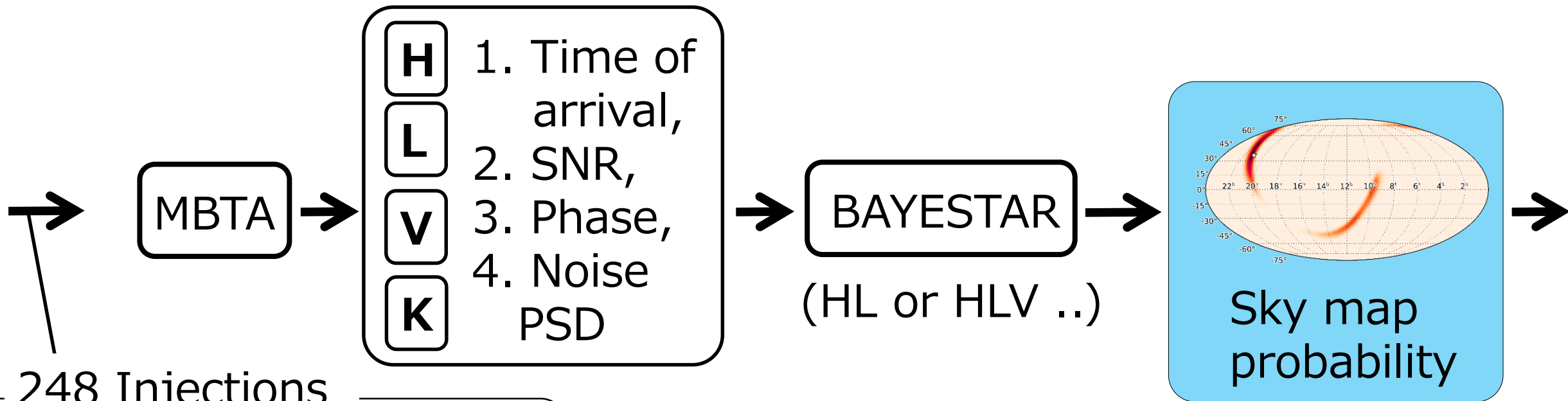


**Orientation**  
(with LIGO antenna pattern)

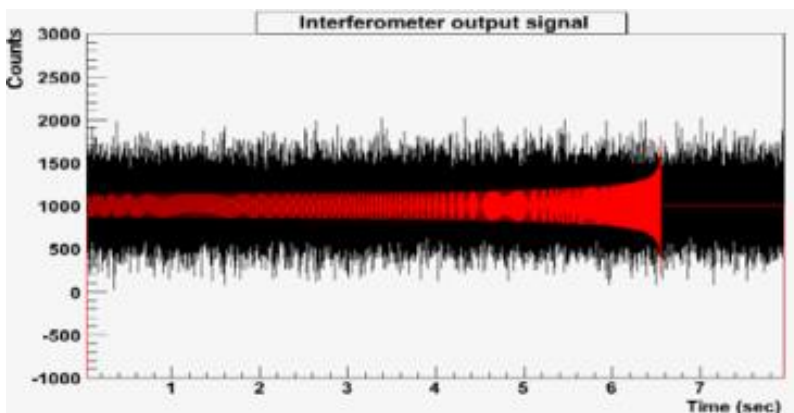


**detected by LIGO network in [1], and randomly selected.**  
[1] LIGO-P1300187

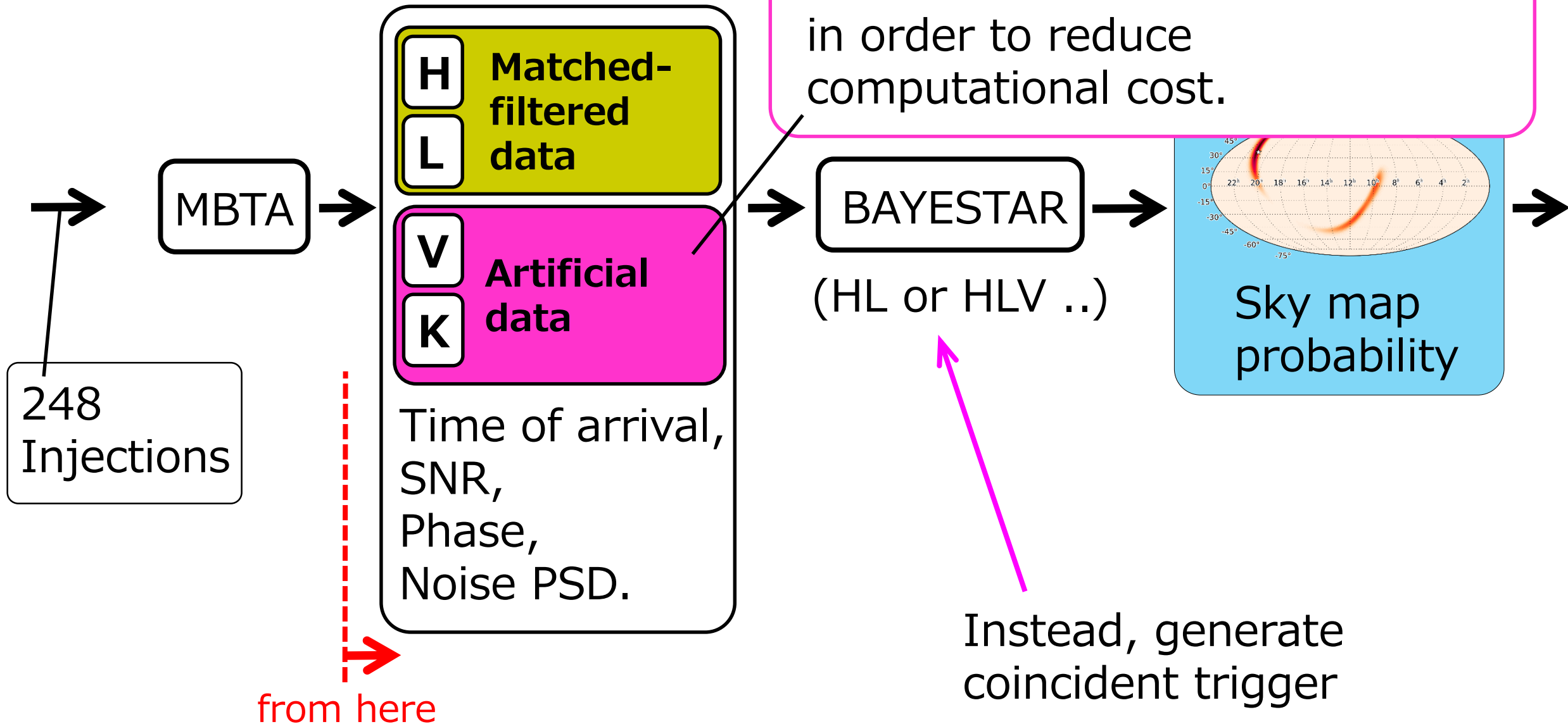
# Main flow:



248 Injections



# Main flow:





# Generating coincident triggers, doubles, triples, ..

→ In the real life,  
**Not all triggers are related to real GW signals.**  
Sometimes triggers are from noise

**In order to realize this,**

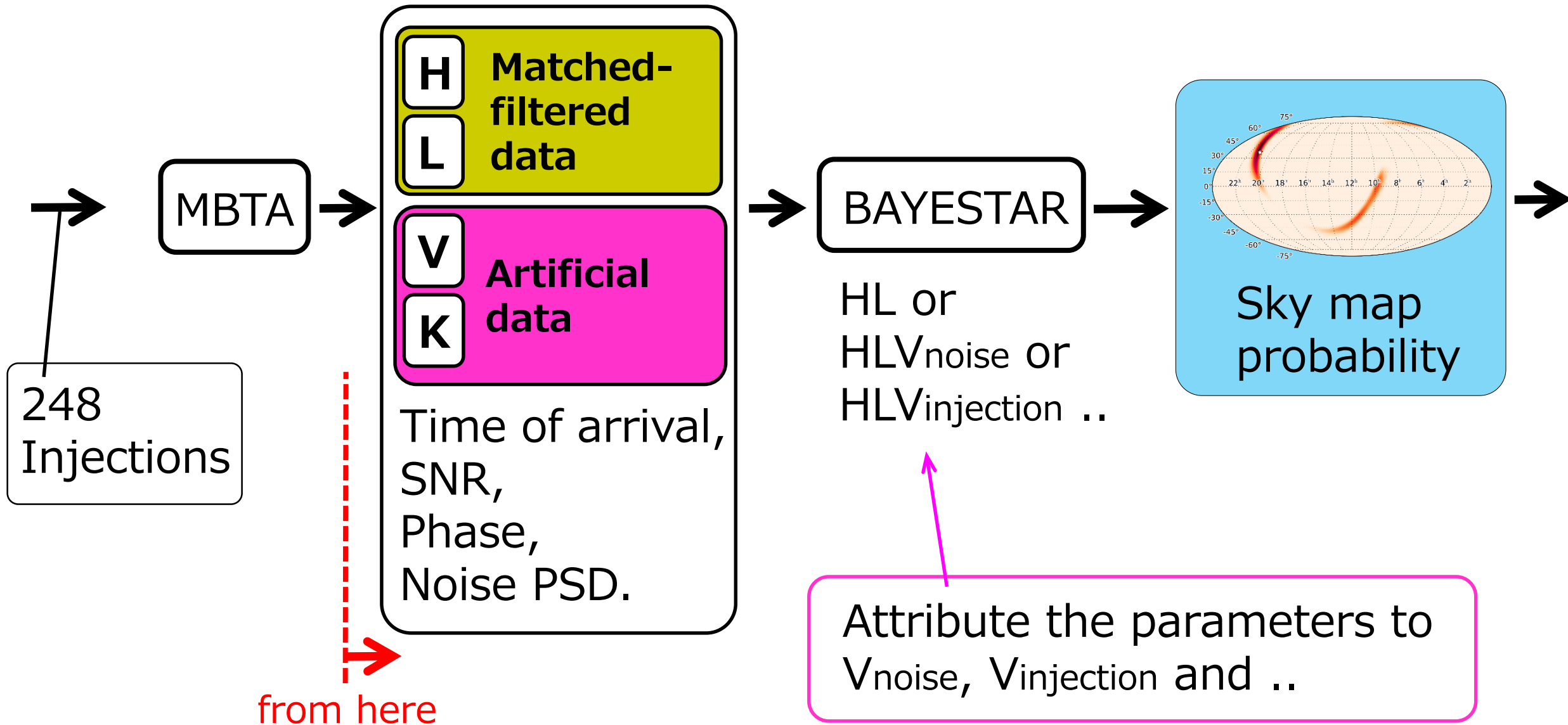
As an example, in LIGO-Virgo network case:

(  $\text{SNR} > \text{SNR}_{\text{th}}$  ) and ( no noise trigger ) →  $\text{HLV}_{\text{injection}}$

(  $\text{SNR} < \text{SNR}_{\text{th}}$  ) and ( no noise trigger ) → HL

( noise trigger ) →  $\text{HLV}_{\text{noise}}$

# Main flow:



# Making artificial **V/K** triggers

(dist. = distribution)

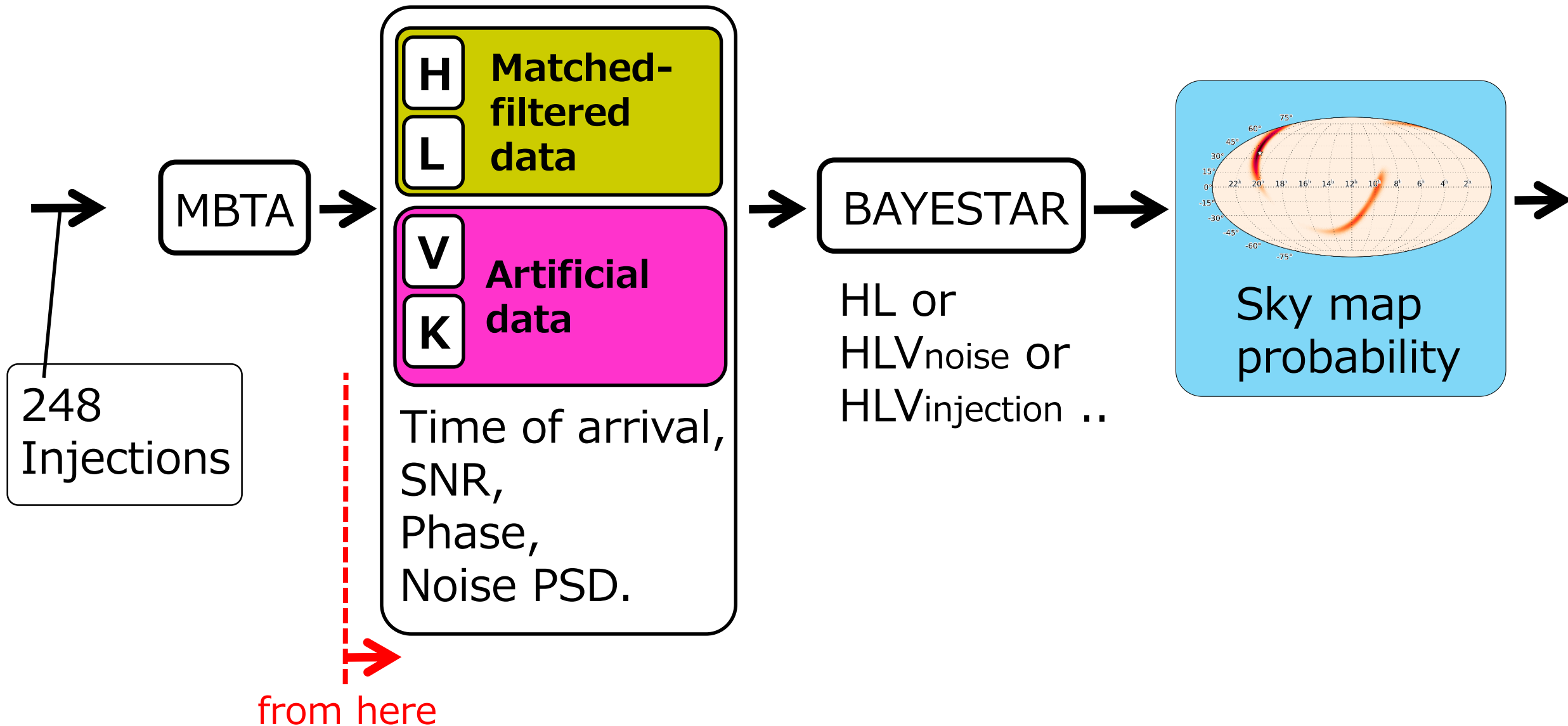
## Noise trigger:

$$\begin{bmatrix} \text{SNR} \\ \text{Time} \\ \text{phase} \end{bmatrix} = \begin{bmatrix} \text{Random number from a measured dist.} \\ \text{Time}_{\text{LIGO}} + \text{Random number from } \mathbf{uniform} \text{ dist.} \\ \text{Random number from } \mathbf{uniform} \text{ dist.} \end{bmatrix}$$

## Injection trigger:

$$\begin{bmatrix} \text{SNR} \\ \text{Time} \\ \text{phase} \end{bmatrix} = \begin{bmatrix} \text{Expected} \end{bmatrix} + \begin{bmatrix} \text{Random number} \\ \text{from } \mathbf{Gaussian} \text{ dist.} \end{bmatrix}$$

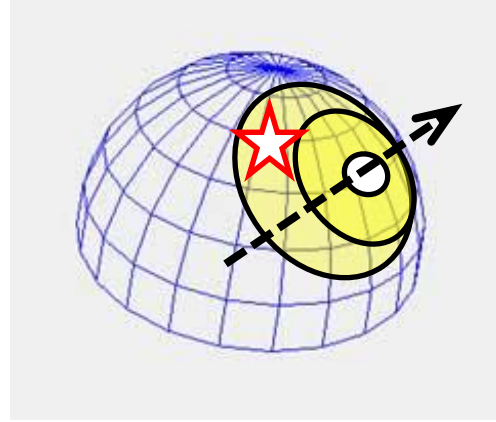
# Main flow:



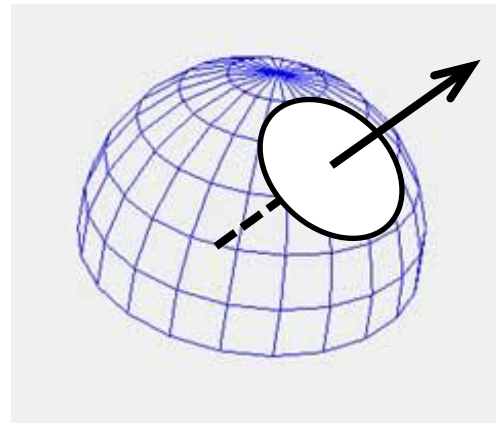
# Main flow:

## Localization performance

- 1) **Accuracy**  
→ Searched area (deg<sup>2</sup>)



- 2) **Precision**  
→ 90 % confidence area (deg<sup>2</sup>)



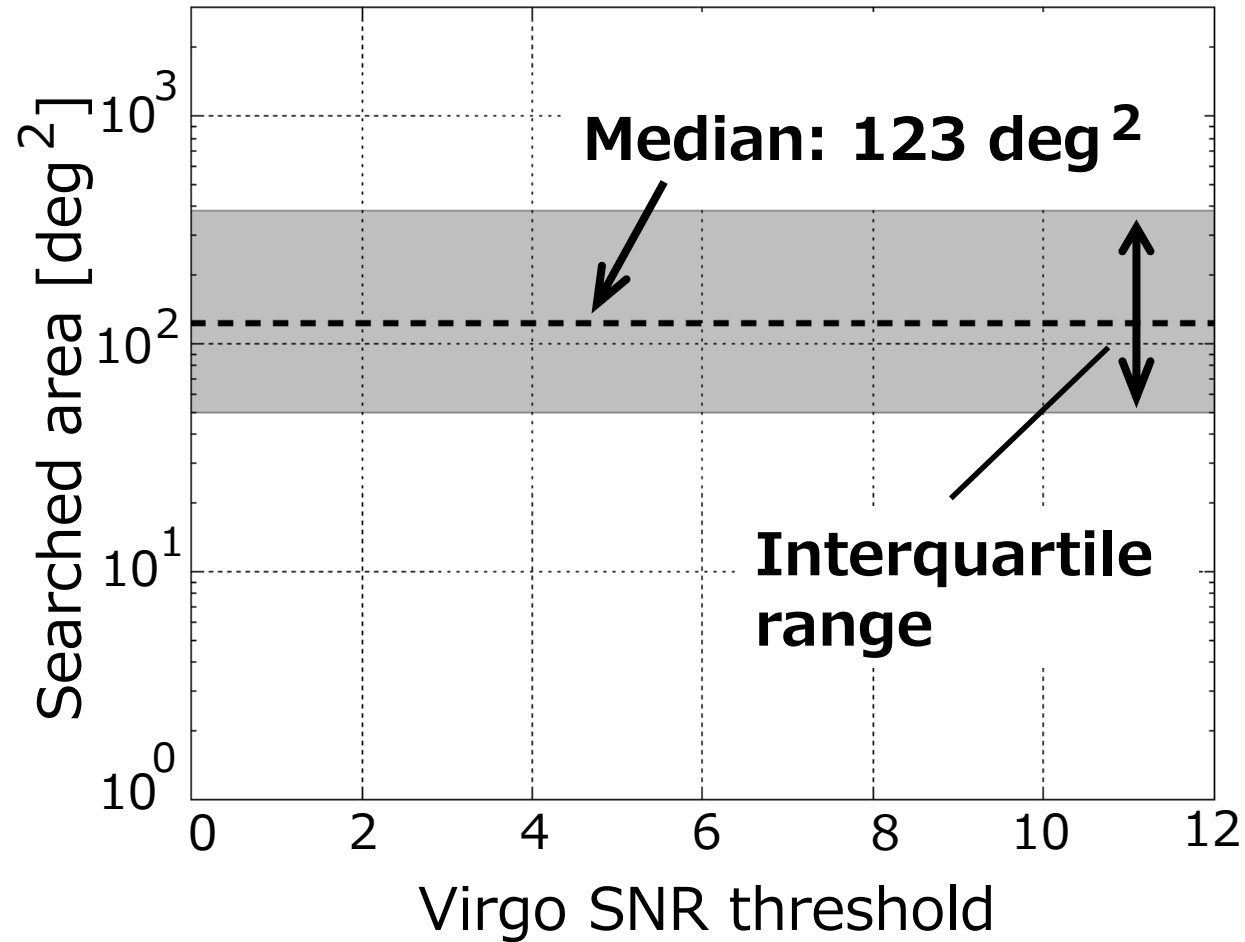
*For both,  
**smaller**  
is  
**better.***

Median values  
for 248 events

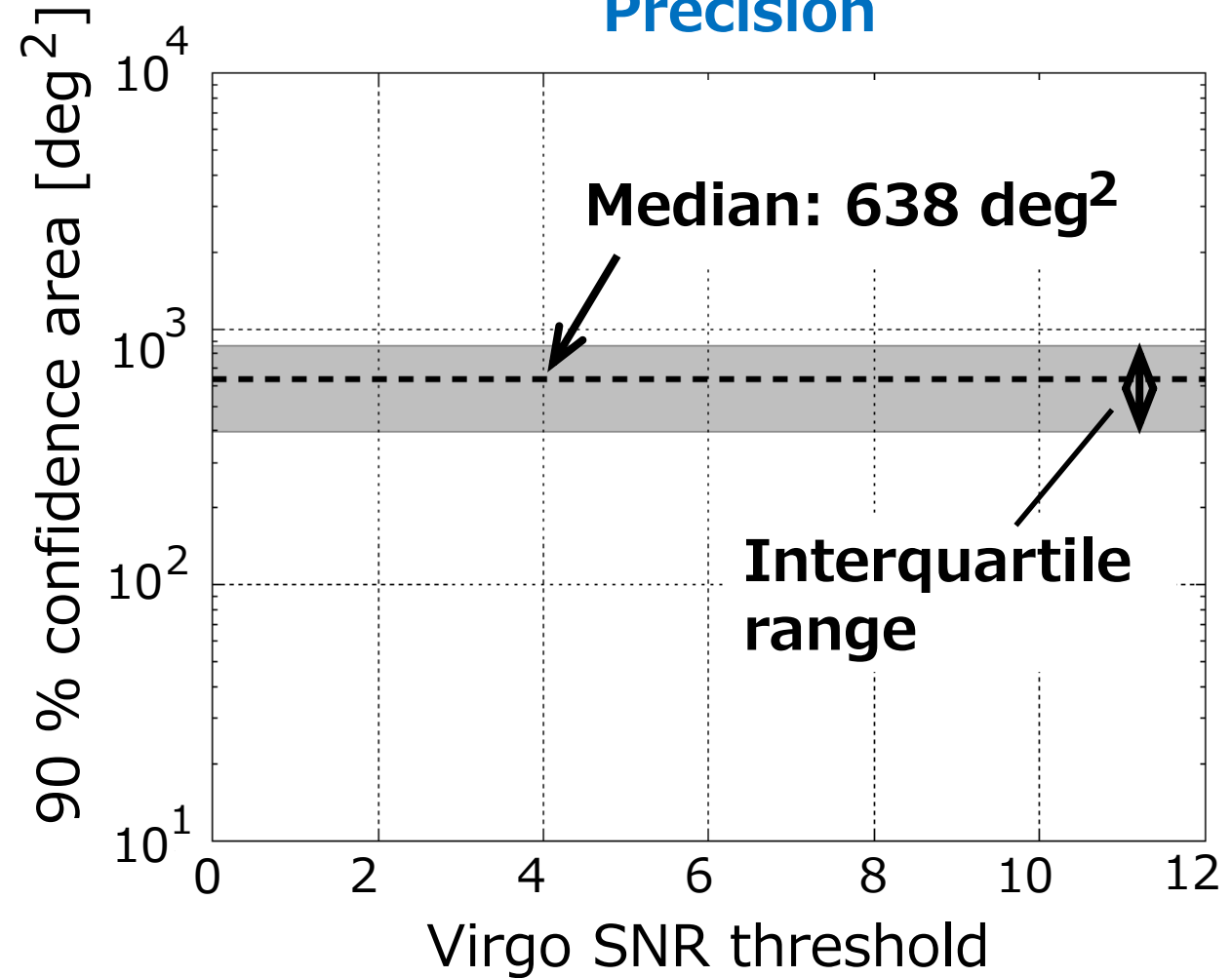
# Performance (HL):

(SNR threshold for H, L = 5., 5.)

## Accuracy



## Precision

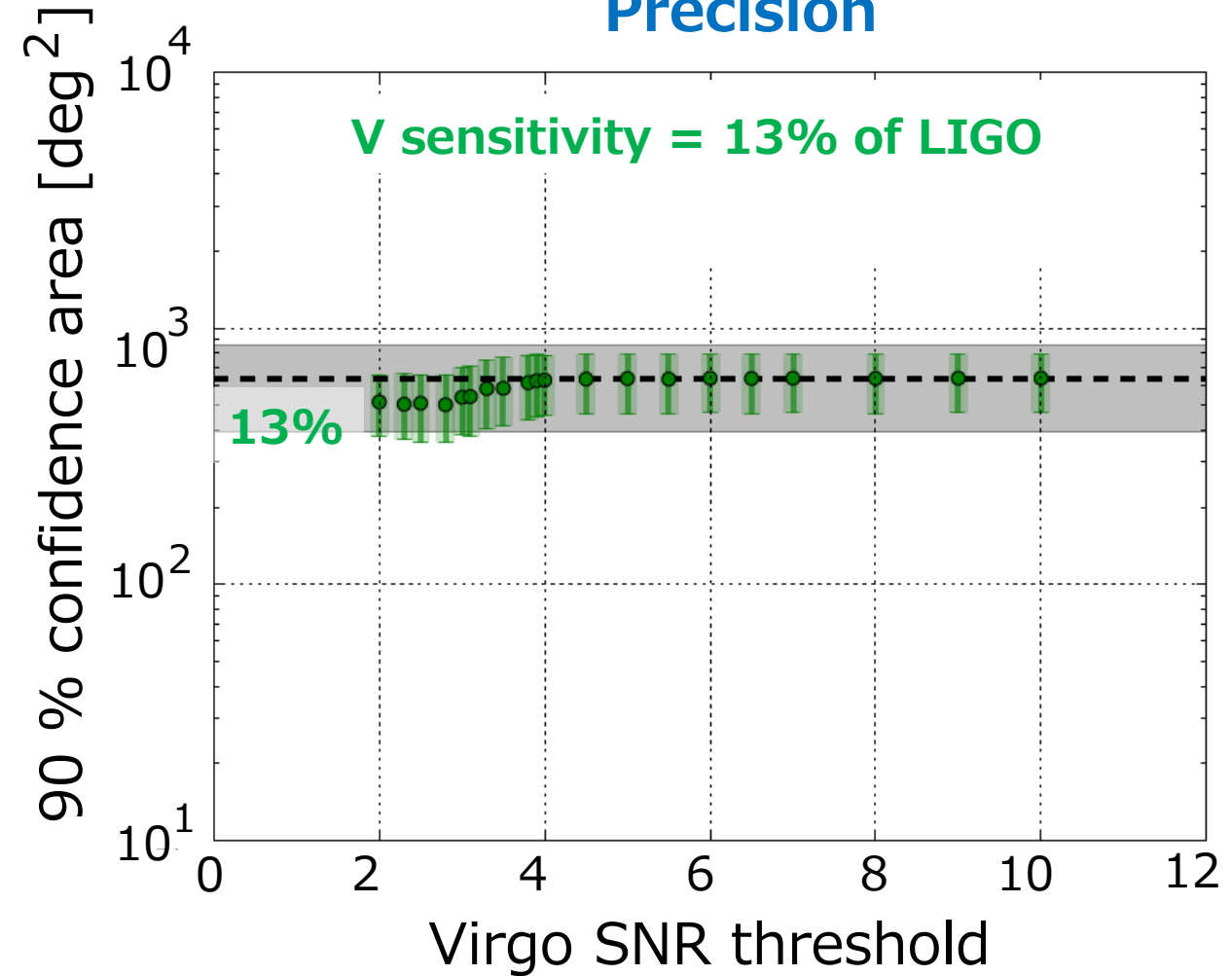
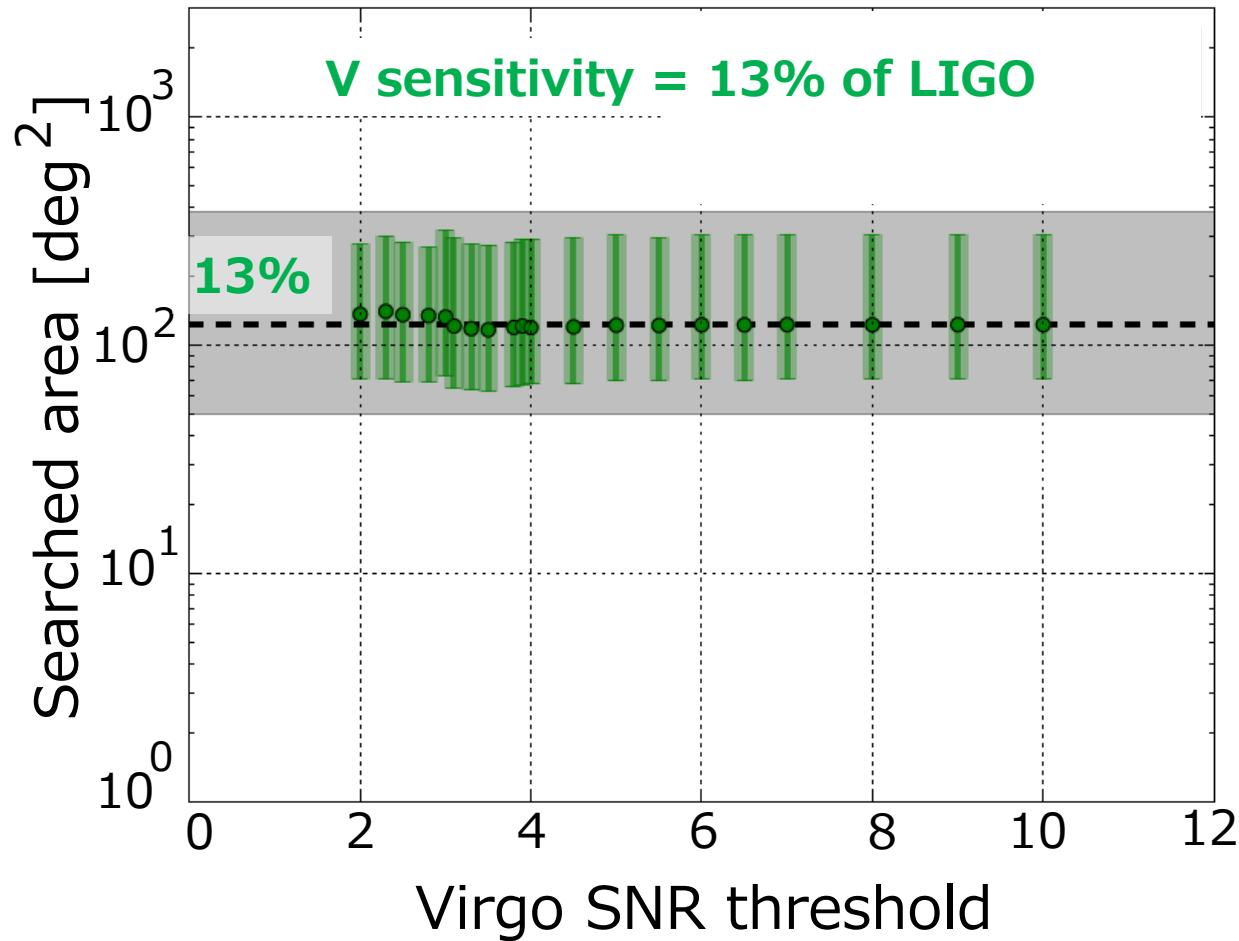


# Performance (HLV):

(SNR threshold for H, L = 5., 5.)

## Accuracy

## Precision

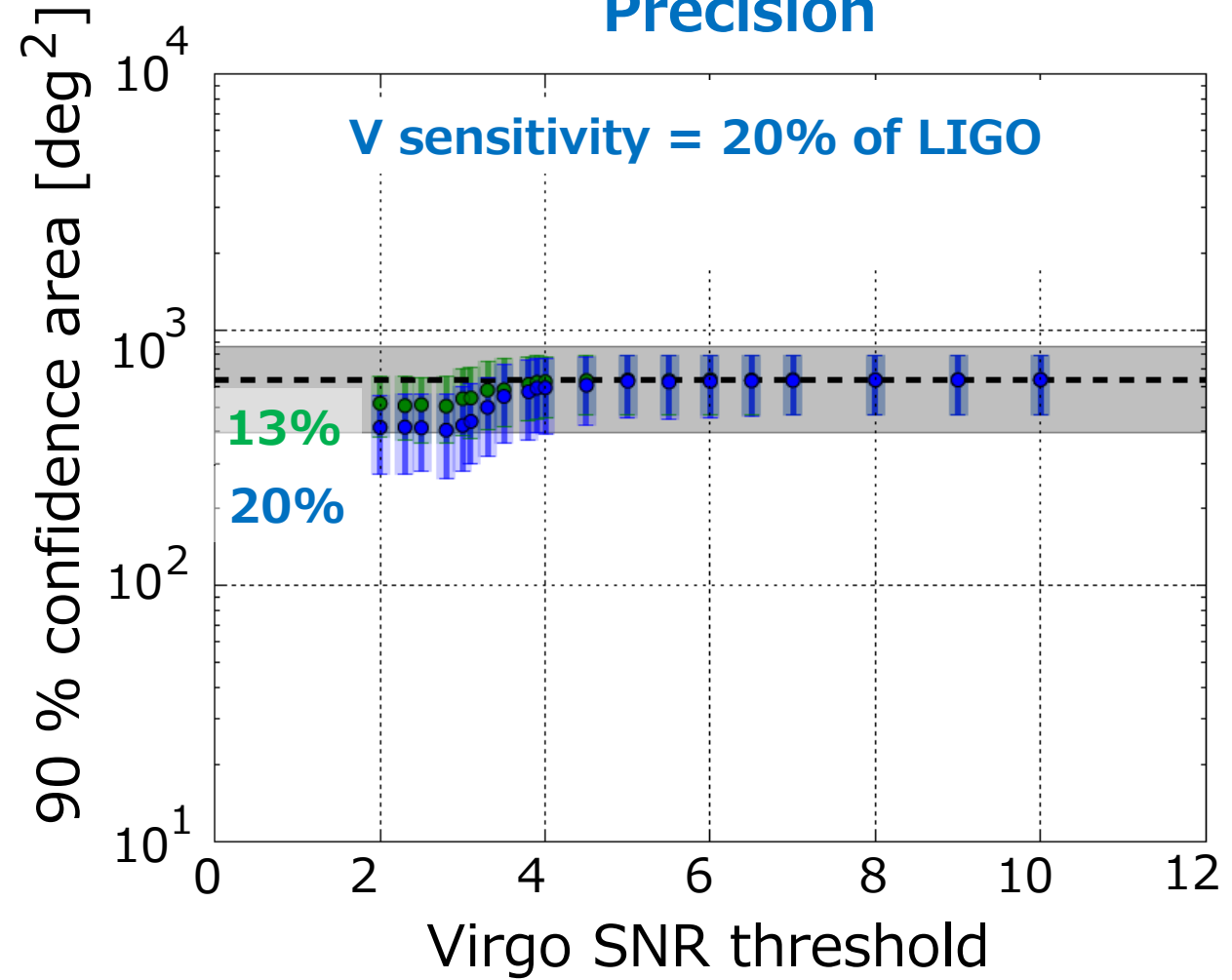
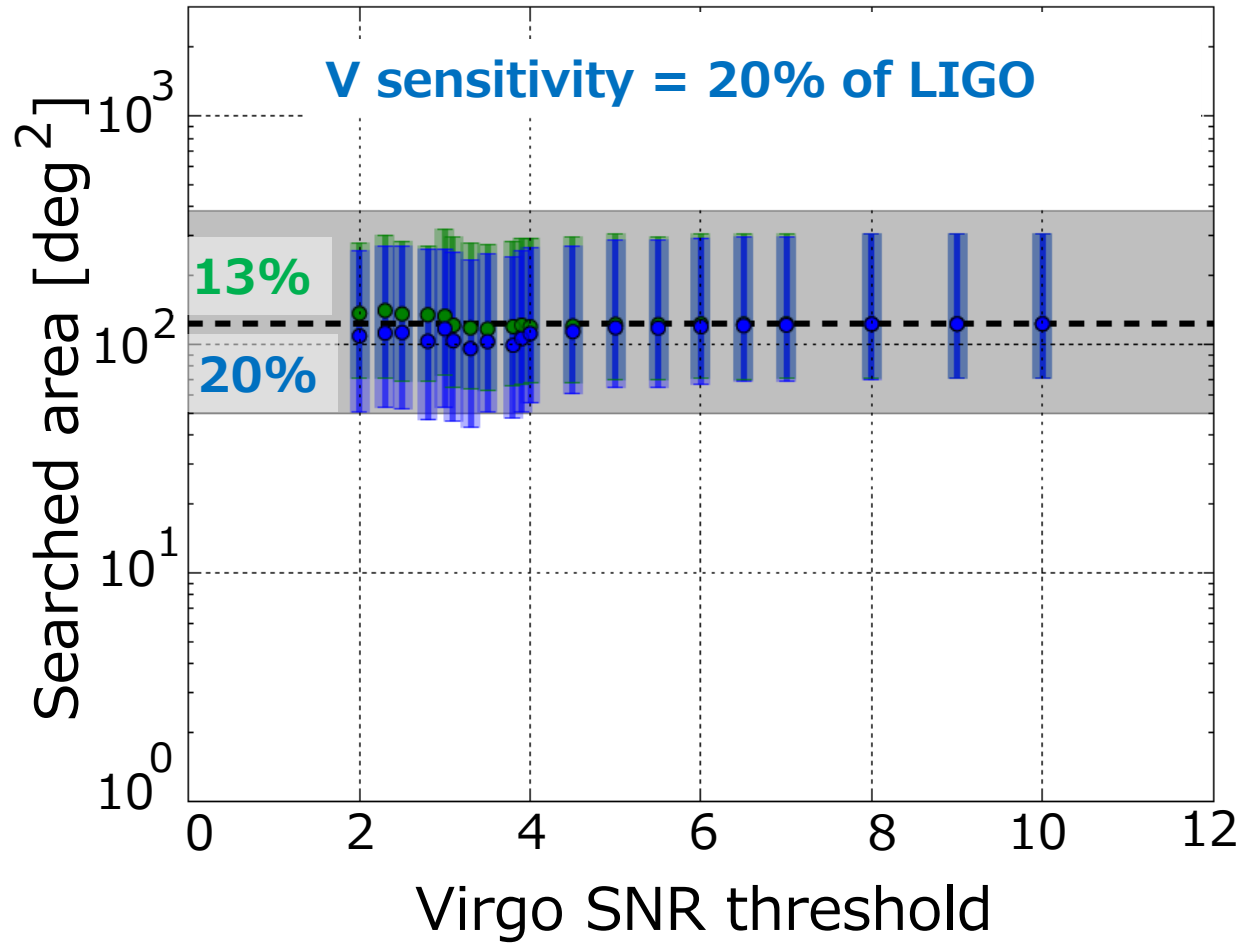


# Performance (HLV):

(SNR threshold for H, L = 5., 5.)

## Accuracy

## Precision

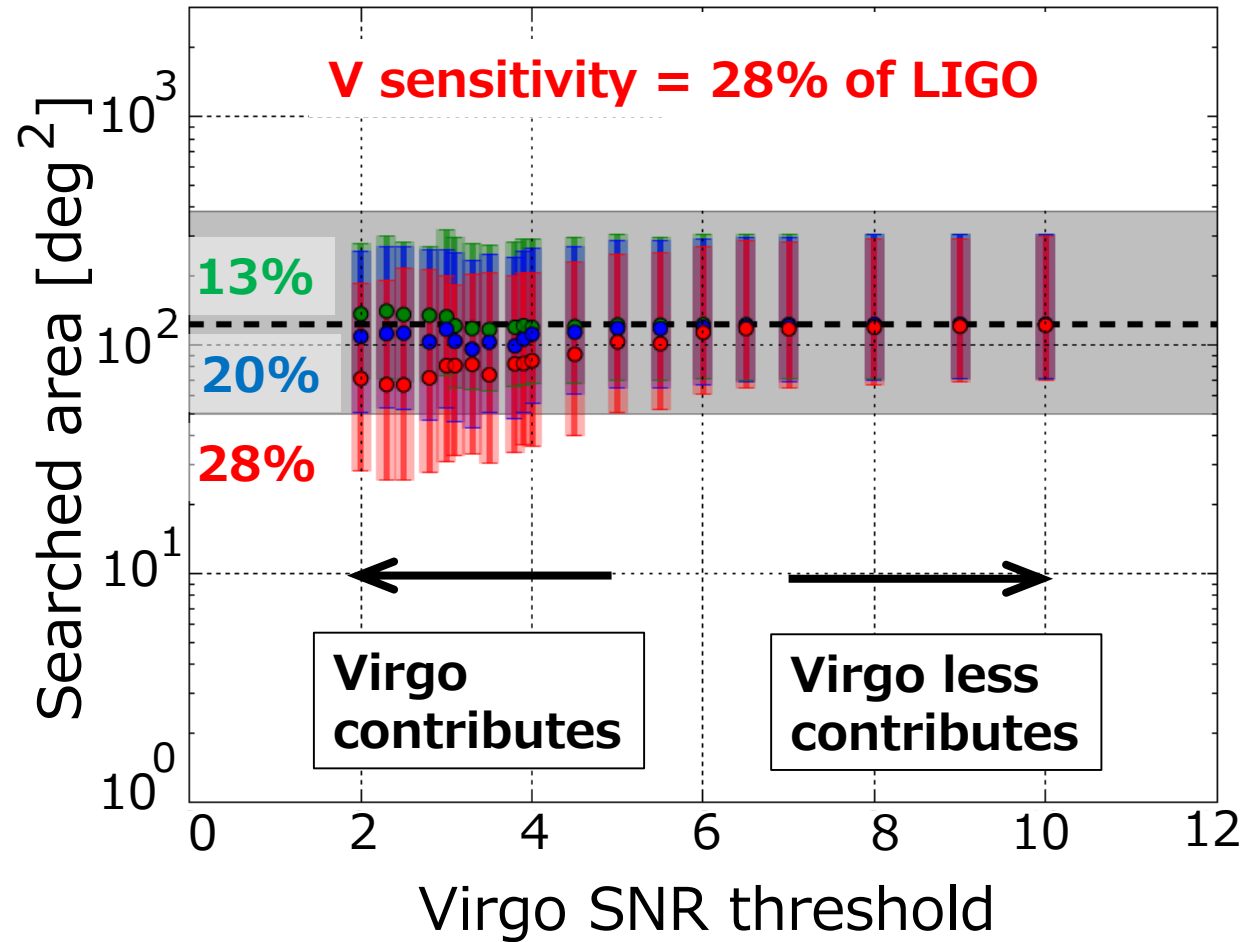




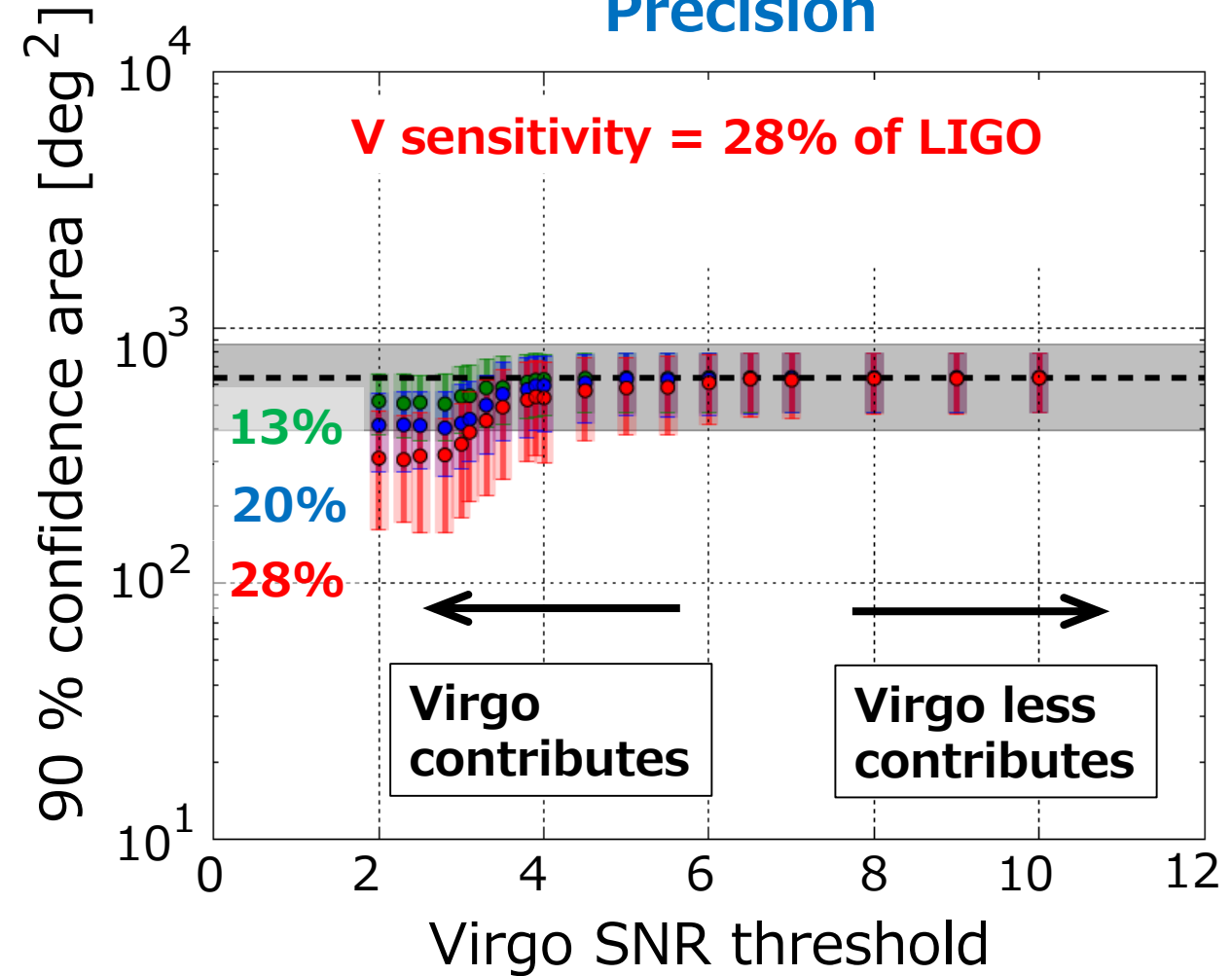
# Performance (HLV):

(SNR threshold for H, L = 5., 5.)

## Accuracy



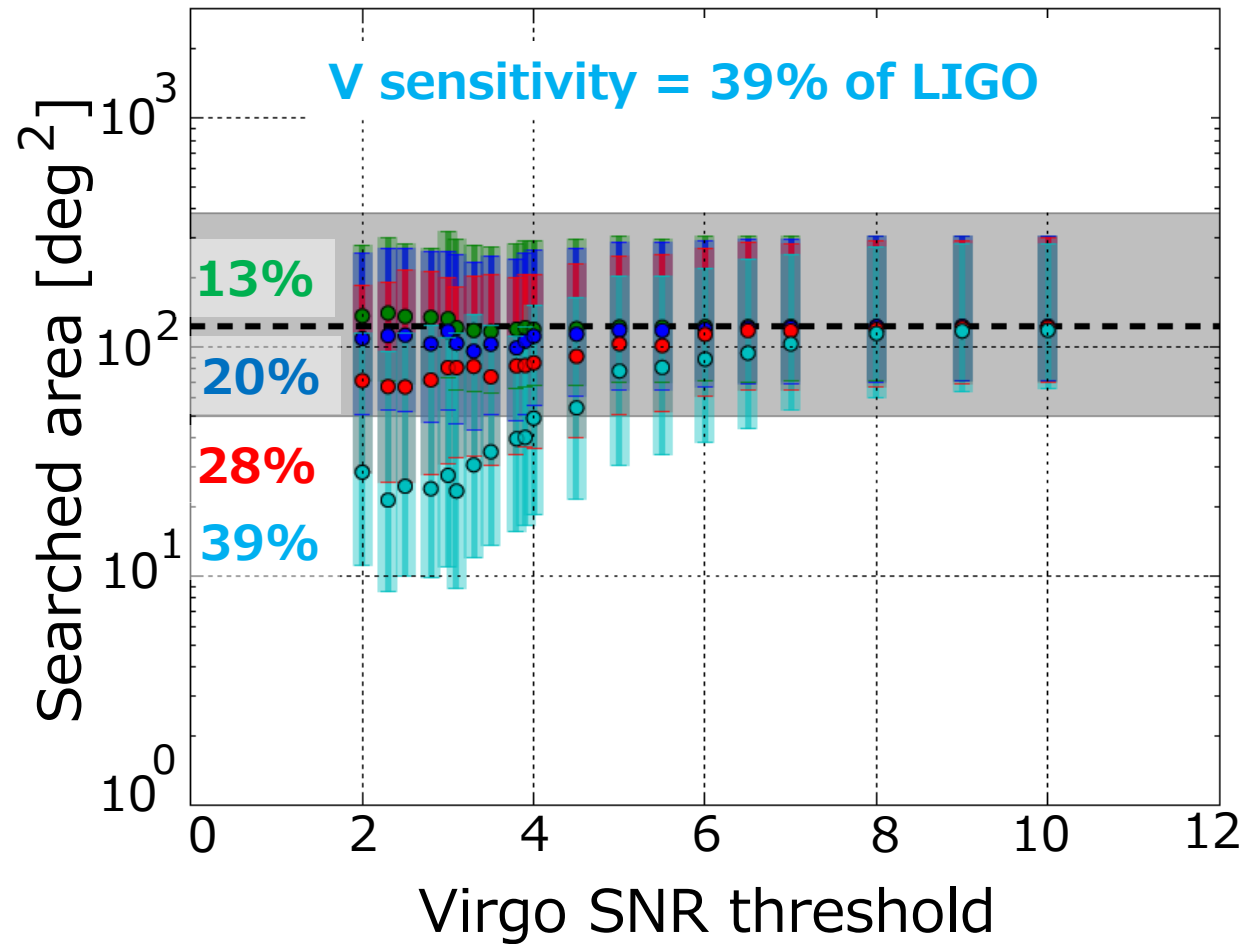
## Precision



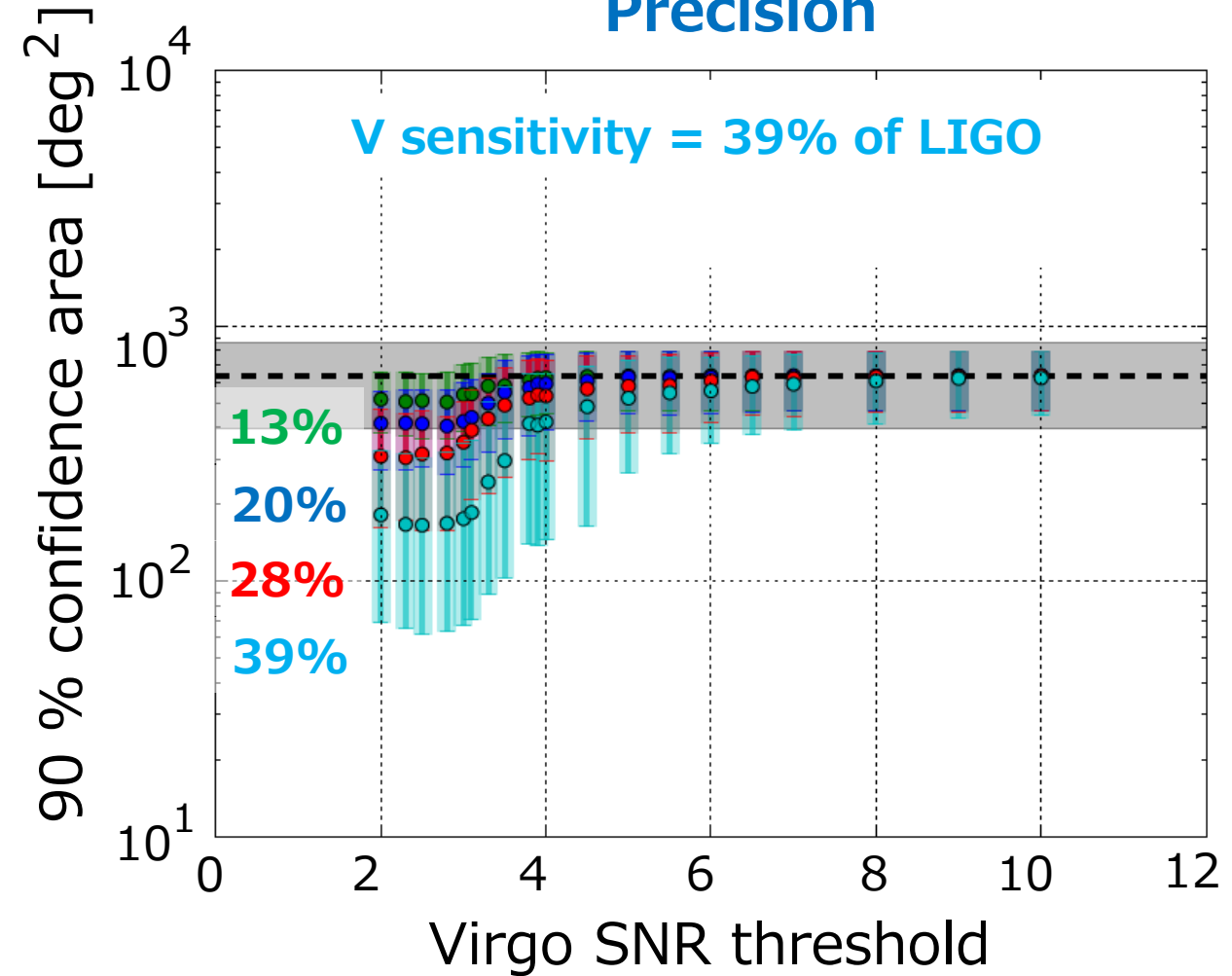
# Performance (HLV):

(SNR threshold for H, L = 5., 5.)

## Accuracy



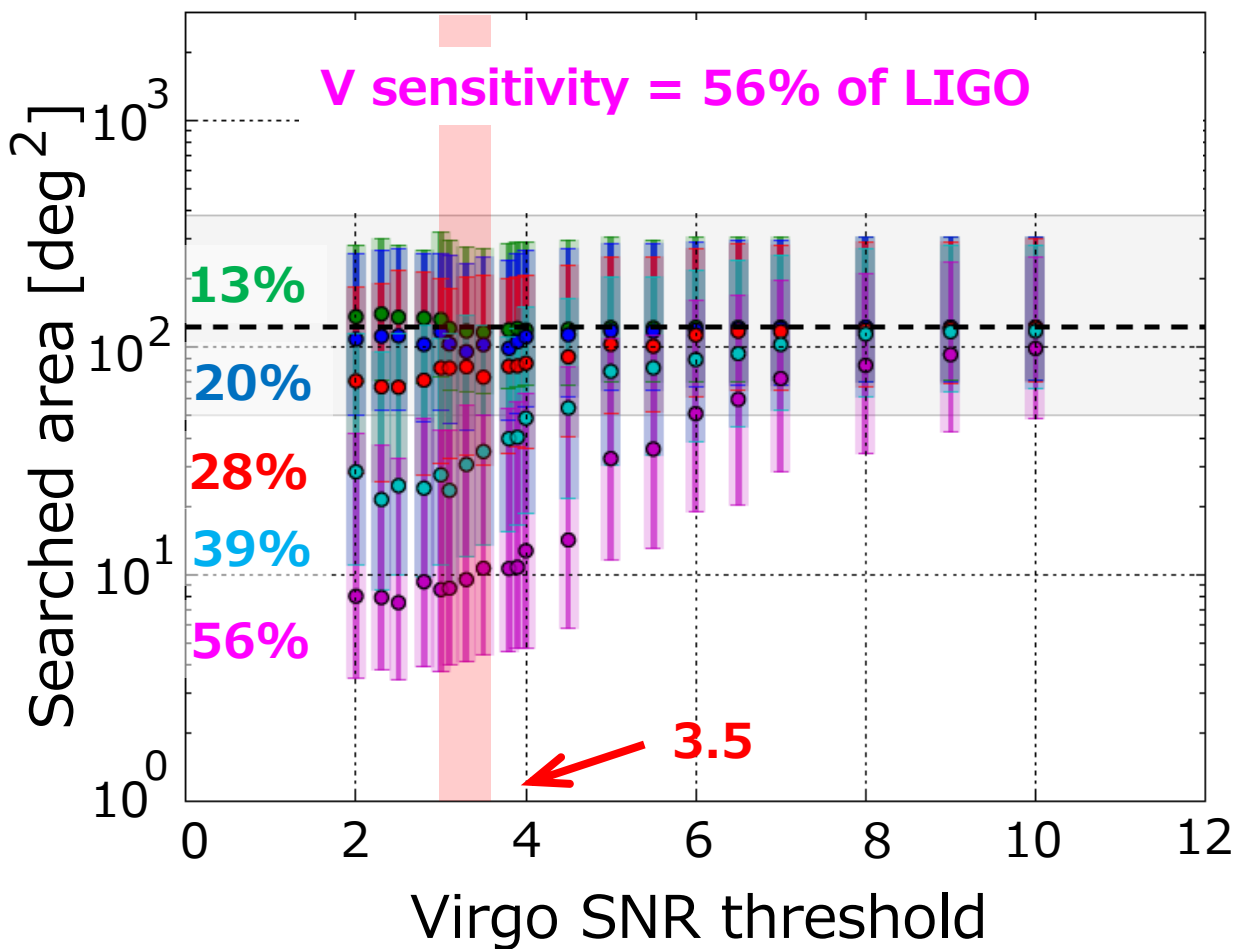
## Precision



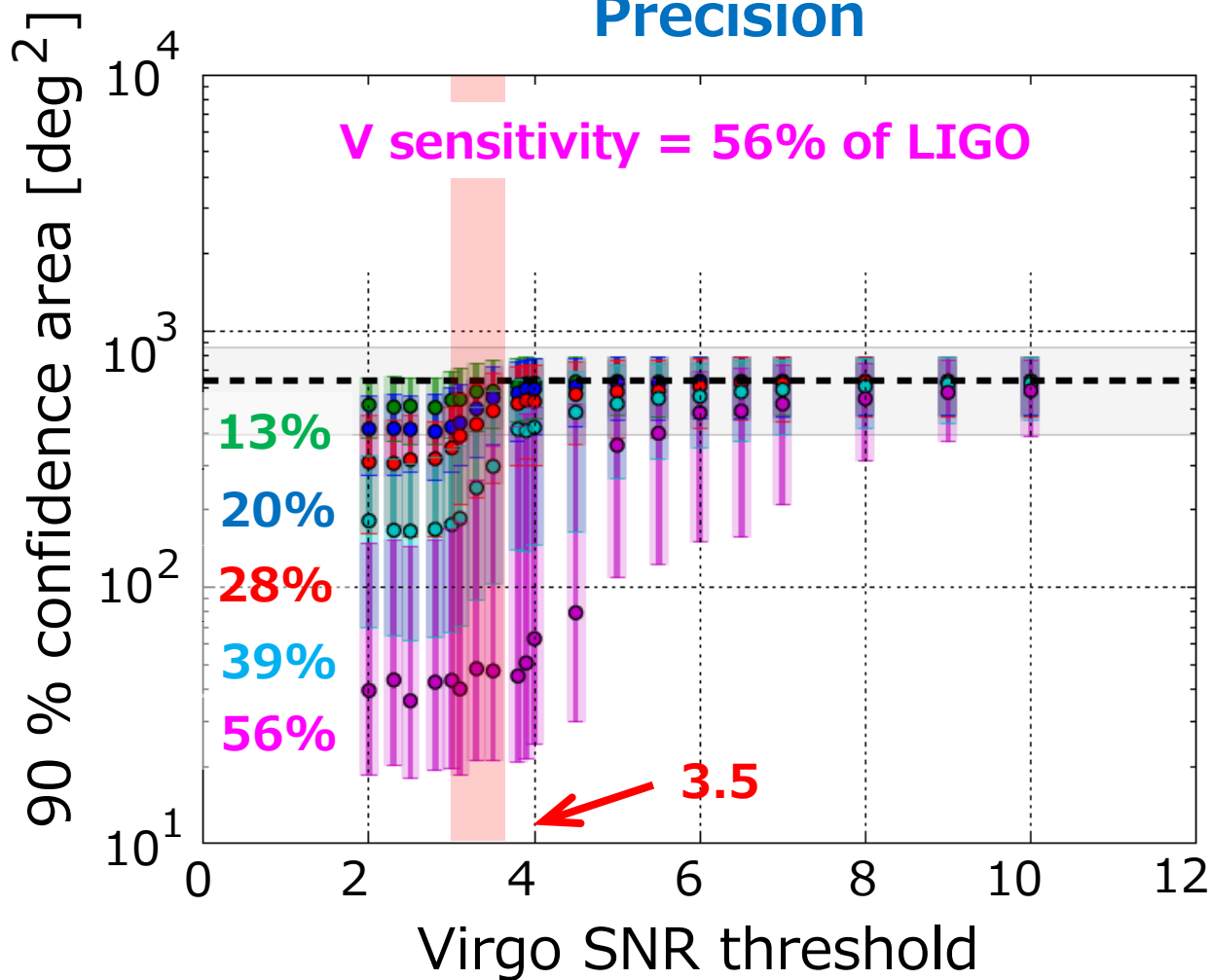
# Performance (HLV):

(SNR threshold for H, L = 5., 5.)

## Accuracy



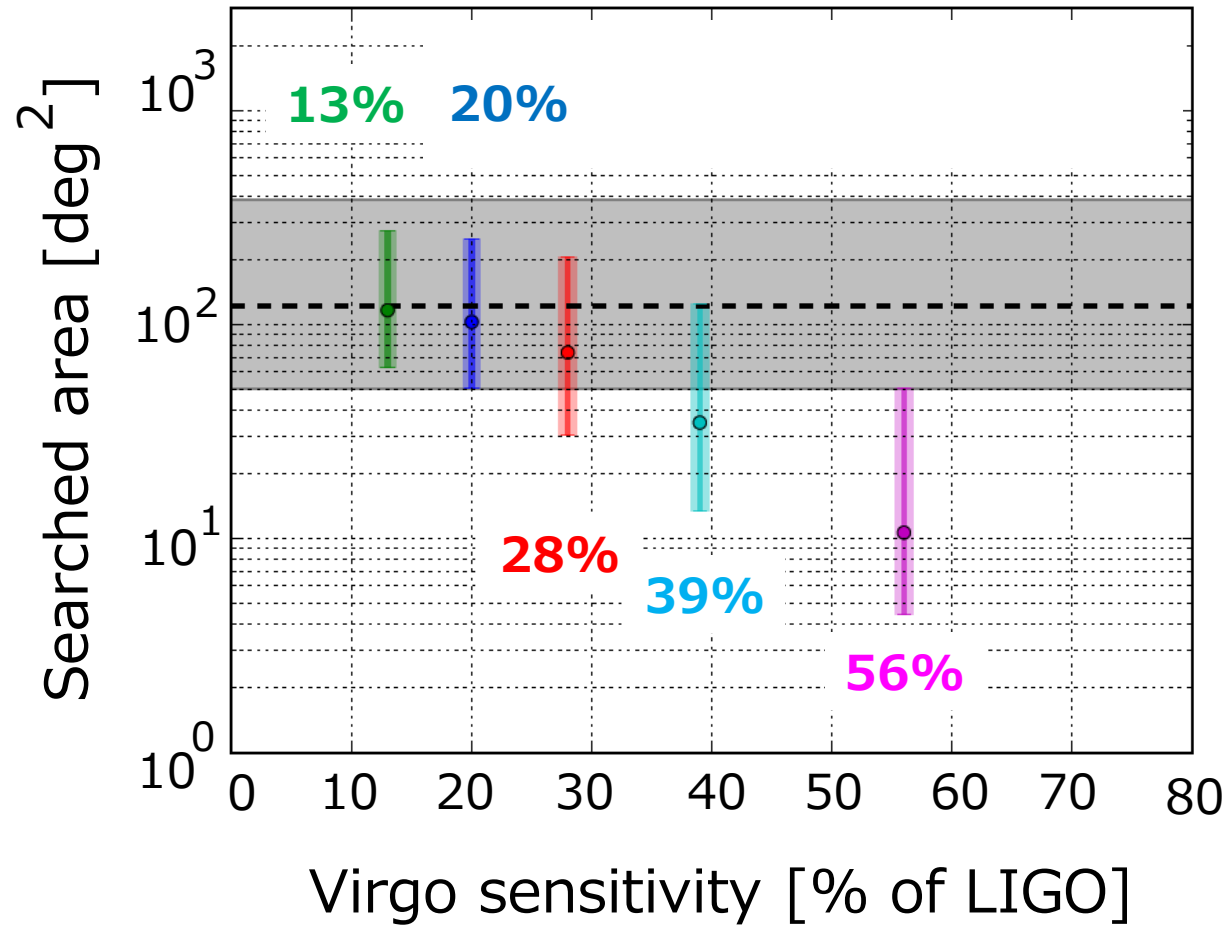
## Precision



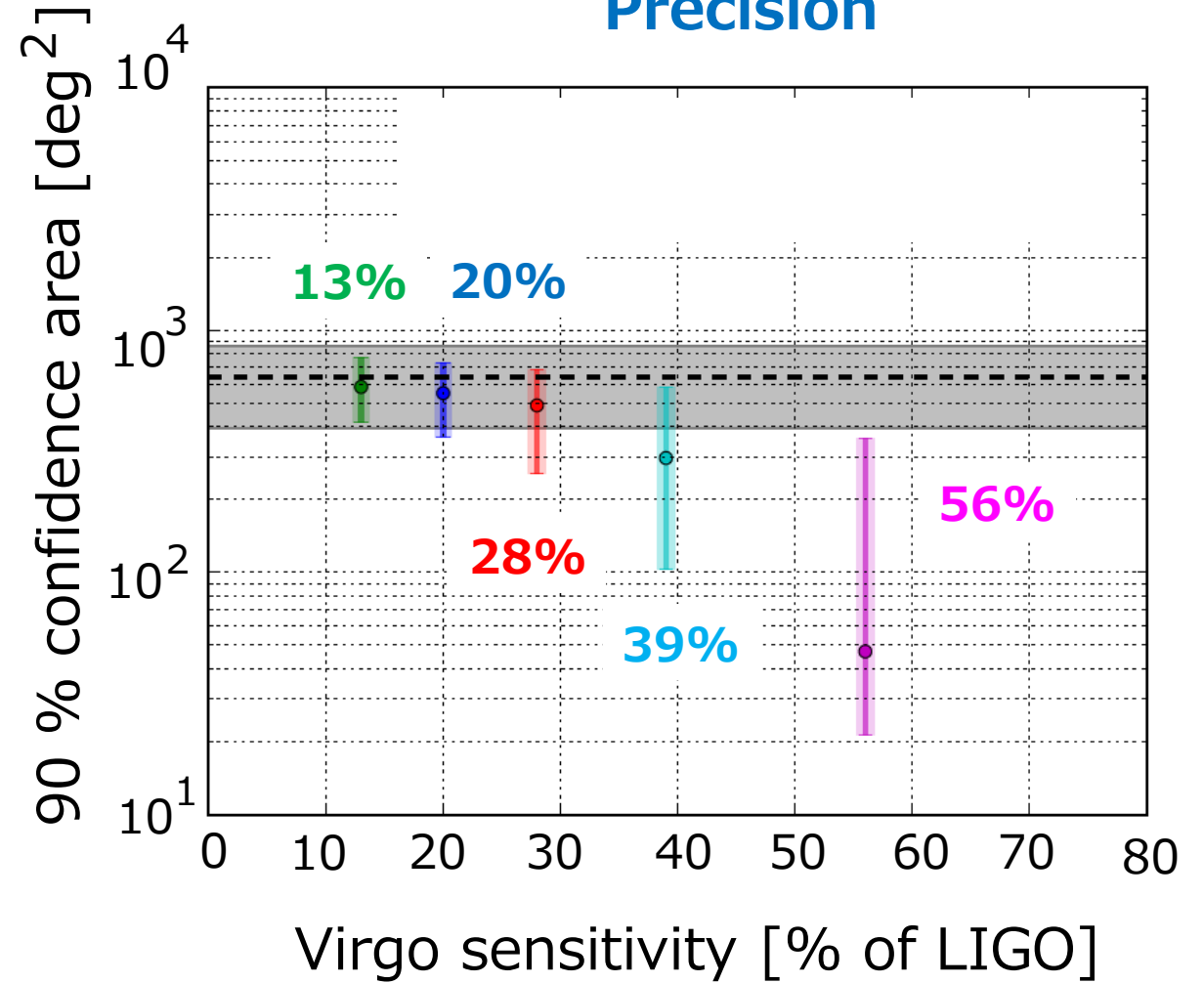
V SNR threshold = 3 ~ 3.5

# Performance (HLV): (SNR threshold for H, L, V = 5, 5, 3.5)

## Accuracy



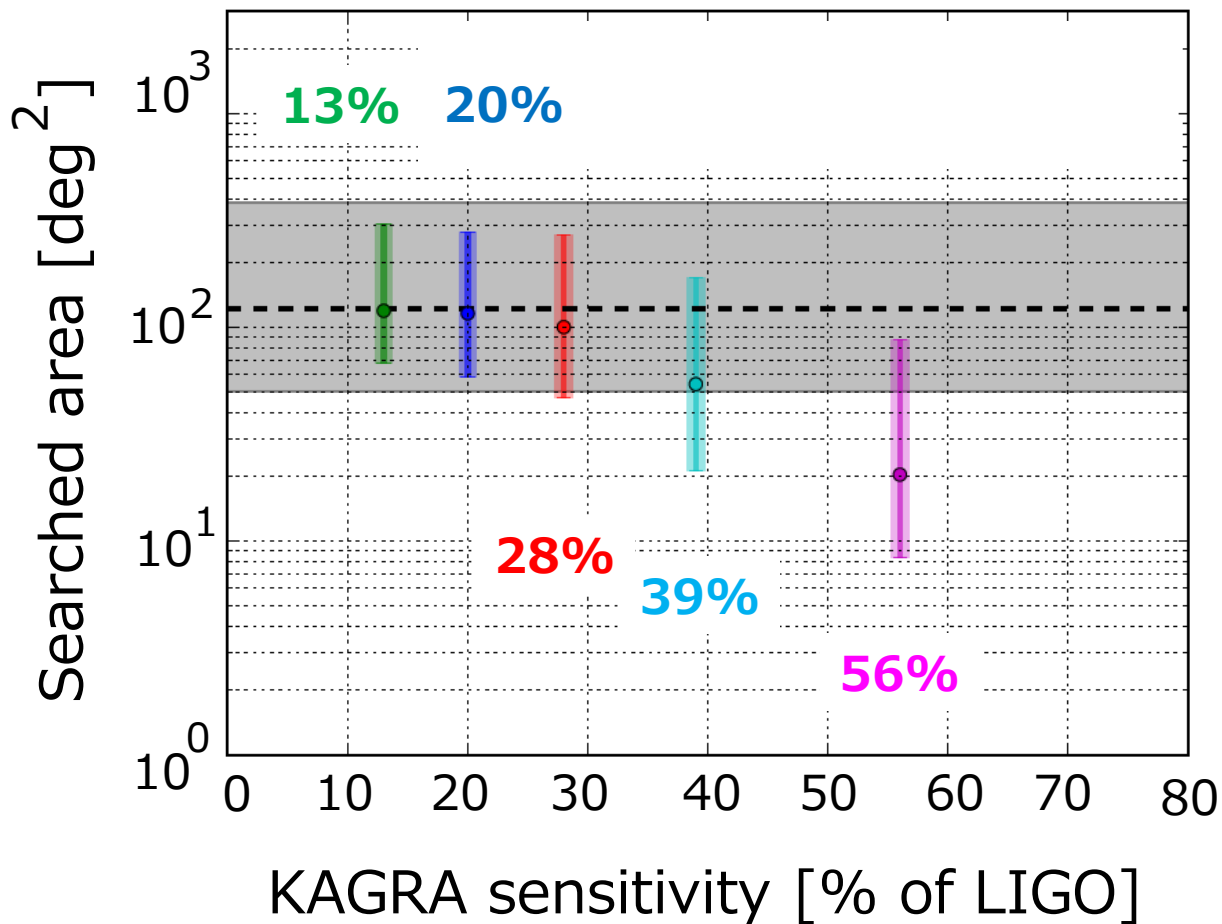
## Precision



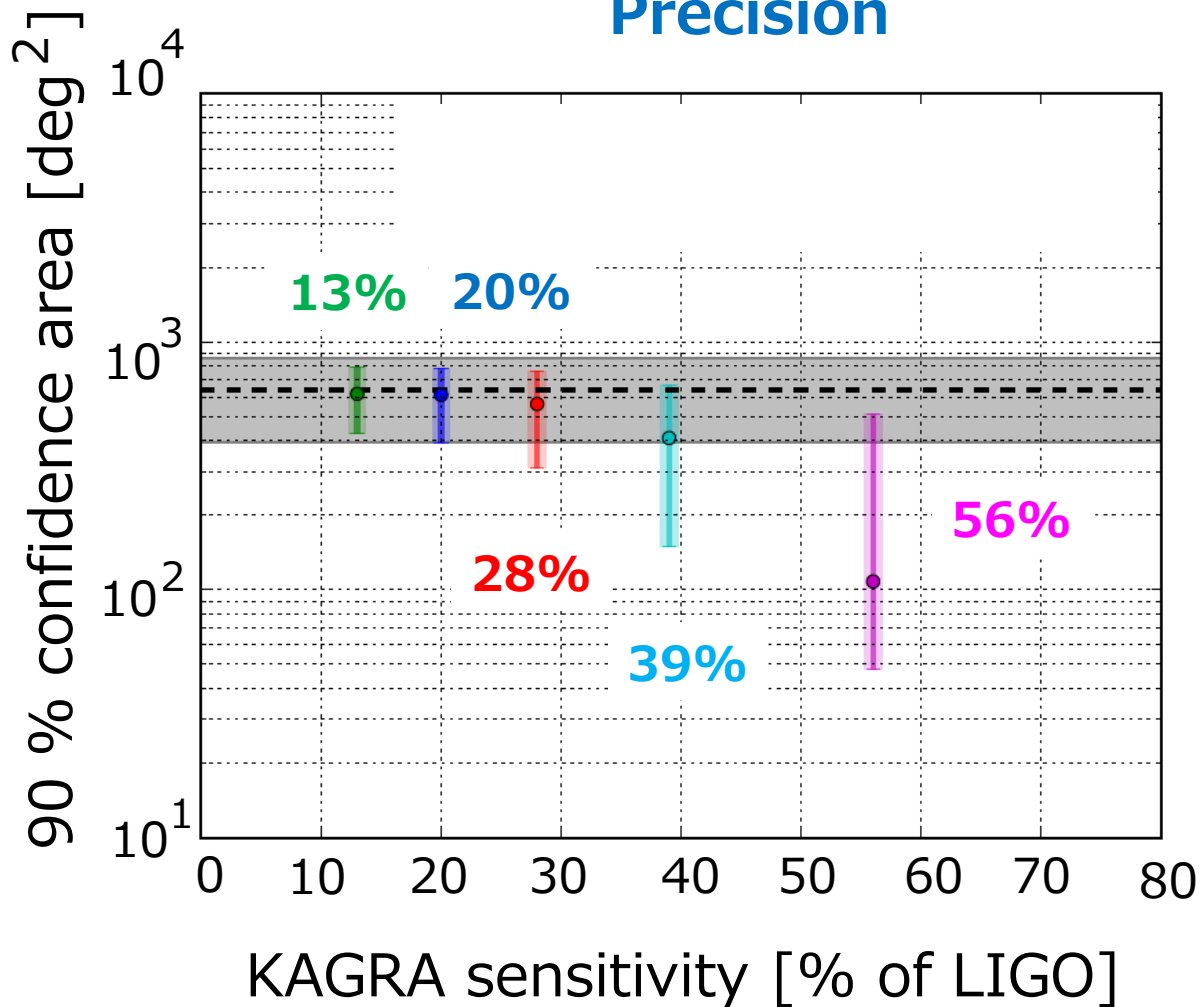
Required: Virgo sensitivity > 20% of LIGO

# Performance (HLK): (SNR threshold for H, L, K = 5, 5, 3.5)

## Accuracy



## Precision



Required: KAGRA sensitivity > 28% of LIGO



# Hierarchical approach by 4-detector network

**Assuming that:**

**1. Relative sensitivity**

$$\text{Virgo} = 0.5 * \text{LIGO}$$

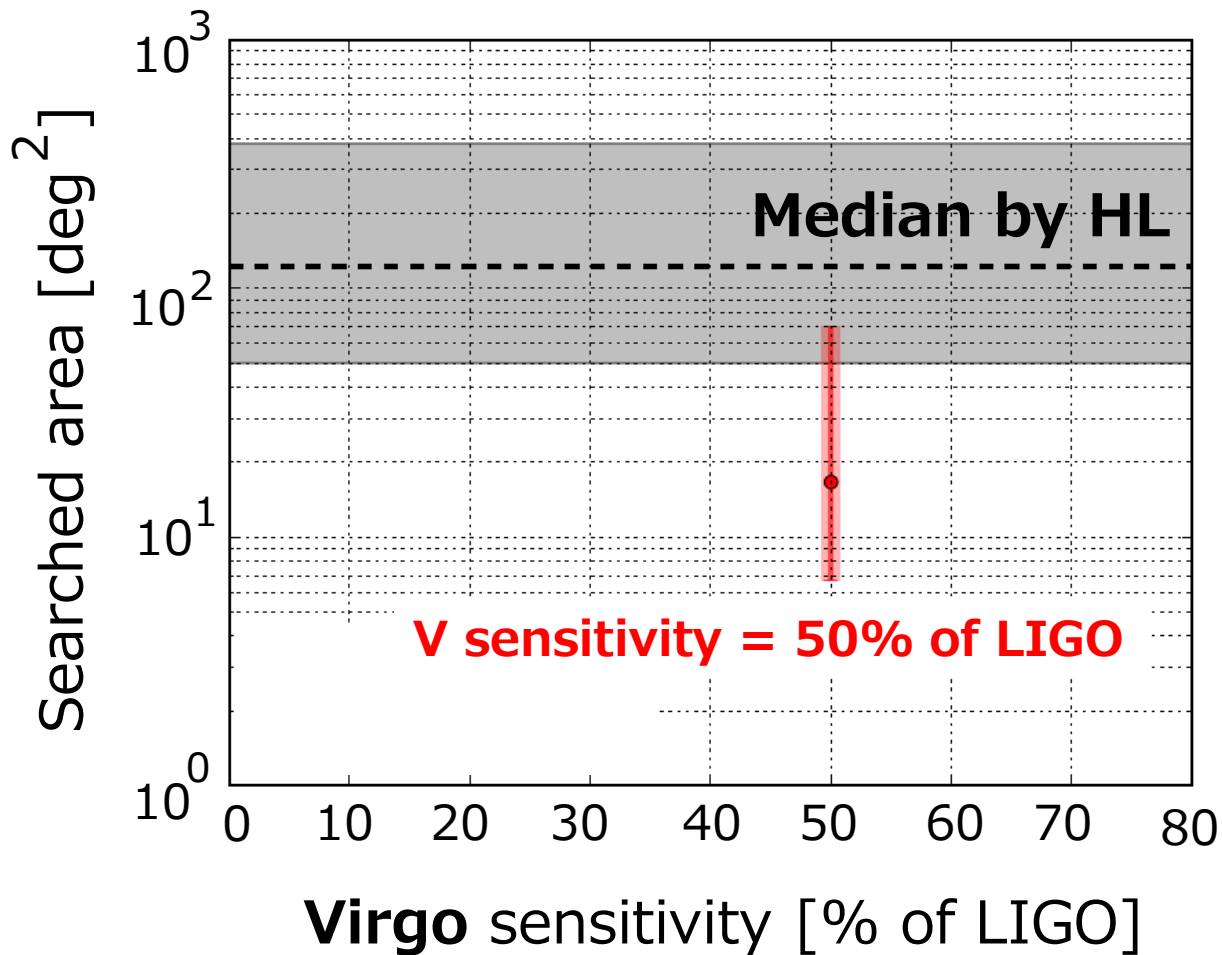
**2. SNR threshold**

$$\text{LIGO} = 5$$

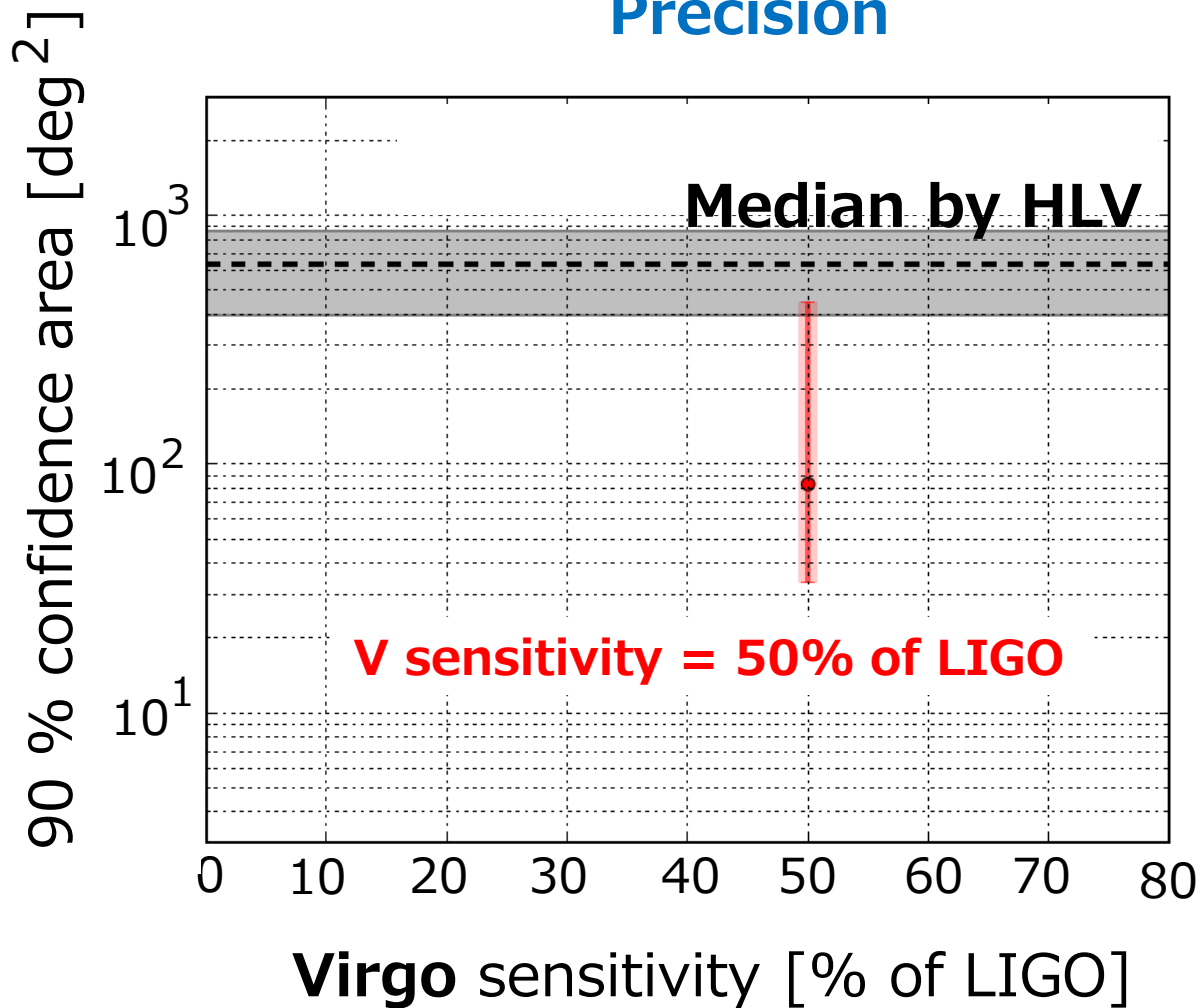
$$\text{Virgo} = 3.5$$

# Performance (HLV): (SNR threshold for H, L, V = 5, 5, **3.5**)

Accuracy

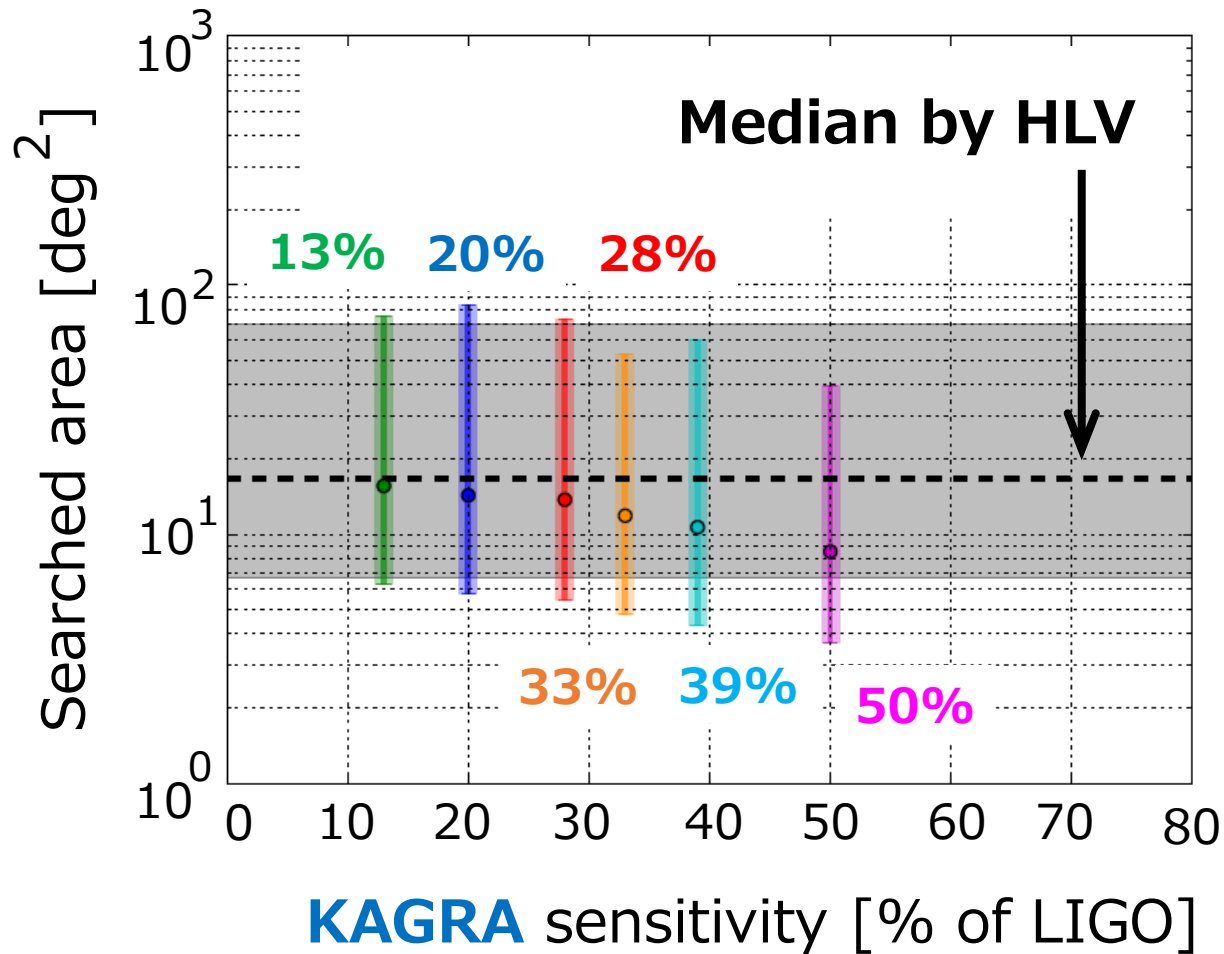


Precision

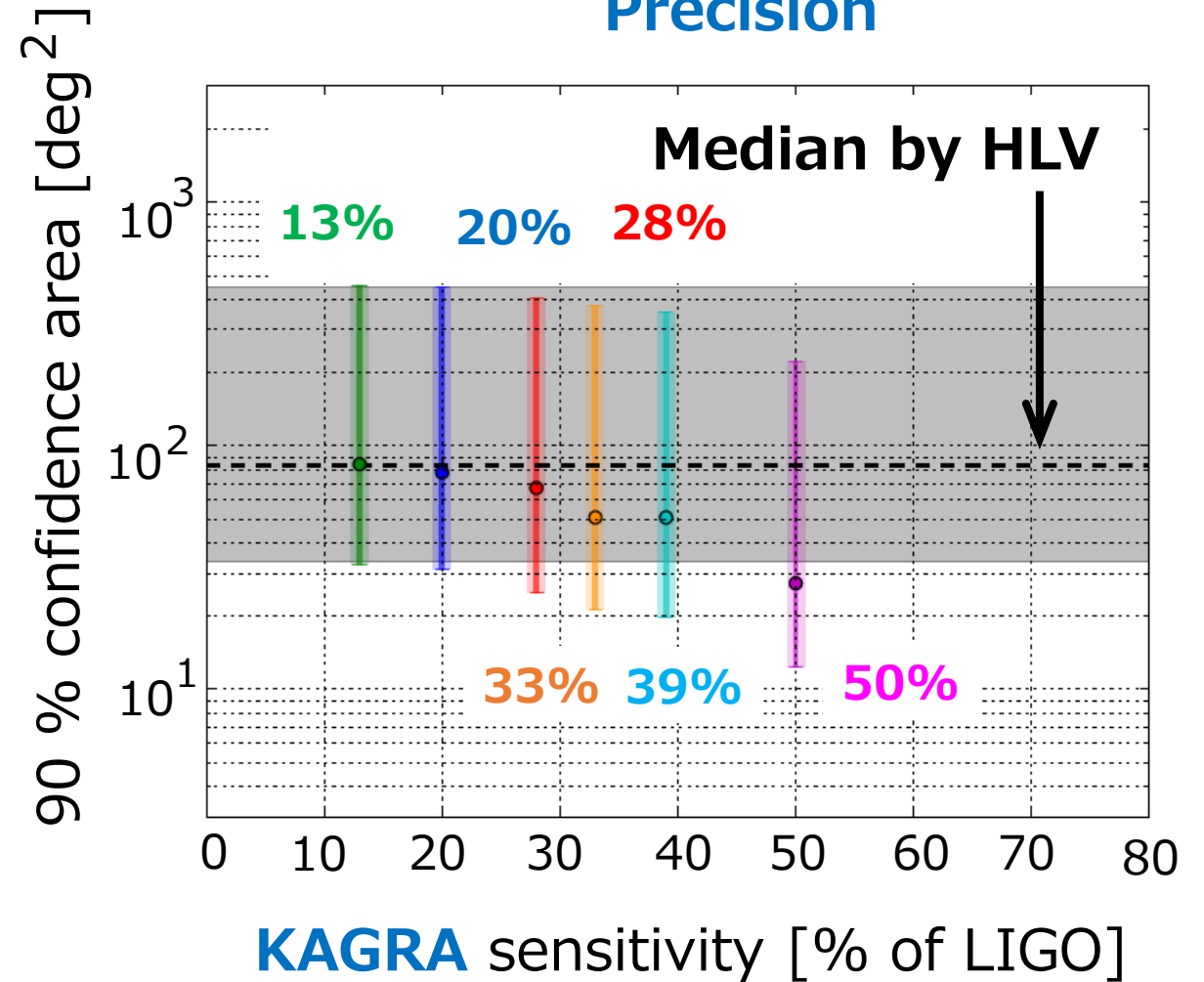


# Performance (HLV $K$ ): (SNR threshold for H, L, V, K = 5, 5, 3.5, 3.5)

## Accuracy



## Precision



Required: KAGRA sensitivity > 28% of LIGO

# Summary of hierarchical approach

\* Required detector sensitivity (at SNR threshold 3.5):

## Relative sensitivity

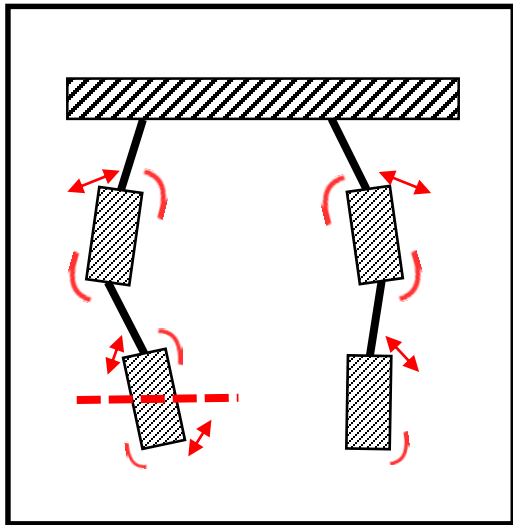
- **HLV-network:** Virgo sensitivity  $> 0.2 * \text{LIGO}$
- **HLK-network:** KAGRA sensitivity  $> 0.28 * \text{LIGO}$
- **HLVK-network:** KAGRA sensitivity  $> 0.28 * \text{LIGO}$

→ **The hierarchical approach improves the fast localization in the heterogeneous network, using existing low-latency infrastructure.**

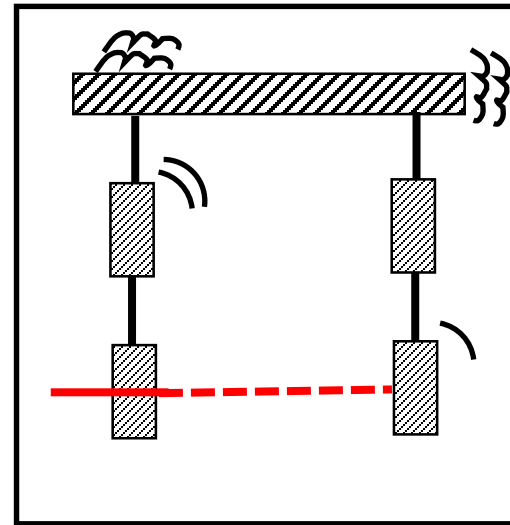
**Not only** fast localization,  
**but also** higher network duty cycle → **key for EM follow up**

**As more practical aspect,**  
**Robust operation of fourth detector**

**Cannot operate  
interferometer**



**Demanded for  
stable operation**



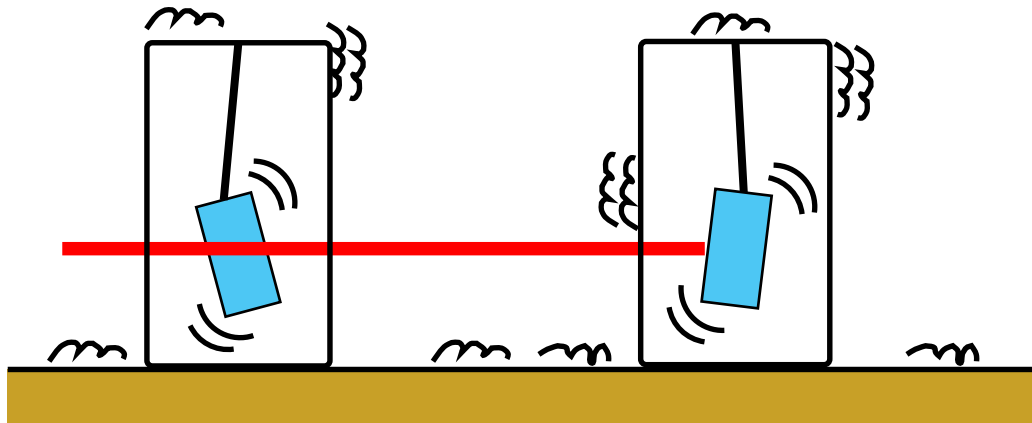


# Thesis contents

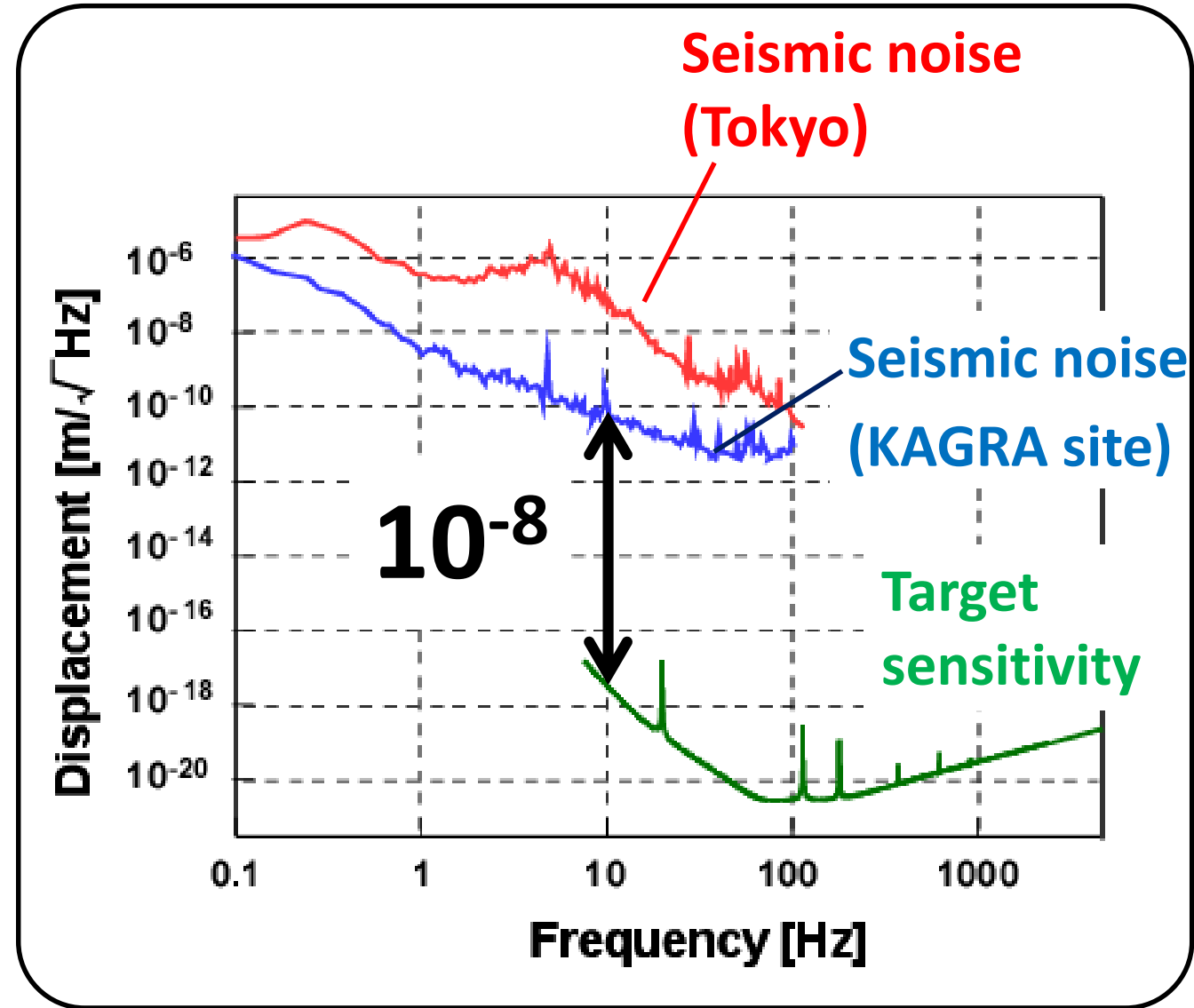
My main research

1. Introduction
  2. Benefit of adding detectors to the observation network
  - 3. Low frequency vibration isolation
  4. KAGRA seismic attenuation system
  5. Suspension control design
  6. Performance test of local control for KAGRA Type-A suspension
  7. Summary
- **Type-A suspension controls toward lock acquisition**

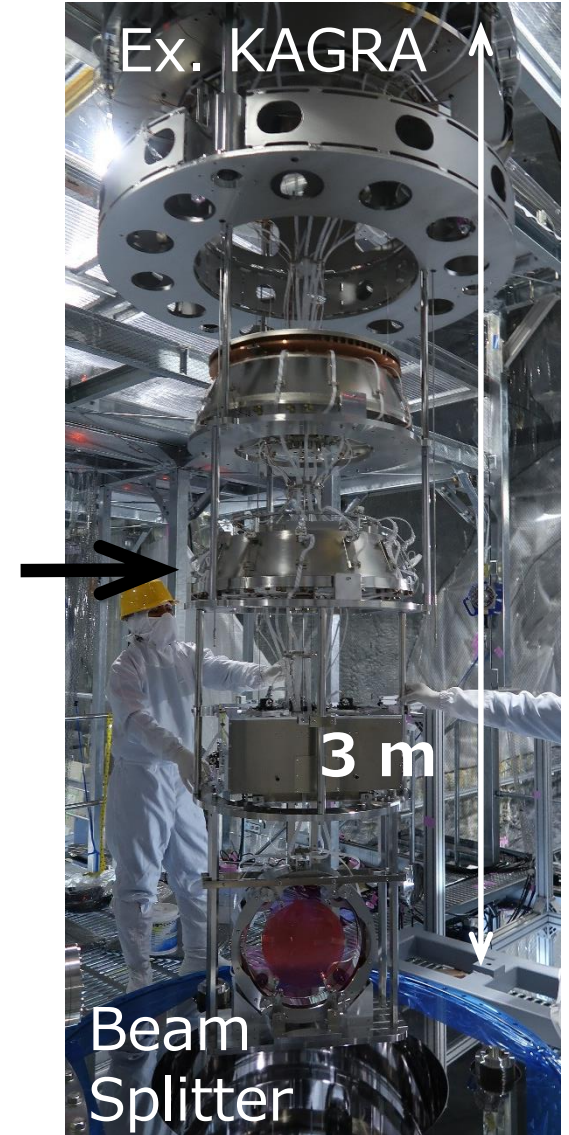
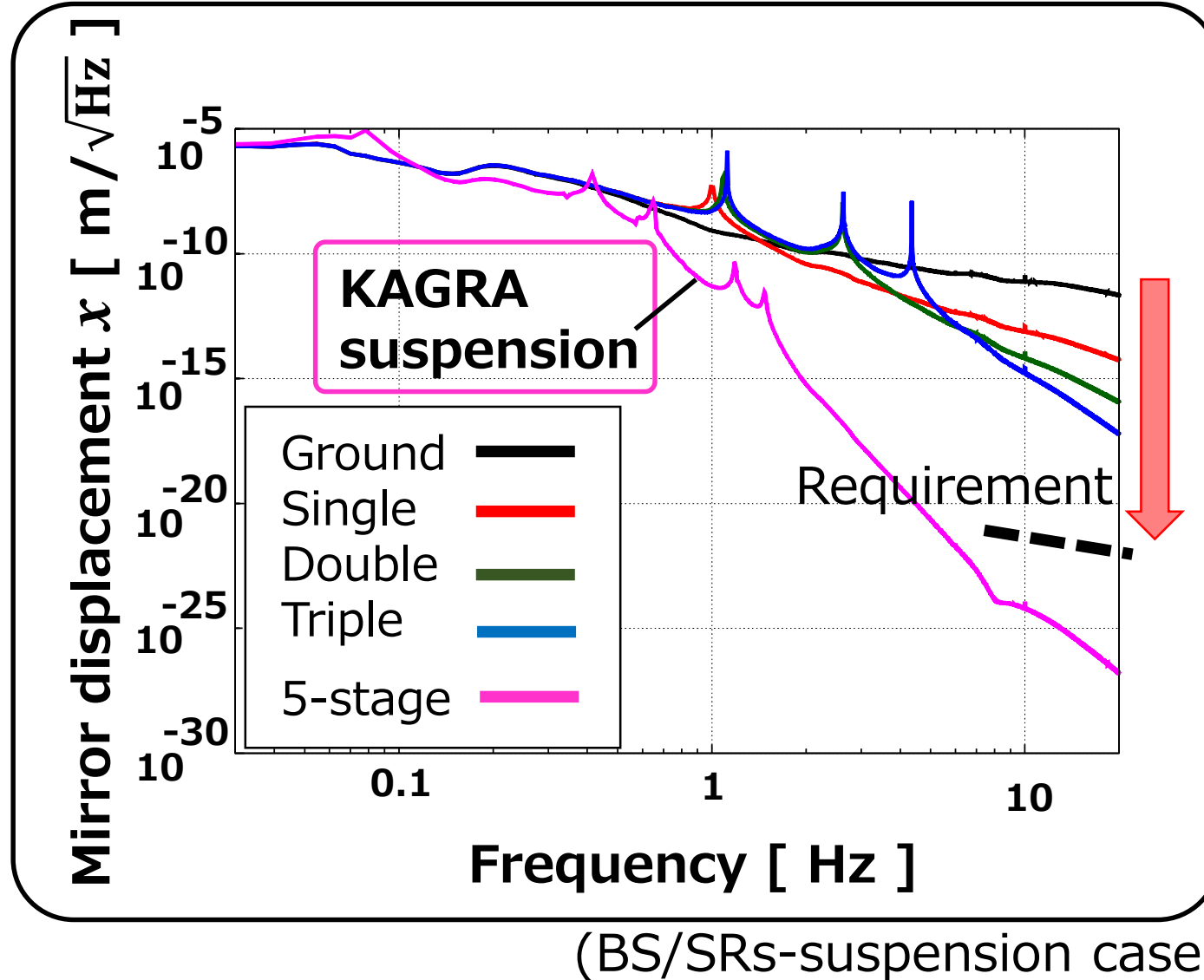
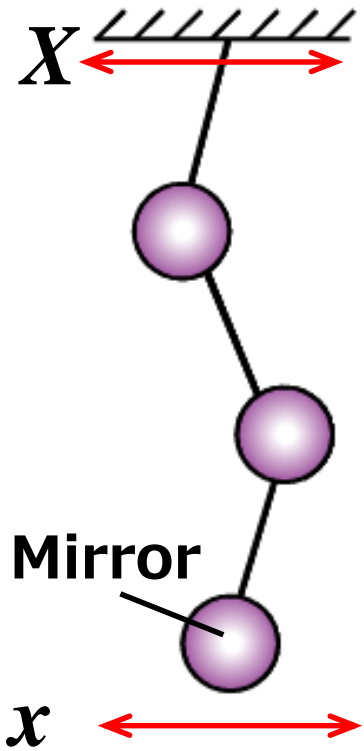
# Why pendulum?



→ To treat seismic noise



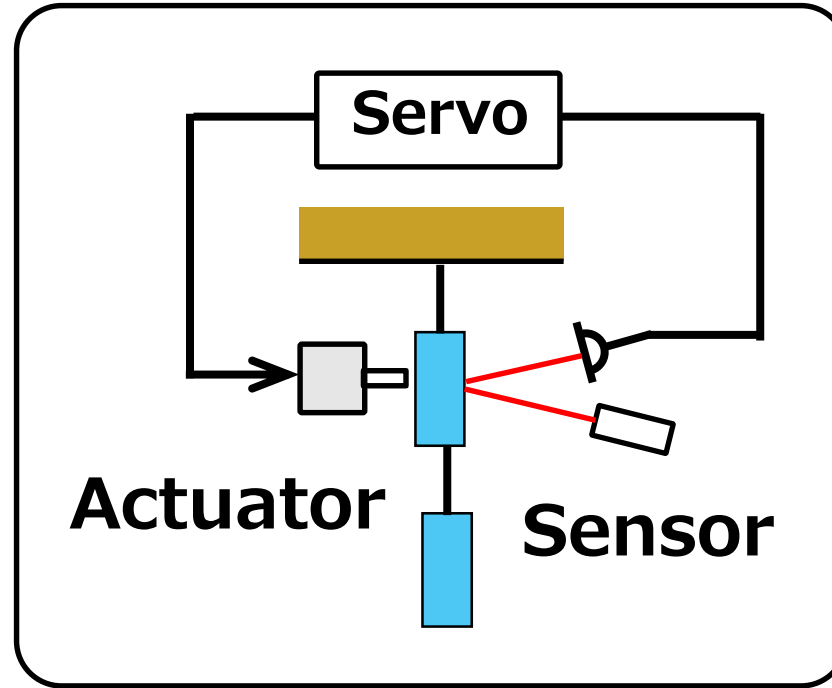
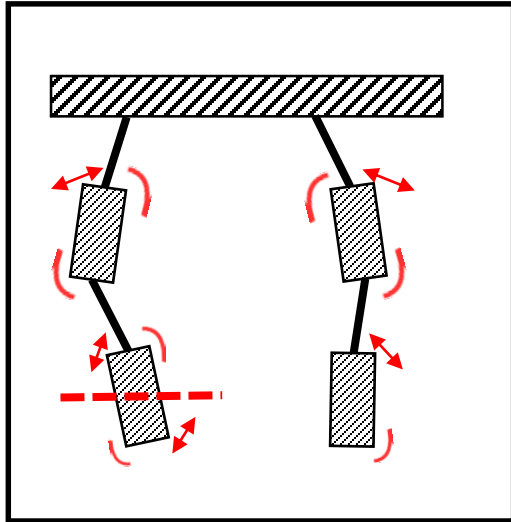
# Seismic noise attenuation → pendulum



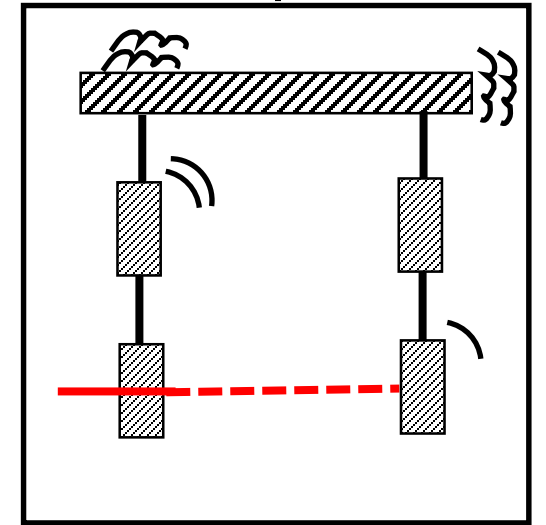
# Resonance damping / Mirror Alignment → necessary

→ Control system

Cannot operate  
interferometer



Demanded for  
stable operation



\* Damp resonances.

\* Freeze the mirrors

# Thesis contents

My main research

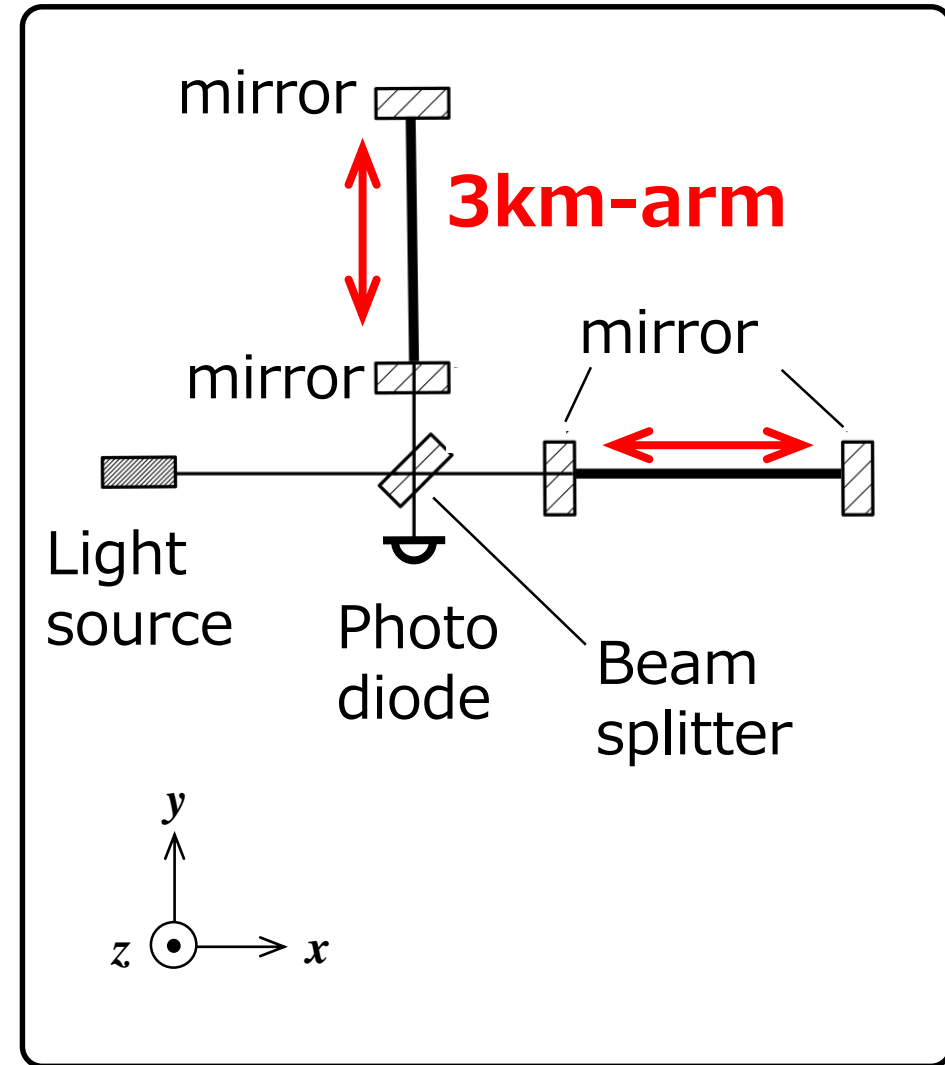
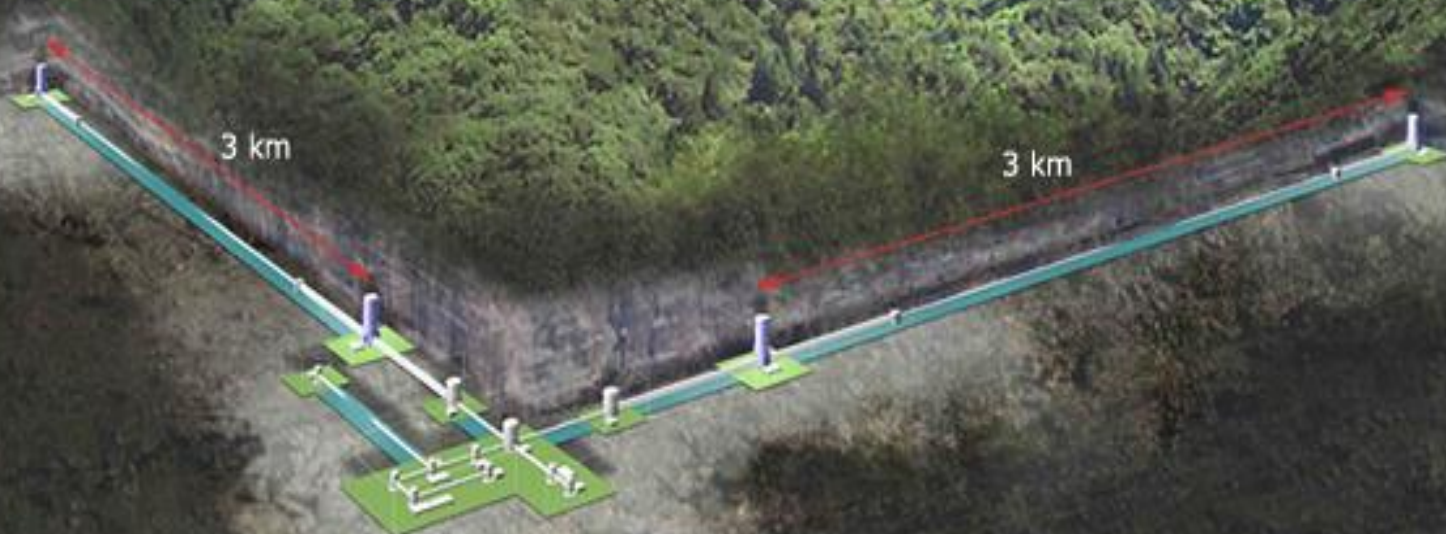
1. Introduction
2. Benefit of adding detectors to the observation network
3. Low frequency vibration isolation
- 4. KAGRA seismic attenuation system
5. Suspension control design
6. Performance test of local control for KAGRA Type-A suspension
7. Summary

→ **TypeA suspension controls toward lock acquisition**

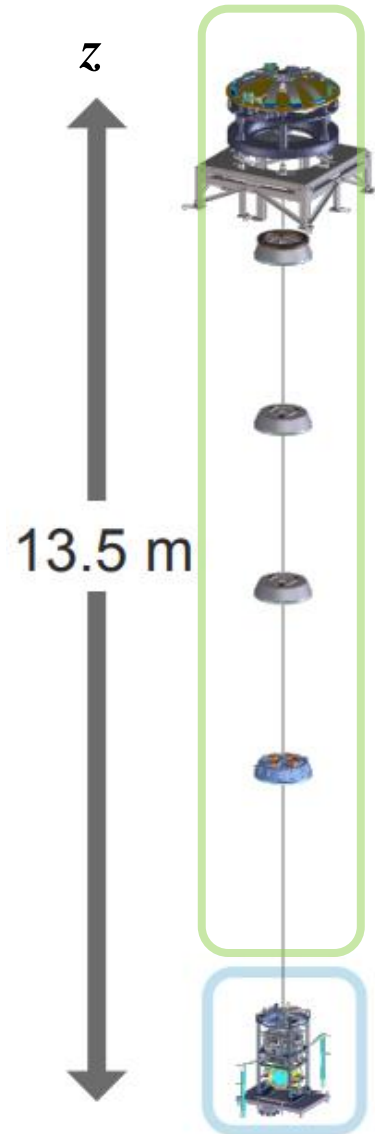
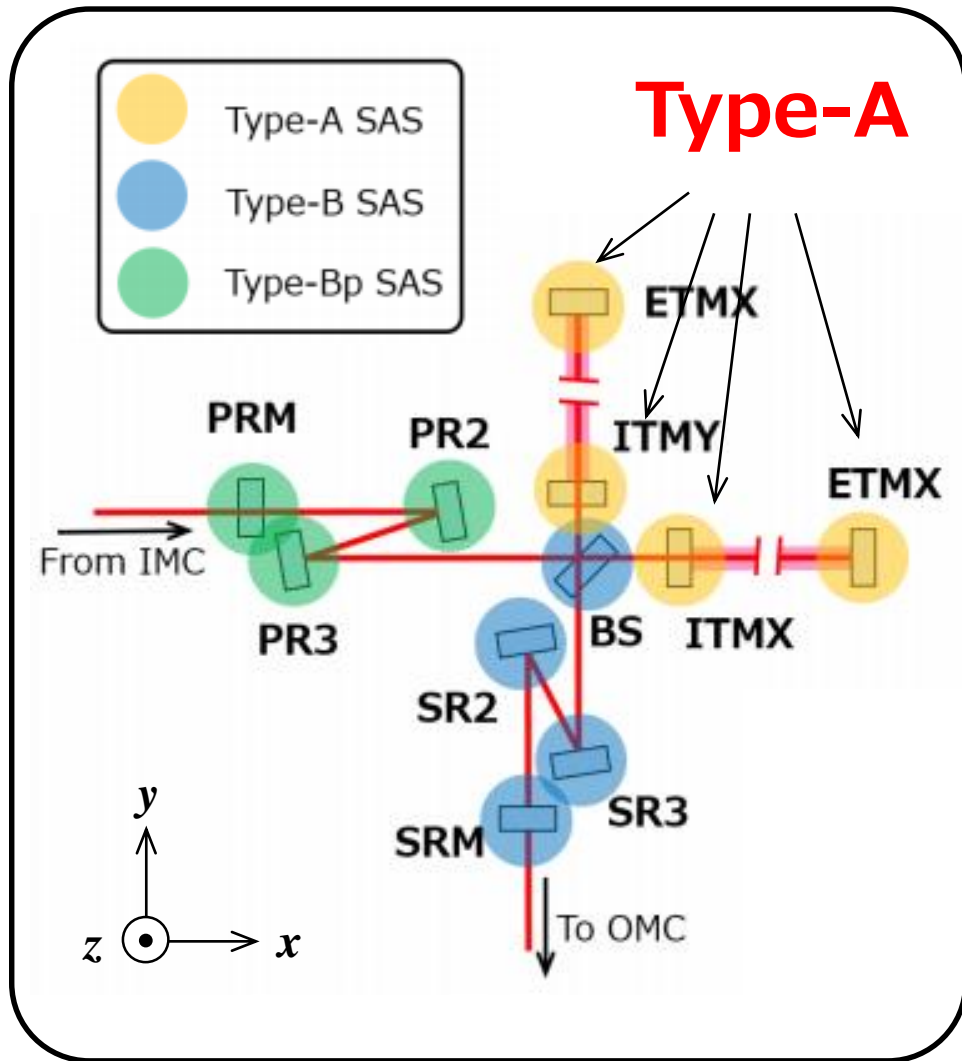


# KAGRA detector

1. Underground
2. Cryogenic operation



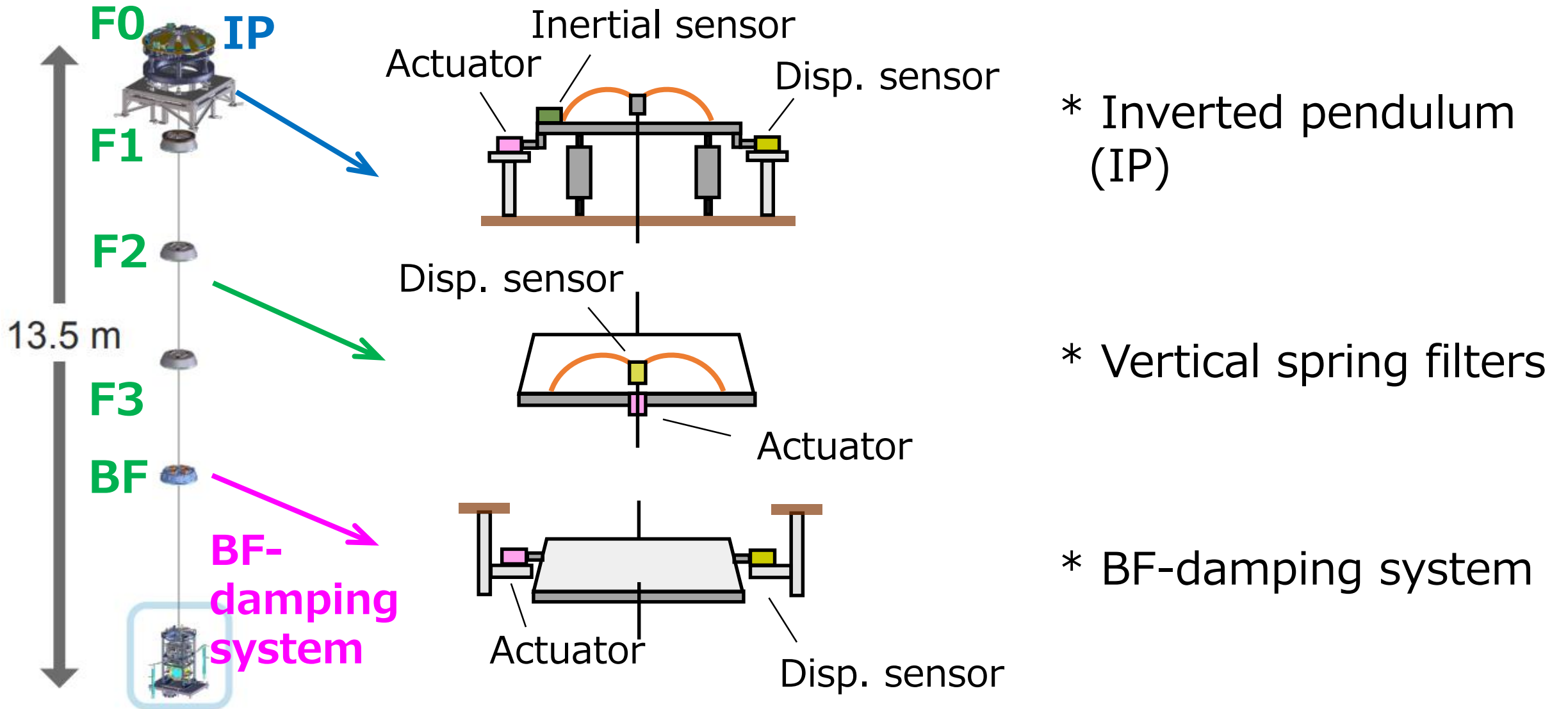
# Type-A suspension:



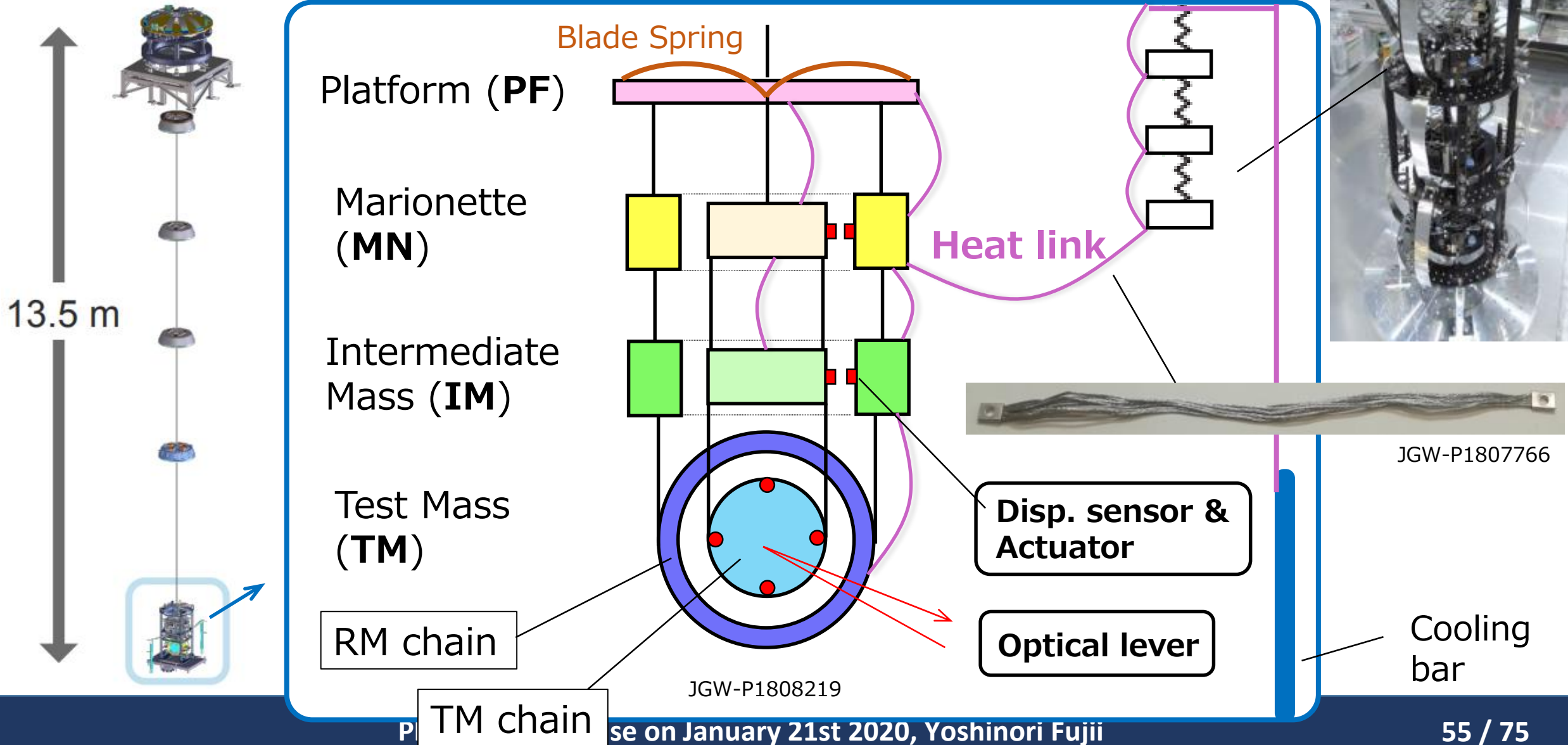
→ The longest suspension in KAGRA

- Upper 5 stages: room-temperature
- Lower 4 stages: cryogenic-temperature

# Components of room-temperature part:



# Components of cryogenic part:





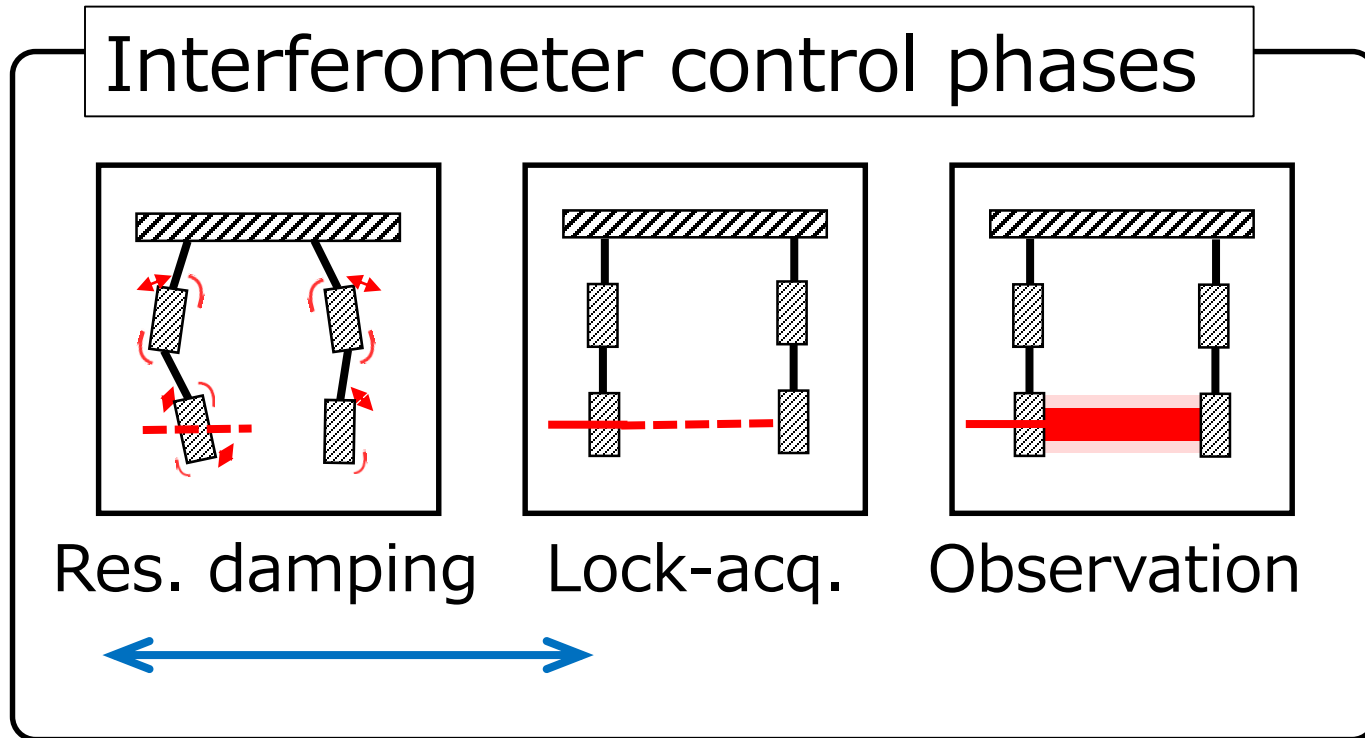
# Thesis contents

My main research

1. Introduction
2. Benefit of adding detectors to the observation network
3. Low frequency vibration isolation
4. KAGRA seismic attenuation system
- 5. Suspension control design
6. Performance test of local control for KAGRA Type-A suspension
7. Summary

→ **TypeA suspension controls toward lock acquisition**

# My work: Local control for full Type-A suspension



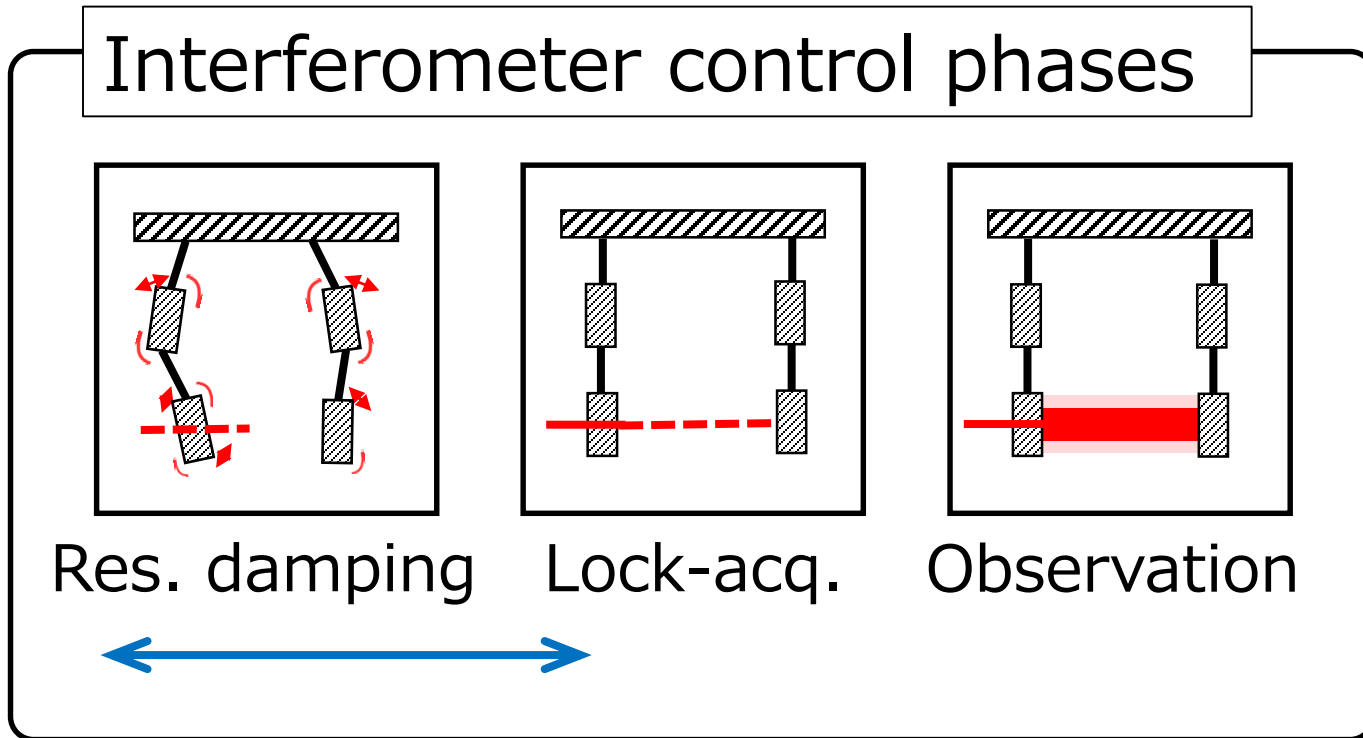
## Goal:

To construct suspension local control system of full Type-A to allow interferometer locking.

- \* Implementation
- \* Performance test



# My work: Local control for full Type-A suspension



## Goal:

To construct suspension local control system of full Type-A to allow interferometer locking.

Data acq. system & digital system

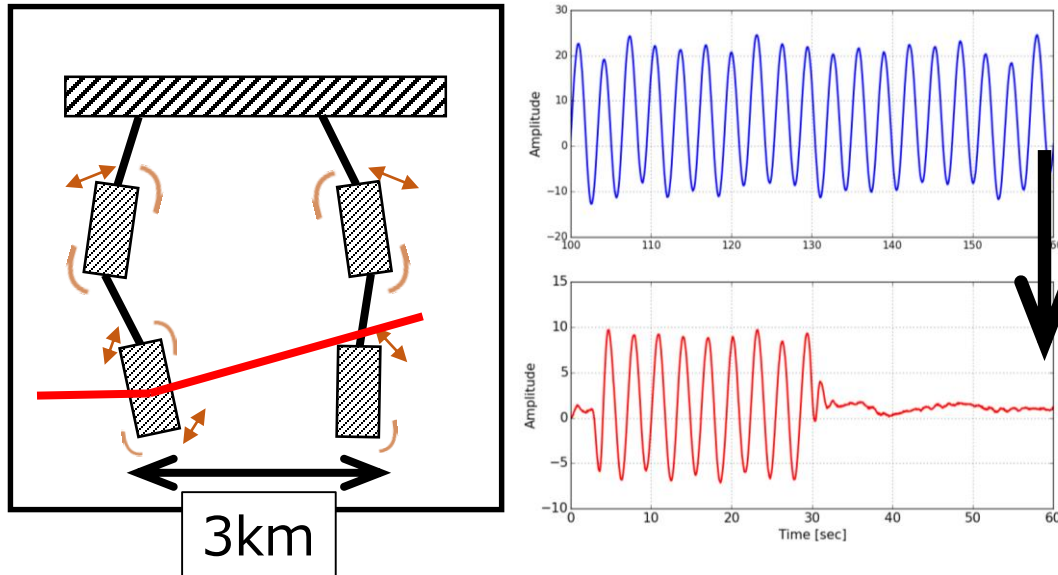
Mechanical system

**Already done**

\* Control system in observation (→ future work)

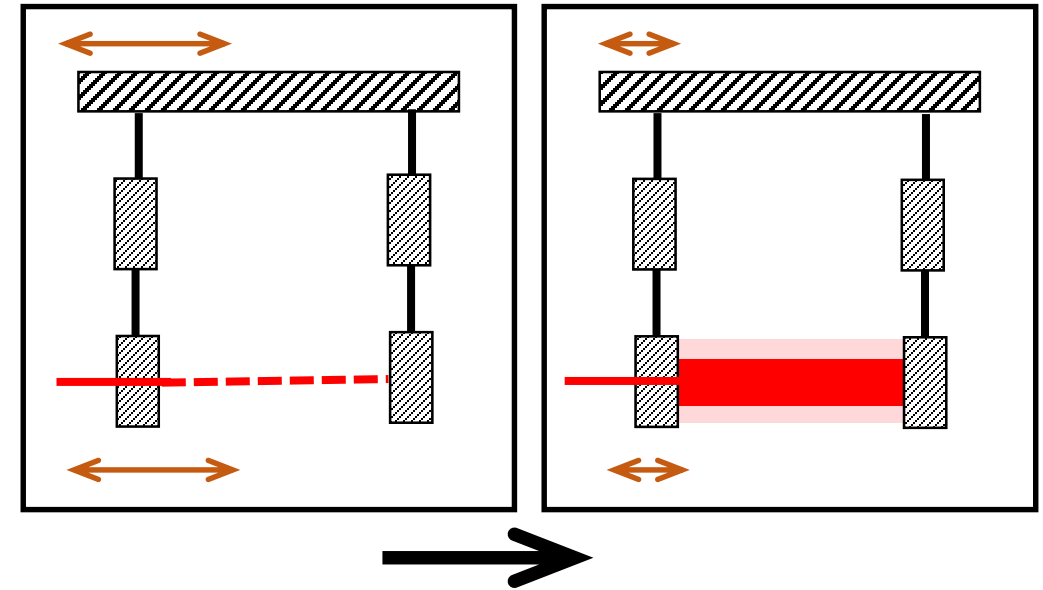
# What is necessary for the local control toward lock acquisition:

To damp resonances



→ Reduce lock loss time

To suppress mirror motion



→ Stable operation

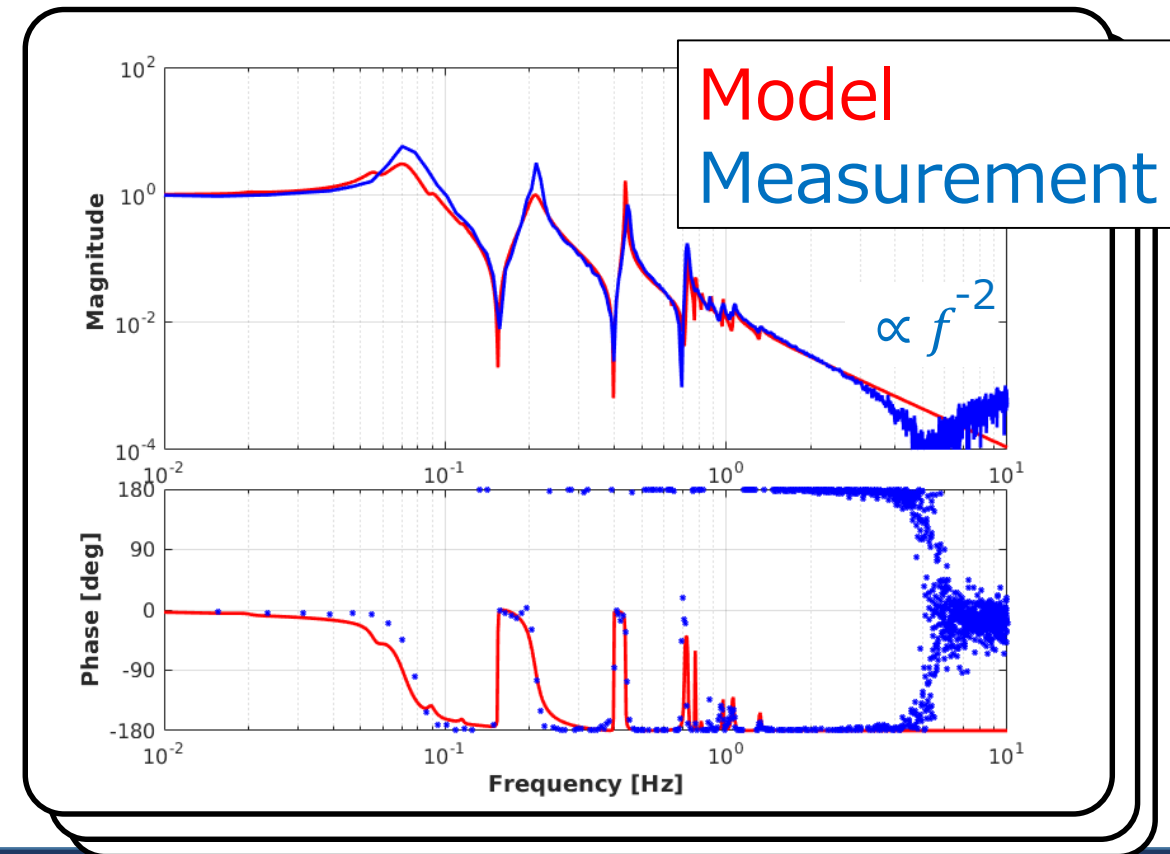
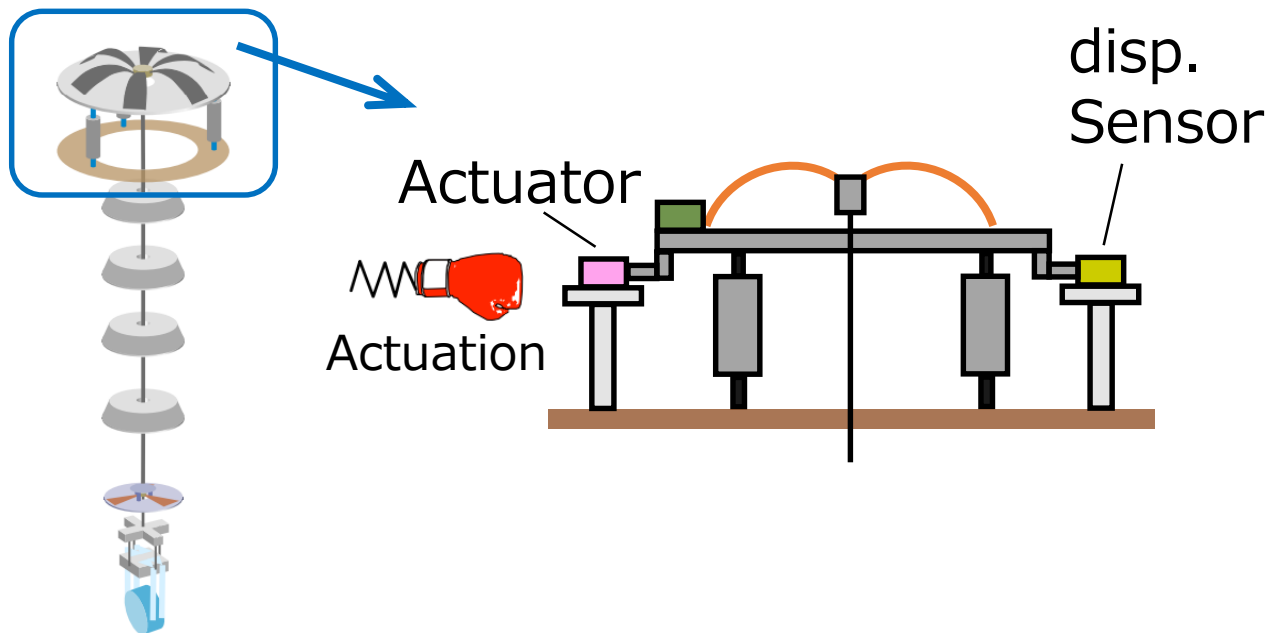
# What I did:

1. Frequency response check for mechanical system
2. Resonance damping
3. Mirror residual motion suppression

# 1. Frequency response check:

- **Target:** Confirm the system has characteristics of pendulum
- **Measurement:** Frequency responses from actuators to sensors

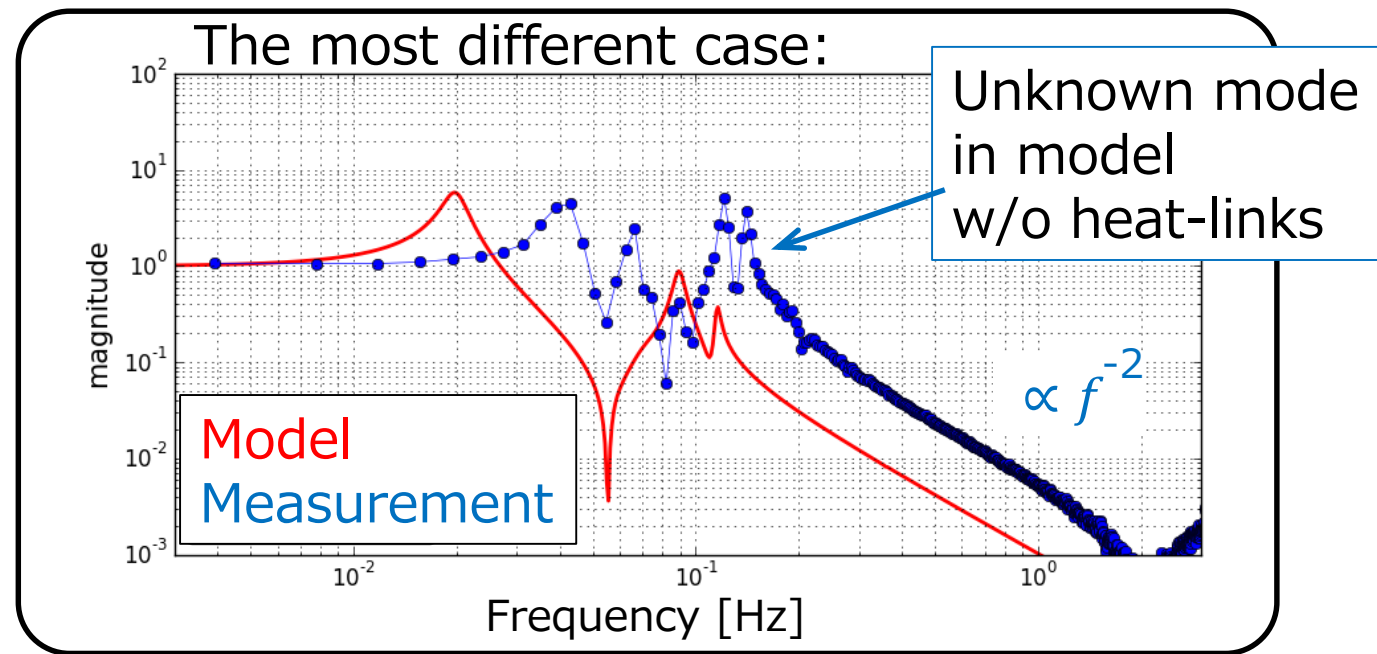
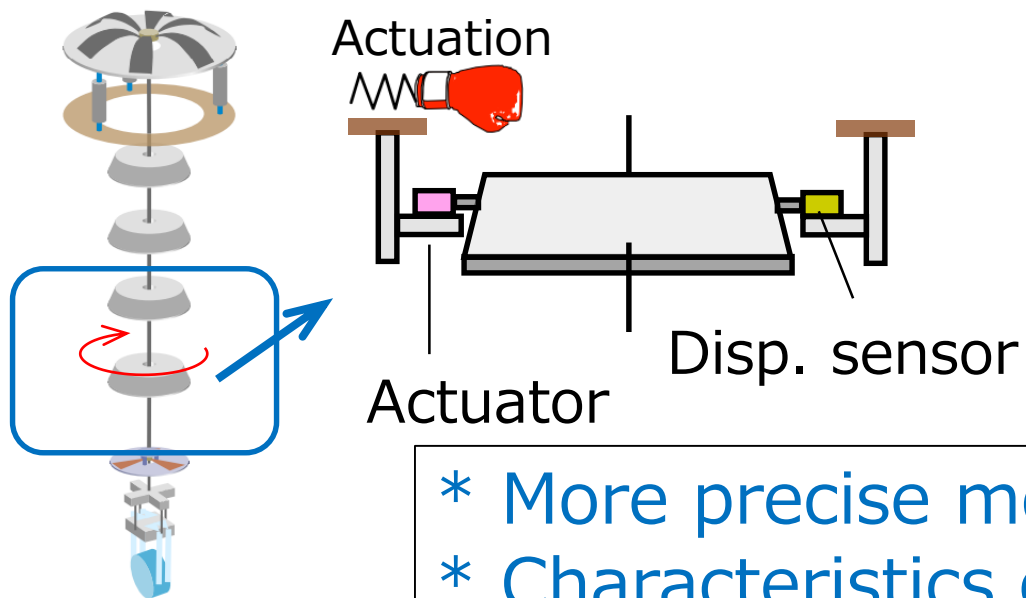
\* By each component



# 1. Frequency response check:

- **Target:** Confirm the system has characteristics of pendulum
- **Measurement:** Frequency responses from actuators to sensors

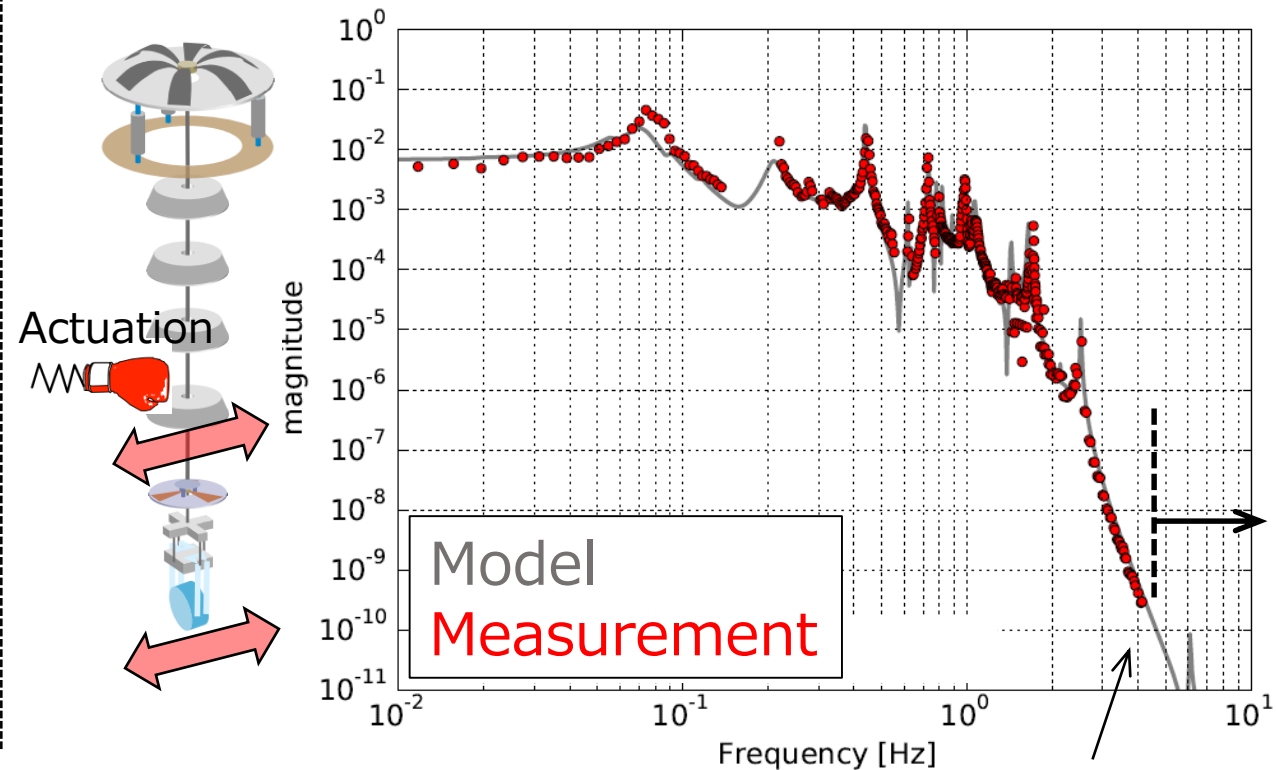
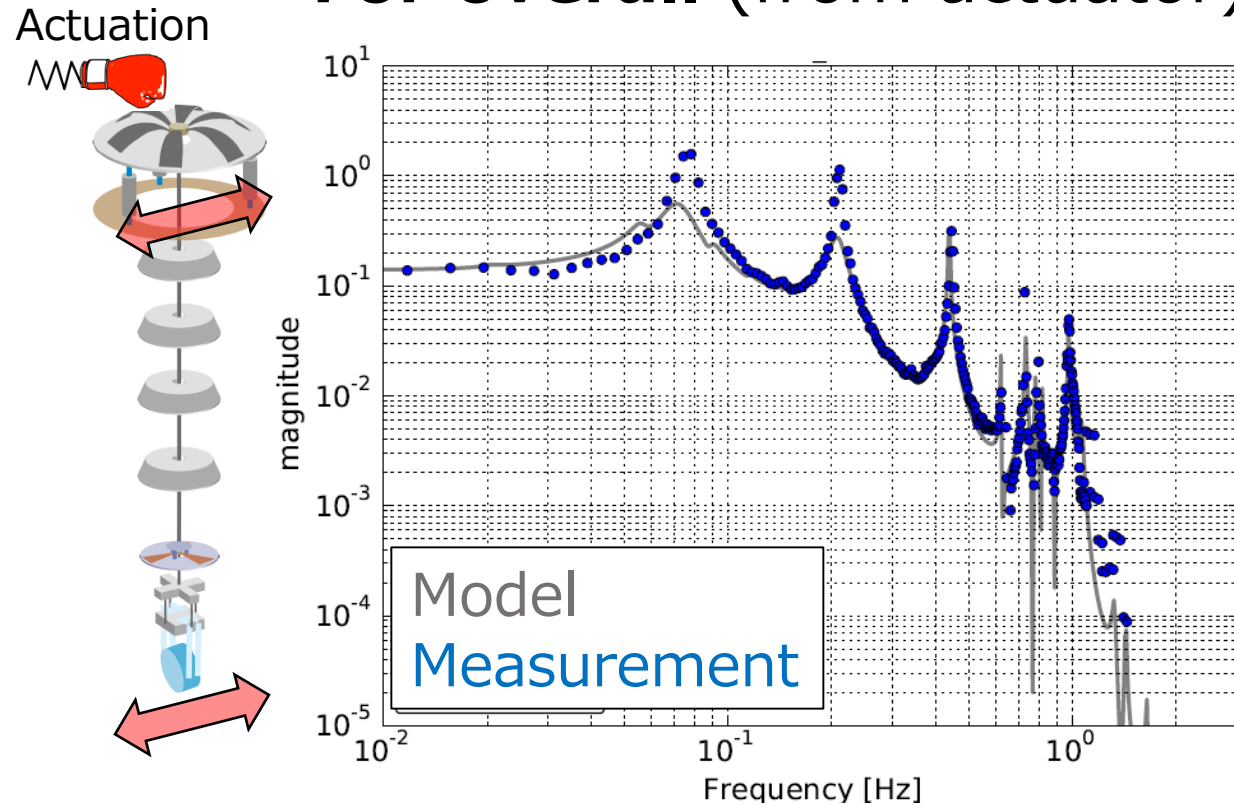
\* **By each component**



- \* More precise model tuning → Necessary
- \* Characteristics of pendulum  
→ Okay to build control for lock acquisition

# 1. Frequency response check:

\* For overall (from actuator)



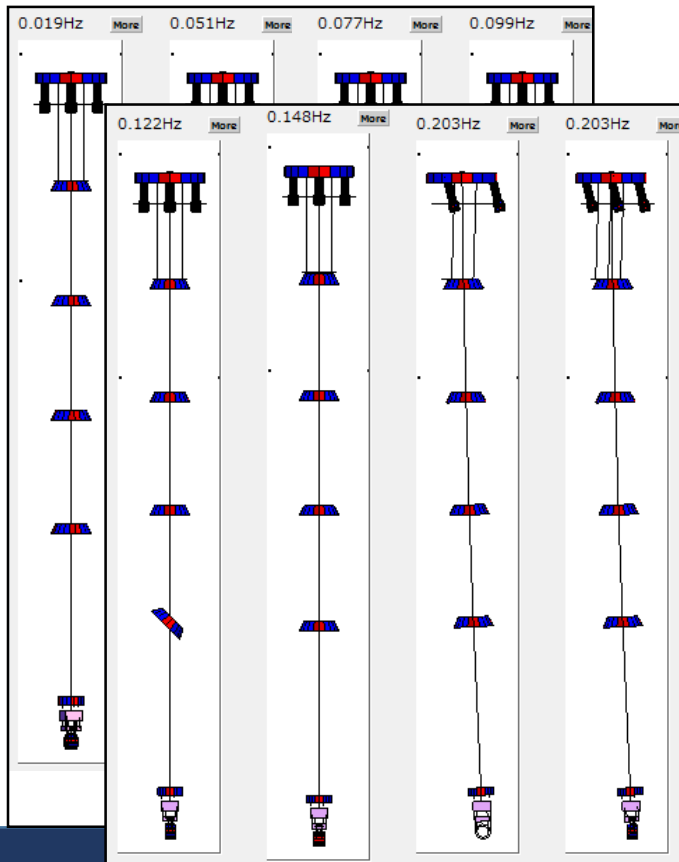
More sensitive interferometer is necessary.

- For overall performance, (model tuning is also necessary though)
- Type-A suspension has characteristics of pendulum up to 4.2 Hz.
- Assuming extrapolation, disp. noise at 10 Hz is attenuated.



## 2. Resonance damping:

- **Target:** To damp all the resonances disturbing the lock acquisition, within 1 min as  $1/e$  decay time.



### Number of resonances:

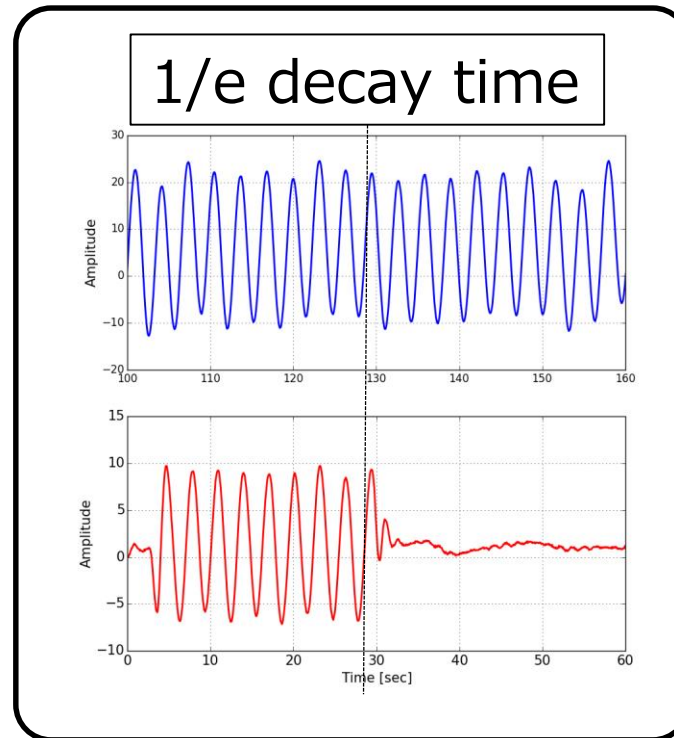
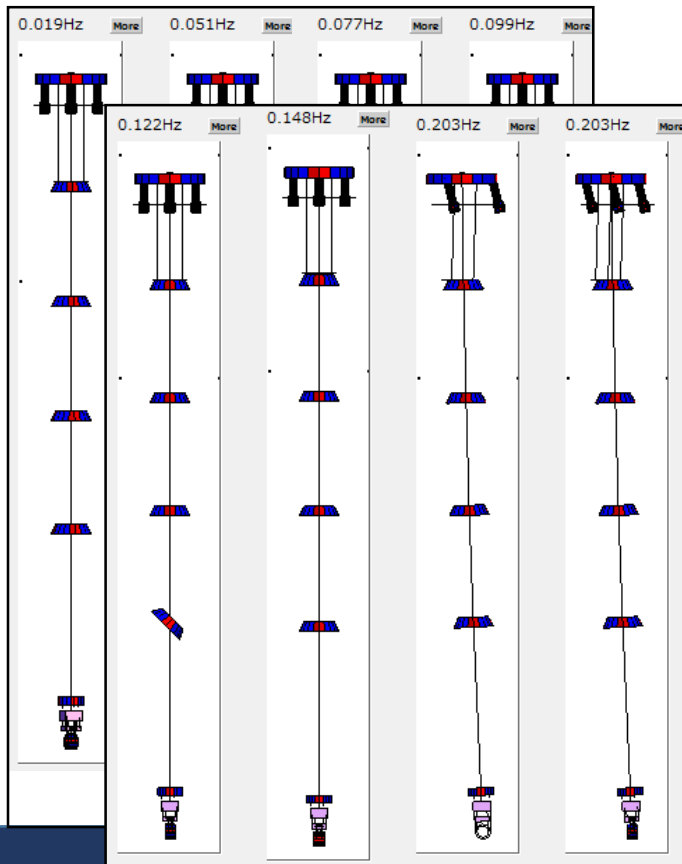
Assuming rigid-bodies  
→ 75 modes

From sensor & actuator availability  
Measured:

→ For 53 modes (res. frequency < 30Hz)

## 2. Resonance damping:

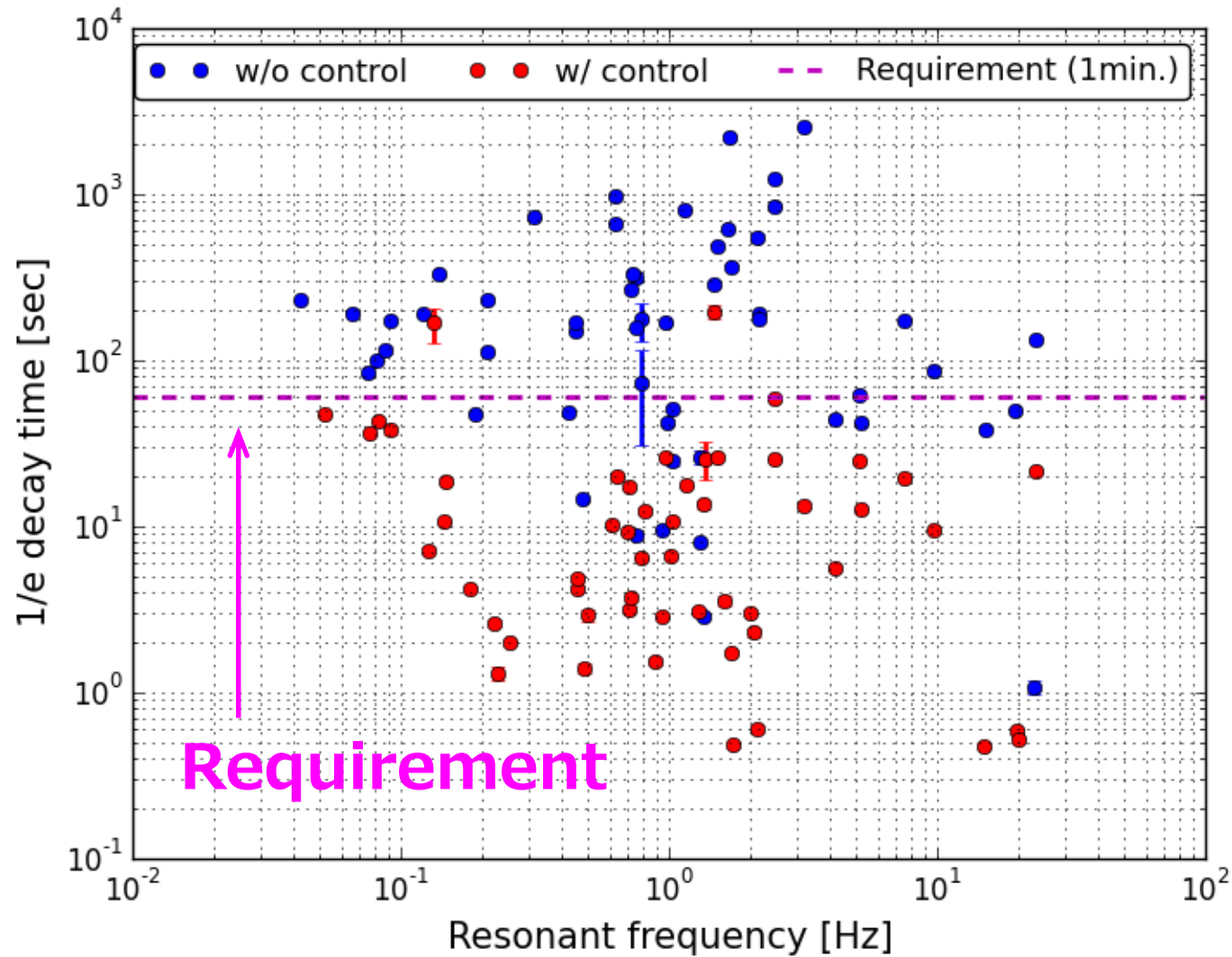
- **Target:** To damp all the resonances disturbing the lock acquisition, within 1 min as  $1/e$  decay time.
- **Measurement:**  $1/e$  decay time constant of each resonant mode



\* Excite resonant mode one by one, (as much as possible)

by sending a sinusoidal signal to implemented actuators.

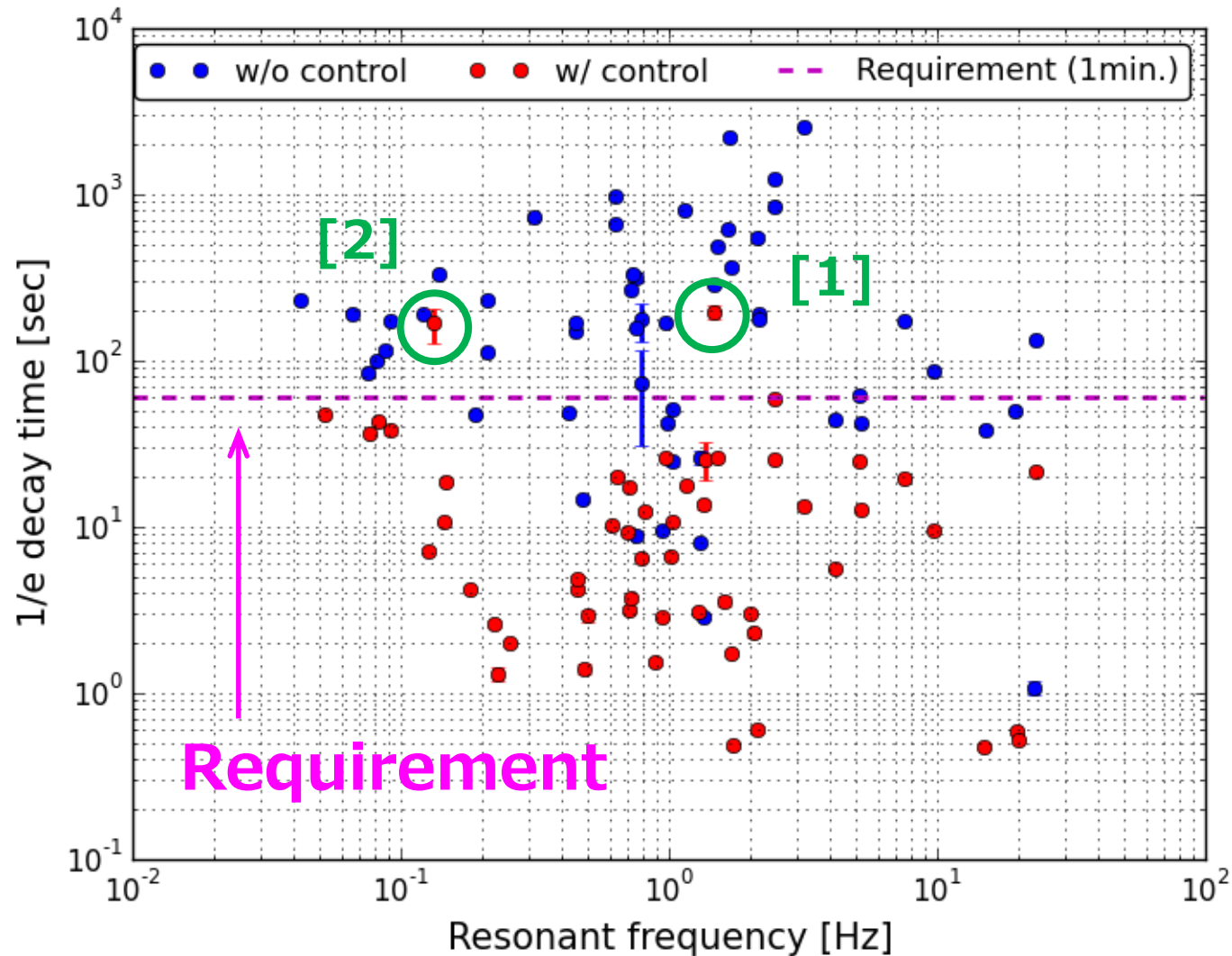
## 2. Resonance damping:



w/o control

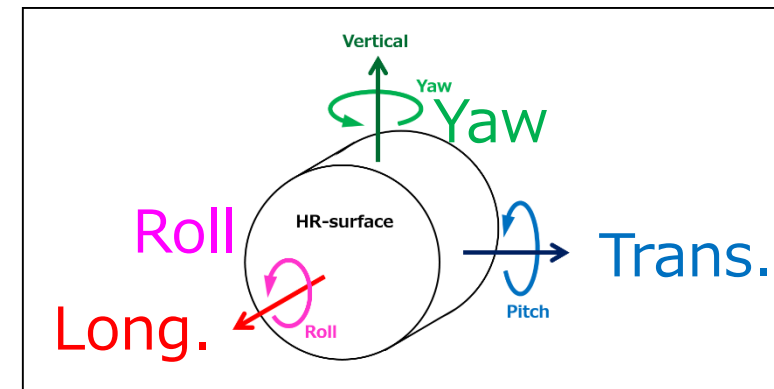
w/ control

## 2. Resonance damping:



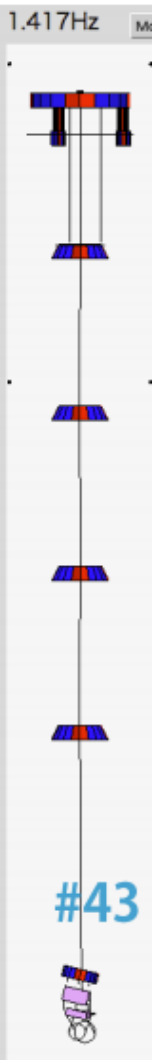
[1] #43: 1.5Hz

Roll / Trans. motion  
 → Not disturbs  
 the lock acquisition.



[2] 0.14Hz

unknown Yaw motion  
 → The model  
 w/o heat-link system  
 failed to predict.

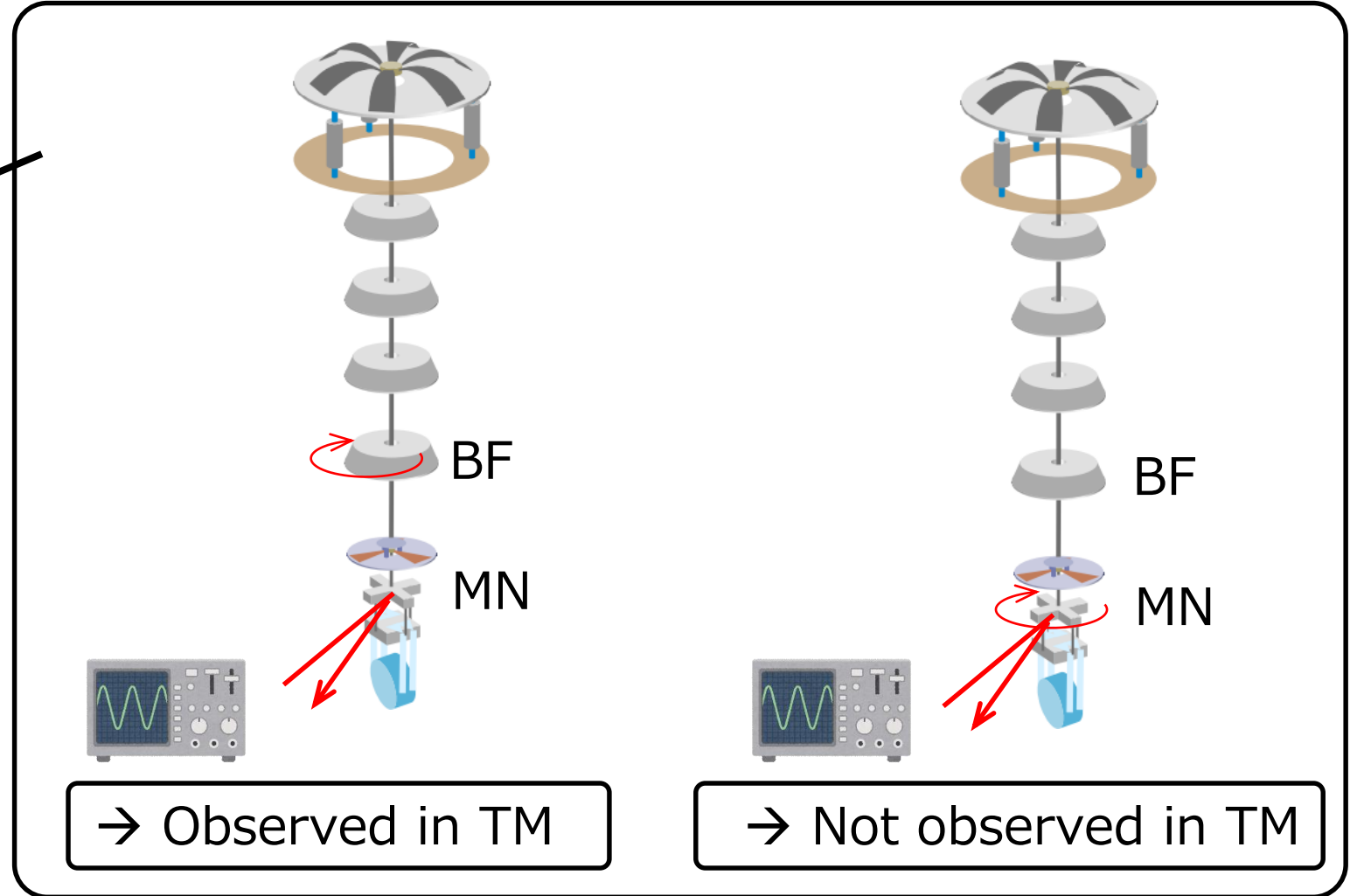


## 2. Resonance damping:

### [2] 0.14Hz mode

1. This will be excited when BF-stage actuated.
2. for interferometer control: only payload is controlled.

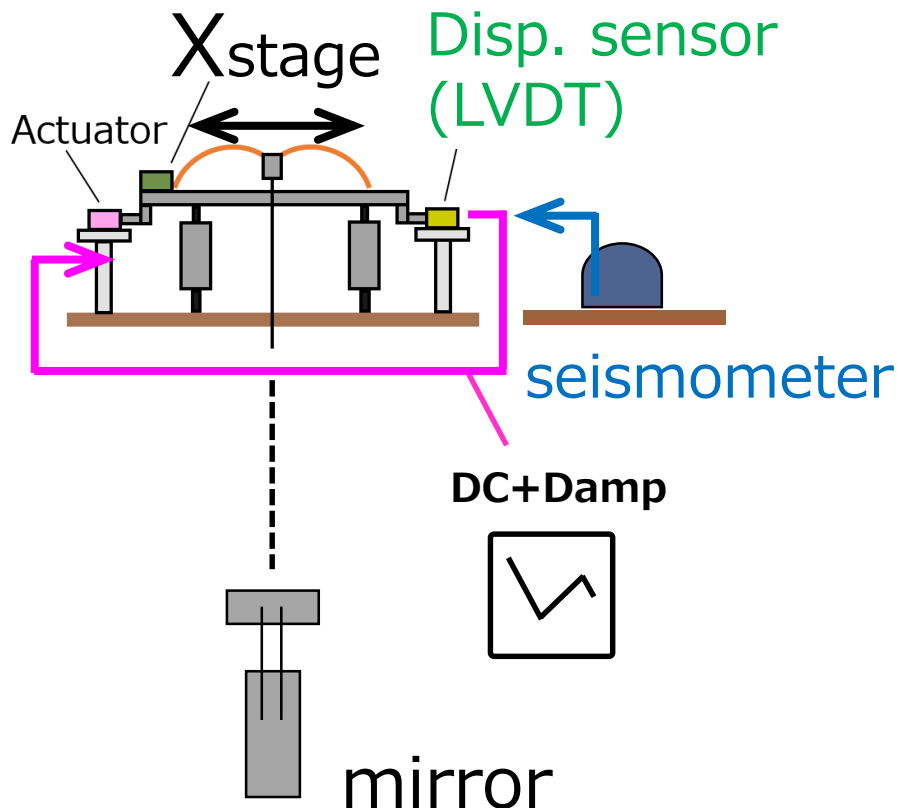
→ This mode will NOT be excited at lock loss.



→ The control system damps all the resonances disturbing the lock acquisition **for the lock-recovery mode.**

### 3. Mirror residual motion suppression:

- **Target:** To suppress mirror velocity & displacement so that the interferometer lock is acquired.



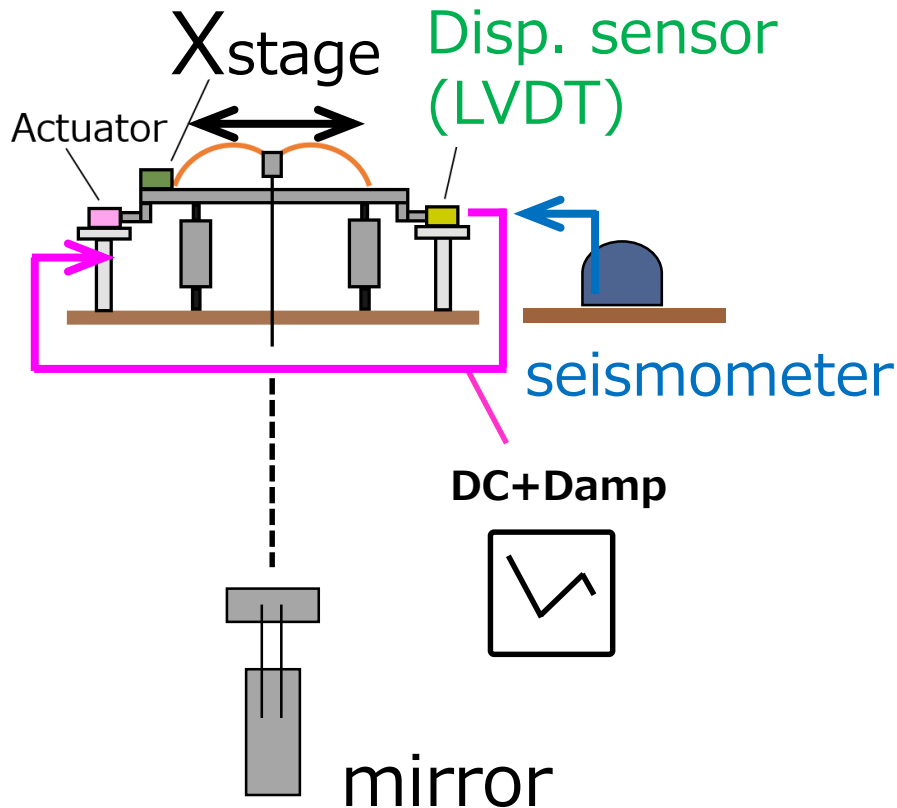
$$X_{sensor}^{virtual} = \left[ \underbrace{X_{stage} - X_{ground}}_{\substack{\text{Displacement} \\ \text{sensor} \\ \text{signal}}} + \underbrace{X_{ground}^{seis}}_{\substack{\text{Seismometer} \\ \text{signal}}} \right]$$

→ Cut the seismic noise injection via disp. sensor. (→ sensor correction)



### 3. Mirror residual motion suppression:

- **Target:** To suppress mirror velocity & displacement.
- **Measurement:** Frequency response from ground to mirror

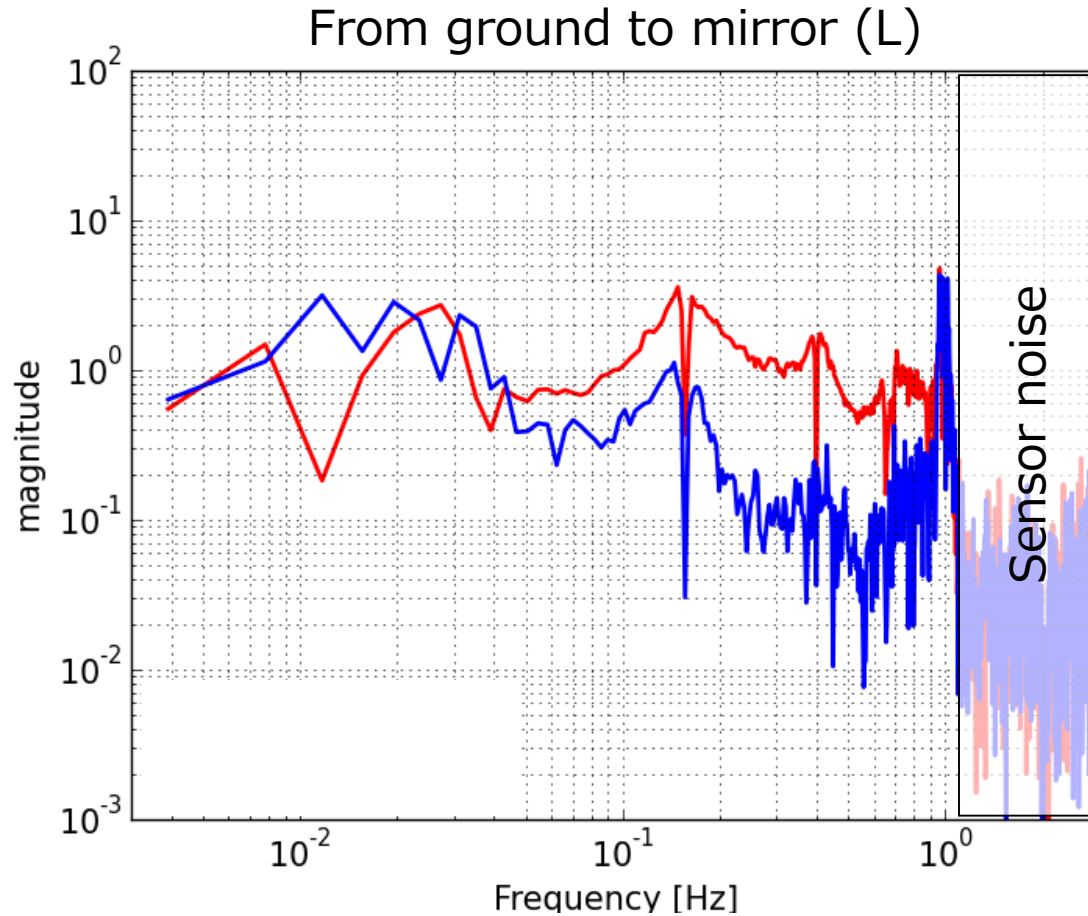
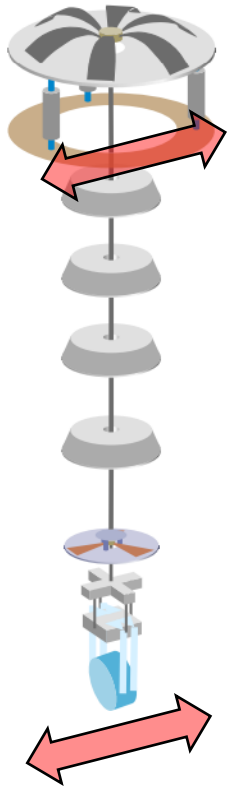


$$X_{sensor}^{virtual} = \left[ \underbrace{X_{stage} - X_{ground}}_{\substack{\text{Displacement} \\ \text{sensor} \\ \text{signal}}} + \underbrace{X_{ground}^{seis}}_{\substack{\text{Seismometer} \\ \text{signal}}} \right]$$

→ Cut the seismic noise injection via disp. sensor. (→ sensor correction)

# 3. Mirror residual motion suppression:

\* Frequency response from ground to mirror

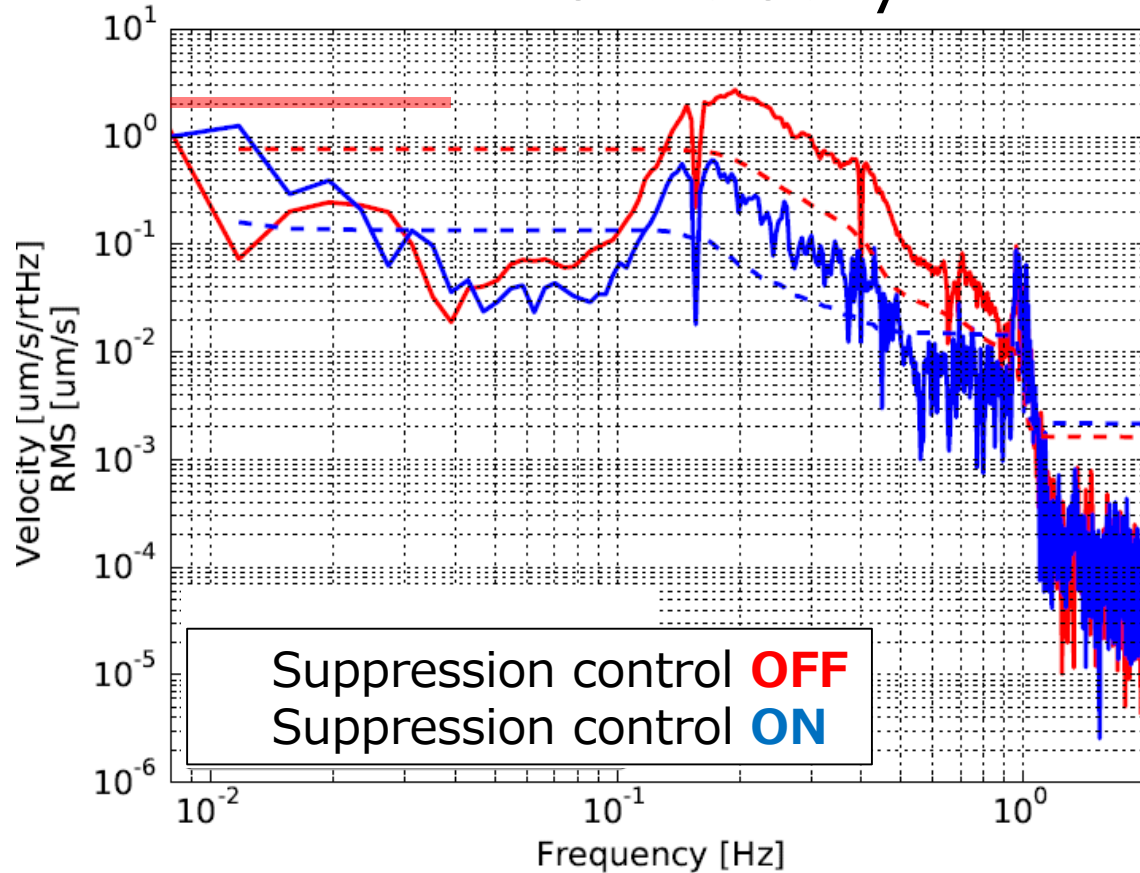


w/o sensor correction

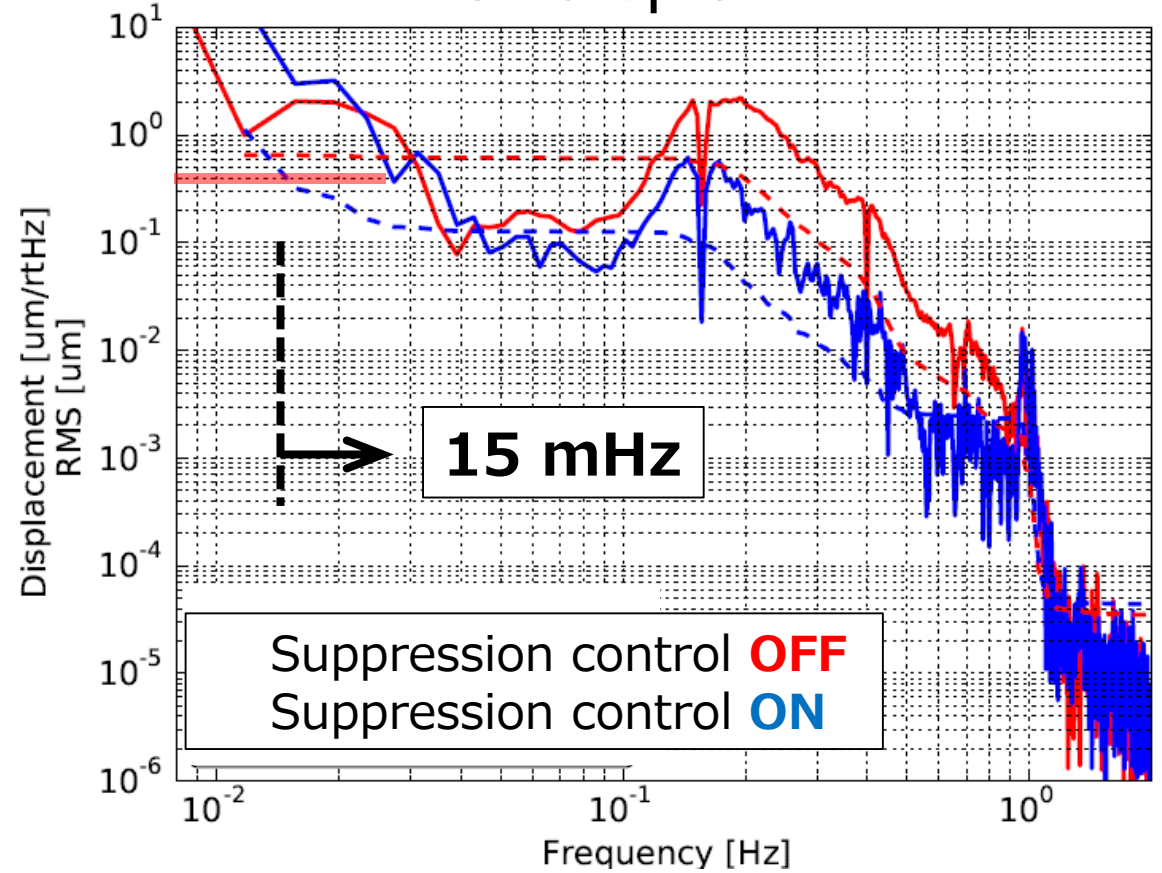
w/ sensor correction

# 3. Mirror residual motion suppression (w/ 90%tile seismic motion)

## Mirror velocity



## Mirror displacement



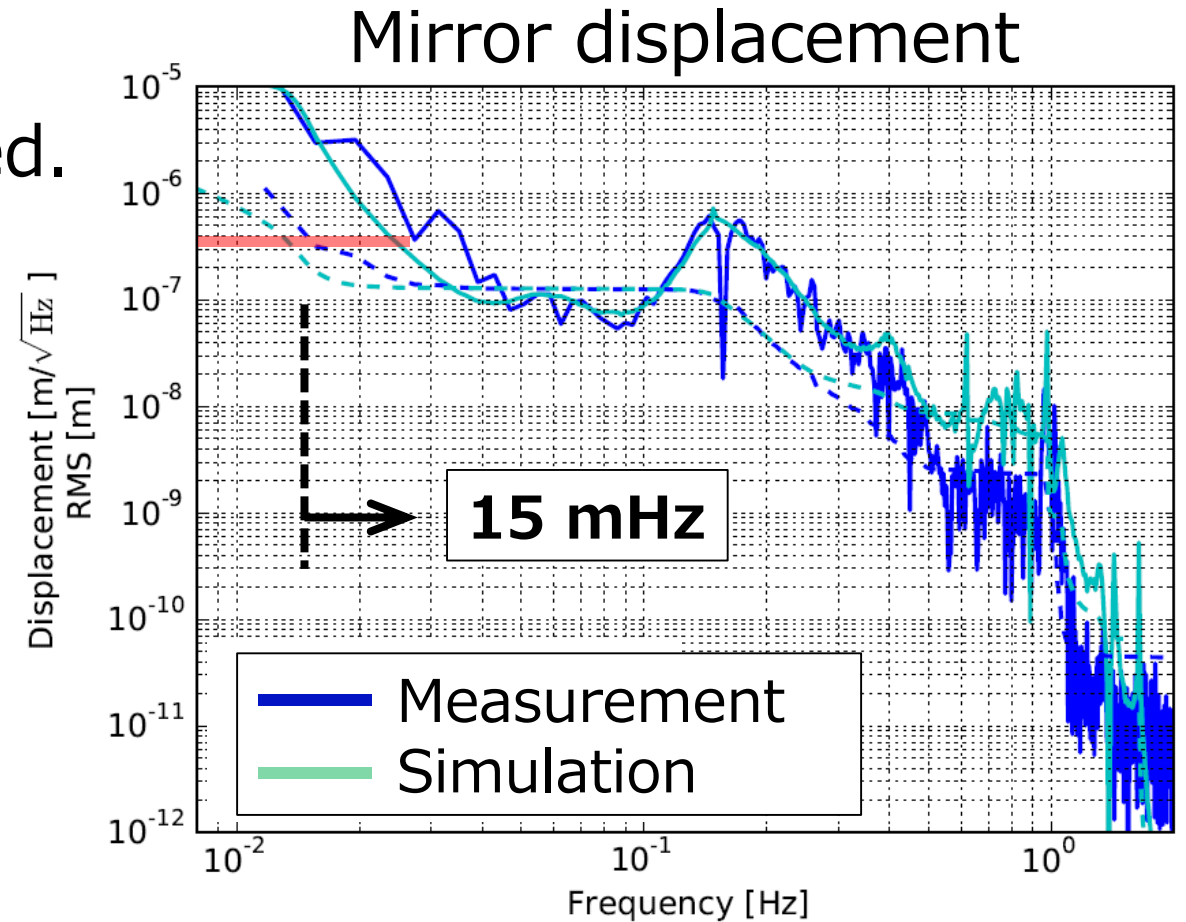
→ The control system locally suppresses the residuals and satisfies the requirement for in the time scale of 1 min.

### 3. Mirror residual motion suppression (w/ 90%tile seismic motion)

\* Measurement agrees with simulation. → works as designed.

\* Performance at < 15 mHz:  
→ due to noise coupling from seismometers.  
→ For further stabilization,  
1. local seismometer corr. system (with tilt-meter), or  
2. global control with interferometer signal is necessary. → **Task of the observation phase control.**

→ Local control system for lock acquisition has been realized.



# Summary: performance of local control system

## 1. Frequency response check

- Type-A suspension has characteristics of pendulum.
- the unexpected frequency response → further model tuning.
- Enough for lock acq. phase control.

## 2. Resonance damping

- The control system damped all the resonances disturbing the lock acquisition for the lock-recovery mode within 1min in  $1/e$  decay time.

## 3. Mirror residual motion suppression

- The control system locally suppresses the residual mirror motion in the time scale of 1 min.

→ Local control system for lock acquisition has been realized.

This is the first time to control KAGRA full Type-A suspension.

# Summary of this research:

## 1. Fast localization simulation by current network with hierarchical approach

→ If  $V(K)$  sensitivity  $> 0.2$  (0.28) of LIGO, the hierarchical search improves the fast localization performance in the heterogeneous network using existing low-latency infrastructure.

## 2. TypeA suspension controls toward lock acquisition

→ I've constructed local control system for full Type-A suspension of KAGRA toward acquiring interferometer lock.

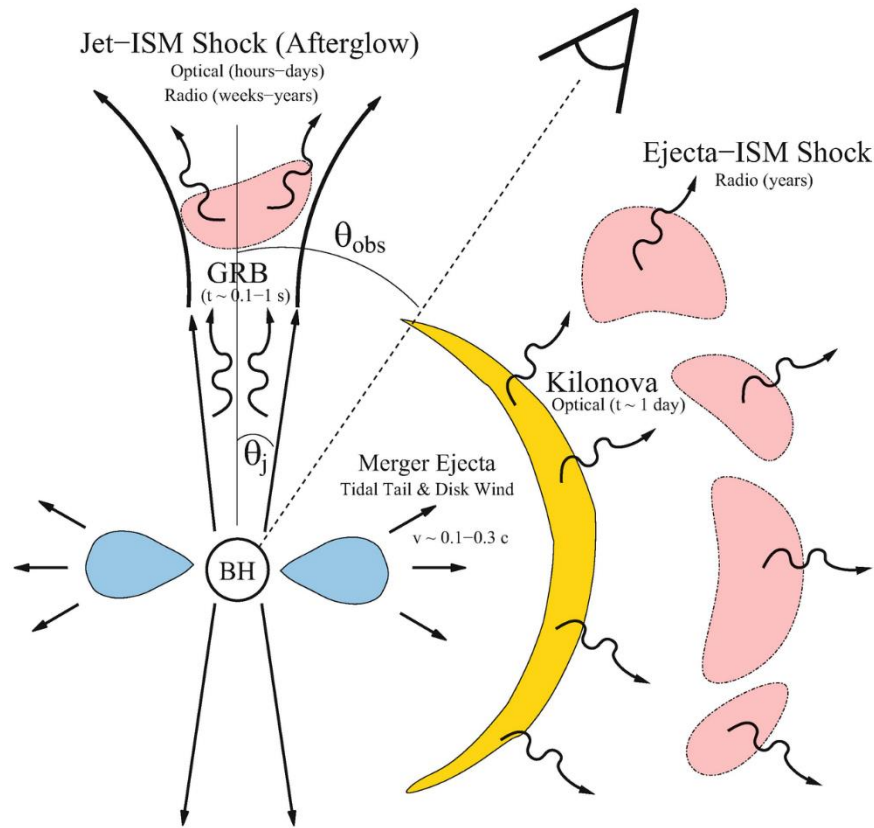
→ **This contributes to KAGRA joining to the network as the 4th detector.**



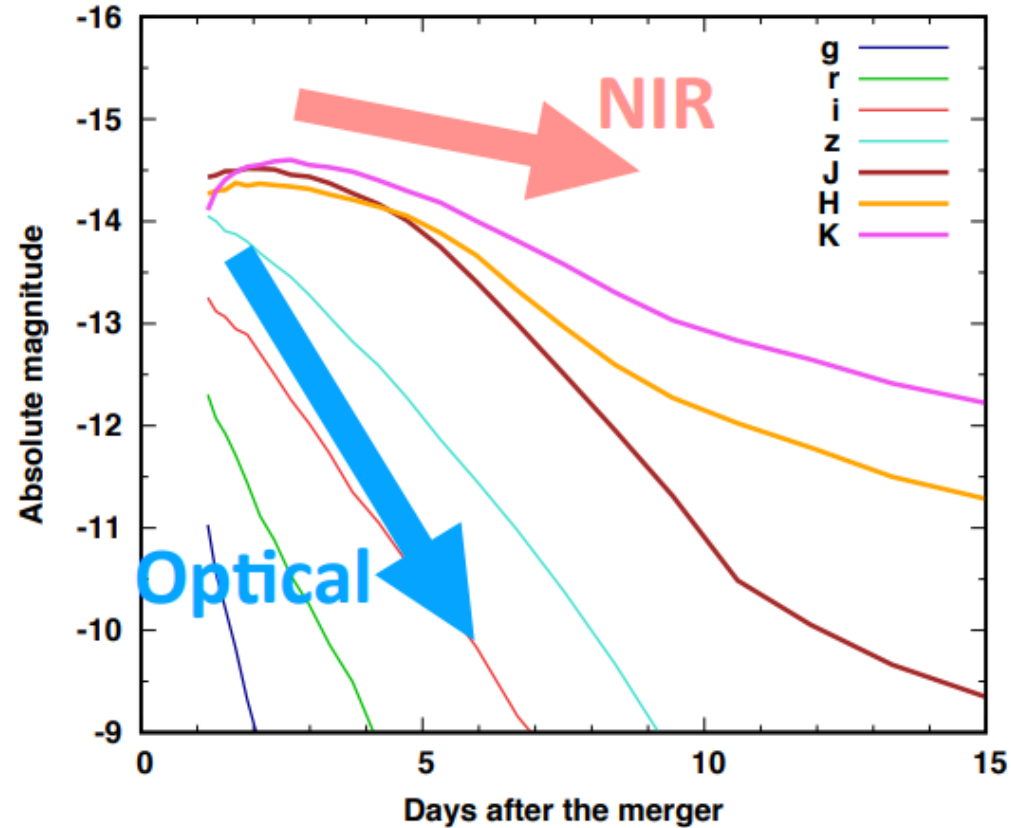
# Backups

Note: fast localization

**Kilonova:** Electromagnetic emission powered by radioactive decays of r-process nuclei, given by ejected material from neutron star mergers. [ref] <https://iopscience.iop.org/article/10.3847/1538-4357/aaa0cb/pdf>



Metzger & Berger 2012

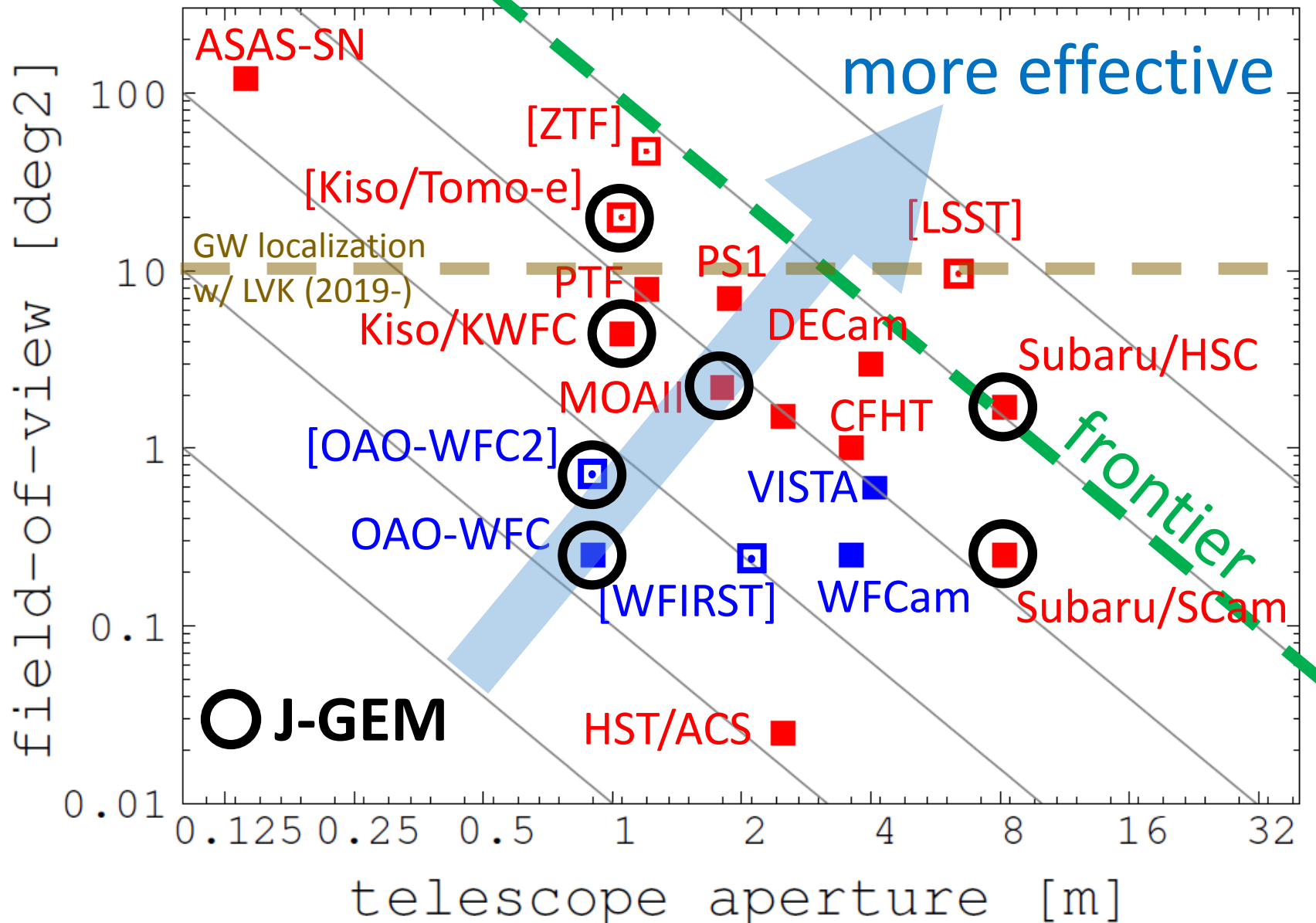


[http://www.icehap.chiba-u.jp/activity/180326MultiMessenger/3-26/tanaka\\_20180326.pdf](http://www.icehap.chiba-u.jp/activity/180326MultiMessenger/3-26/tanaka_20180326.pdf)

# FOV vs. Area by GWs

## 世界の可視近赤外広視野望遠鏡・装置

可視:赤 赤外:青 []:将来計画



[ref] <http://www.icrr.u-tokyo.ac.jp/JPSOCR/2016S/yoshida.pptx>

# Detector response:

## The signal (I)

Signal sensed by detector is a combination of two polarizations

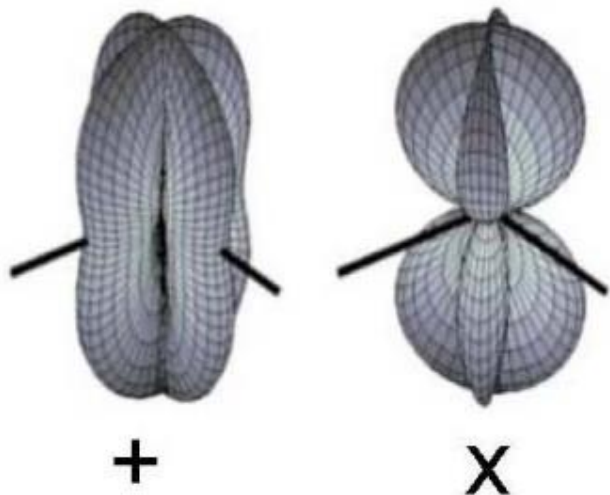
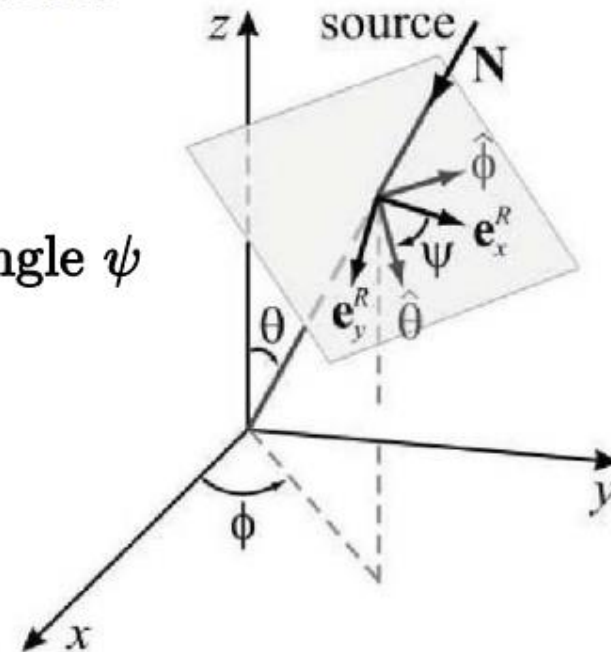
$$h(t) = F_+(\theta, \phi, \psi) h_+(t) + F_\times(\theta, \phi, \psi) h_\times(t)$$

$F_+$  and  $F_\times$ : detector response functions

depend on sky location  $(\theta, \phi)$  and polarization angle  $\psi$

$$F_+ = -\frac{1}{2}(1 + \cos^2 \theta) \cos 2\phi \cos 2\psi - \cos \theta \sin 2\phi \sin 2\psi$$

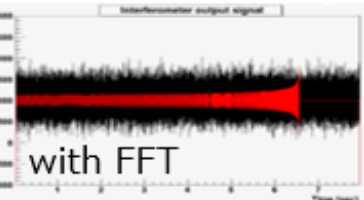
$$F_\times = \frac{1}{2}(1 + \cos^2 \theta) \cos 2\phi \sin 2\psi - \cos \theta \sin 2\phi \cos 2\psi$$



$F_+$  and  $F_\times$  can be approximated as constant over length of CBC signals in ground based detectors

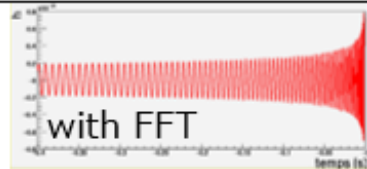
# Matched filtering

Detector output

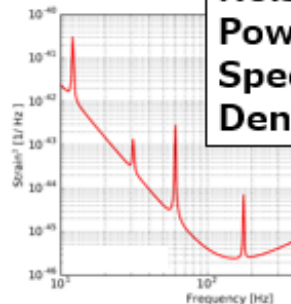


×

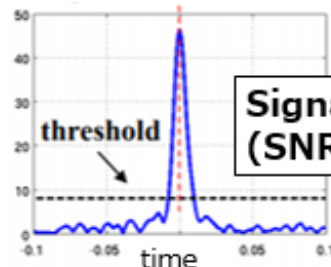
Theoretical waveform  
(Template)



Noise  
Power  
Spectrum  
Density



JGW-P1707567



Signal-to-Noise ratio  
(SNR)

We introduce the reference time  $t_c$  as the time of the coalescence. We can rewrite the template (that is, normalized waveform) centering on  $t_c$  as  $u(t; t_c) = u'(t - t_c)$ . Thus,

$$\begin{aligned}\tilde{u}(f) &= \int_{-\infty}^{\infty} u'(t - t_c) e^{-2\pi i f t} dt \\ &= \int u'(t') e^{-2\pi i f t'} e^{-2\pi i f t_c} dt' \\ &= \tilde{u}'(f) e^{-2\pi i f t_c},\end{aligned}$$

where we assume  $t = t' + t_c$  and  $\tilde{u}'(f)$  is

$$\tilde{u}'(f) = \int u'(t) e^{-2\pi i f t} dt = \int u(t; t_c = 0) e^{-2\pi i f t} dt = \tilde{u}(f; t_c = 0).$$

As a result, Eq.(2.10) can be rewritten as

$$(x, u) = 4\text{Re} \int_0^{\infty} \frac{\tilde{x}(f) \tilde{u}^*(f; t_c = 0)}{S_n(|f|)} e^{2\pi i f t_c} df. \quad (2.11)$$

Because this formula is equivalent to the inverse Fourier transformation from  $f$  to  $t_c$ , we can obtain the time series of  $(x, u)$  for each  $t_c$  by the inverse Fourier transformation. The calculation of Eq.(2.11) can be done efficiently with the Fastest Fourier Transform, such as FFTW.



# SNR maximization:

## Matched filtering in practice (II)

- The phase of the chirp signal is unknown

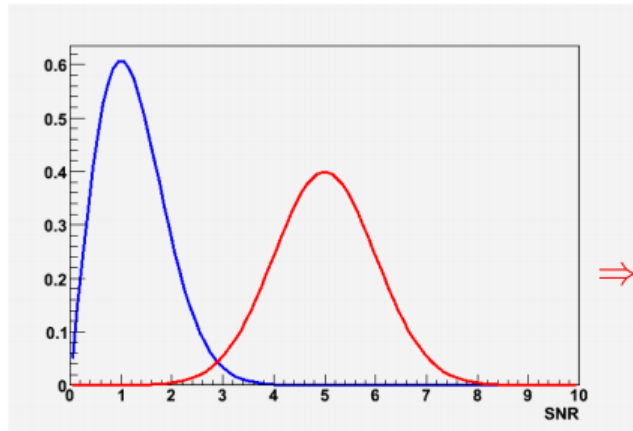
$$h(t) = A [h_c(t) \cos \Phi + h_s(t) \sin \Phi]$$

cosine and sine phases of the waveform

» The SNR has to be maximized over all possible values of  $\Phi$

Filter with  $T_{0^\circ}$  and  $T_{90^\circ}$  and take quadratic sum

$$S^2 = \sqrt{S_{0^\circ}^2 + S_{90^\circ}^2}$$

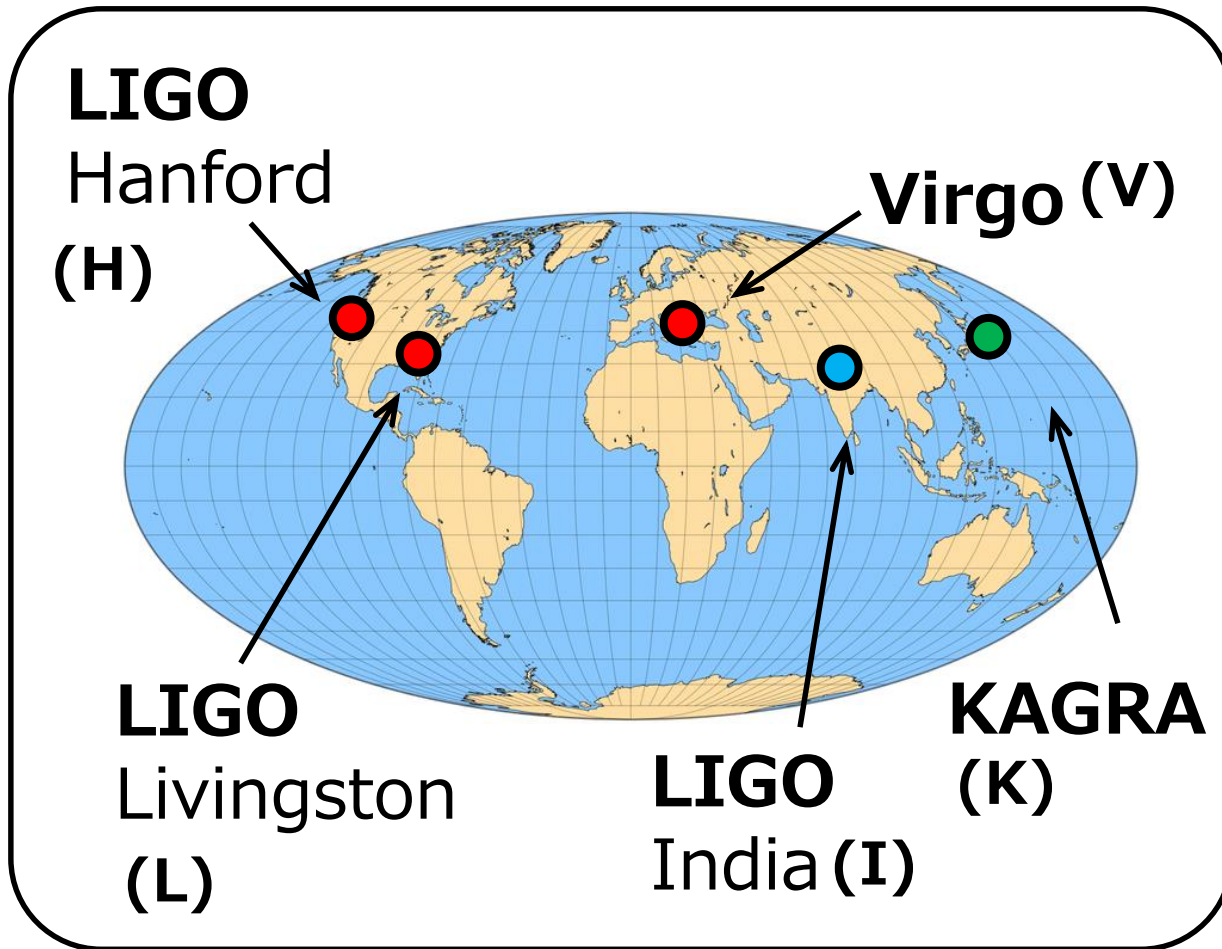


Noise has a  $\chi^2$  distribution  
with 2 degrees of freedom  $p(\rho) = \rho e^{-\rho^2/2}$

Signal has a non-central  $\chi^2$  distribution  
 $\Rightarrow$  Gaussian distribution if signal strong enough

31

# Network by multiple GW detectors:



\* network duty cycle  $D_{\text{net}}$   
 $\sim D_1 * D_2 * D_3 * D_4 * \dots$

ex.) Network duty cycle  
more than 3 detectors

\* if  $D_1 = D_2 = \dots = 80\%$ ,

3-detector network:  $D_{\text{net}} \sim 51\%$

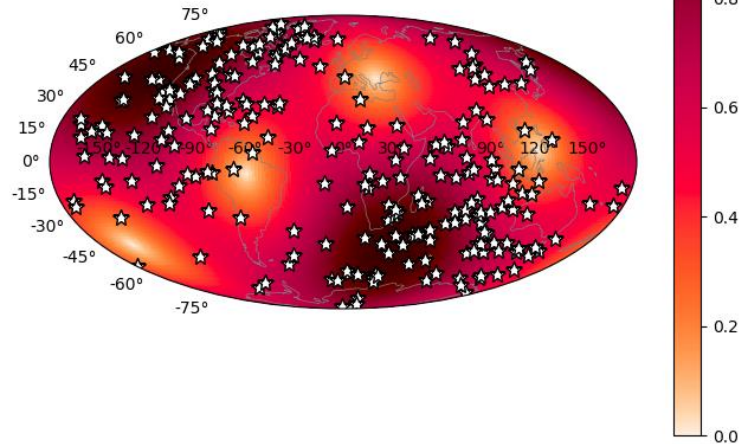


4-detector network:  $D_{\text{net}} \sim 82\%$

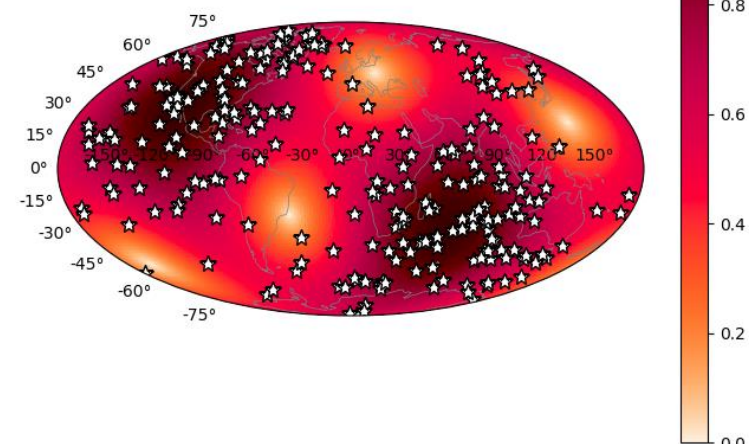


# Antenna pattern & source position

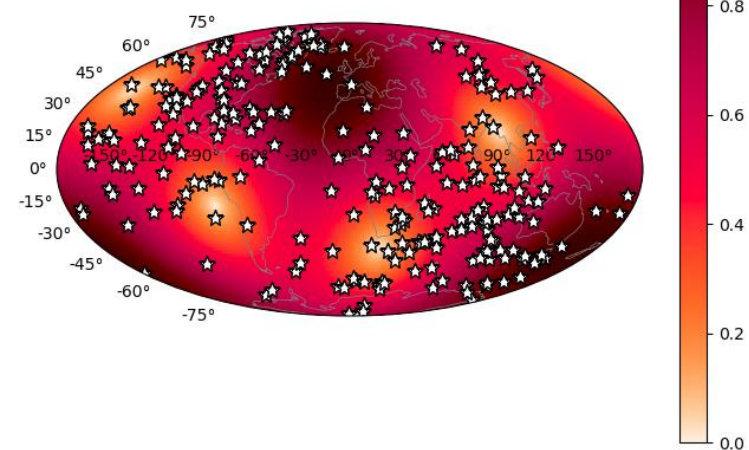
LIGO Hanford



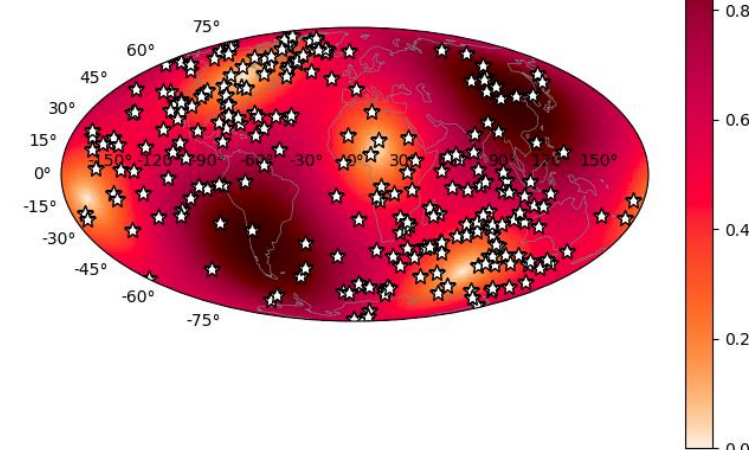
LIGO Livingston



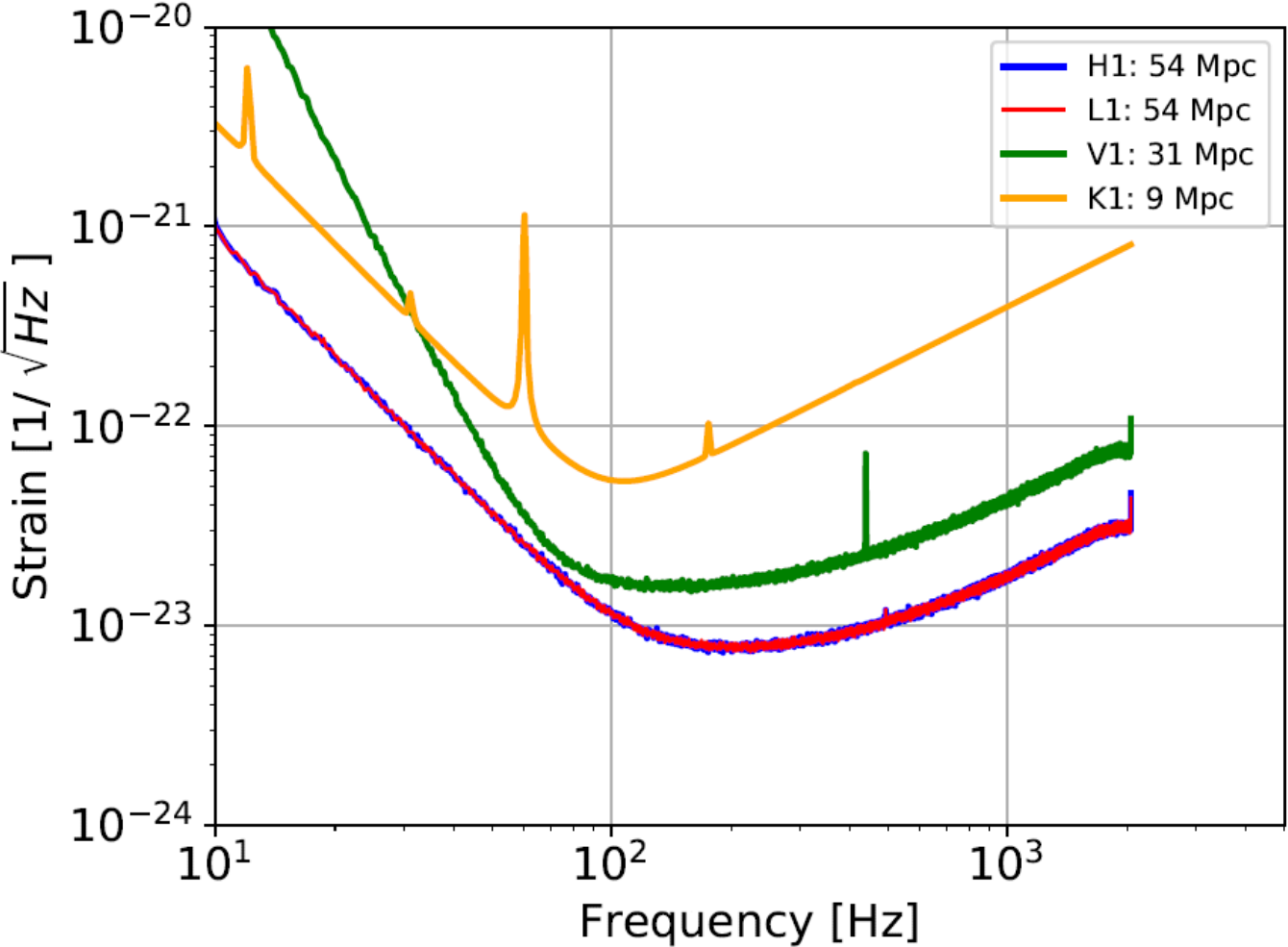
Virgo



KAGRA



# Assumed noise curves:



- For V/K, the curves are scaled.

# Actual threshold in the low-latency analysis in O2:

**Table 1.** Major parameters of O2 online search pipelines based on compact binary merger waveform models.

	PyCBC Live	GstLAL	MBTAOnline
Total mass	$2M_{\odot}$ to $500M_{\odot}$ <sup>a</sup>	$2M_{\odot}$ to $150M_{\odot}$ <sup>a</sup>	$2M_{\odot}$ to $100M_{\odot}$
Mass ratio	1 to 98	1 to 98	1 to 99
Minimum component mass	$1M_{\odot}$	$1M_{\odot}$	$1M_{\odot}$
Spin magnitude ( $m < 2M_{\odot}$ )	0 to 0.05	0 to 0.05	0 to 0.05
Spin magnitude ( $m > 2M_{\odot}$ )	0 to 0.998	0 to 0.999	0 to 0.9899
Single-detector SNR threshold for triggering	5.5	4 <sup>b</sup>	5.5 <sup>c</sup>

<sup>a</sup>The maximum total mass for PyCBC Live and GstLAL is in fact a function of mass ratio and component spins (Dal Canton & Harry 2017; Mukherjee et al. 2018) and we indicate the highest total mass limit over all mass ratios and spins. The offline GstLAL search uses a template bank extended to a larger maximum total mass of  $400M_{\odot}$ .

<sup>b</sup>This threshold was applied to the two LIGO detectors only for the online GstLAL analysis. The minimum trigger SNR in Virgo was not determined by an explicit threshold, but instead by a restriction to record at most 1 trigger per second in a given template.

<sup>c</sup>MBTAOnline uses a higher LIGO SNR threshold (6) to form coincidences with Virgo.



More concretely:

\* Component mass: Uniform [  $1.2 M_{\odot}$  :  $1.6 M_{\odot}$  ]

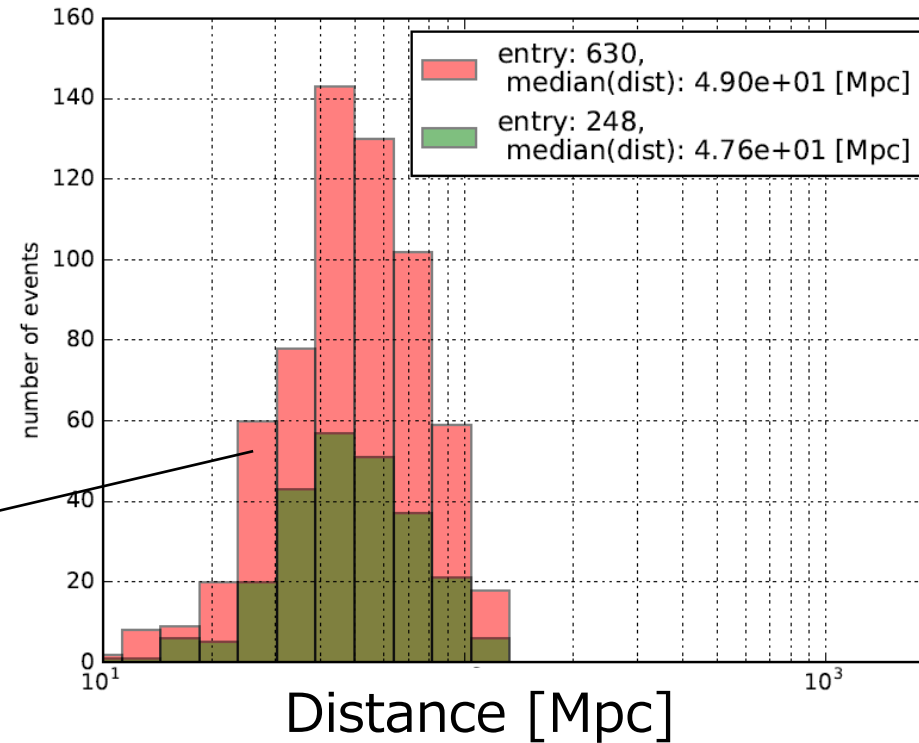
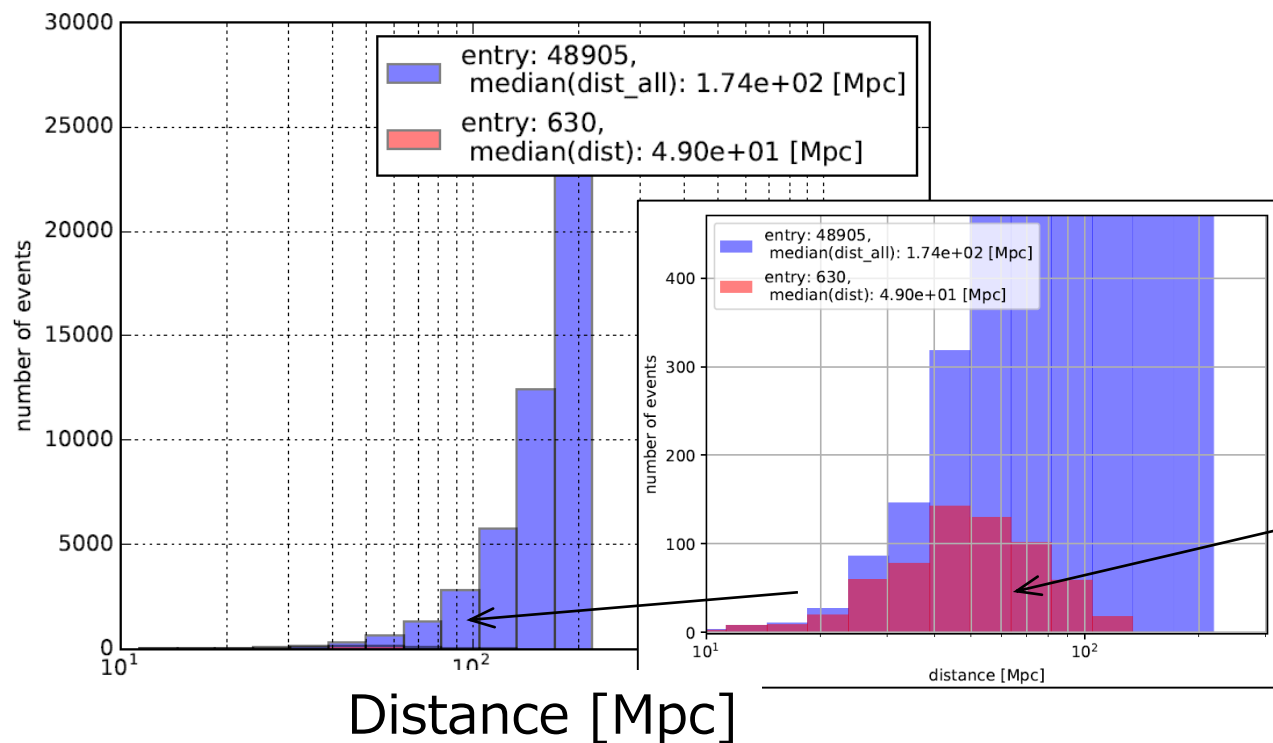
## Injections (number of events: 248)

\* Reuse of another calculation [ref] & detected by HL-network:

All injections  
Random, isotropic  
(48905 events)

Events detected  
by HL  
(630 events)

Randomly selected  
events  
(248 events)





# How the inputs obtained?: 2015 scenario in [1] vs. 2016sim

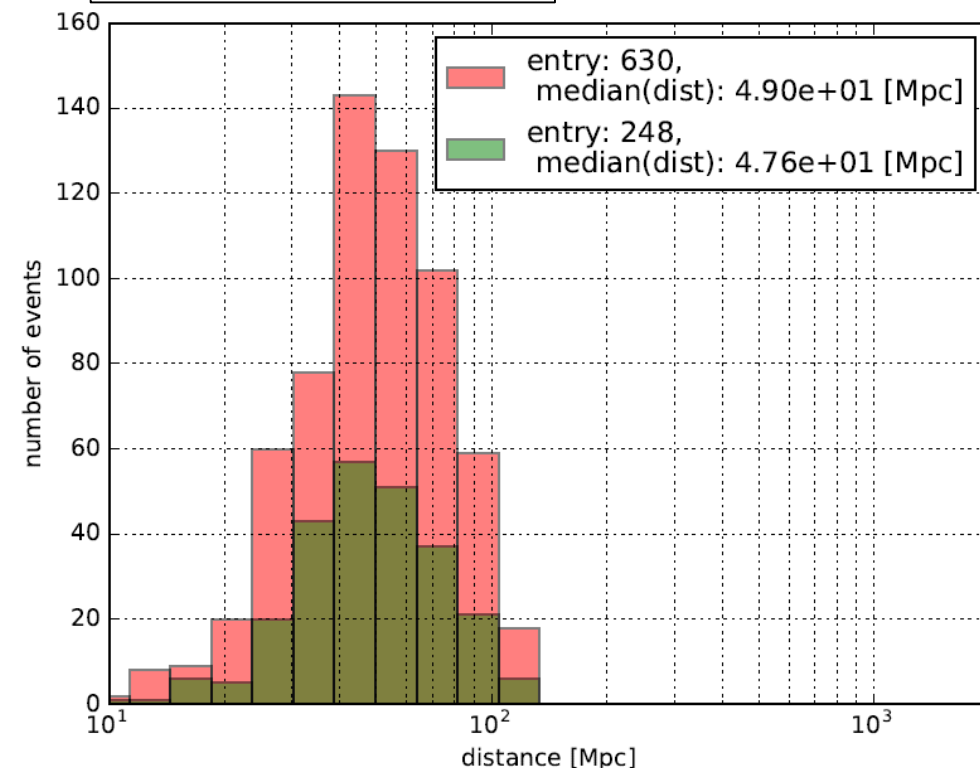
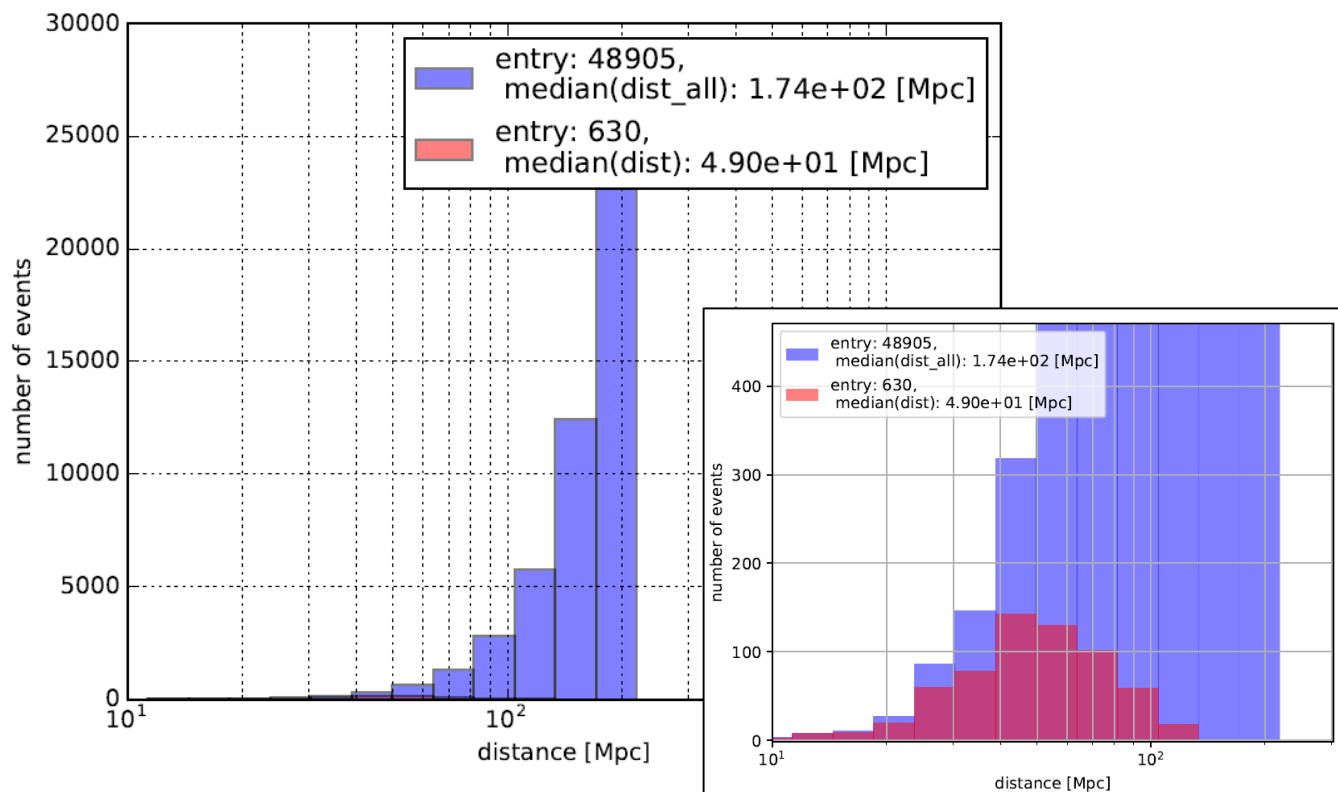
\* Configuration (number of events)

\* Component mass: Uniform [  $1.2 M_{\odot}$  :  $1.6 M_{\odot}$  ]

\* All injections (48905)  $\rightarrow$  \* Found events (630)  $\rightarrow$  \* Used in simulation (248)

Randomly selected in order to save computational cost.

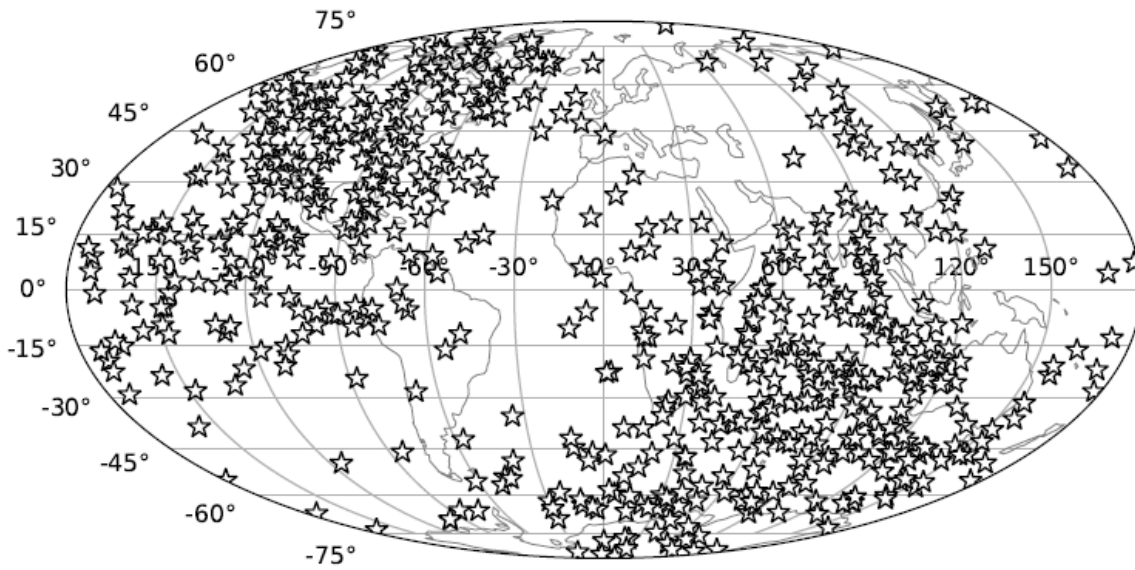
2 events missed



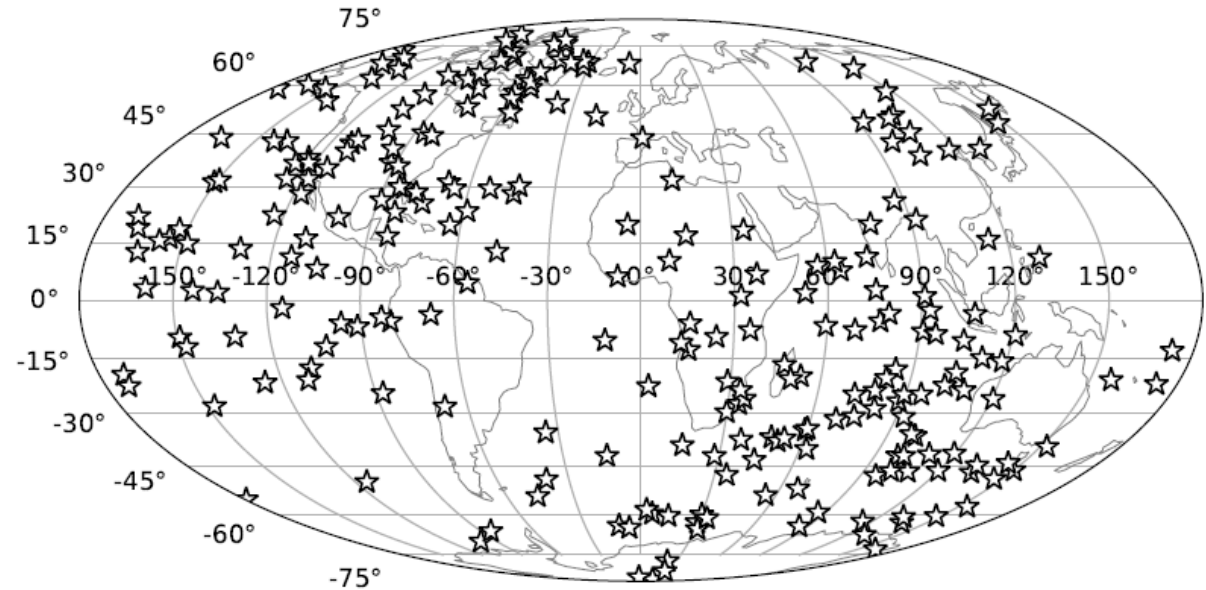
# How the inputs obtained?:

In 2015 scenario in [1]

\* Found events (630)



\* Used events (248)



# Reference: the inputs:

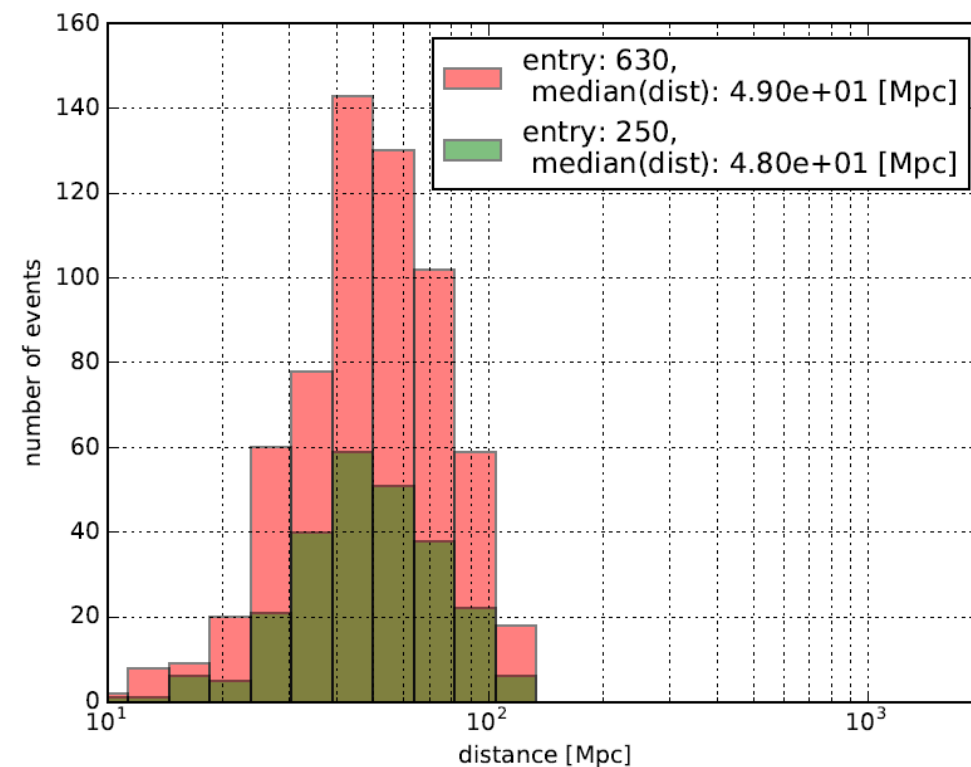
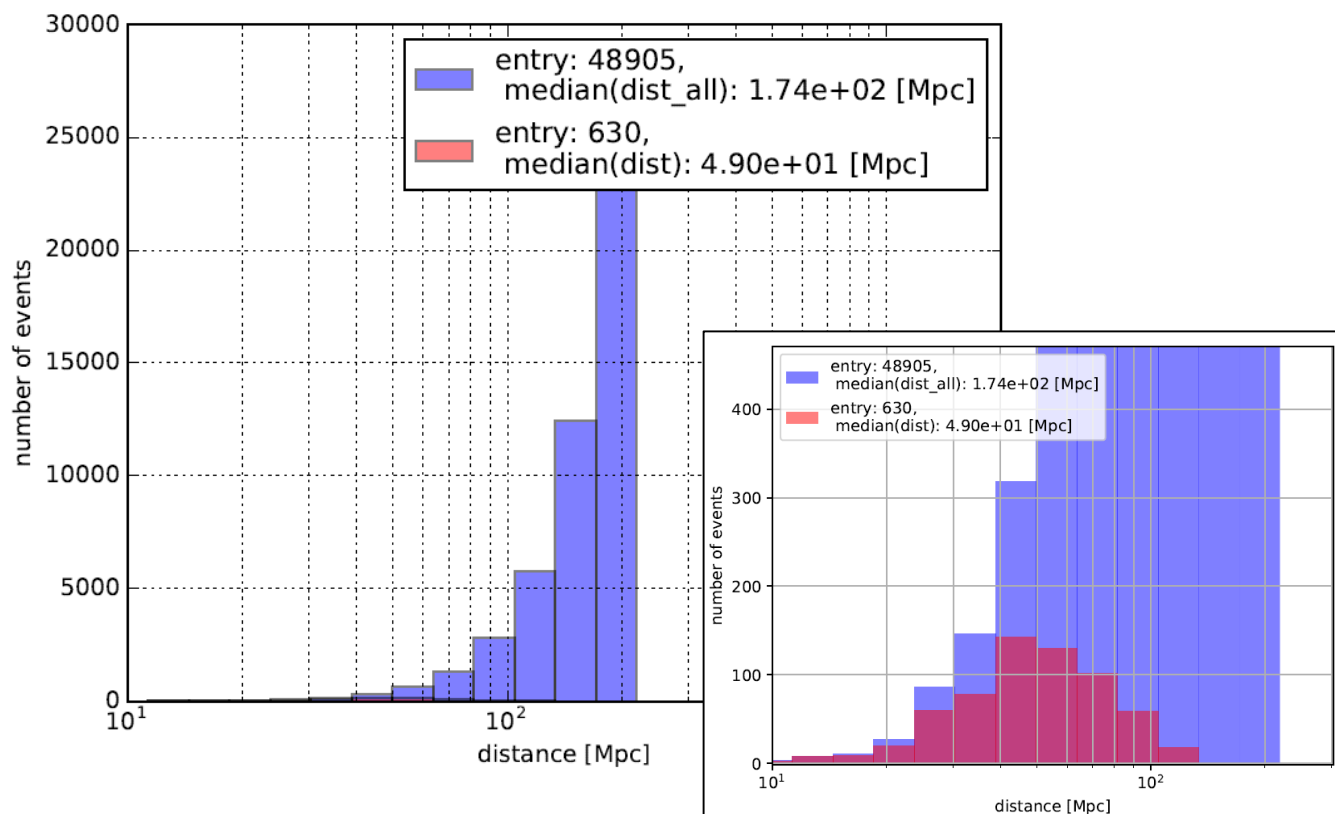
In 2015 scenario in [1]

\* Configuration (number of events)

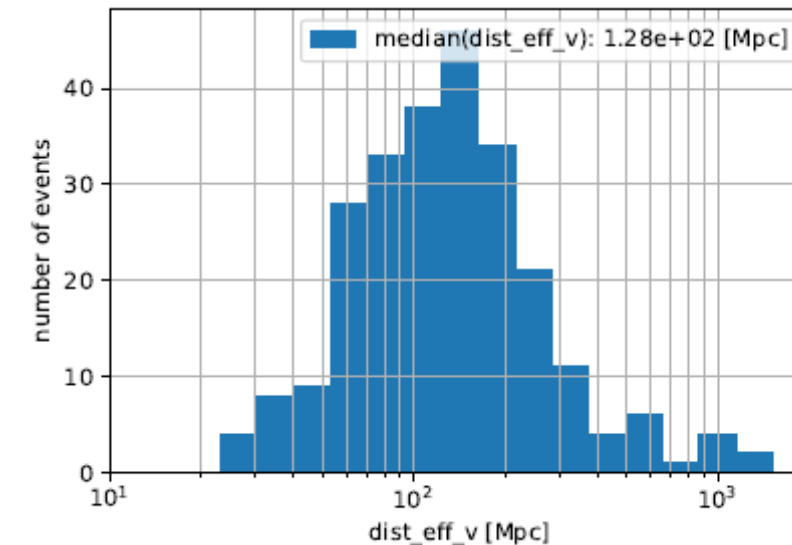
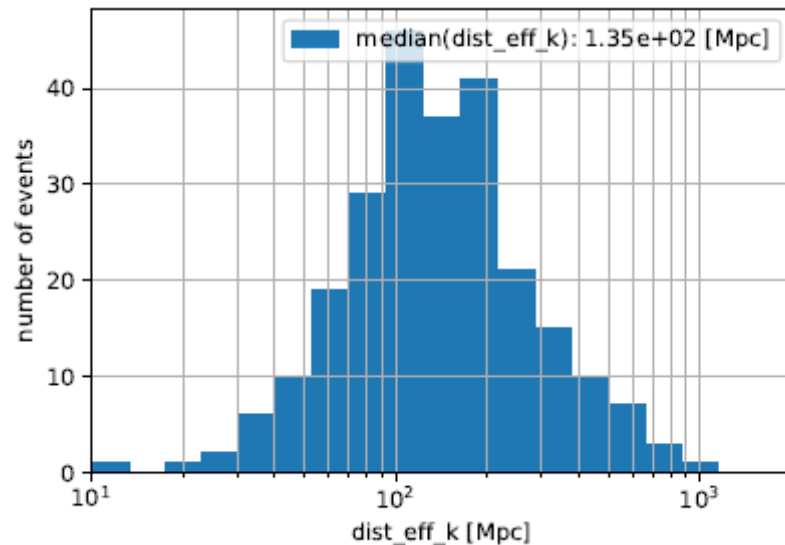
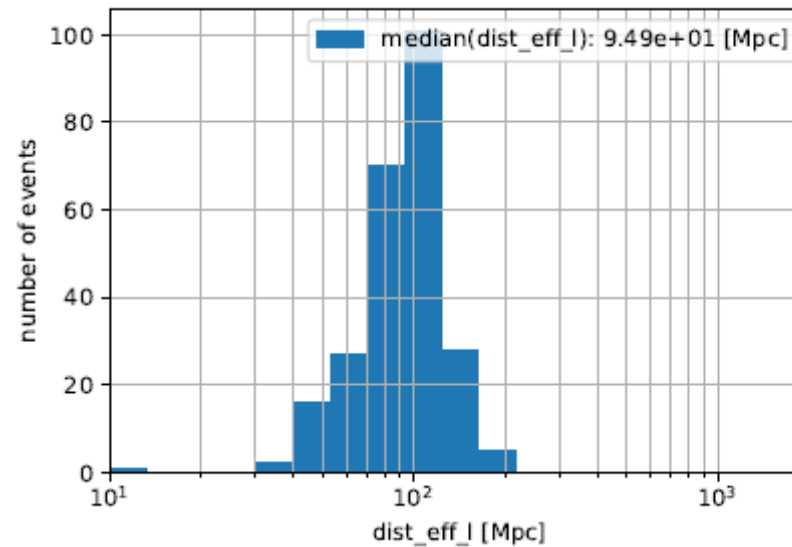
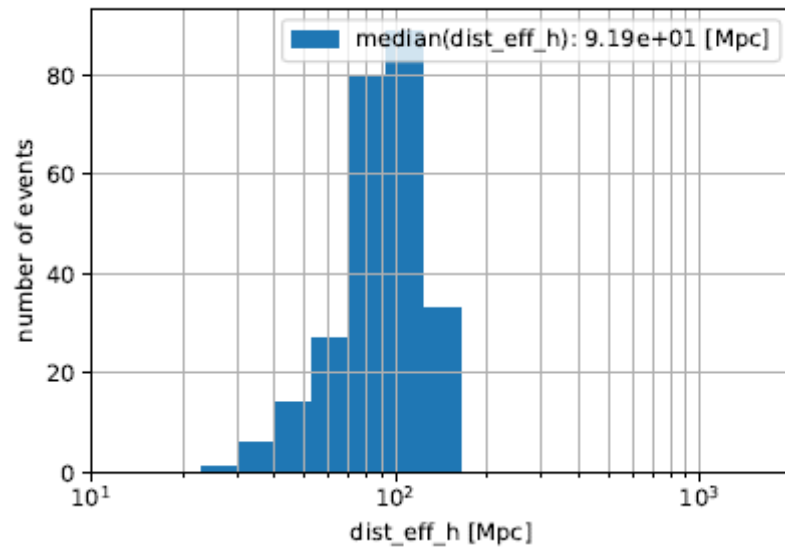
\* Component mass: Uniform [  $1.2 M_{\odot}$  :  $1.6 M_{\odot}$  ]

\* All injections (48905)  $\longrightarrow$  \* Found events (630)  $\longrightarrow$  \* Used in simulation (250)

Randomly selected in order to save computational cost.



# Effective distances of the injections:



Expected SNR,  $\rho$ :

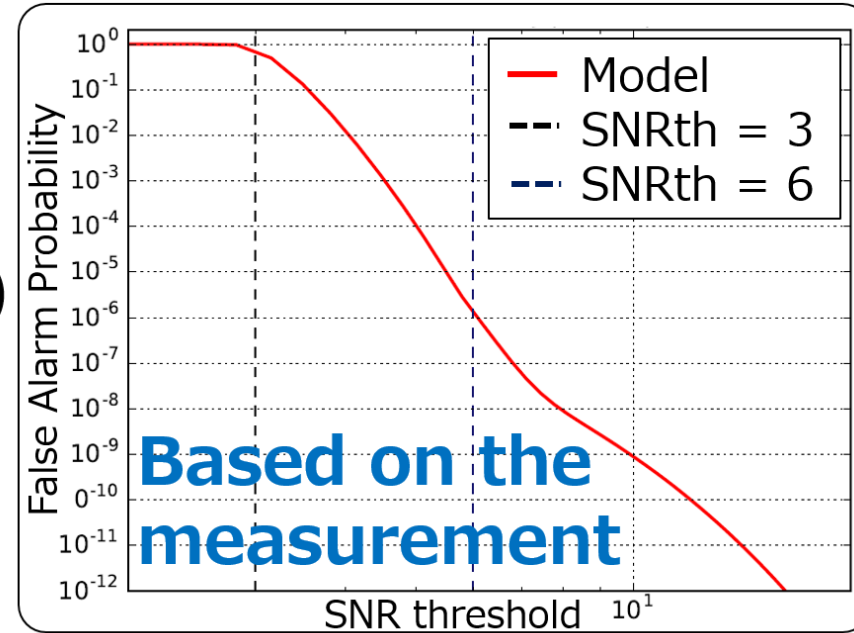
$$\rho = \frac{8 * 2.26 * R_{\text{det}}}{D_{\text{eff}}}$$

# Generating & mixing artificial V triggers

## 2. Mixing HLV triggers

$p = \text{random } [0:1]$   
 $FAP = FAP(SNR)$  or  $FAP(SNR_{th})$

$p < FAP \rightarrow HL V_r$   
 $p > FAP \ \& \ SNR > SNR_{th} \rightarrow HL V_i$   
 $p > FAP \ \& \ SNR < SNR_{th} \rightarrow HL$



noise. (*Right*) False alarm probability (FAP) as a function of the SNR threshold, computed as  $FAP = 1 - \exp(-R T)$ , with  $R$  the rate of triggers above threshold per template, derived from the distribution on the left, and  $T = 70$  ms. At low

Table 2.1: Procedure for generating coincident events for LIGO-Virgo network.  $p_V$  is a random number from a uniform distribution between 0 and 1.  $FAP_V$  is the false alarm probability at a given SNR threshold in Virgo.

Conditions	Generated coincidences
if $p_V < FAP_V(\max(SNR_V^{th}, SNR_V^{expected}))$	H L V <sub>n</sub>
else	
if $SNR_V^{expected} > SNR_V^{th}$	H L V <sub>i</sub>
if $SNR_V^{expected} < SNR_V^{th}$	H L

# Generating & mixing artificial V triggers

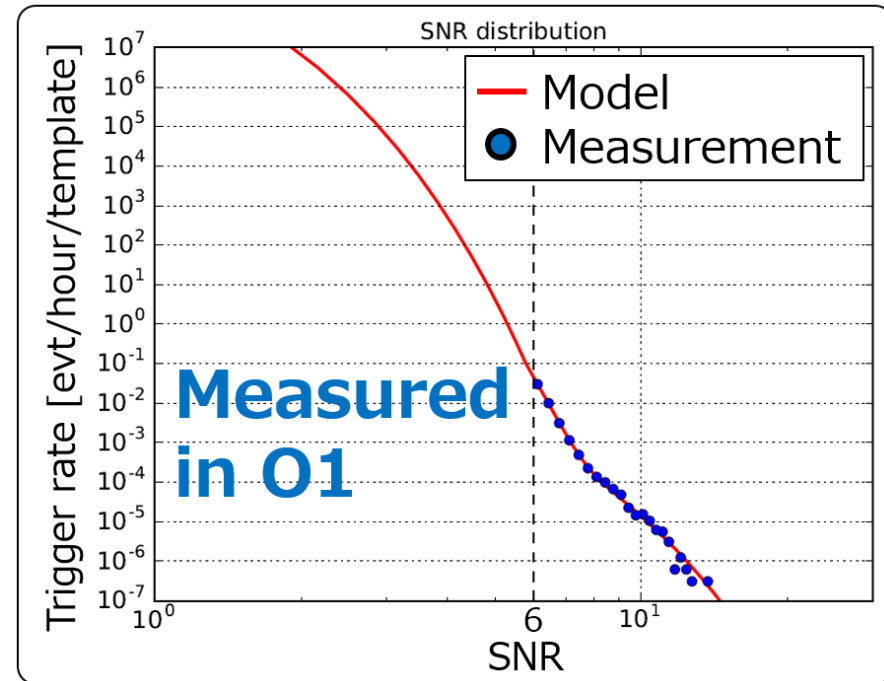
## 1. Generating V triggers

**$V_r$  : V trigger based on random parameters**

$SNR$  = random following measurement

$Time$  =  $t_{H1}$  or  $t_{L1}$   
+ random [-35ms:35ms]

$Phase$  = random  $[0:2\pi]$



**$V_i$  : V trigger based on injection parameters**

$SNR$  = metadata + Gauss(0,1)

$Time$  = metadata + Gauss(0,  $0.66 \text{ ms} * \frac{6}{SNR}$ )

$Phase$  = metadata + Gauss(0, 0.25 rad)

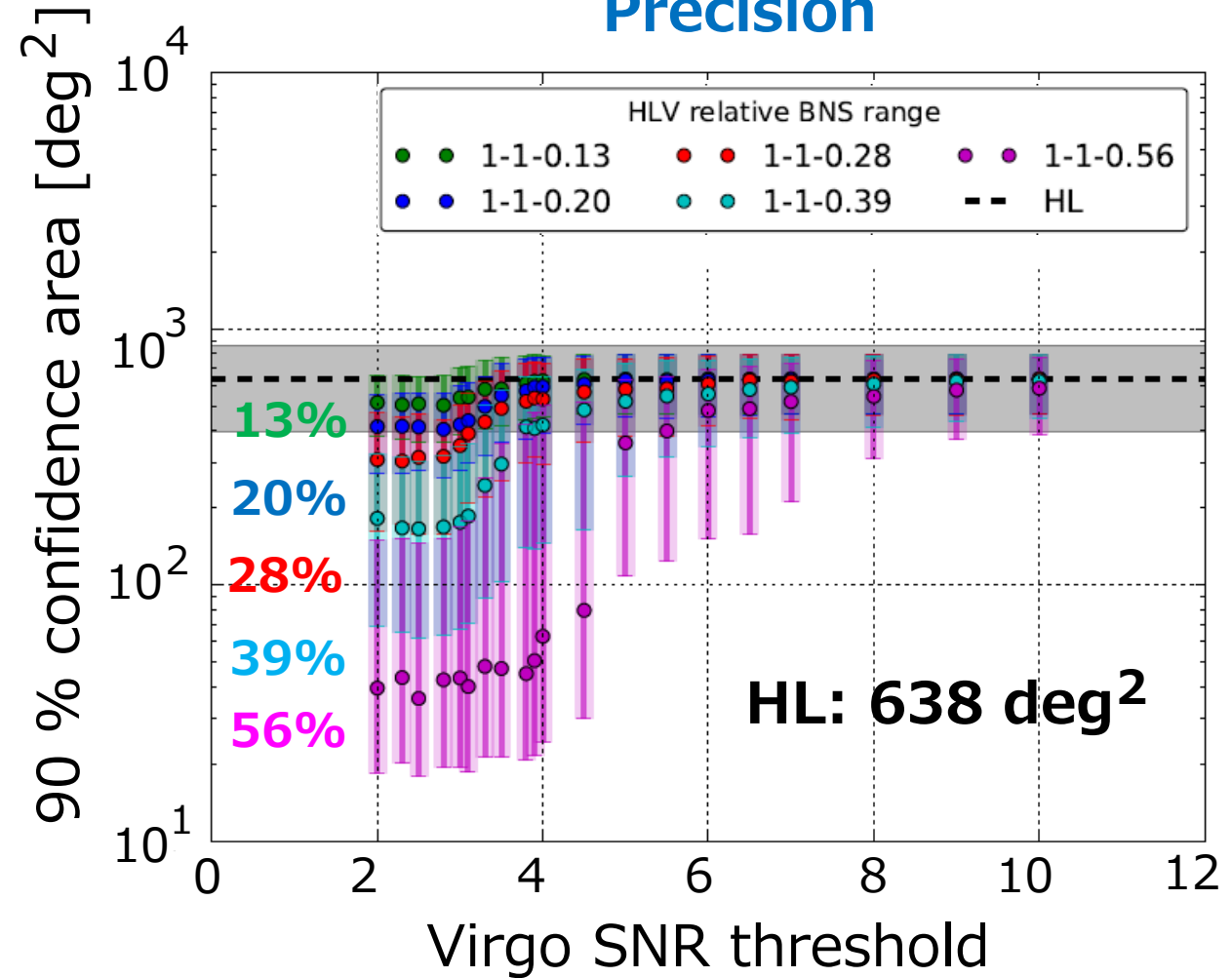
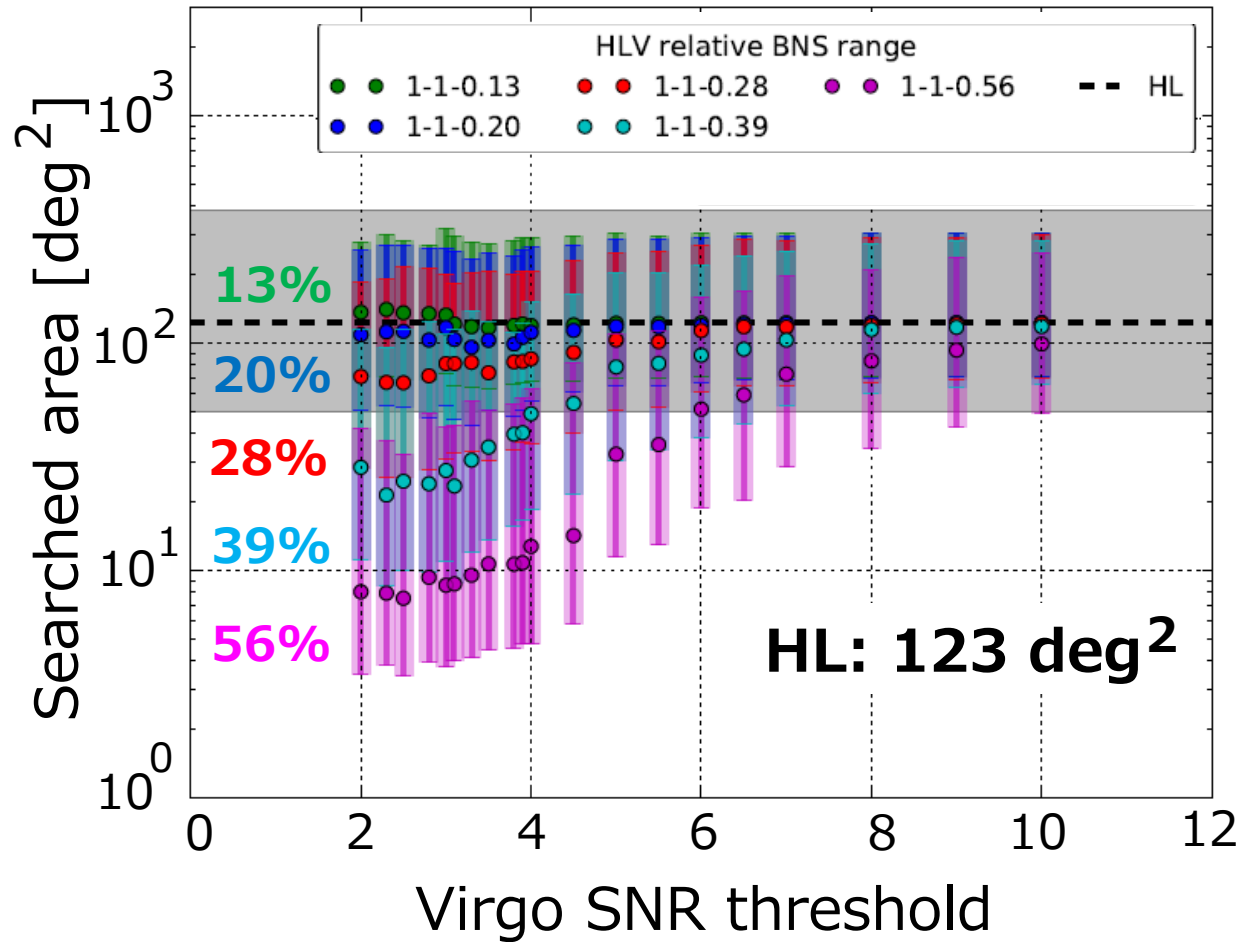


# Performance (HLV):

(SNR threshold for H, L = 5.)

## Accuracy

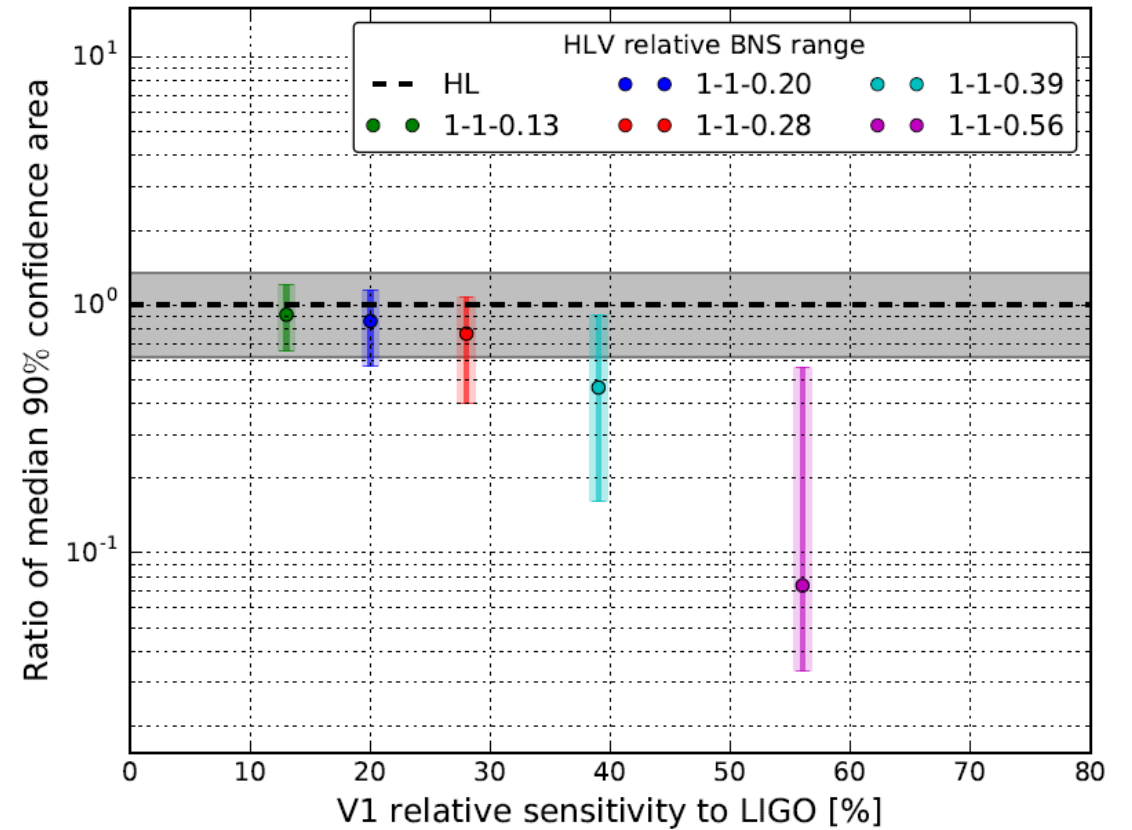
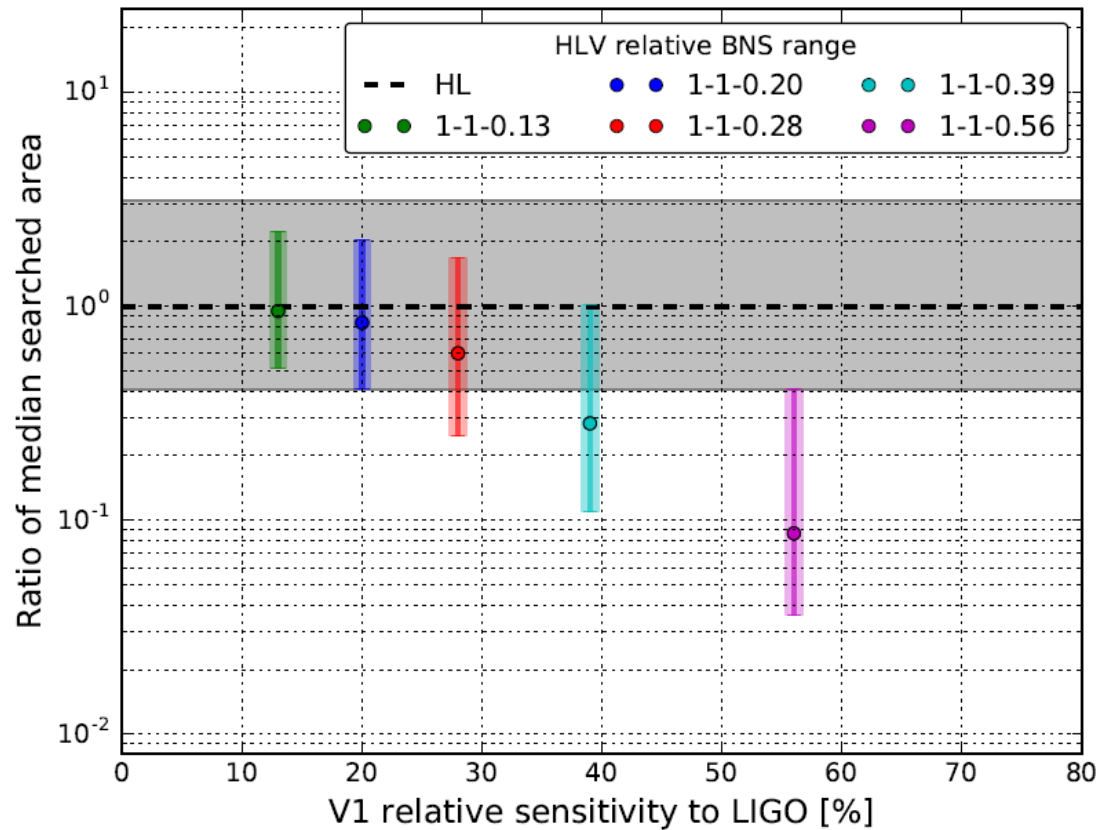
## Precision



# Performance of HL- vs. HLV-hierarchical-network:

RnageH : RangeL = 54 : 54 (Mpc)

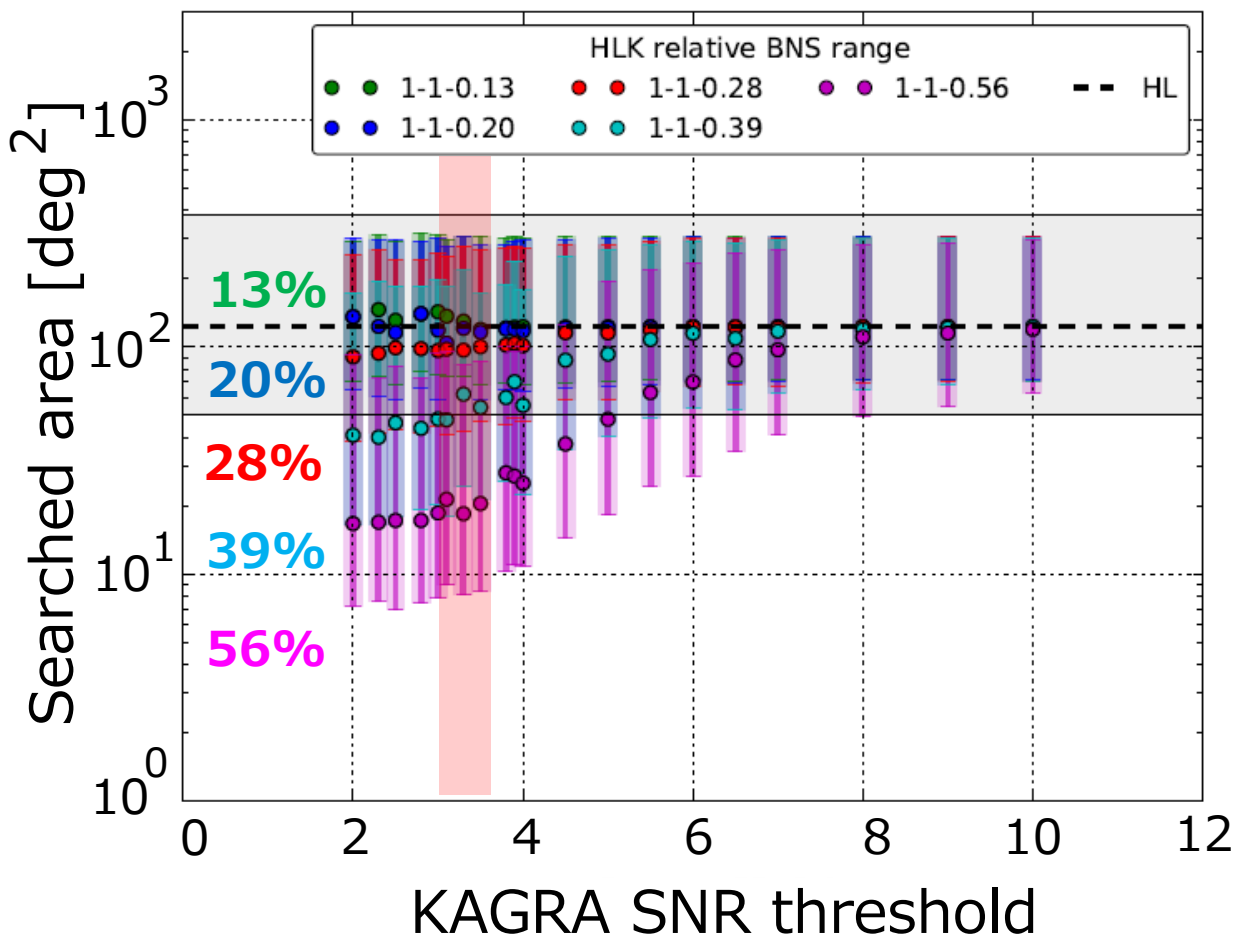
H1th : L1th : V1th = 5 : 5 : 3.5



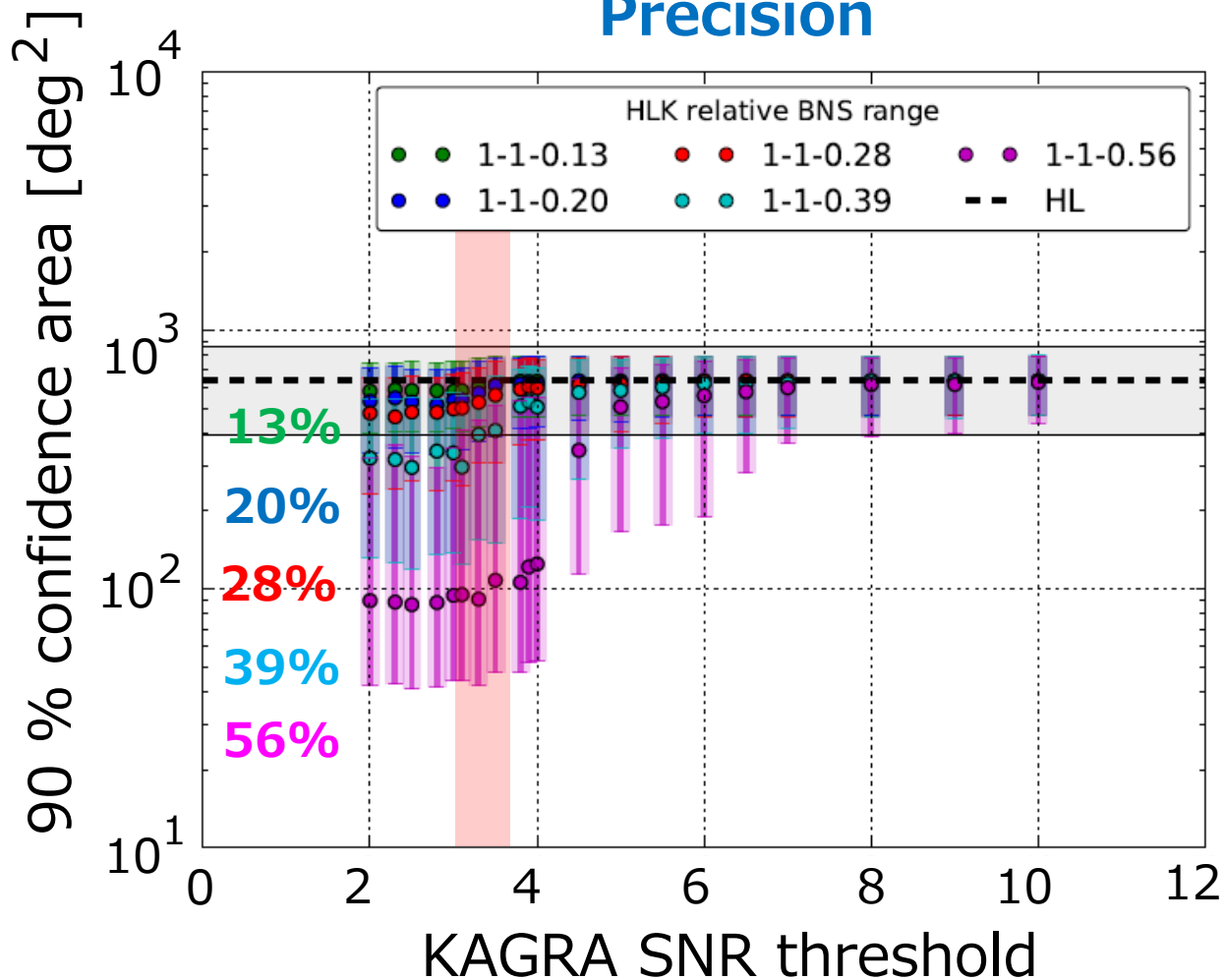
# Performance (HLK):

(SNR threshold for H, L = 5.)

## Accuracy



## Precision

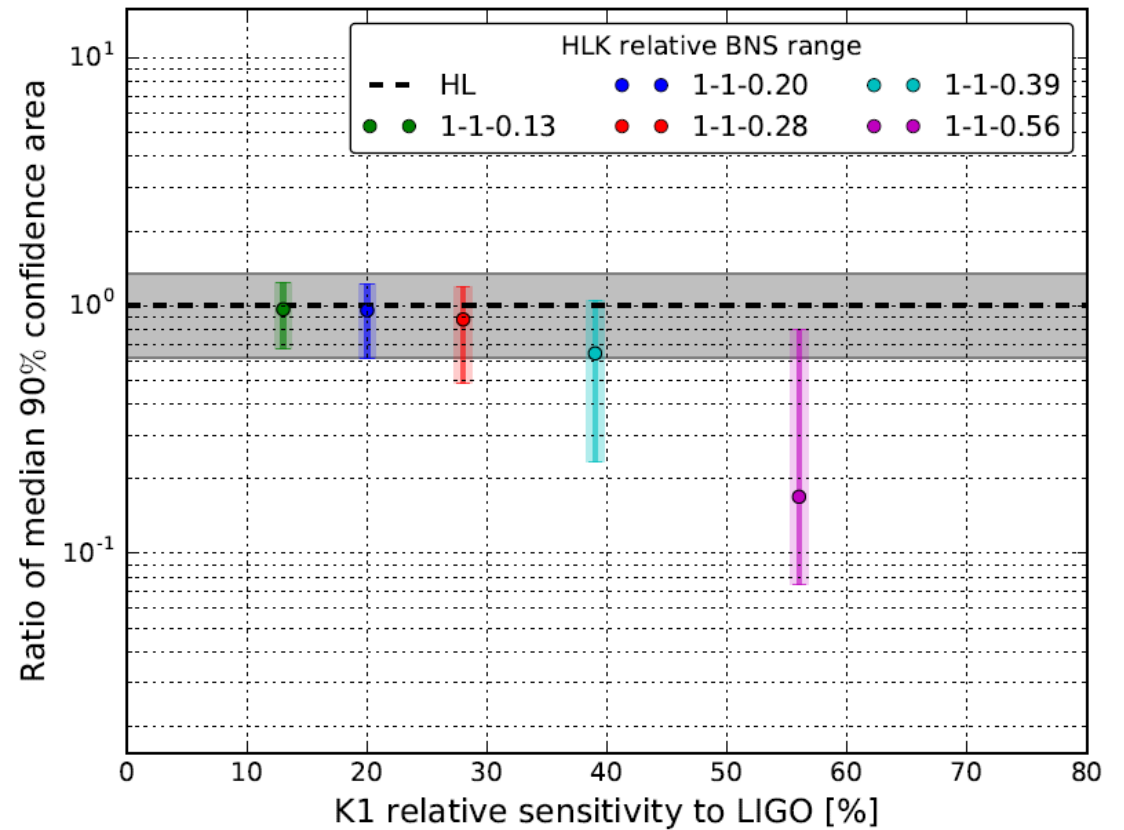
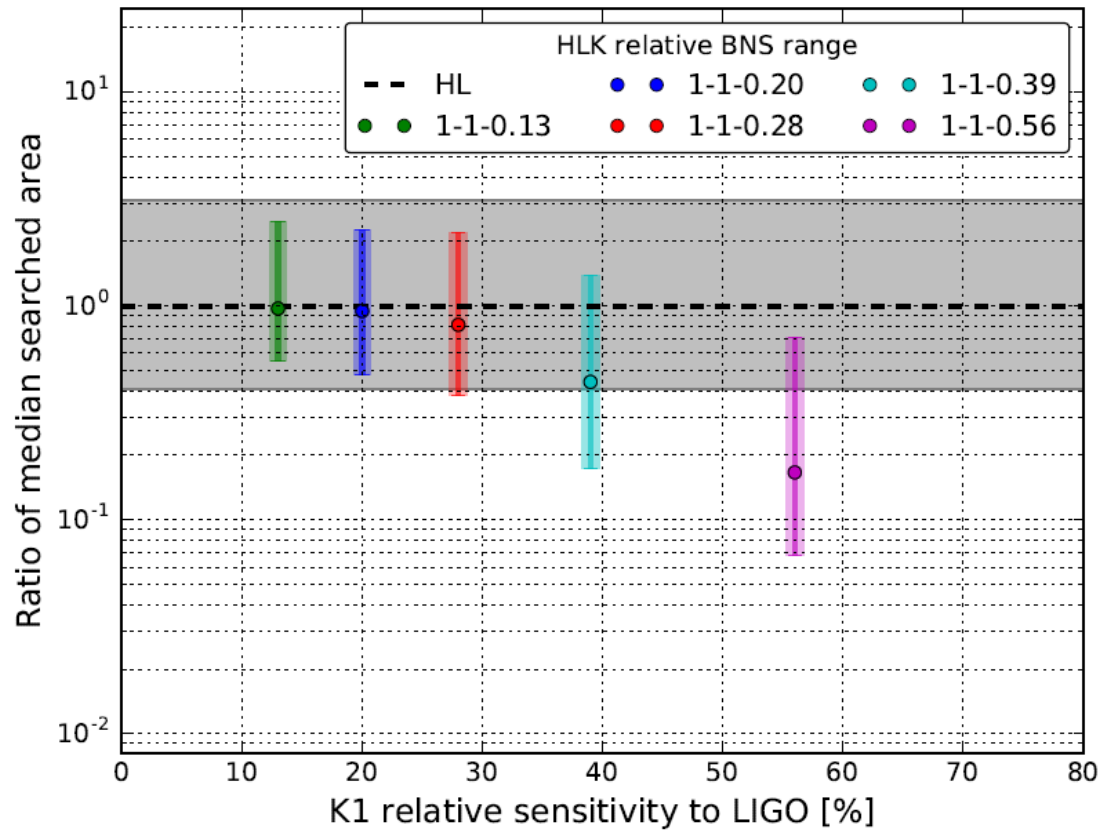


Relative sensitivity = (1, 1, >0.28), SNR threshold = (5, 5, ~3.5)  
→ becomes improved

# Performance of HL- vs. HLK-hierarchical-network:

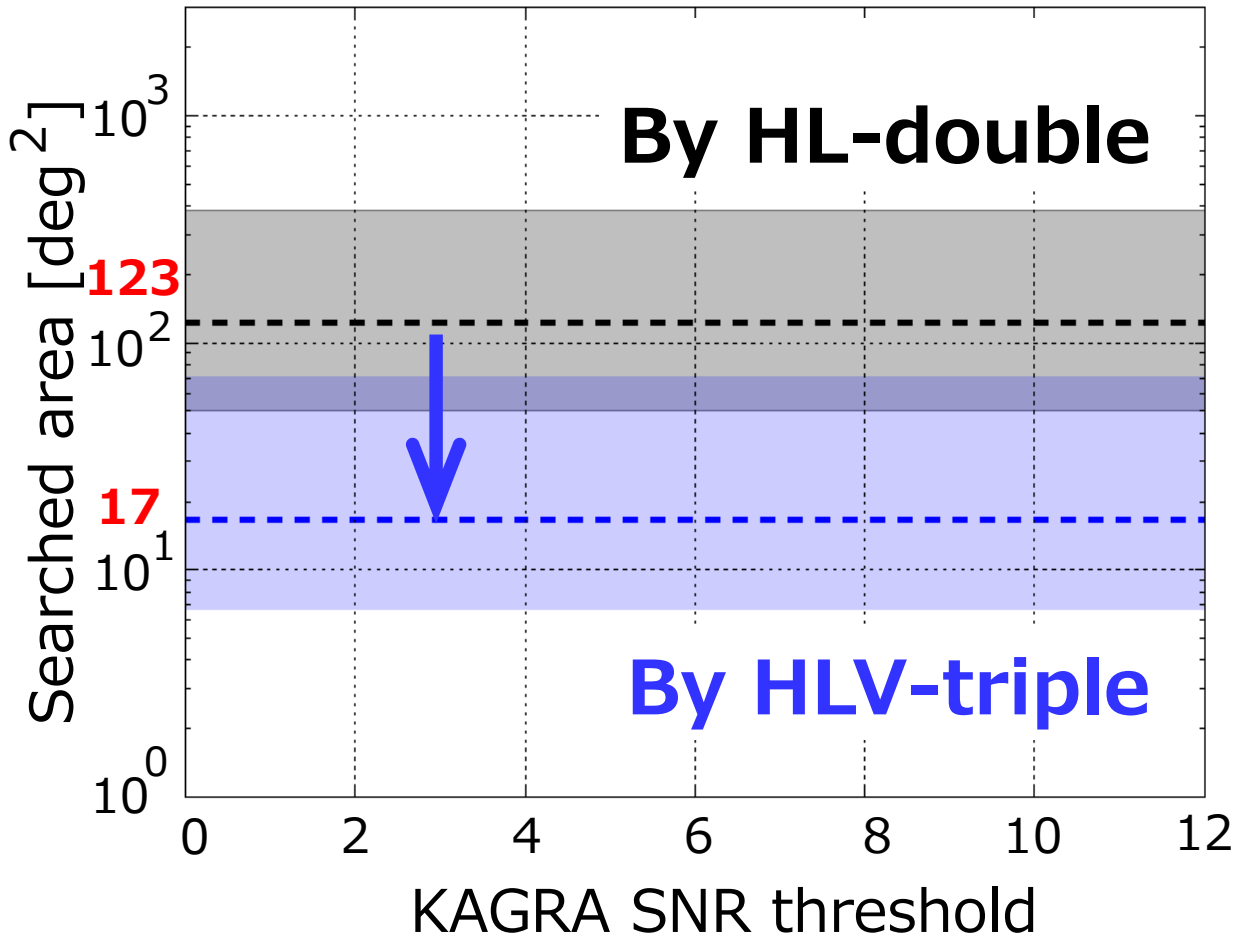
RnageH : RangeL = 54 : 54 (Mpc)

H1th : L1th : K1th = 5 : 5 : 3.5

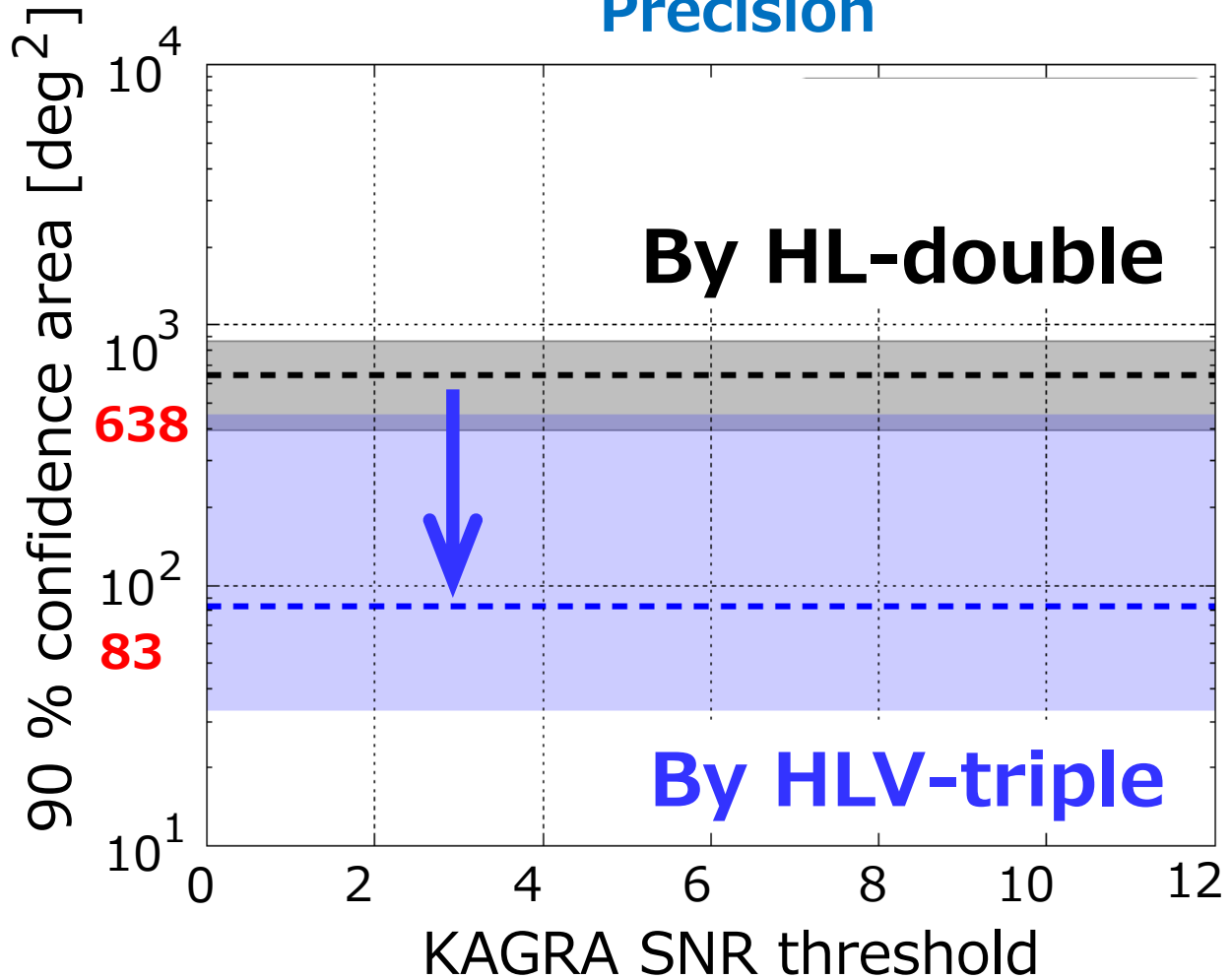


# Performance (HL vs. HLV): (SNR threshold for H, L, V = 5, 5, 3.5)

Accuracy



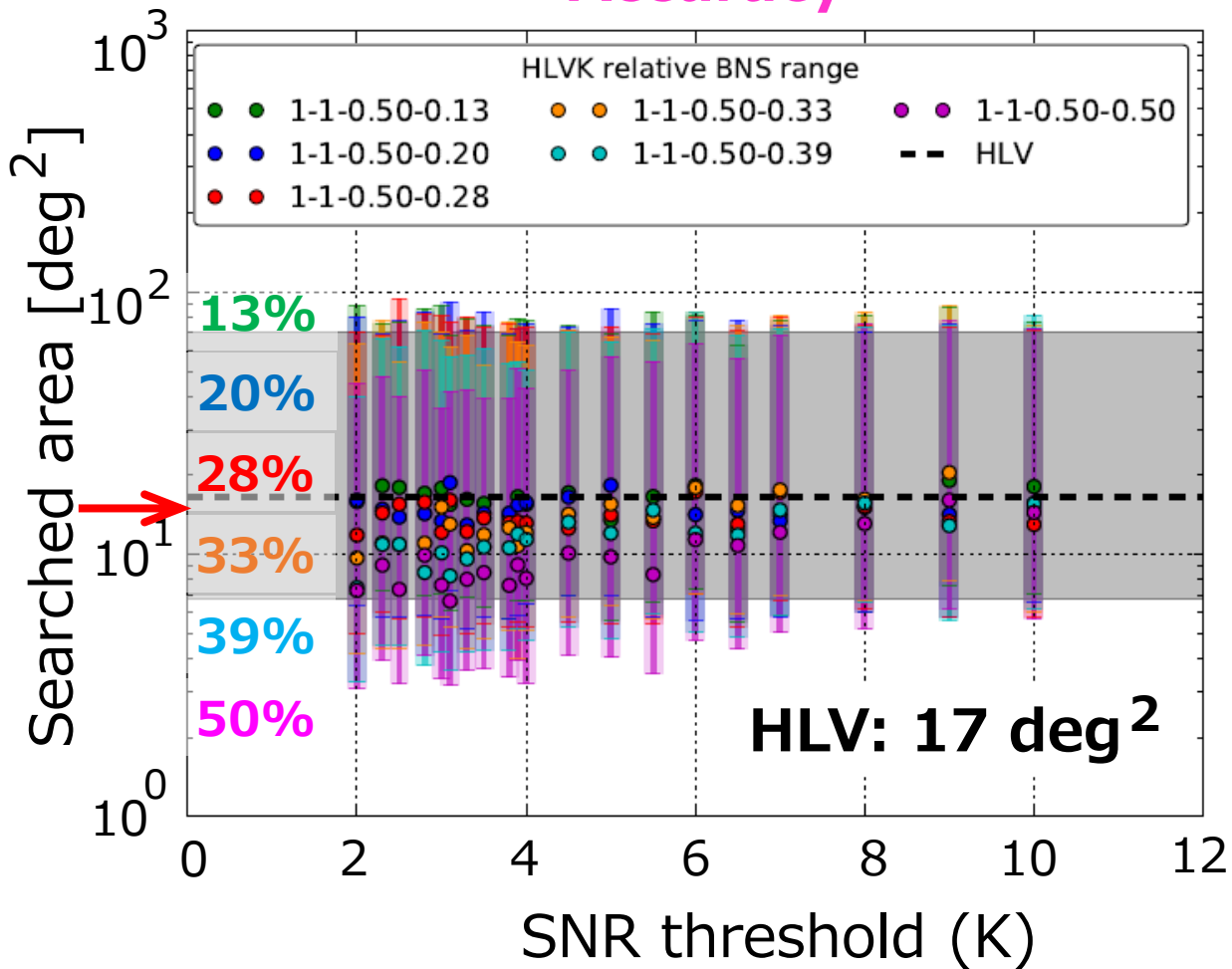
Precision



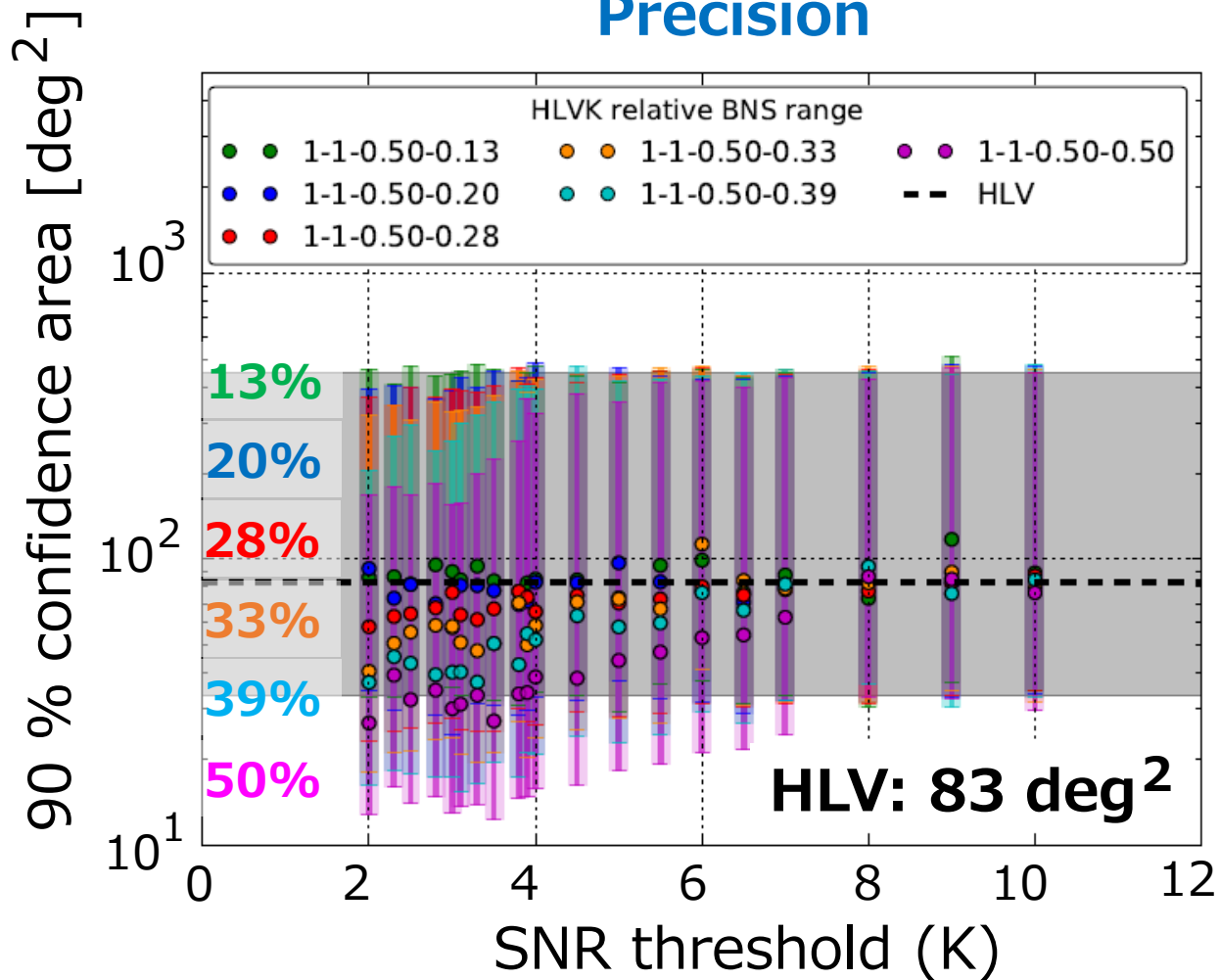
# Performance (HLVK):

(SNR threshold for H, L, V = 5, 5, 3.5)

## Accuracy



## Precision



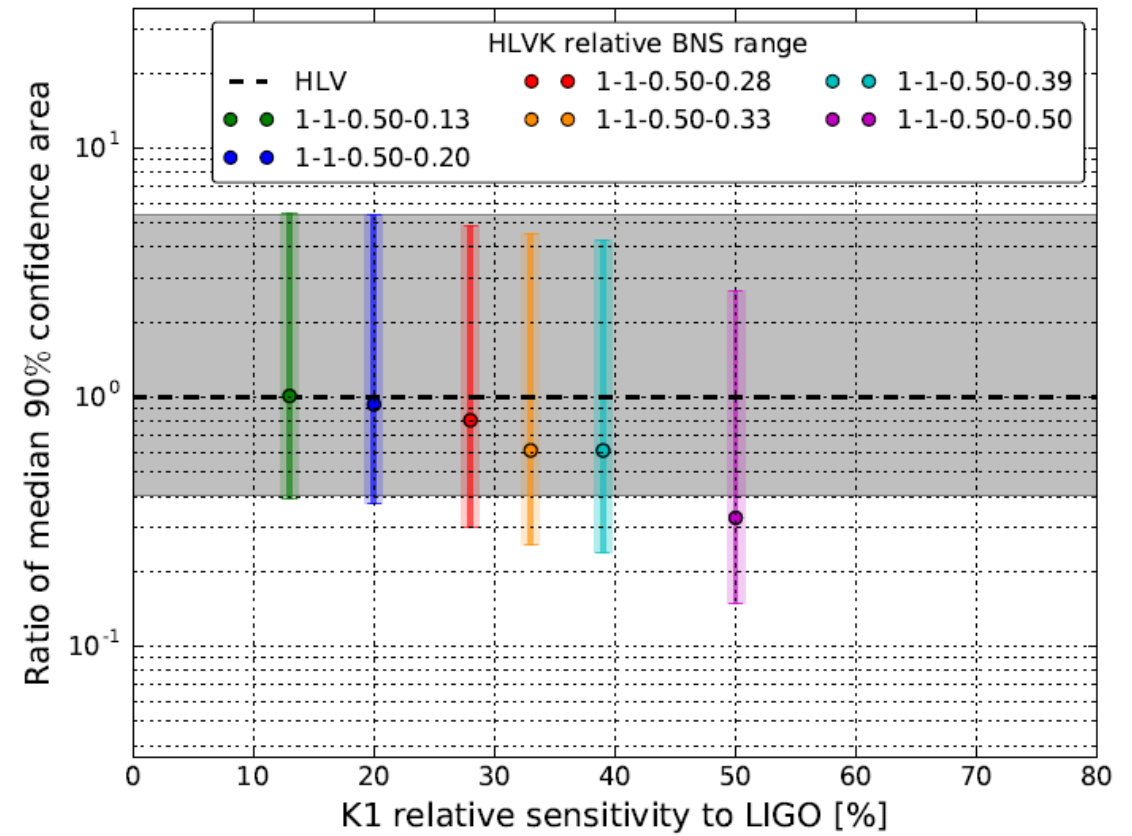
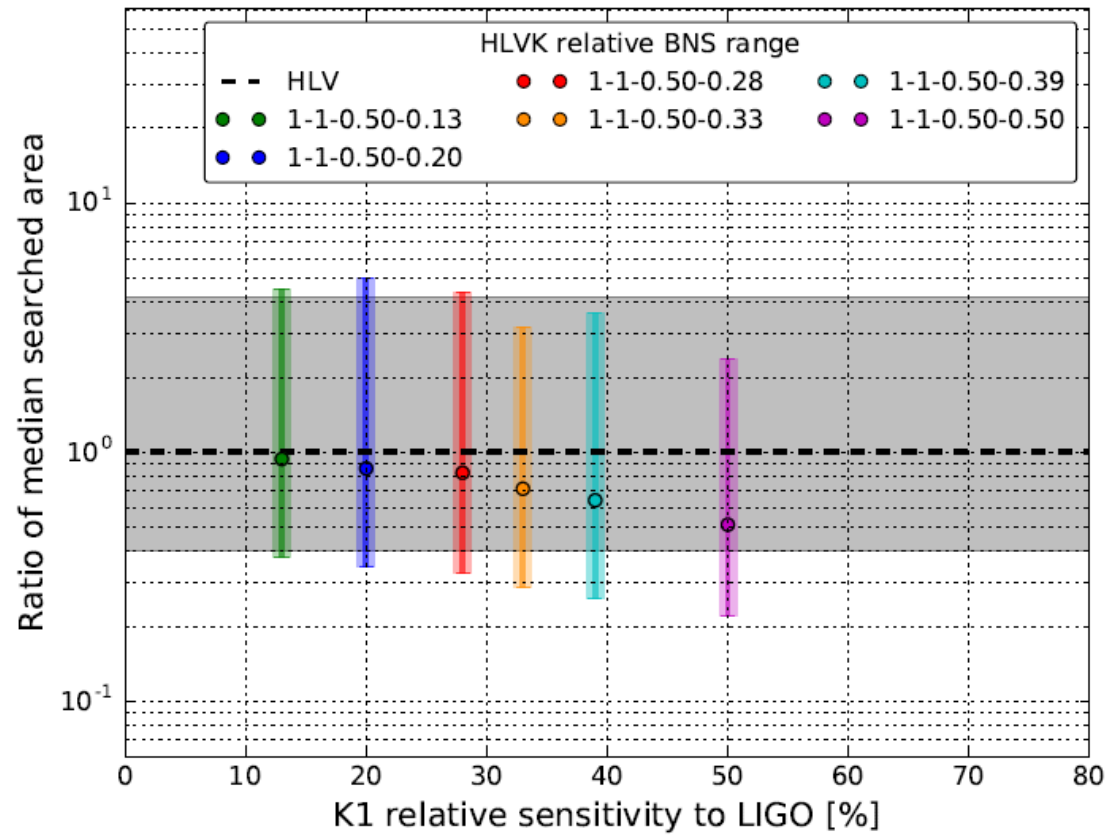
Relative sensitivity = (1, 1, >0.3), SNR threshold = (5, 5, ~3.5)  
→ Effectively improved



# Performance of HL- vs. HLK-hierarchical-network:

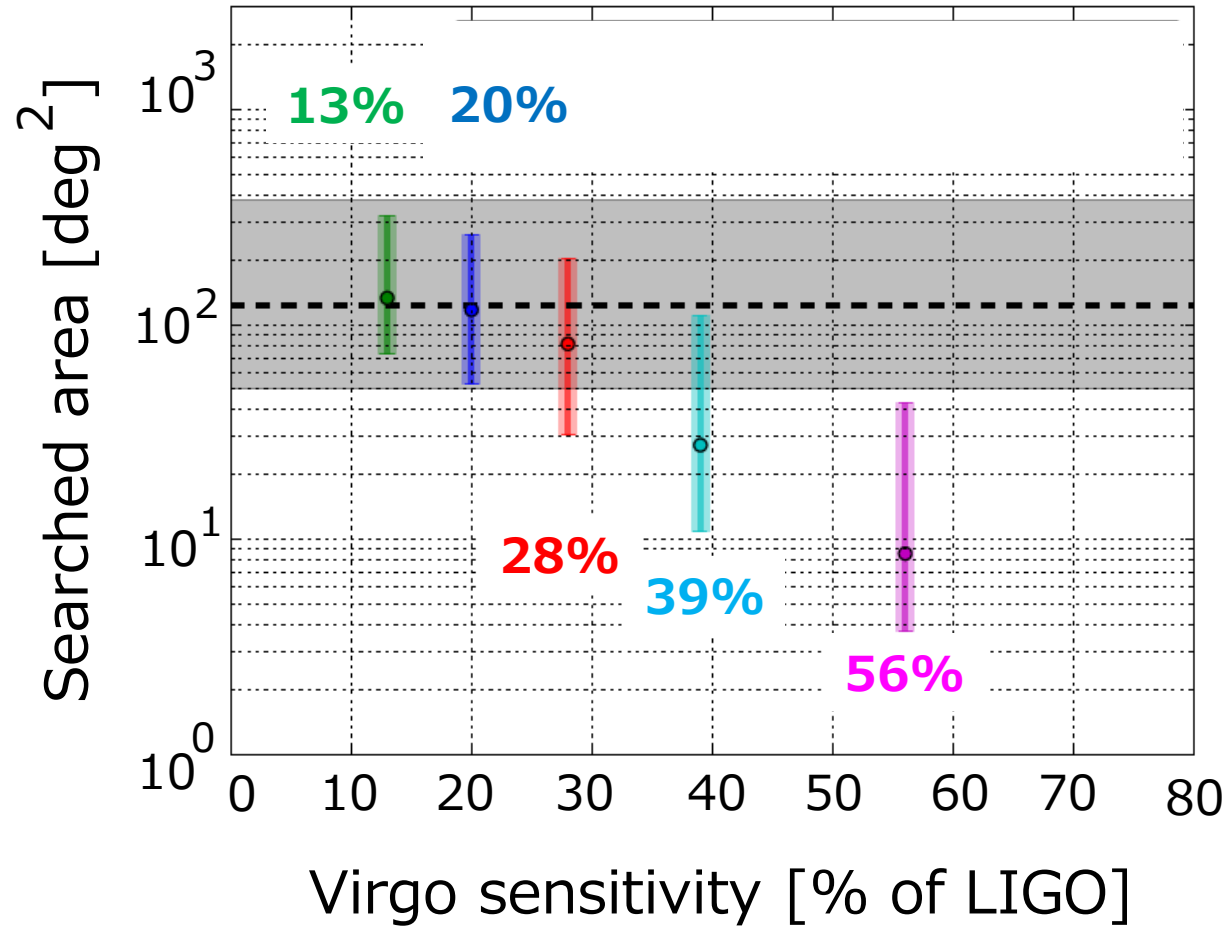
RnageH : RangeL : RangeV = 54 : 54 : 27 (Mpc)

H1th : L1th : V1th : K1th = 5 : 5 : 3.5 : 3.5

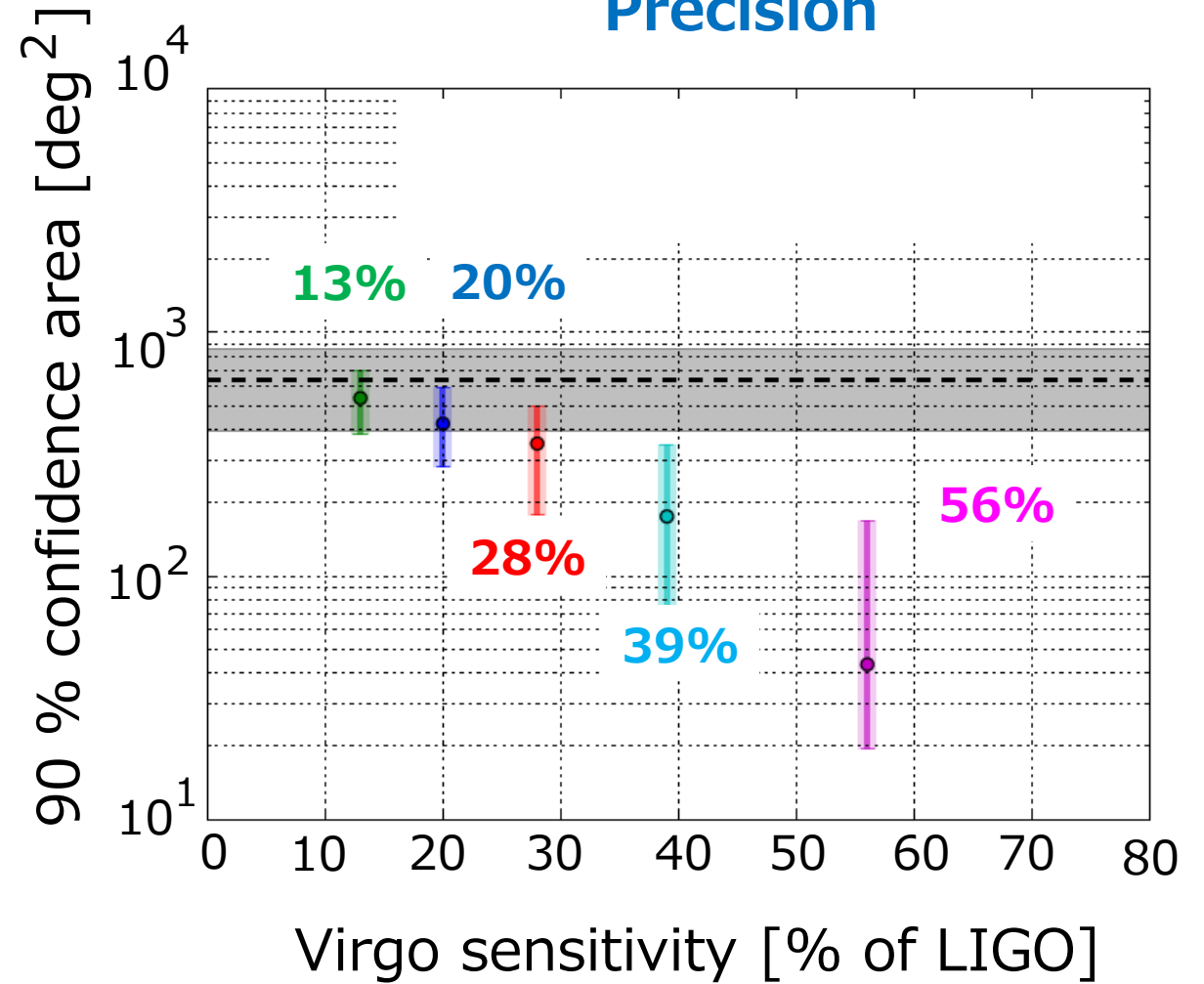


# Performance (HLV): (SNR threshold for H, L, V = 5, 5, 3.0)

## Accuracy



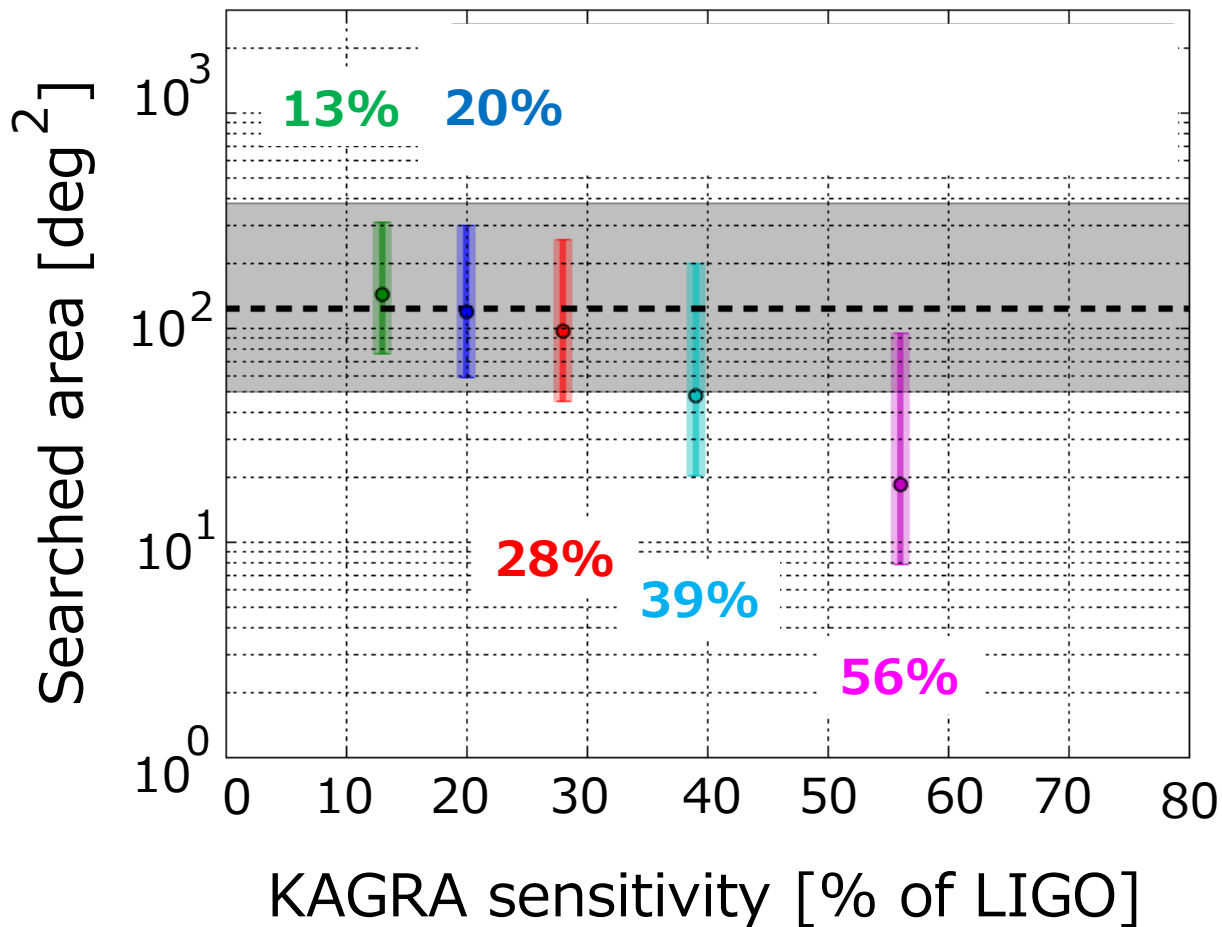
## Precision



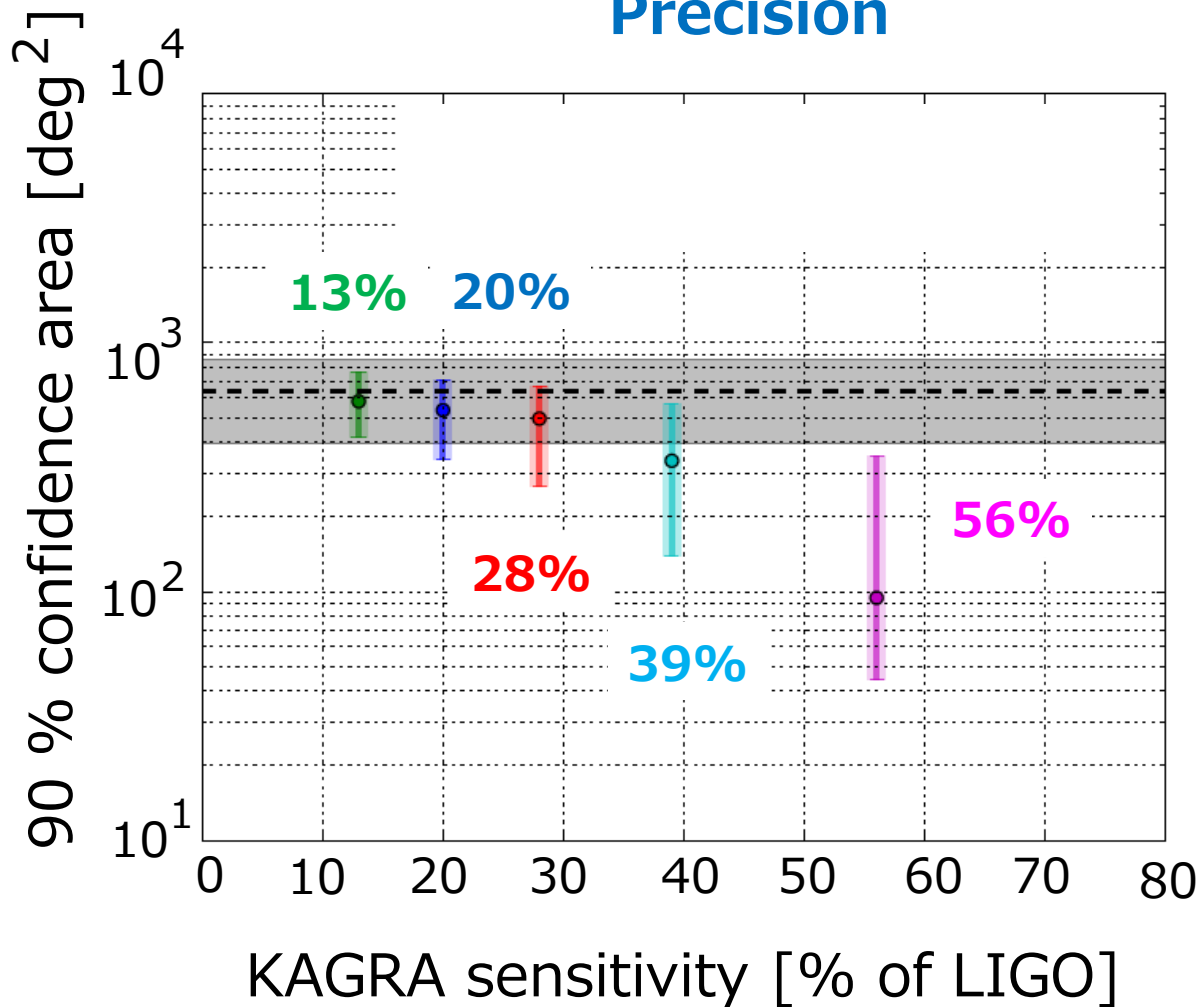
Required: Virgo sensitivity > 20% of LIGO

# Performance (HLK): (SNR threshold for H, L, K = 5, 5, 3.0)

## Accuracy



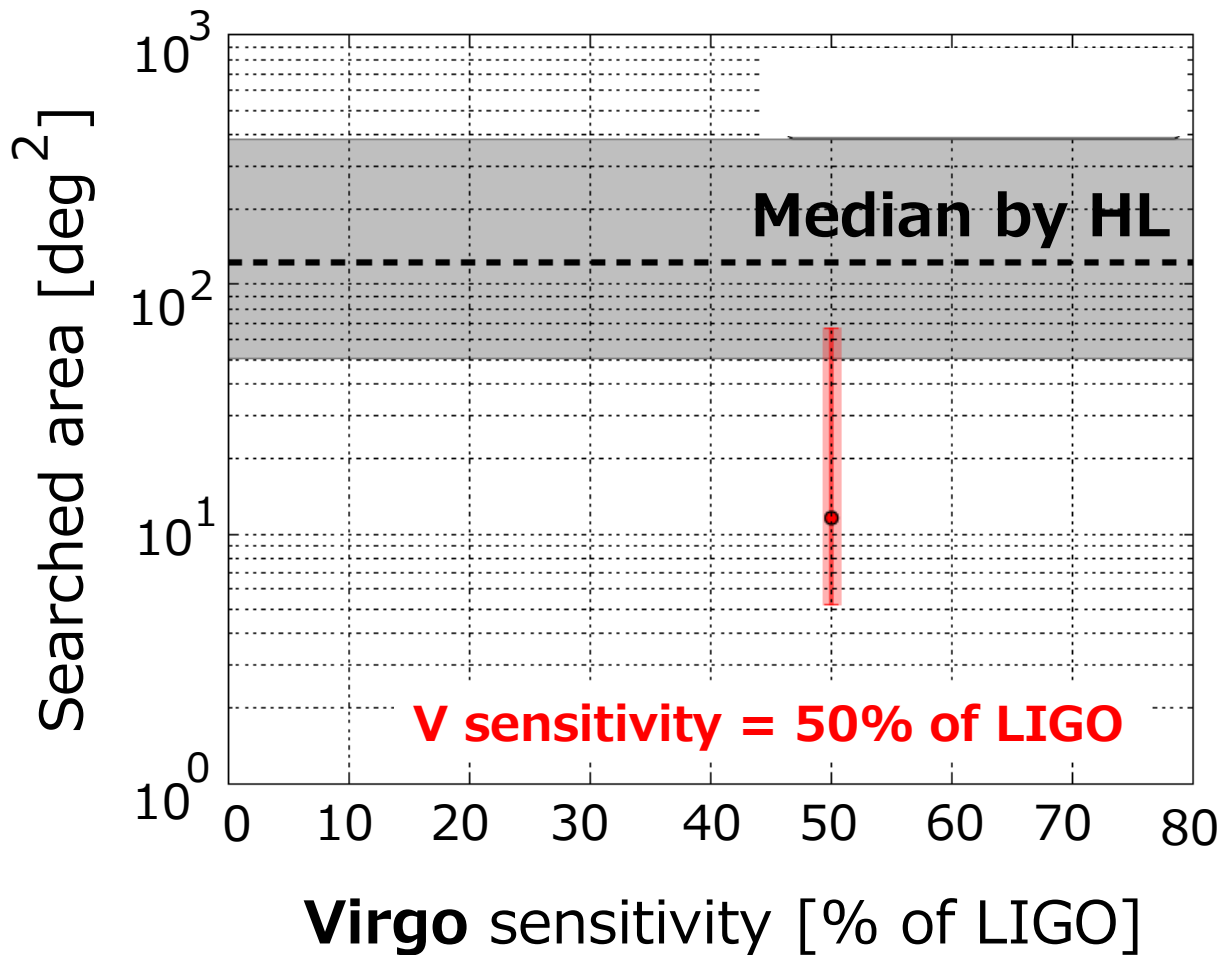
## Precision



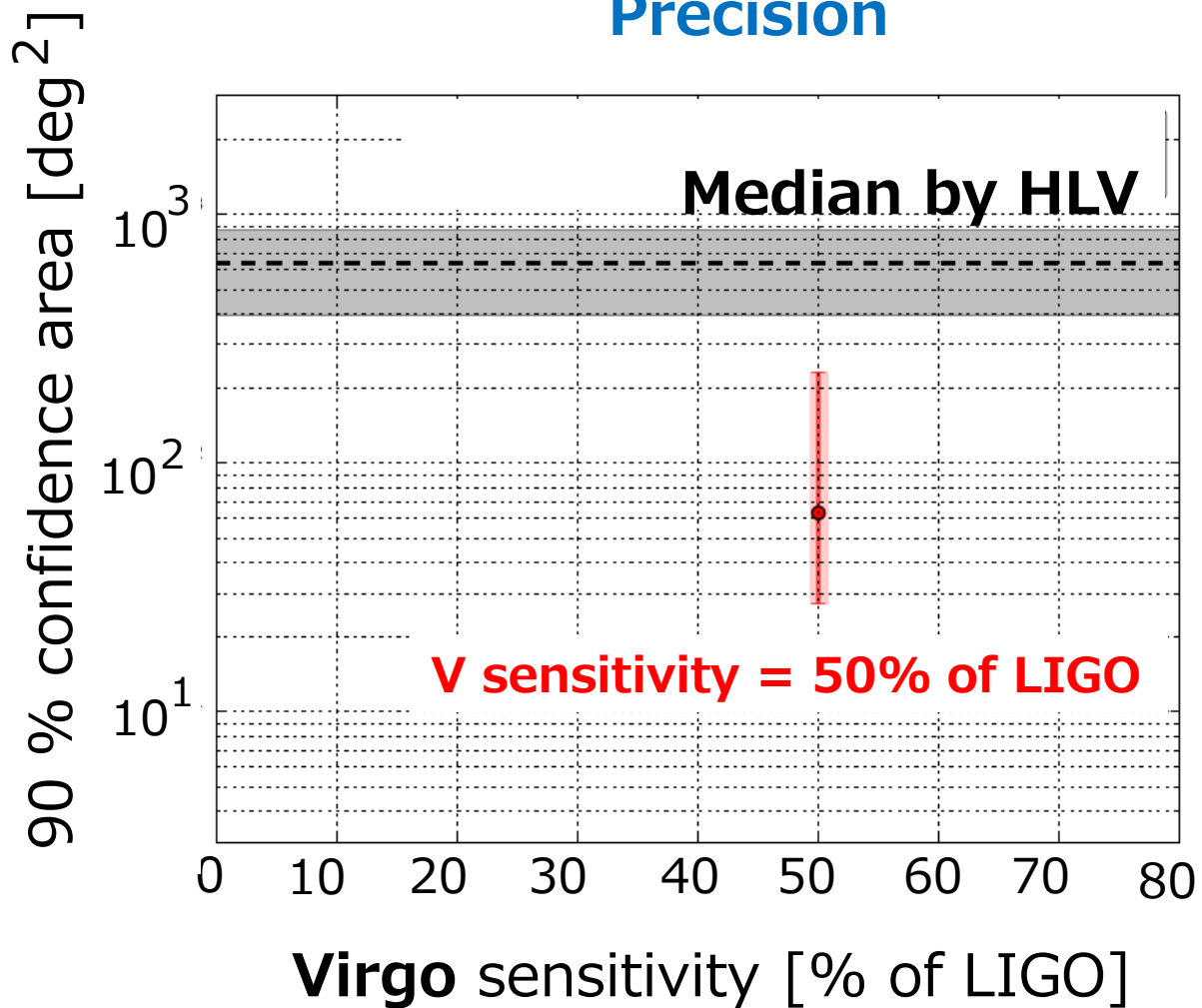
Required: KAGRA sensitivity > 28% of LIGO

# Performance (HLV): (SNR threshold for H, L, V = 5, 5, **3.0**)

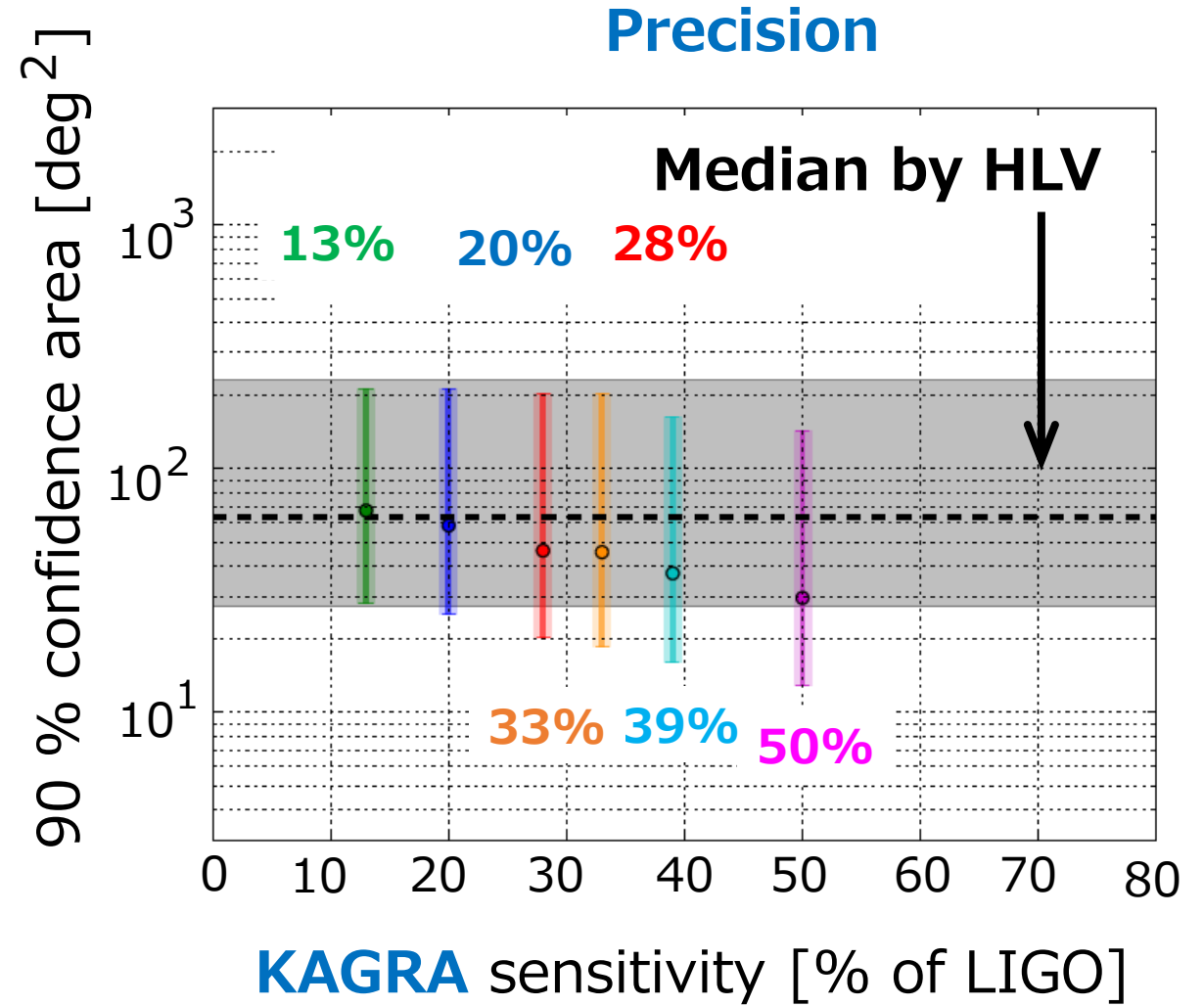
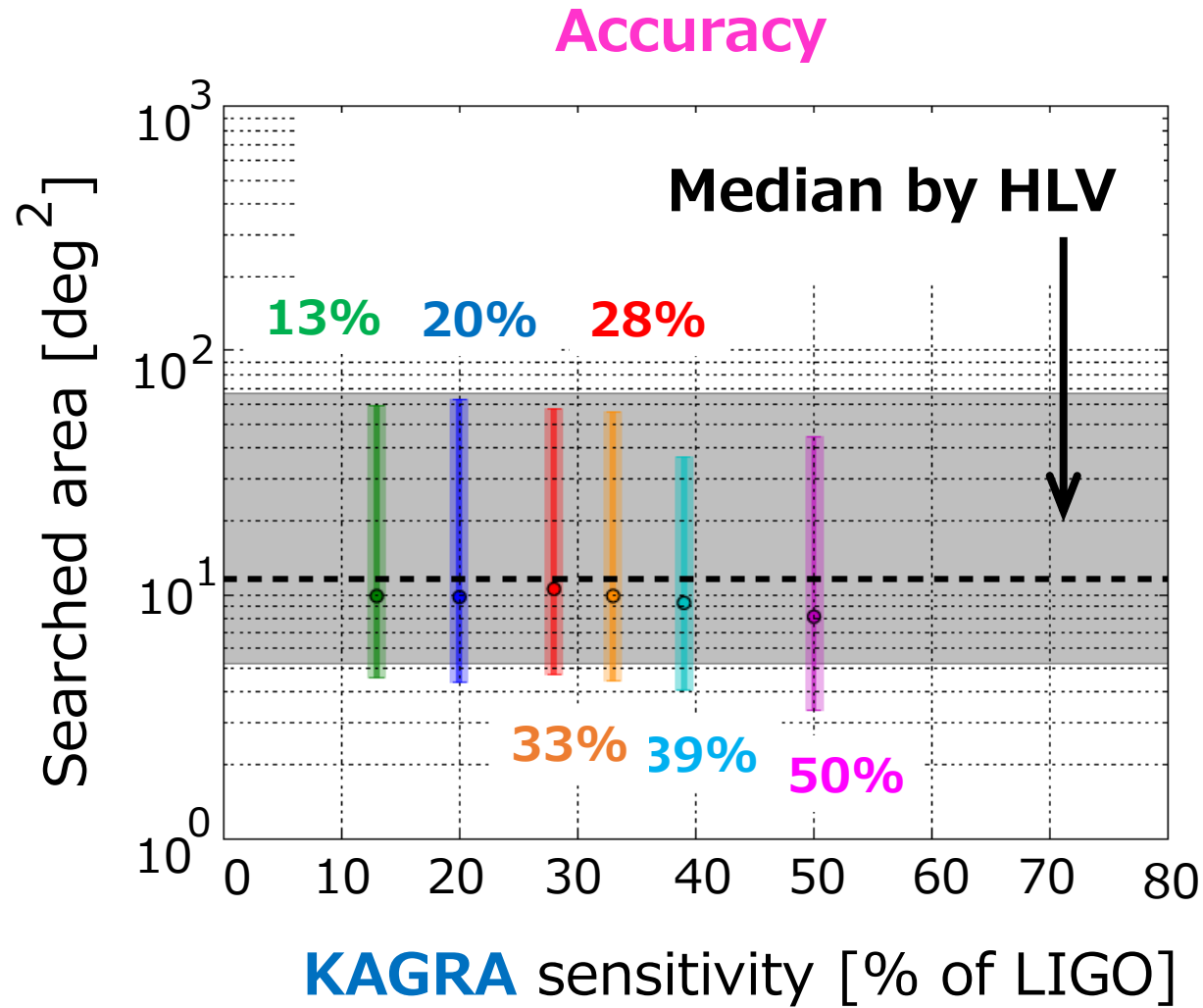
## Accuracy



## Precision



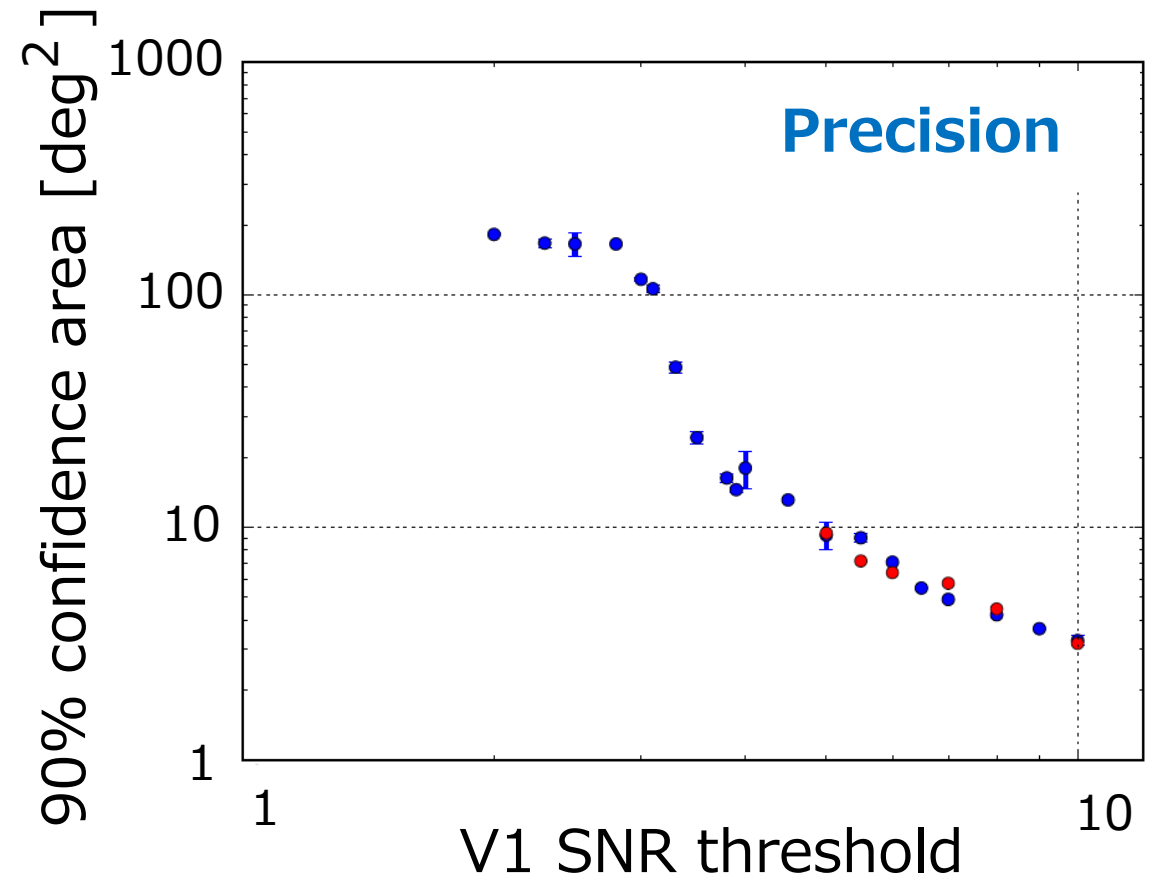
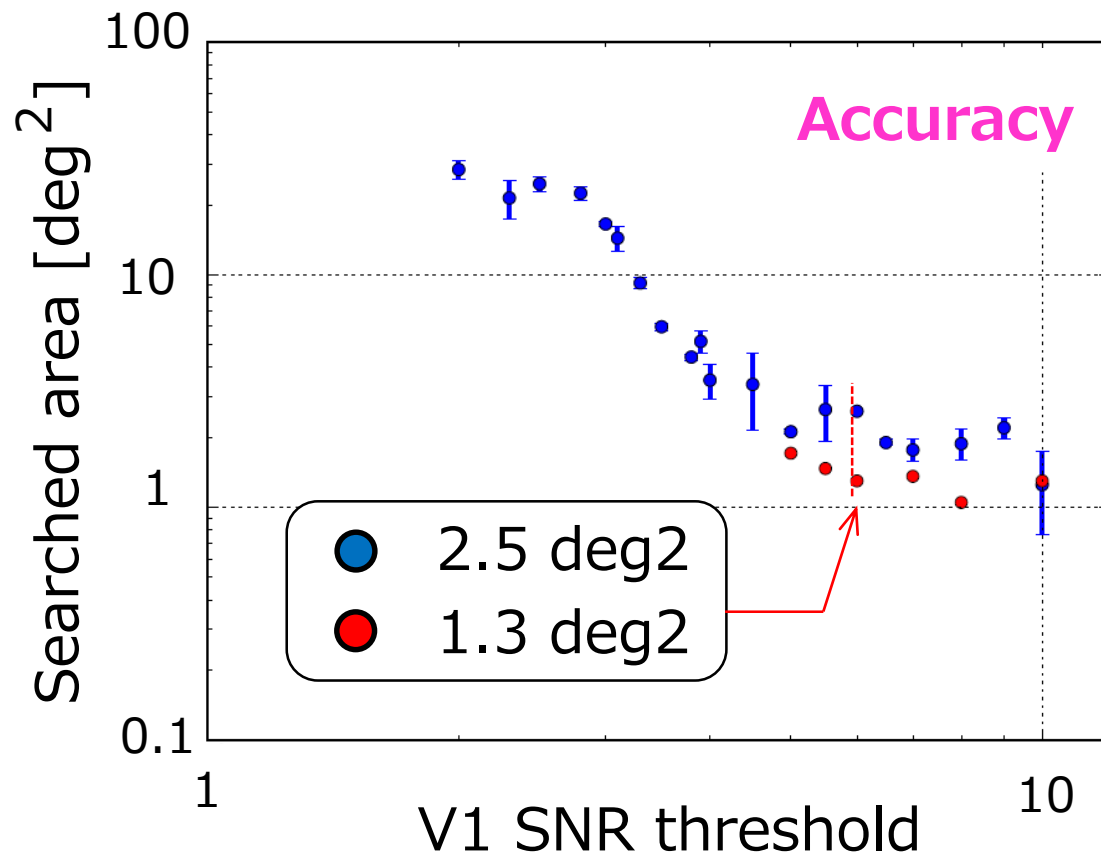
# Performance (HLV $K$ ): (SNR threshold for H, L, V, K = 5, 5, 3.0, 3.0)



Required: KAGRA sensitivity > 28% of LIGO

# Performance of HLV-triggers:

- with artificial triggers
- with actual triggers



Simulation vs. running MBTA → consistent

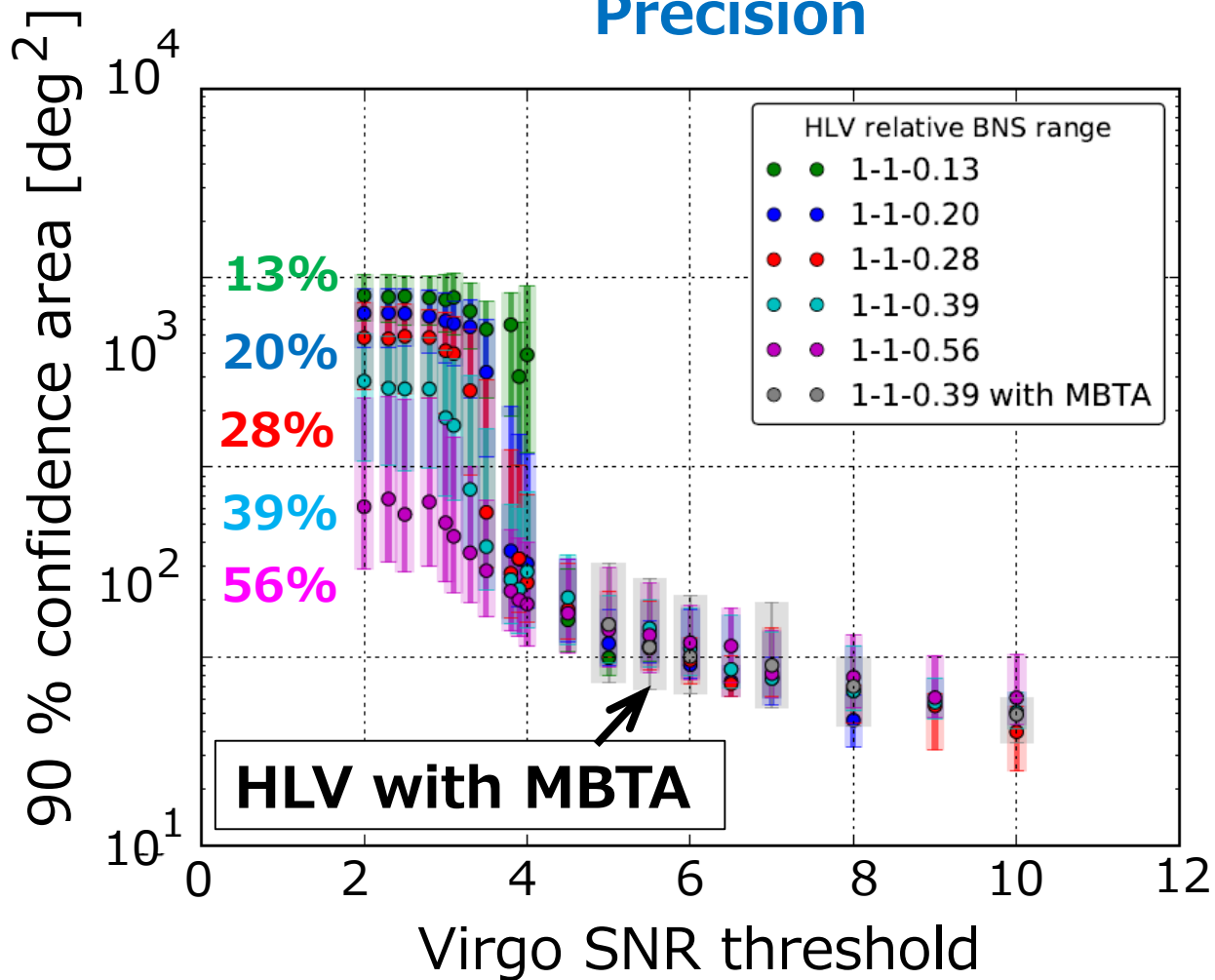
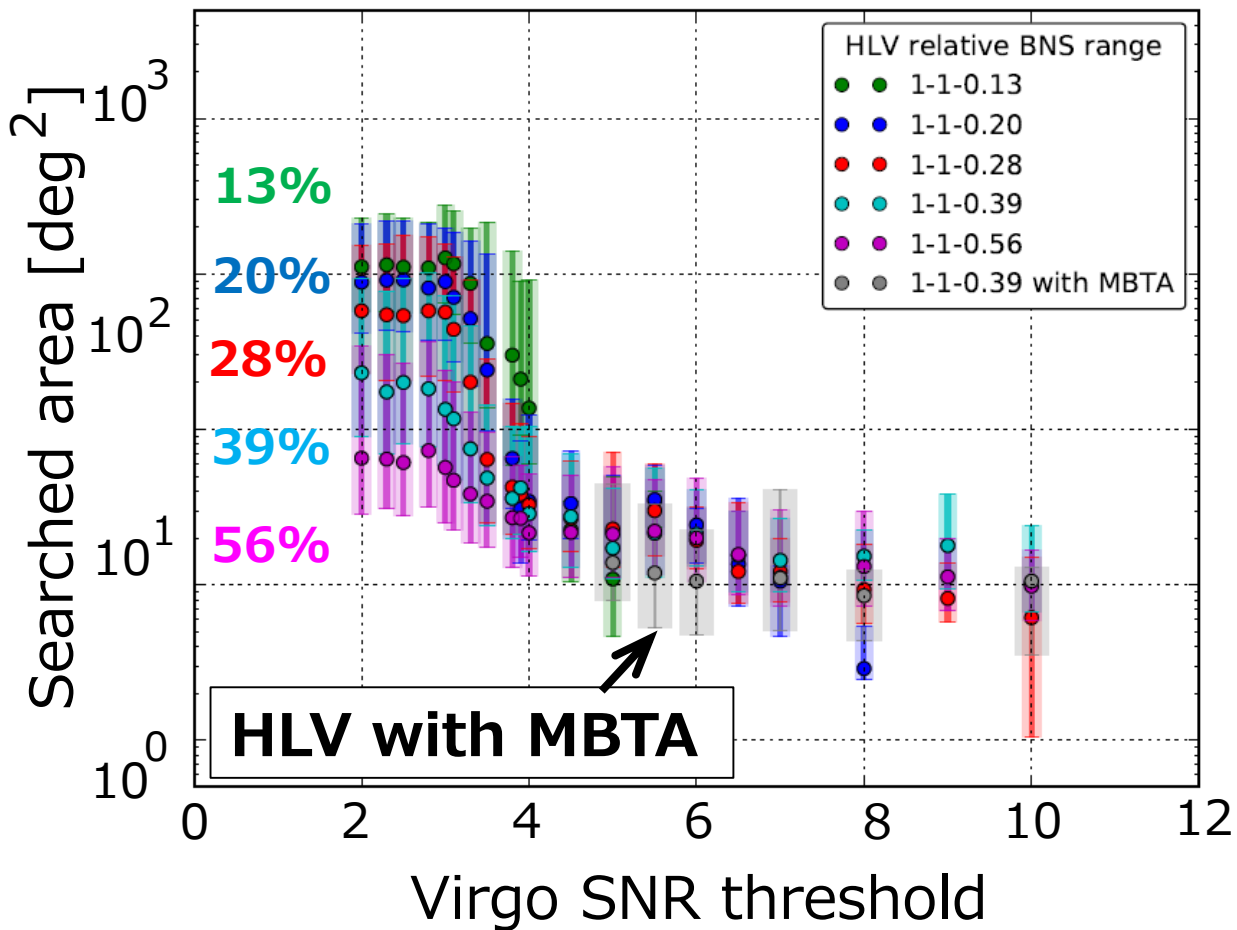


# Performance (HLV):

(SNR threshold for H, L = 5.)

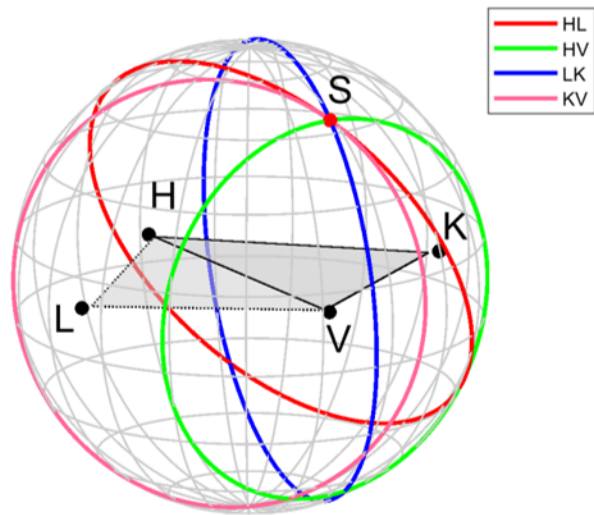
## Accuracy

## Precision

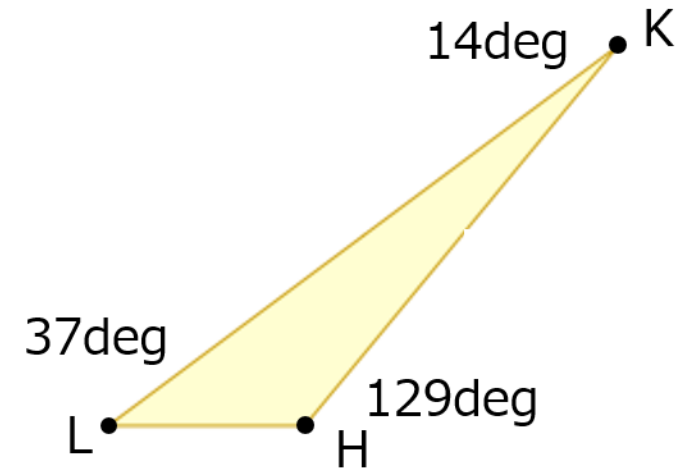
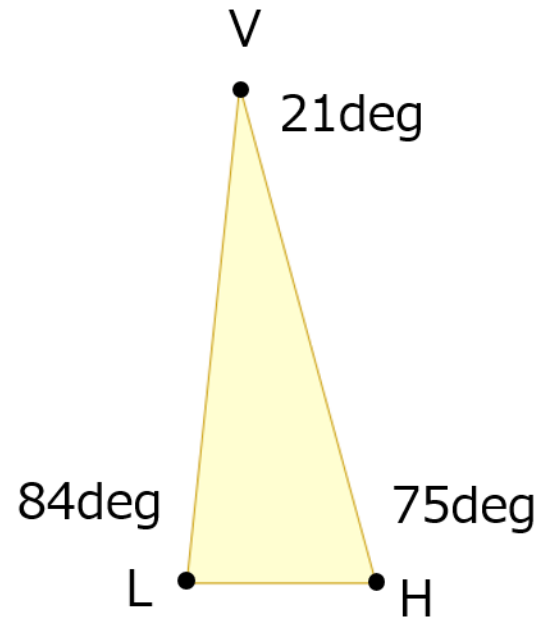


Comparison (HLV\_sim) vs. (HLV\_mbta)

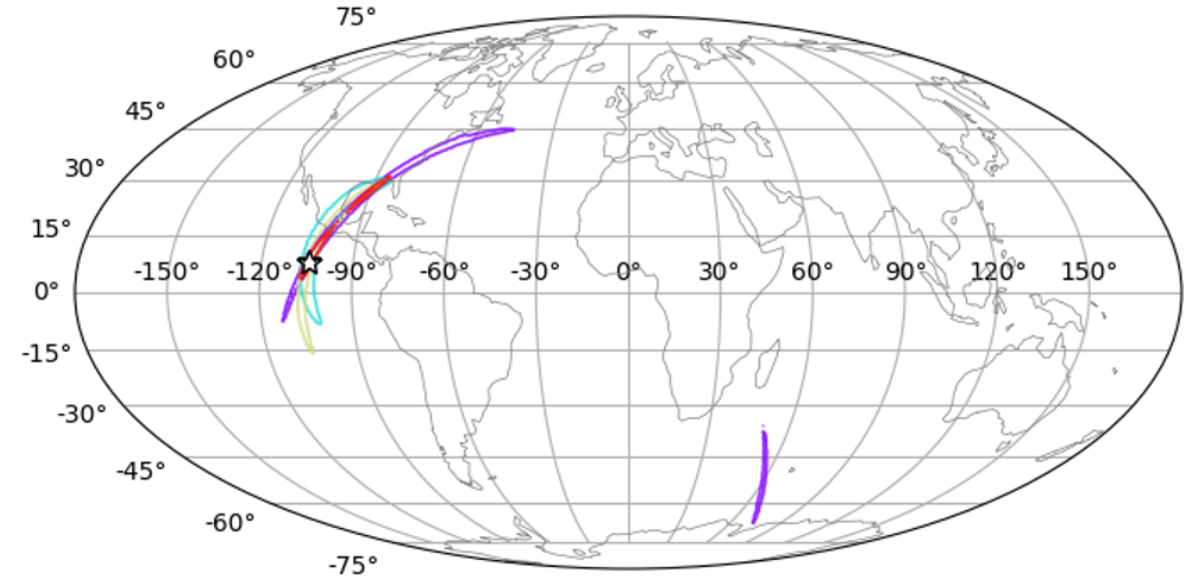
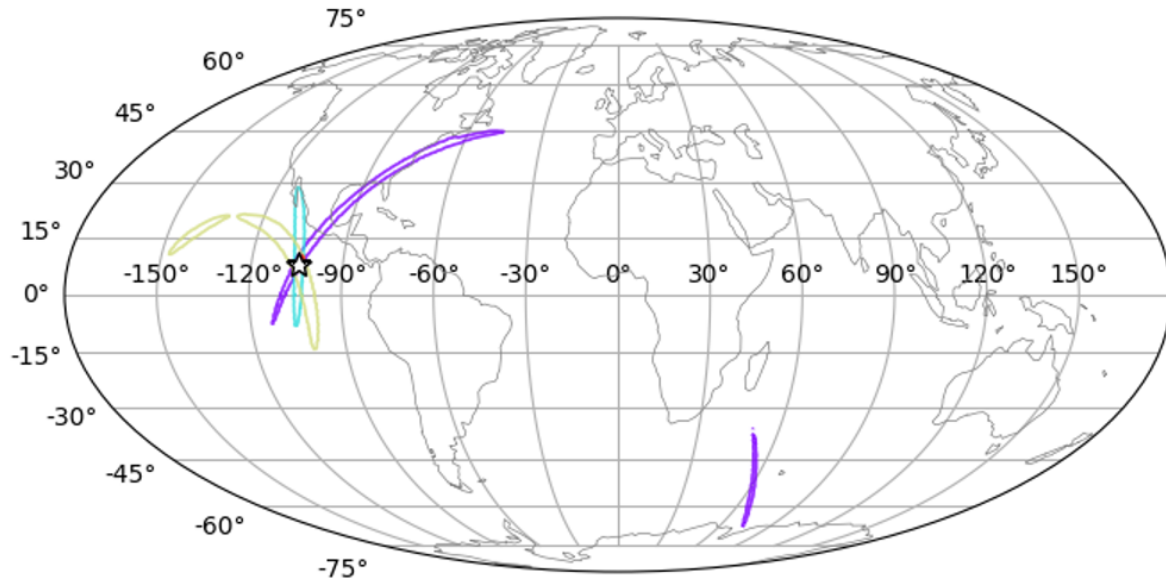
# Difference: from geometry



arXiv: 1304.0670

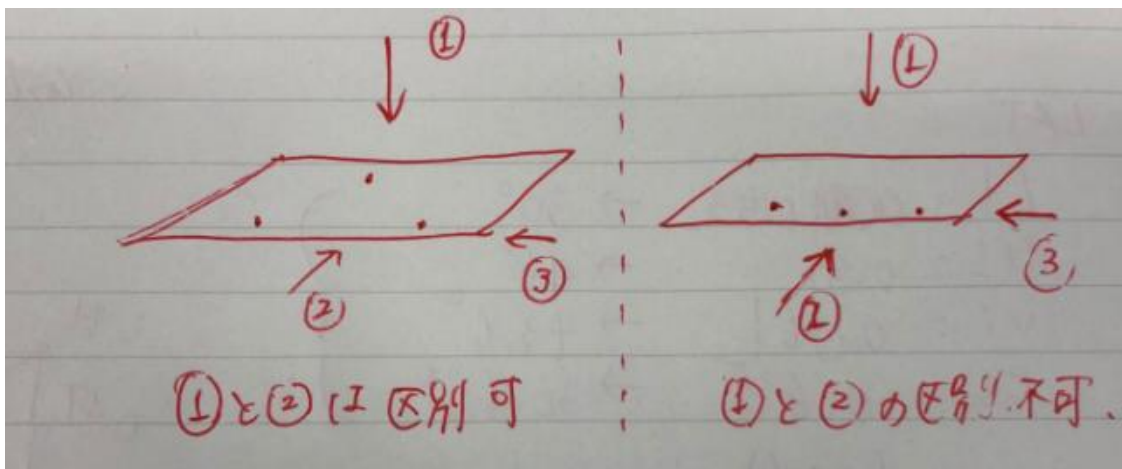


# Difference: from geometry



# Difference: from geometry

\* Flatter triangle would make localization worse.



→ This effect could be evaluated by using:

<https://arxiv.org/pdf/0908.2356.pdf>

<https://arxiv.org/pdf/1010.6192.pdf>

$$p(\mathbf{r}|\mathbf{R}) \propto p(\mathbf{r}) \exp \left[ -\frac{1}{2}(\mathbf{r} - \mathbf{R})^T \mathbf{M}(\mathbf{r} - \mathbf{R}) \right]$$

$$\mathbf{M} = \frac{\mathbf{D}_{12}\mathbf{D}_{12}^T}{\sigma_{12}^2} + \frac{\mathbf{D}_{23}\mathbf{D}_{23}^T}{\sigma_{23}^2} + \frac{\mathbf{D}_{31}\mathbf{D}_{31}^T}{\sigma_{31}^2} \quad (30)$$

Thus  $\mathbf{M}$  has a contribution from each pair of detectors which depends upon the detector separation  $\mathbf{D}_{ij}$  and the pairwise timing uncertainty

$$\sigma_{ij}^2 = \sigma_i^2 + \sigma_j^2 + \frac{\sigma_i^2 \sigma_j^2}{\sigma_k^2} \quad (31)$$

where  $k \neq i, j$ . The timing uncertainty from a given pair of detectors is dependent upon the timing accuracy  $\sigma_k$  in the third detector. Initially, this may seem surprising,

$\mathbf{M}$ : for the localization accuracy based on the detector geometry & timing accuracy.

$$\rightarrow \det(\mathbf{M}_{HLV}) / \det(\mathbf{M}_{HLK}) \sim 2$$

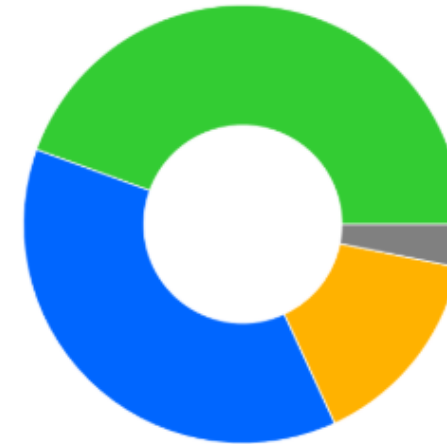
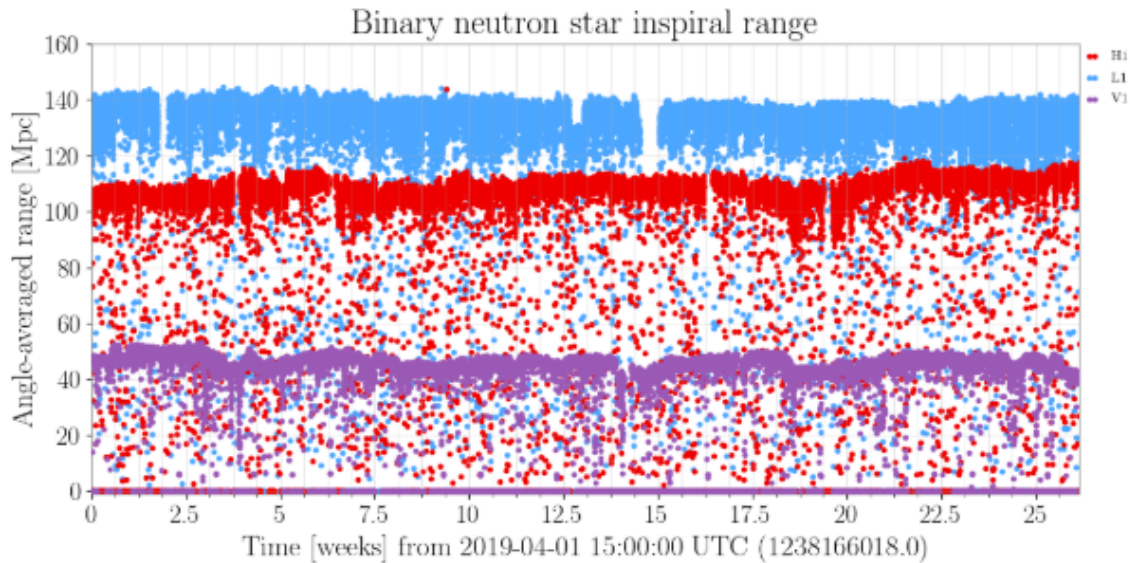
# Actual duty cycle:

**Table 1** Percentage of time during the first and second observing runs that the aLIGO and AdV detectors spent in different operating modes as recorded by the on-duty operator. Since several factors may influence detector operation at any given time, there is a certain subjectivity to the assignments. Maintenance includes a planned 4-h weekly period ( $\sim 2.4\%$  of the total), and unplanned corrective maintenance to deal with equipment or hardware failures. Coincident operation of the aLIGO detectors occurred  $\sim 43\%$  of the time in O1 and  $\sim 46\%$  in O2. After joining O2 on August 1 2017 AdV operated with a duty factor of approximately 85% until the end of the run on August 25 2017.

		O1		O2		
		Hanford	Livingston	Hanford	Livingston	Virgo
Operating mode %	Observing	64.6	57.4	65.3	61.8	85.1
	Locking	17.9	16.1	8.0	11.7	3.1
	Environmental	9.7	19.8	5.8	10.1	5.6
	Maintenance	4.4	4.9	5.4	6.0	3.1
	Commissioning	2.9	1.6	3.4	4.7	1.1
	Planned engineering	0.1	0.0	11.9	5.5	—
	Other	0.4	0.2	0.2	0.2	2.0

# Actual performance of online detectors:

<https://summary.ligo.org/~detchar/summary/O3a/>



- Triple interferometer [44.5%]
- Double interferometer [37.4%]
- Single interferometer [15.0%]
- No interferometer [3.2%]



- Observing [71.2%]
- Ready [0.7%]
- Locked [3.0%]
- Not locked [25.0%]



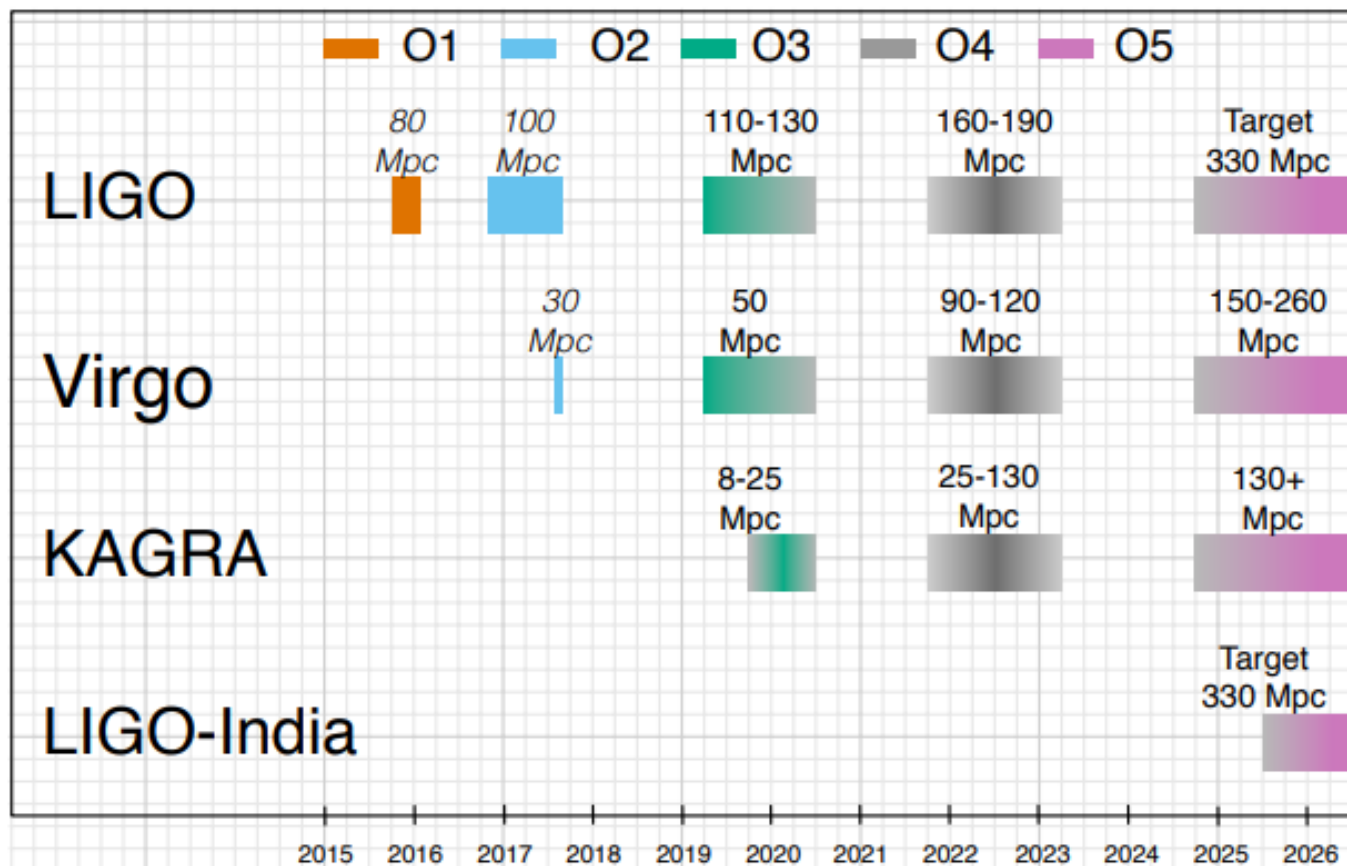
- Observing [75.8%]
- Ready [0.4%]
- Locked [3.7%]
- Not locked [20.1%]



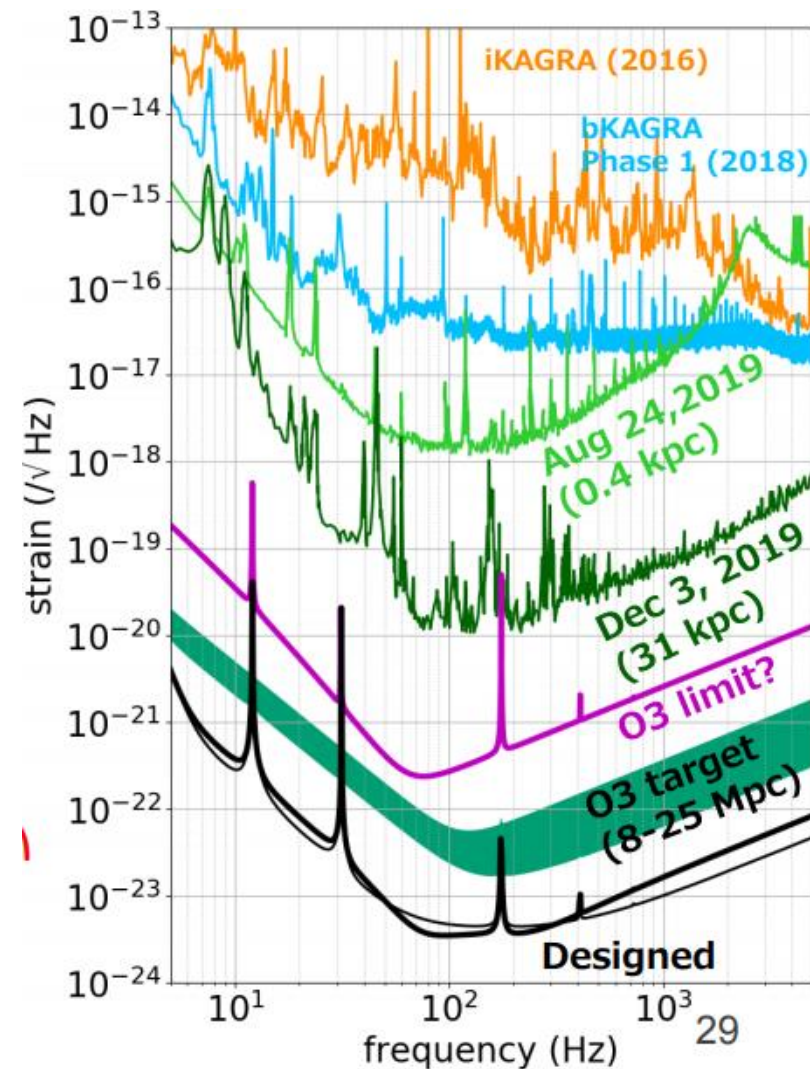
- Observing [76.3%]
- Locked [6.1%]
- Not locked [17.7%]



# Prospects for observation & current KAGRA



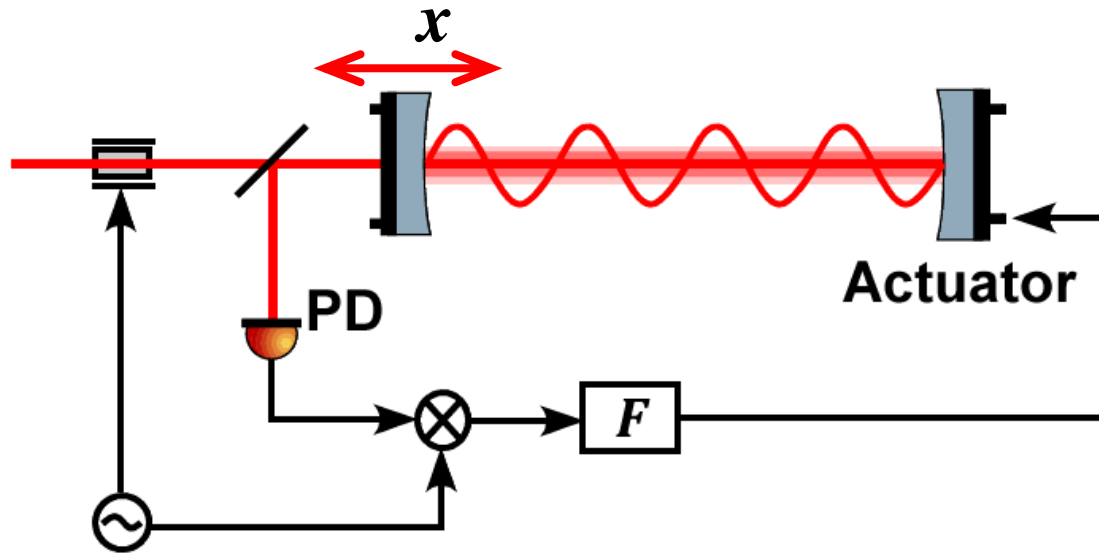
arXiv: 1304.0670



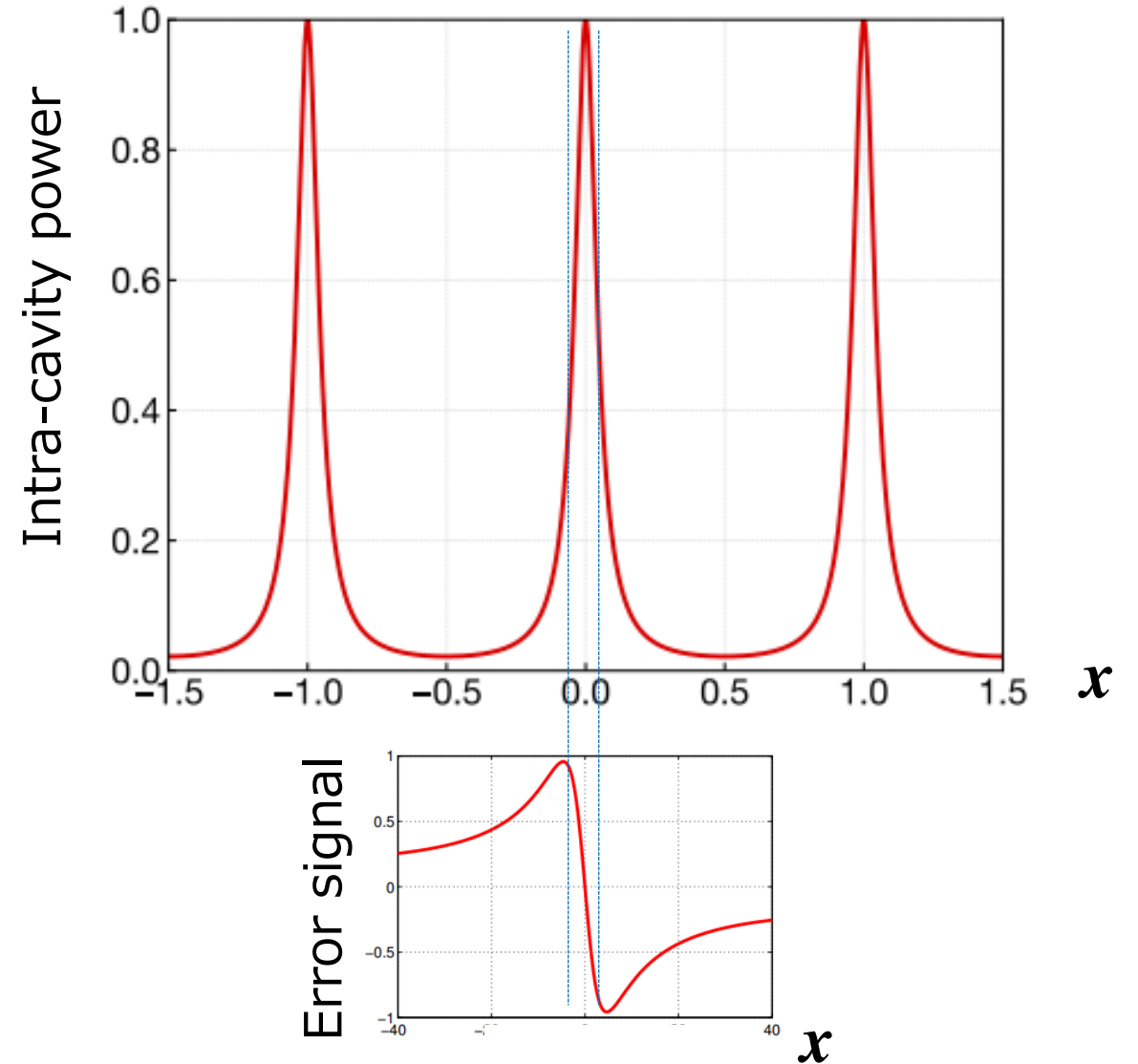
JGW-G1911123

# Interferometer locking:

Pound-Drever-hall (PDH) technique:

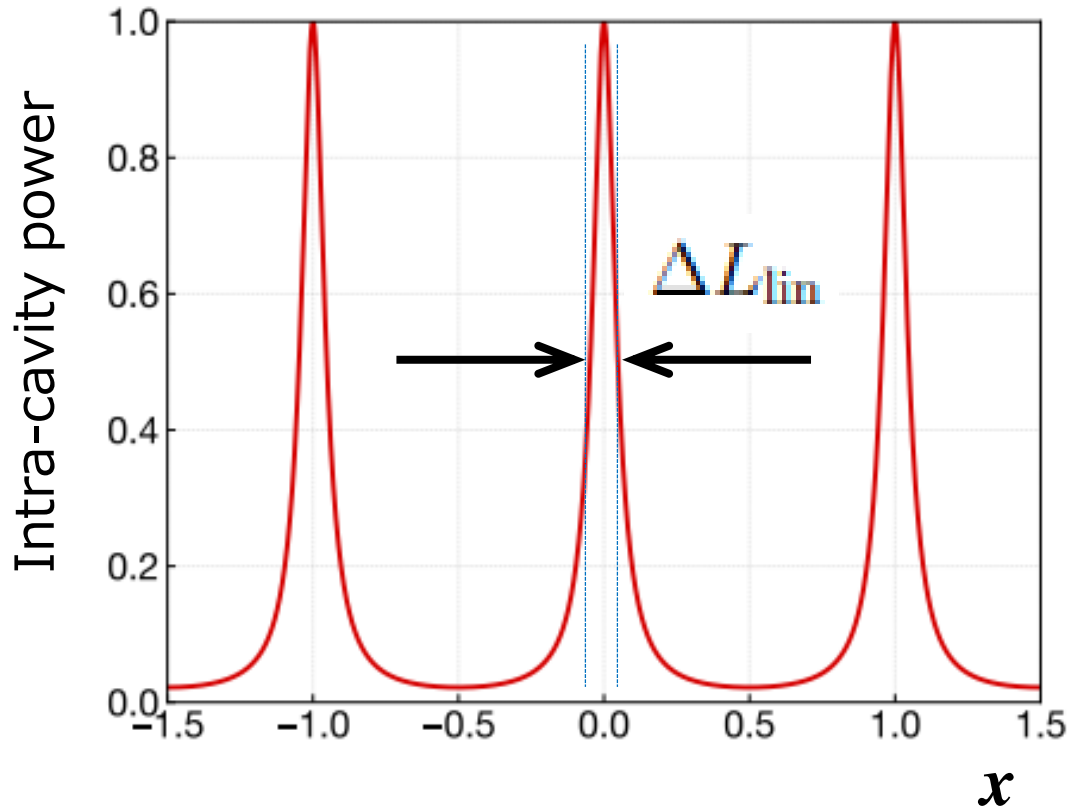


[ref] <https://gwdoc.icrr.u-tokyo.ac.jp/cgi-bin/private/DocDB/ShowDocument?docid=4739>

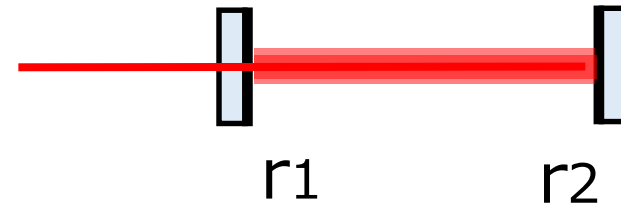


Feedback control only works within linewidth (FWHM).

# Cavity linewidth:



$$\Delta L_{lin} = \frac{\lambda}{2\mathcal{F}}, \quad \left( \mathcal{F} = \frac{\pi\sqrt{r_1 r_2}}{1 - r_1 r_2} \right)$$



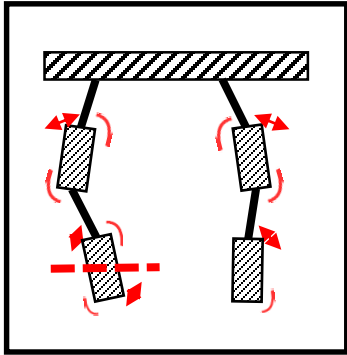
$$wb \cdot \text{del\_L\_lin} = (2 \cdot \pi \cdot \text{UGF}) \cdot \text{lumbda} / 2 / \mathcal{F}$$

DoFs	UGF [Hz]	Finesse	lambda [nm]	wb*del_L_lin [um/s]	del_L_lin [nm]
ARM_IR		1550	1064		0.34
ARM_GR	10e3	50	532	334	53.24
MICH	50 for BS	1	1064	167	226
PRCL	50 for PRM	57	1064	2.93	9.33
SRCL	50 for SRM	38	1064	4.398	14

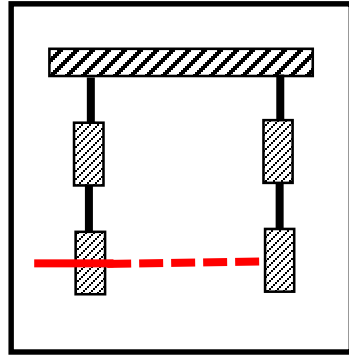
# My work for Type-A:

Local control system

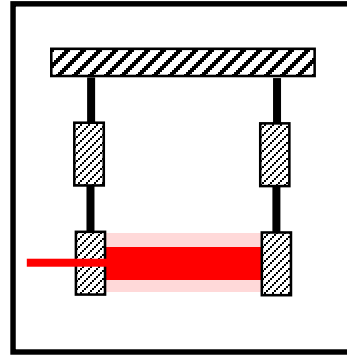
## Implementation & Performance test



Res. damping



Lock-acq.



Observation

With full Type-A:

My work

## Goal:

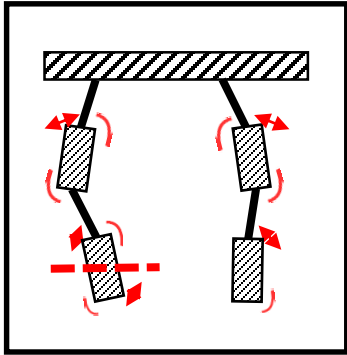
To construct local control system of full Type-A to allow interferometer locking.

- \* Control system in observation:
  - much depends on interferometer control (*global control*) in addition.
  - set as future work.

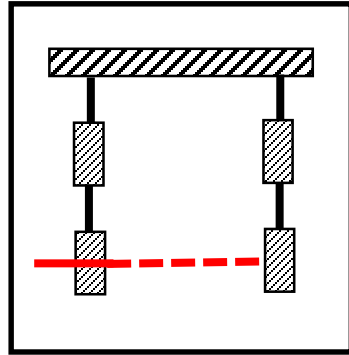
# My work for Type-A:

Local control system

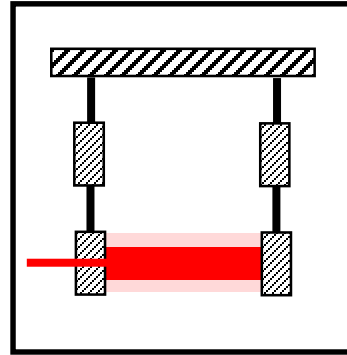
## Implementation & Performance test



Res. damping



Lock-acq.



Observation

With full Type-A: **My work**

Data acq. system & digital system

Mechanical system

**Already done**

## Goal:

To construct local control system of full Type-A to allow interferometer locking.

- \* Control system in observation:
  - much depends on interferometer control (*global control*) in addition.
  - set as future work.

# What has been already done & not done for Type-A:

## Mechanical system

### Basic designing

#### Suspension system:

[T. Sekiguchi internal doc.(2014)]+

#### Cryogenic system:

[D. Chen PhD thesis(2015)]+

### Installation (& characterization)

#### Room-temp. part:

[K. Okutomi PhD (2019)]

#### Cryogenic temp. part:

[T. Yamada master's(2018)]+

[CQG **36** (2019) 165008]+

## Data acq. system & digital system

[PTEP (2018) 013F01]+



Room-temp. part

Cryogenic-temp. part

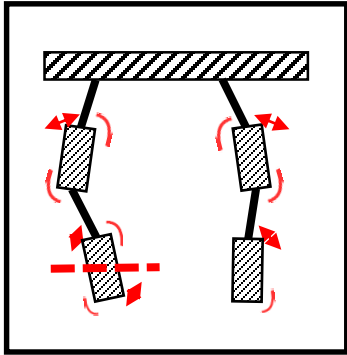
Basic mechanical-  
system development  
→ Already finished.



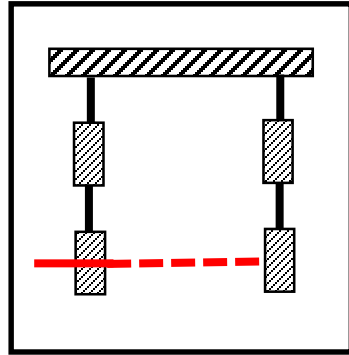
# What has been already done & not done for Type-A:

Local control system

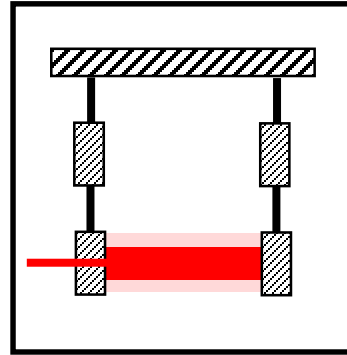
## Implementation & Performance test



Res. damping



Lock-acq.



Observation



**With room-temp. part:**

[K. Okutomi PhD (2019)]<sup>(\*1)</sup>



Room-temp. part

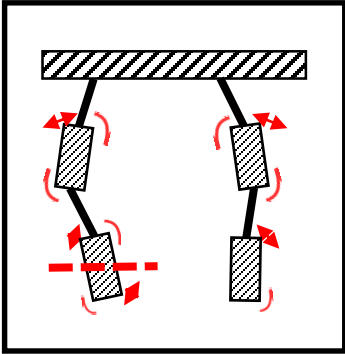


(\*1) for arm-cavity lock.

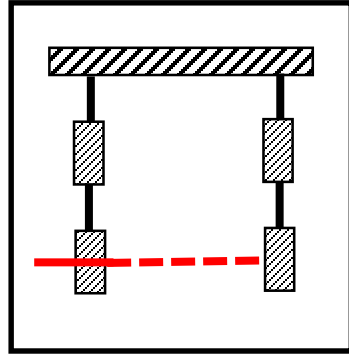
# What has been already done & not done for Type-A:

Local control system

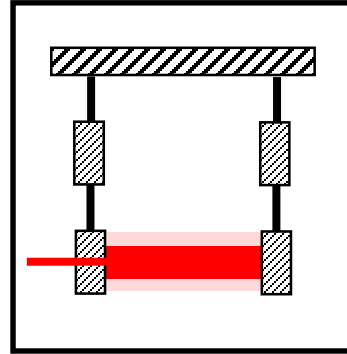
## Implementation & Performance test



Res. damping



Lock-acq.



Observation



**With room-temp. part:**

[K. Okutomi PhD (2019)]<sup>(\*1)</sup>



**With full Type-A:**

**My work**

**Goal:**

**To construct local control system of full Type-A for acquiring interferometer lock.**

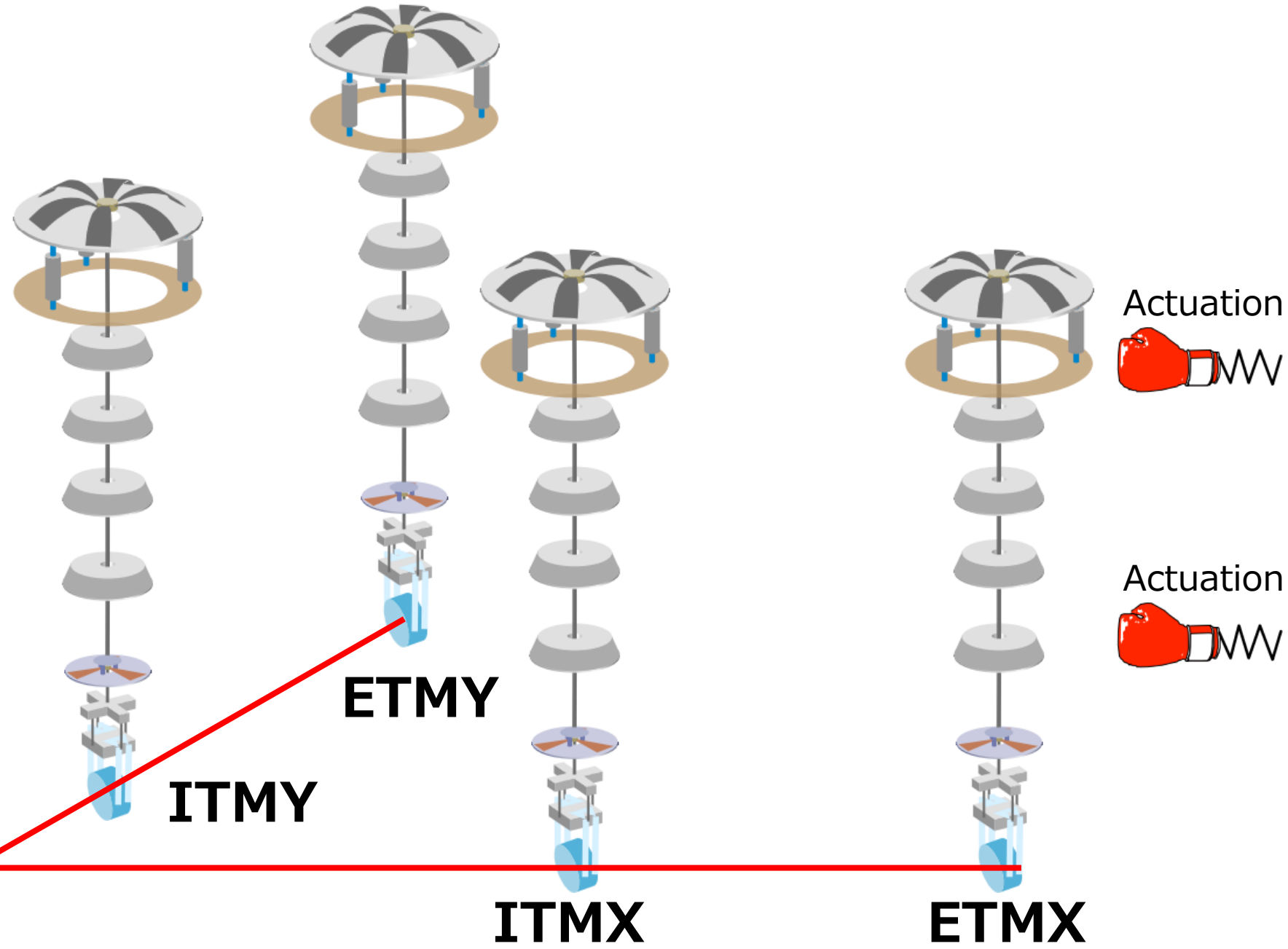
- \* Control system in observation:
  - much depends on interferometer control (*global control*) in addition.
  - set as future work.

(\*1) for arm-cavity lock.

Note: verification of suspension performance

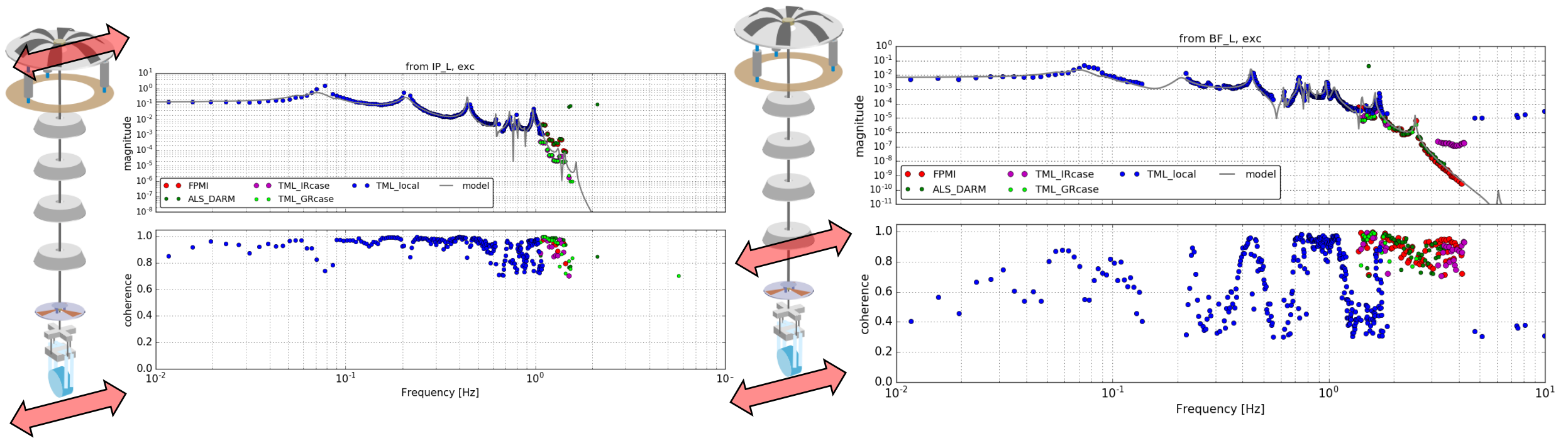
# Measurement:

## Mechanical suspension response to DARM



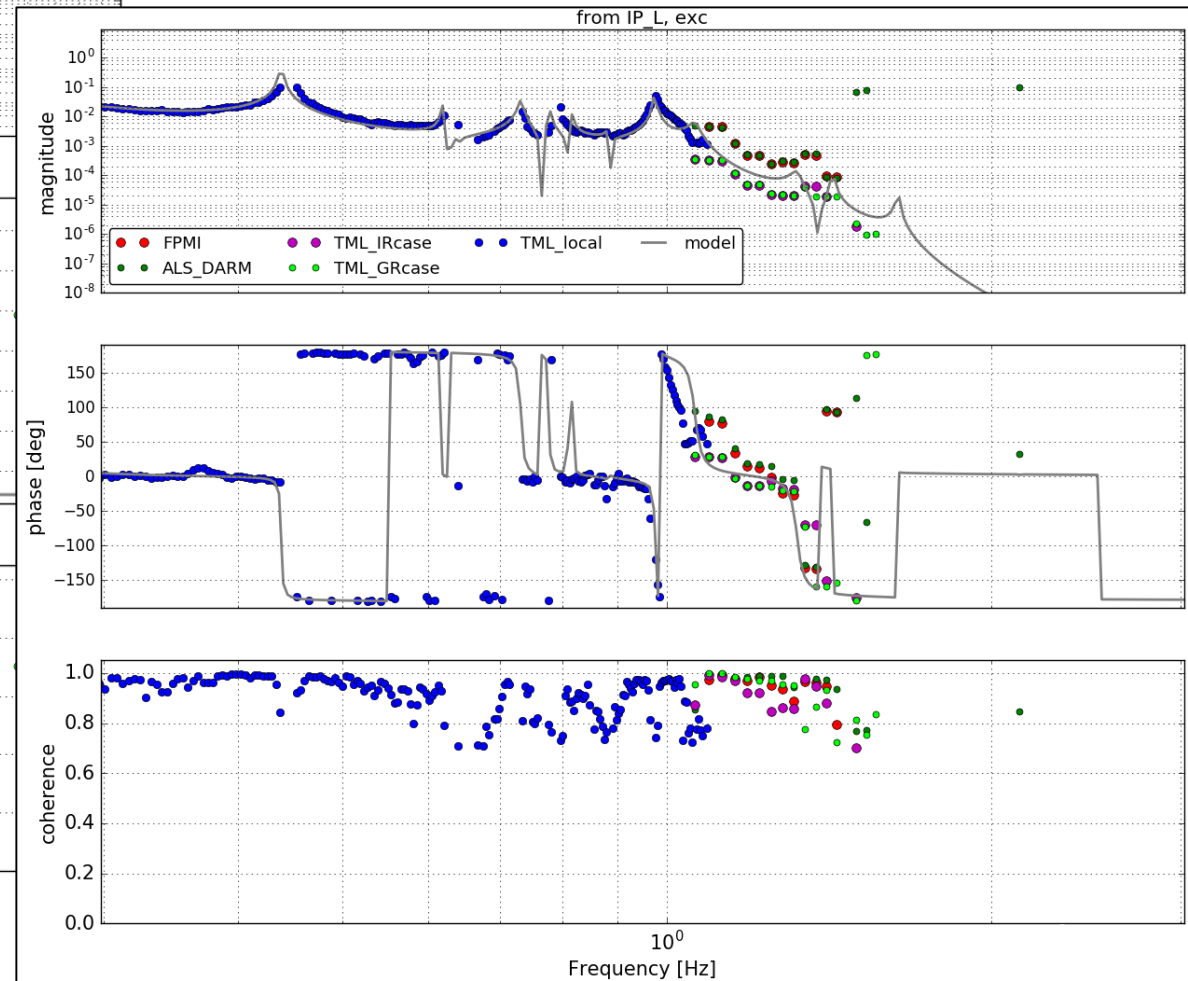
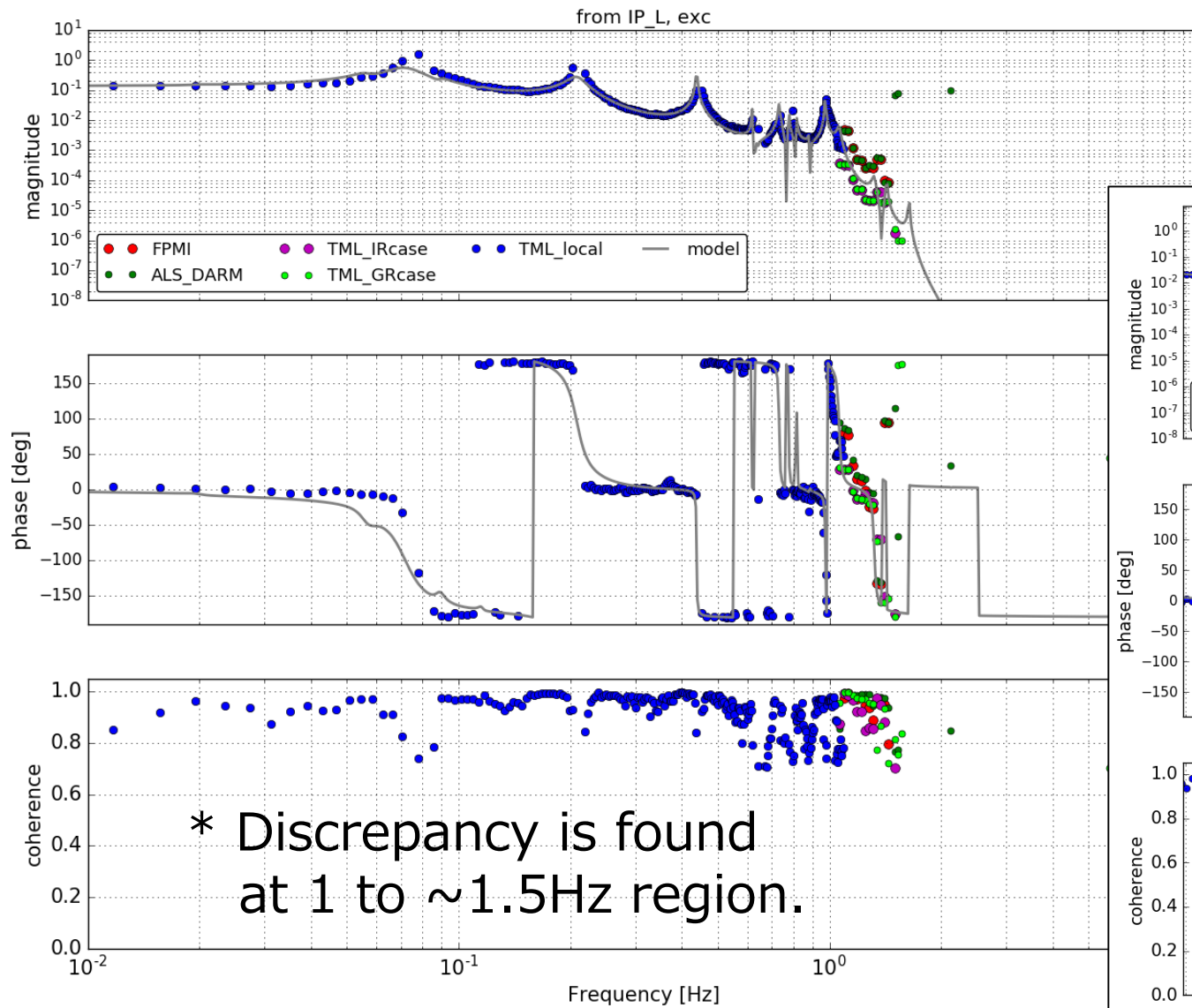
# 1. Mechanical system characterization:

\* By checking vibration isolation



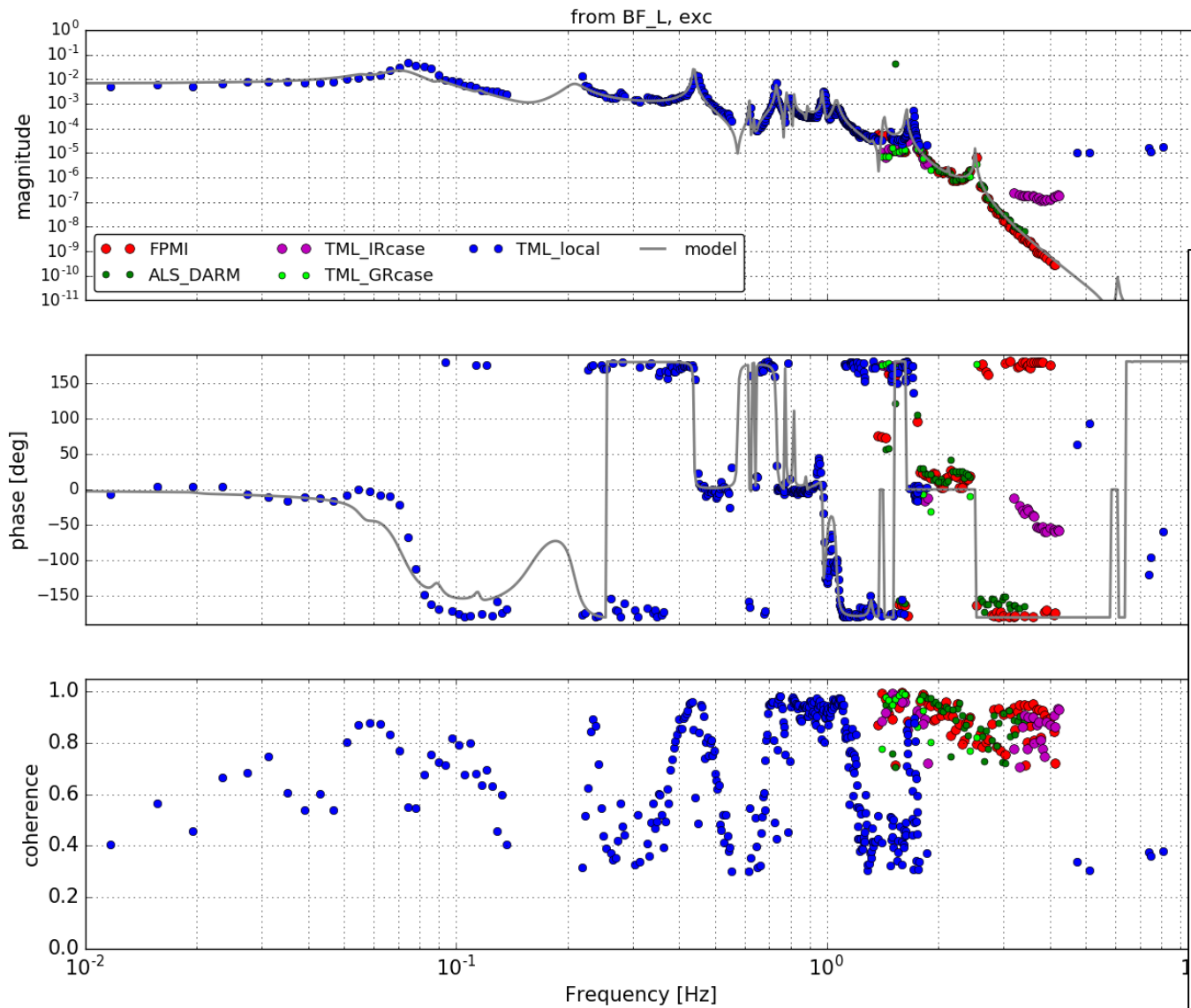
→ Type-A suspension has characteristics of pendulum up to 4 Hz.  
→ discrepancy at 1 Hz to 1.4 Hz is worth to investigate for further improvement.

# Results: force transfer functions, from IPL

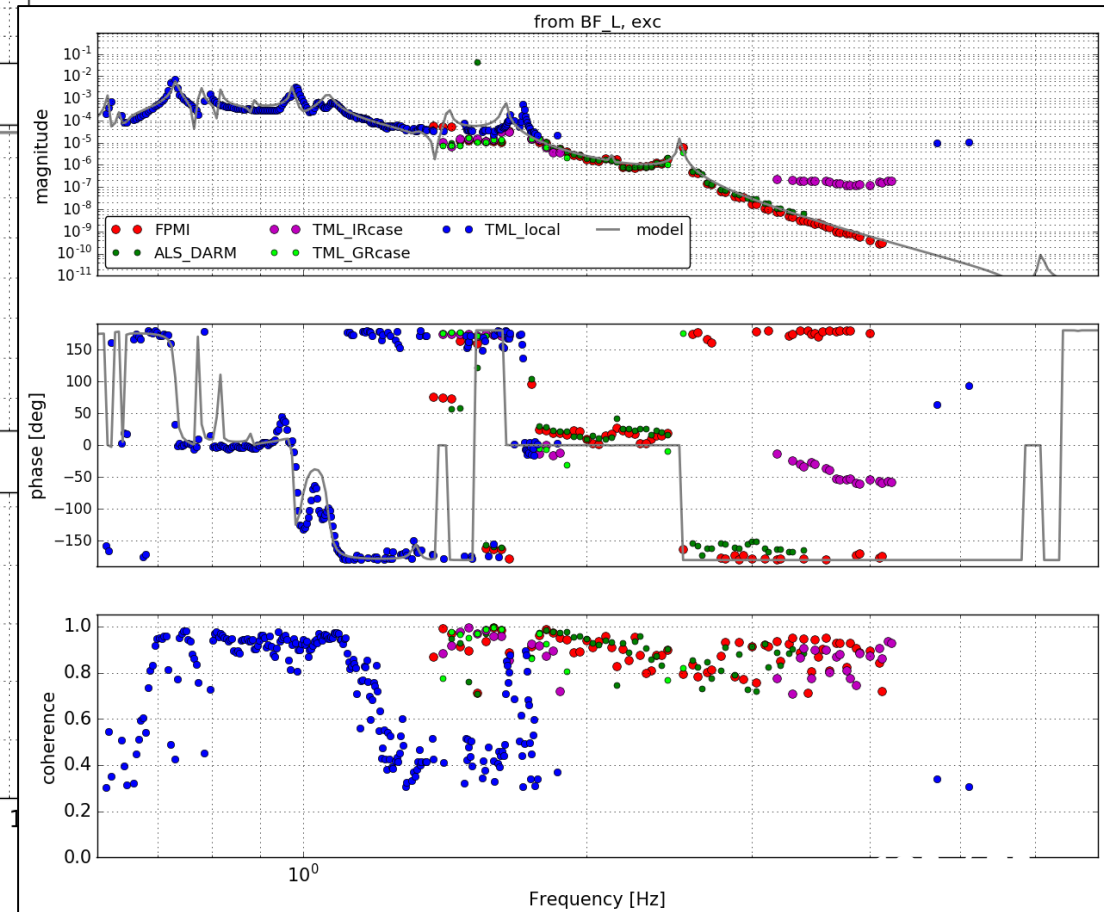




# Results: force transfer functions, from BFL



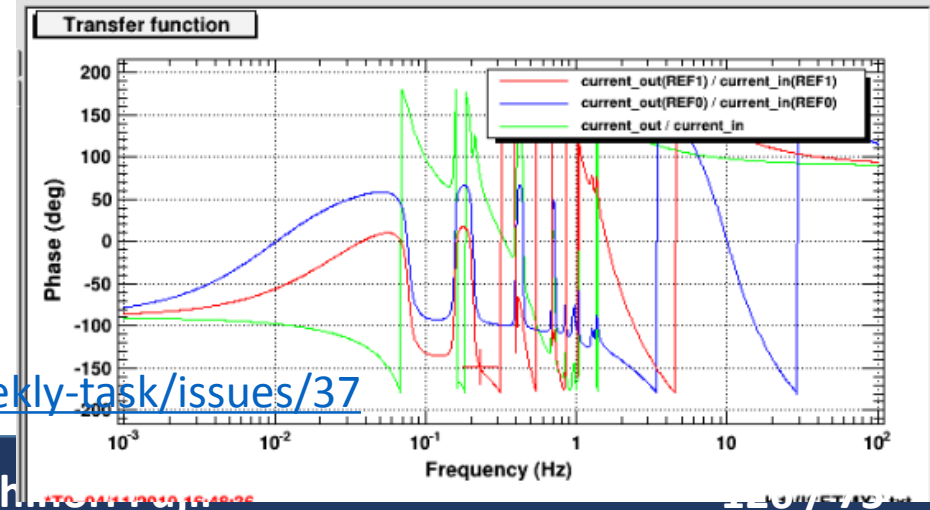
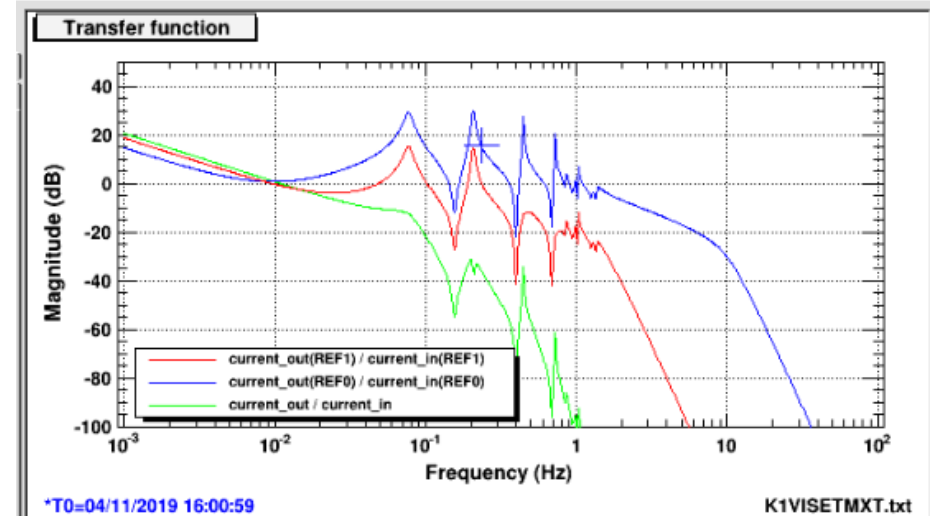
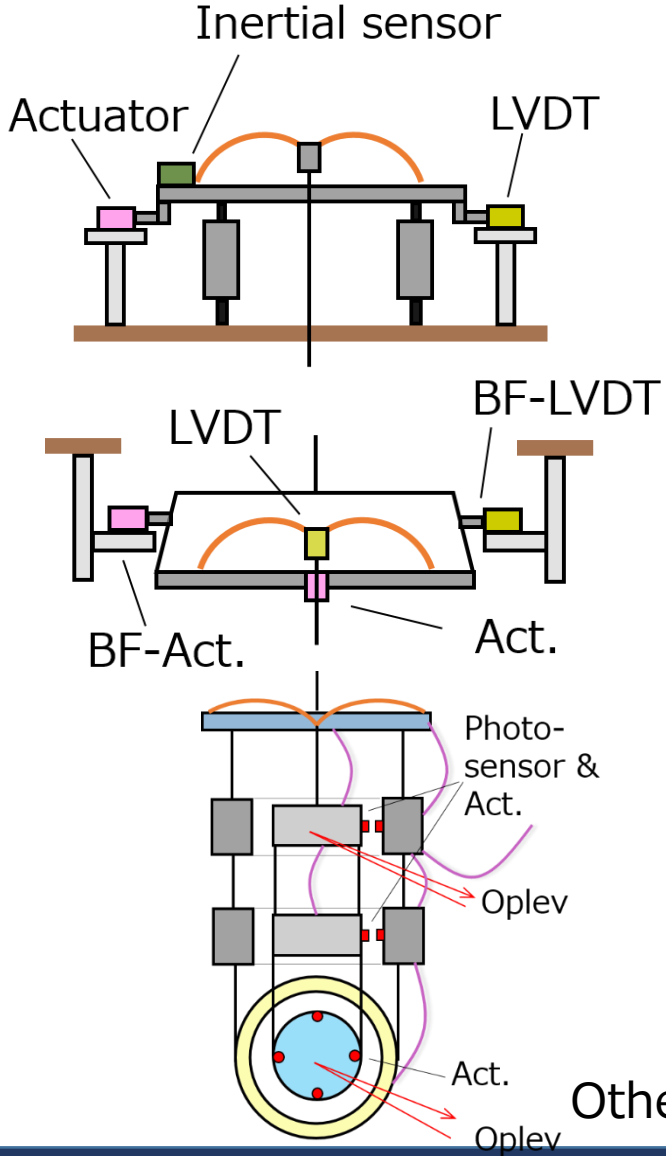
The transfer function up to 4.2 Hz agree with the model.



# Settings for the measurement w/o controls:

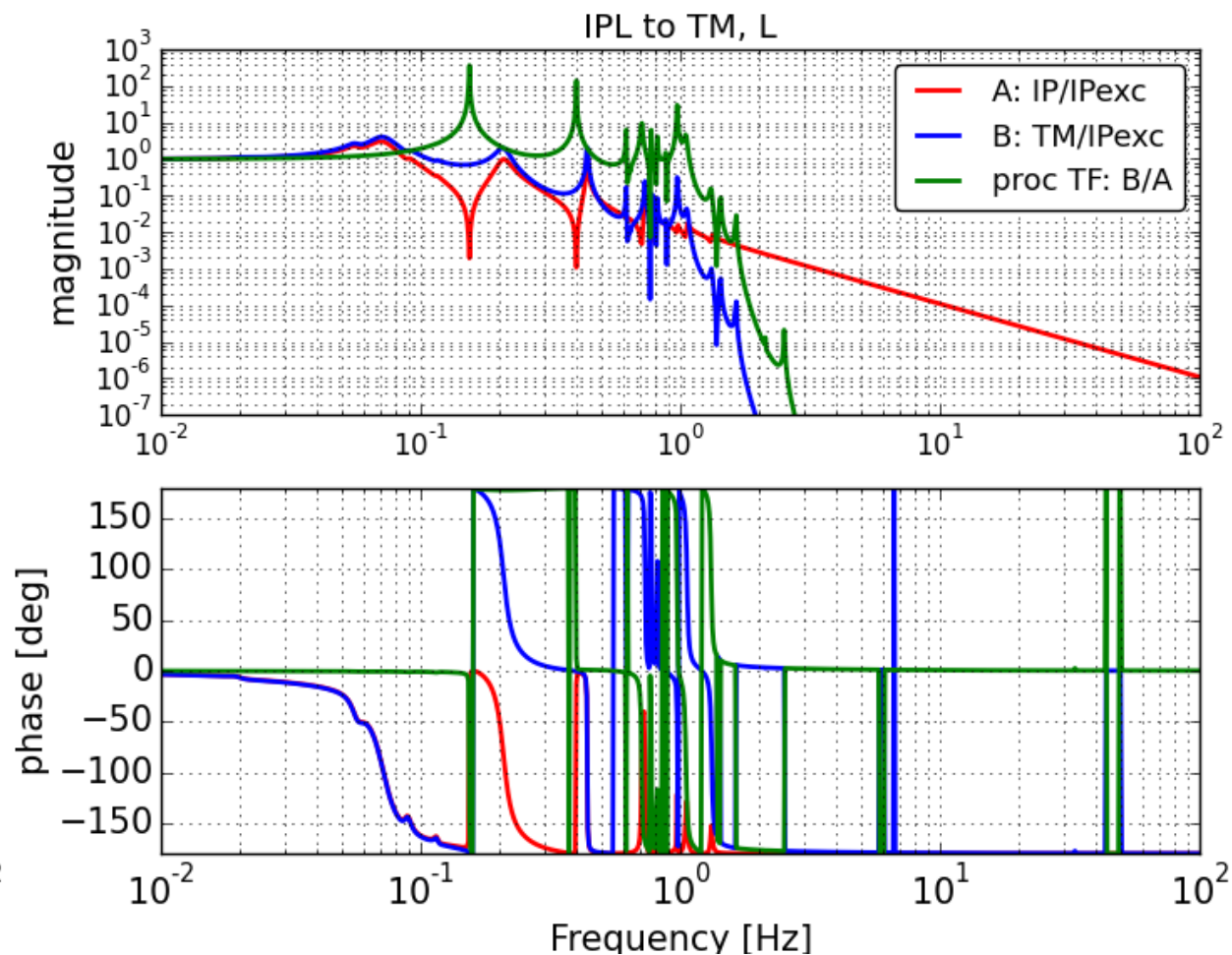
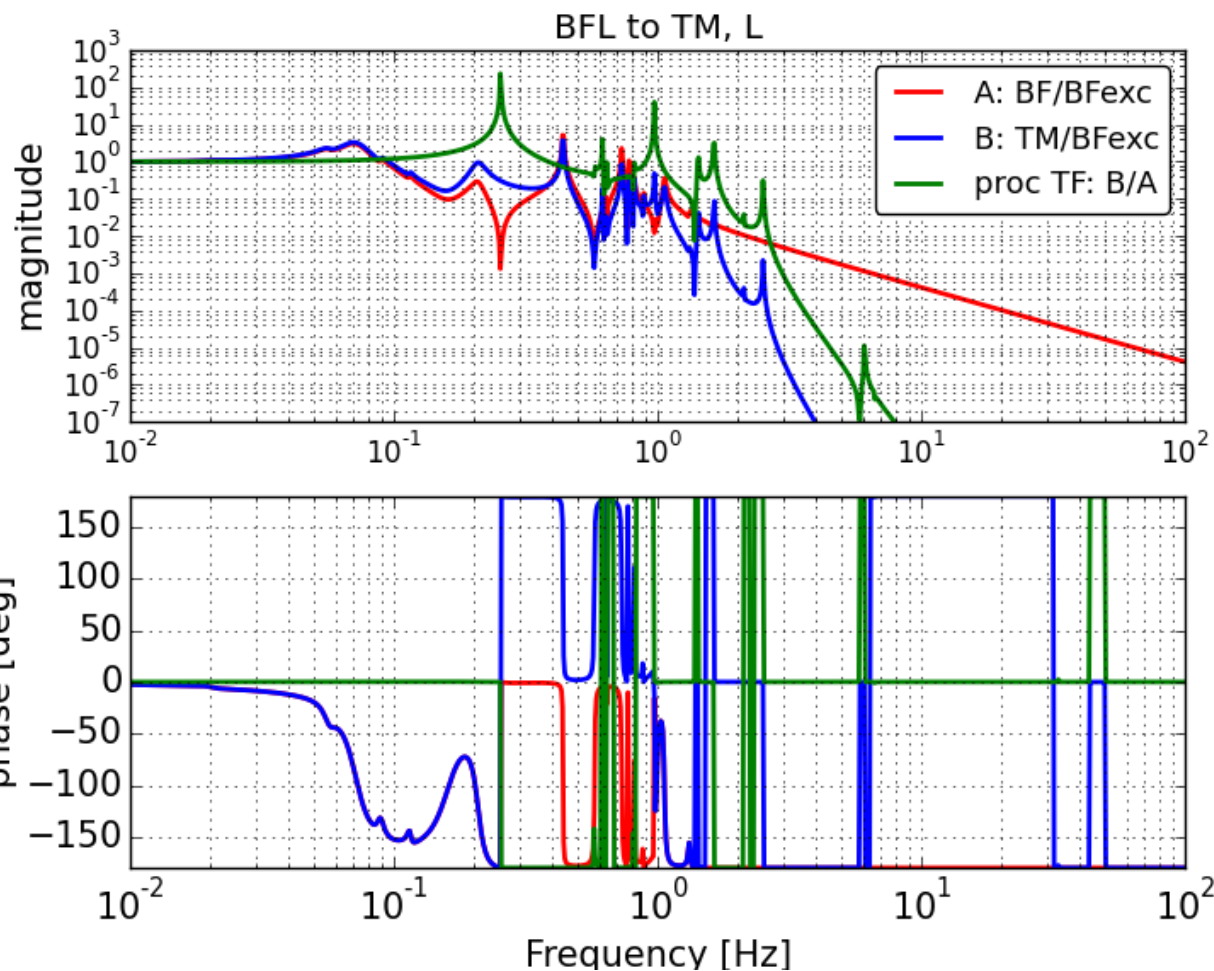
With Tower-damped state,

- ordinal L-loop (blue) was opened at IP satge.
- instead,
- green curve loop was used for the ALS\_DARM measurement,
- red curve loop was used for the FPMI\_DARM measurement.



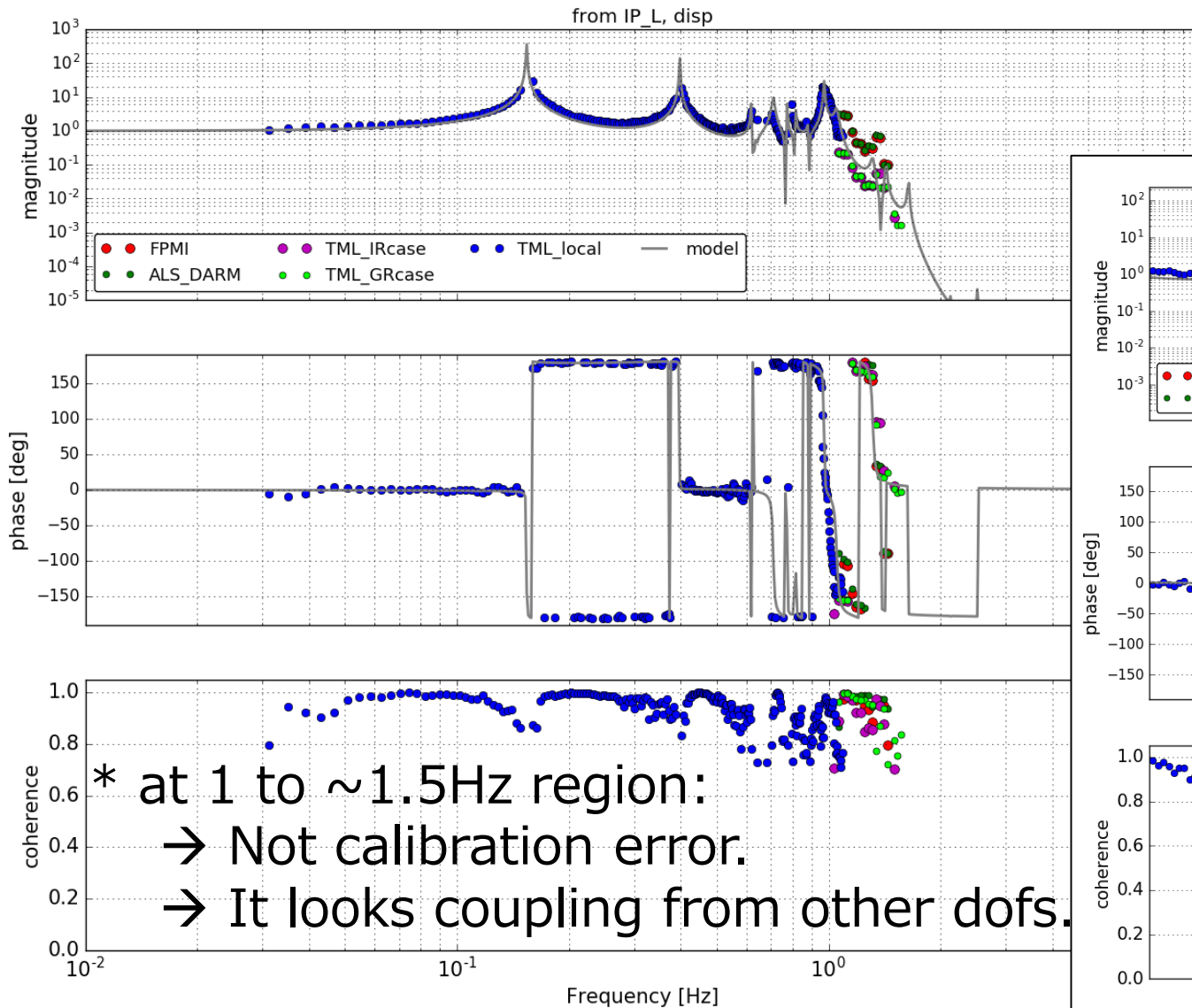
Other ref: <https://github.com/YoshinoriFujii/Weekly-task/issues/37>

# Simulation models:

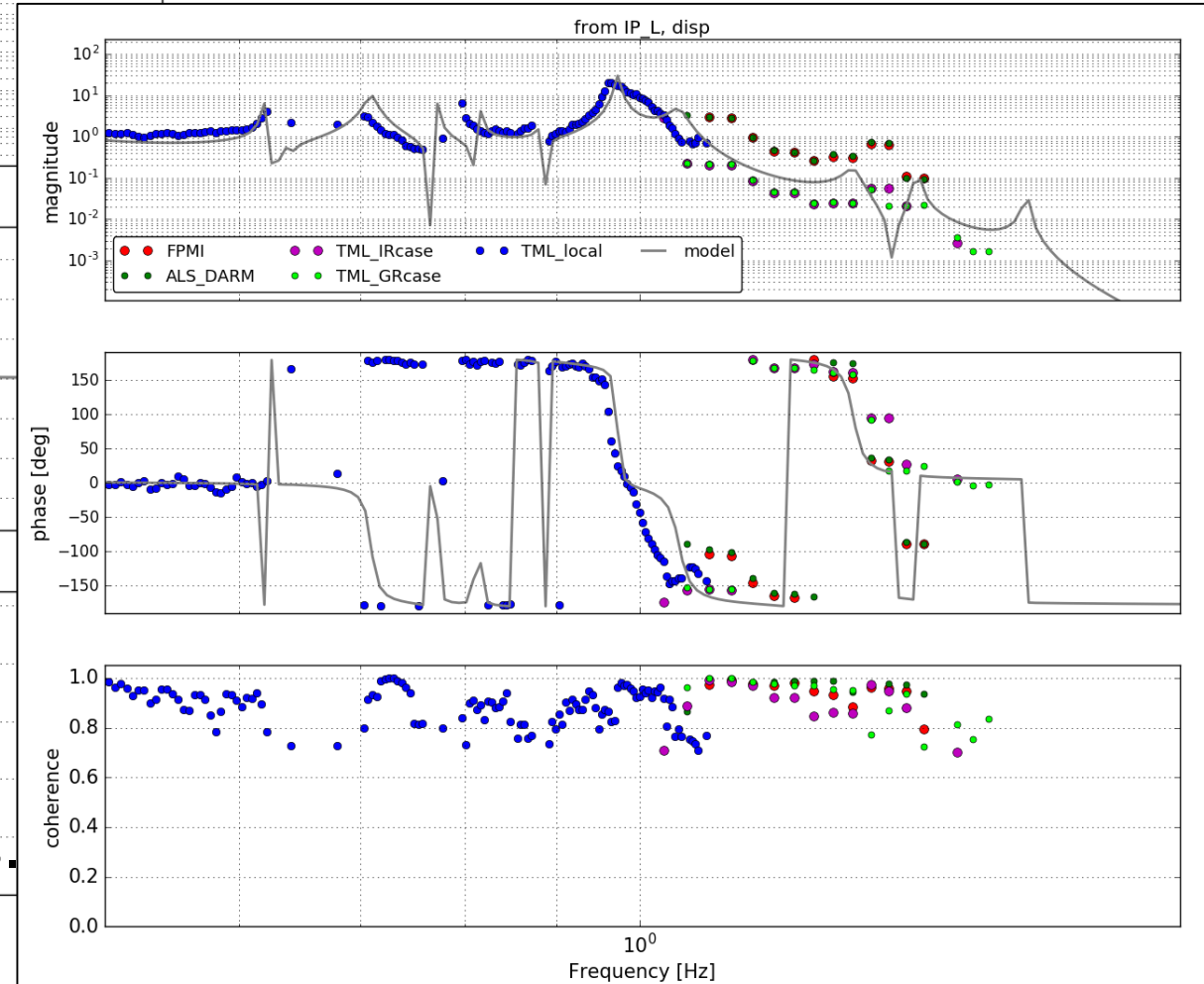


# Results: displacement transfer functions, from IPL

It seems that model have to be tuned at 1 to  $\sim 1.5$ Hz region.



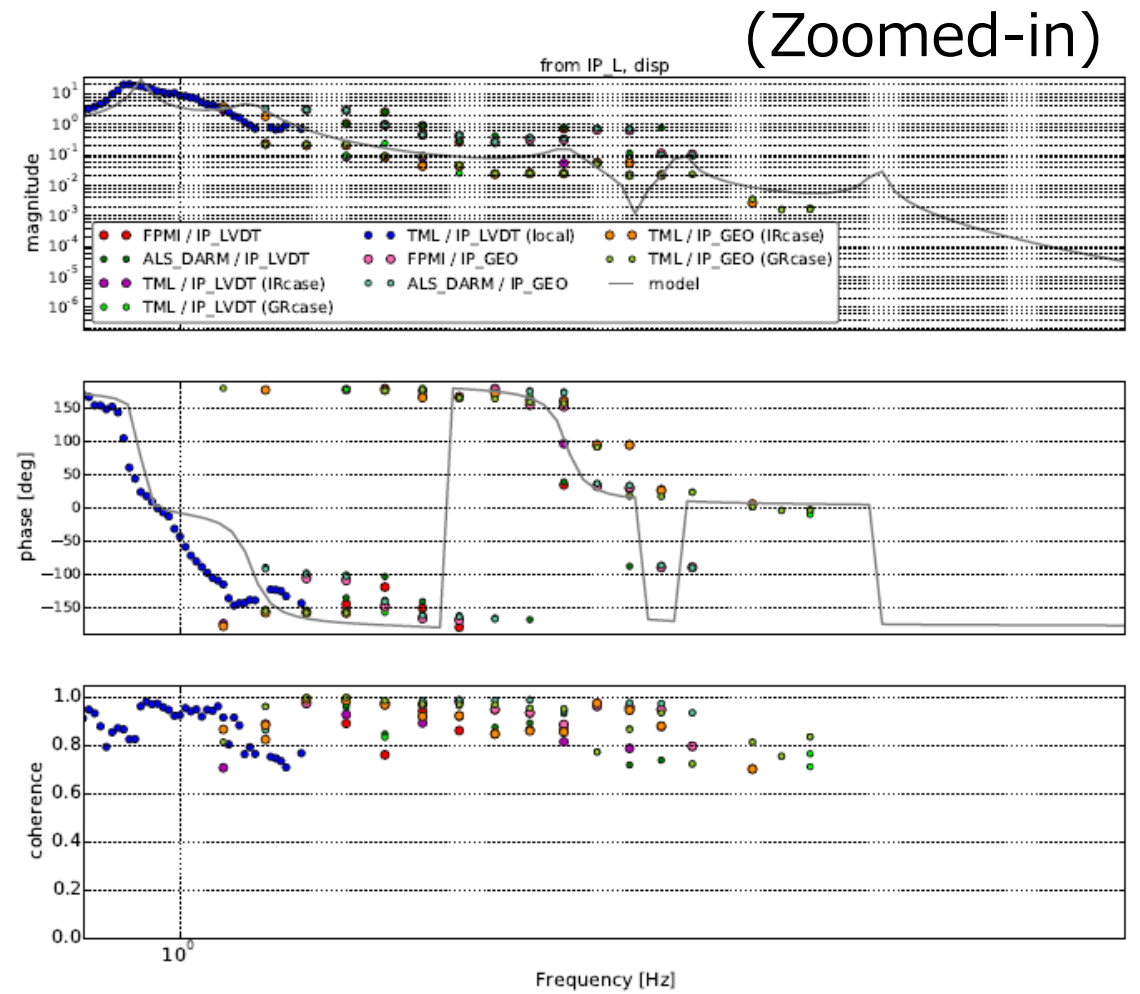
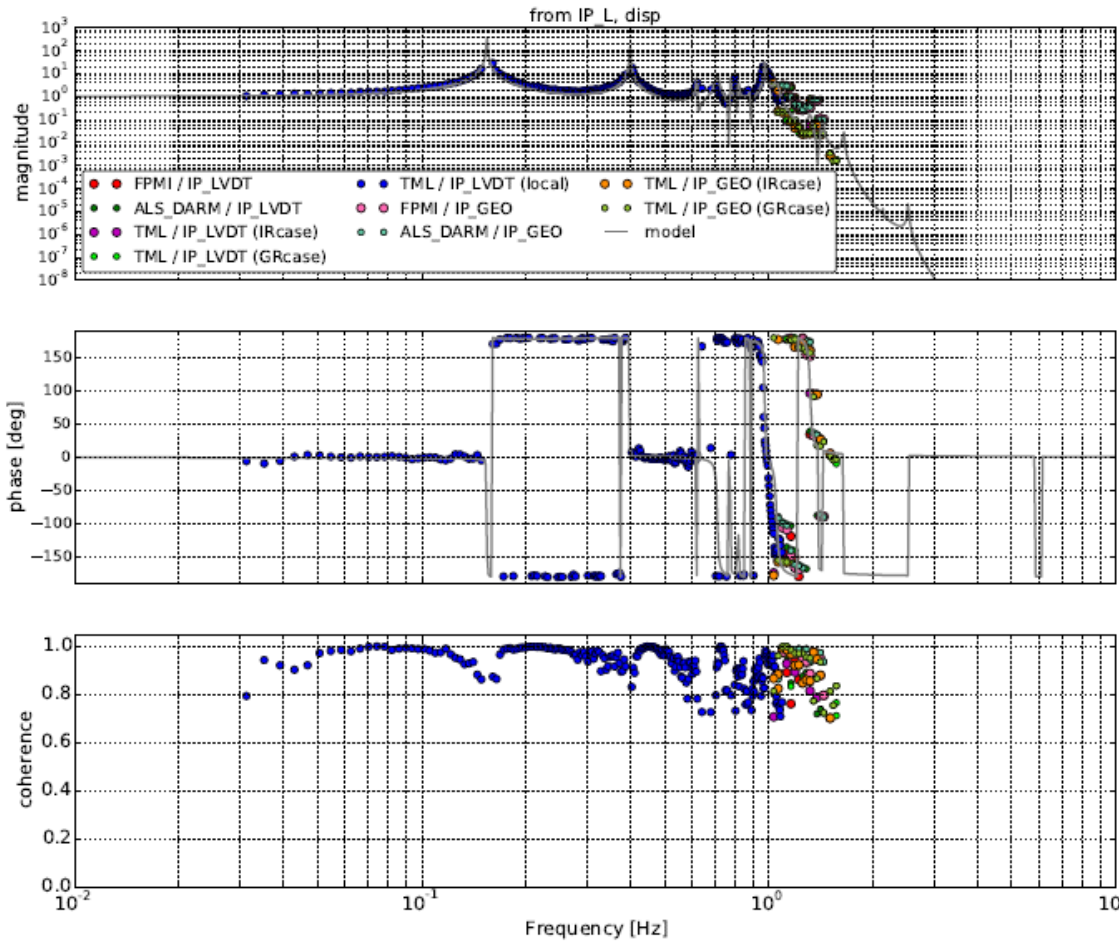
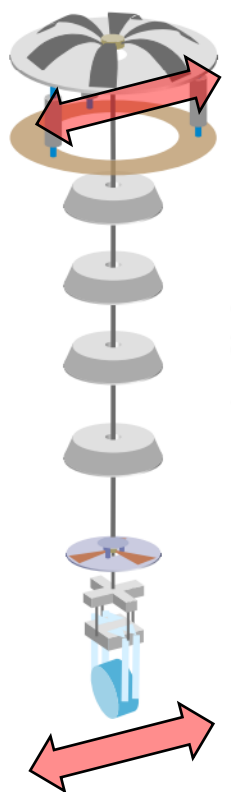
\* at 1 to  $\sim 1.5$ Hz region:  
→ Not calibration error.  
→ It looks coupling from other dofs.





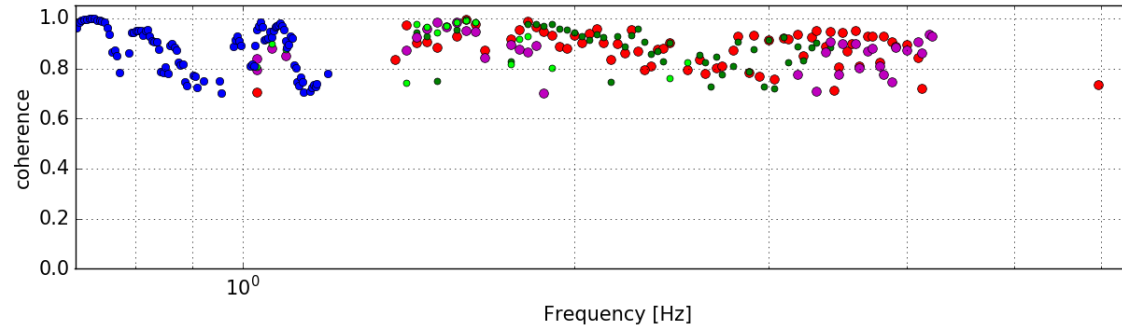
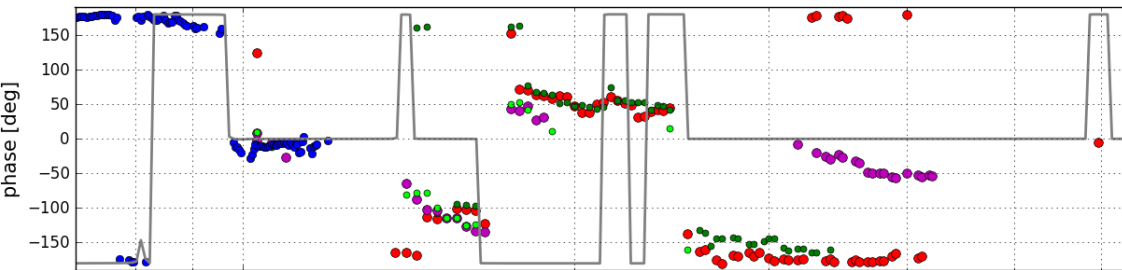
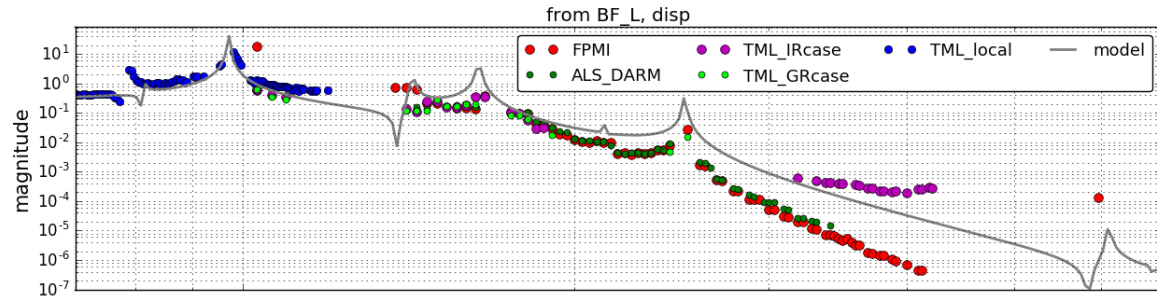
# Results: displacement transfer functions, from IPL

\* Including IP(geo) signal.

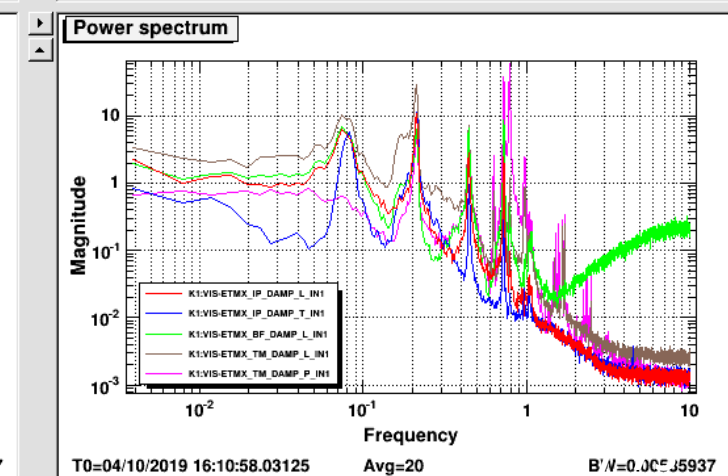
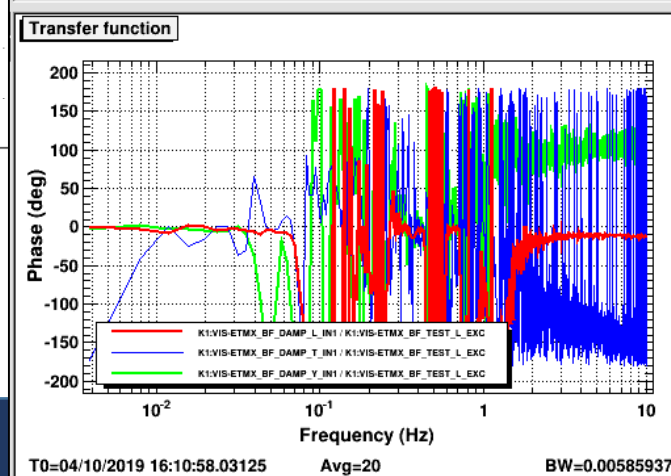
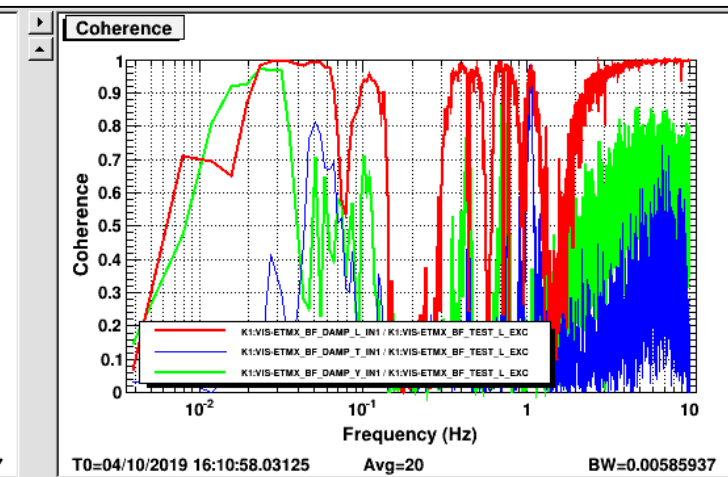
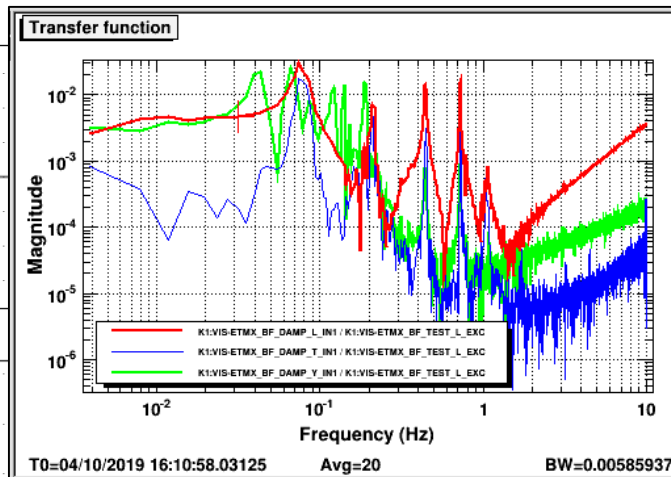


# Results: displacement transfer functions, from BFL

It seems that the discrepancy comes from the issue of LVDT, the direct sensor-actuator coupling.



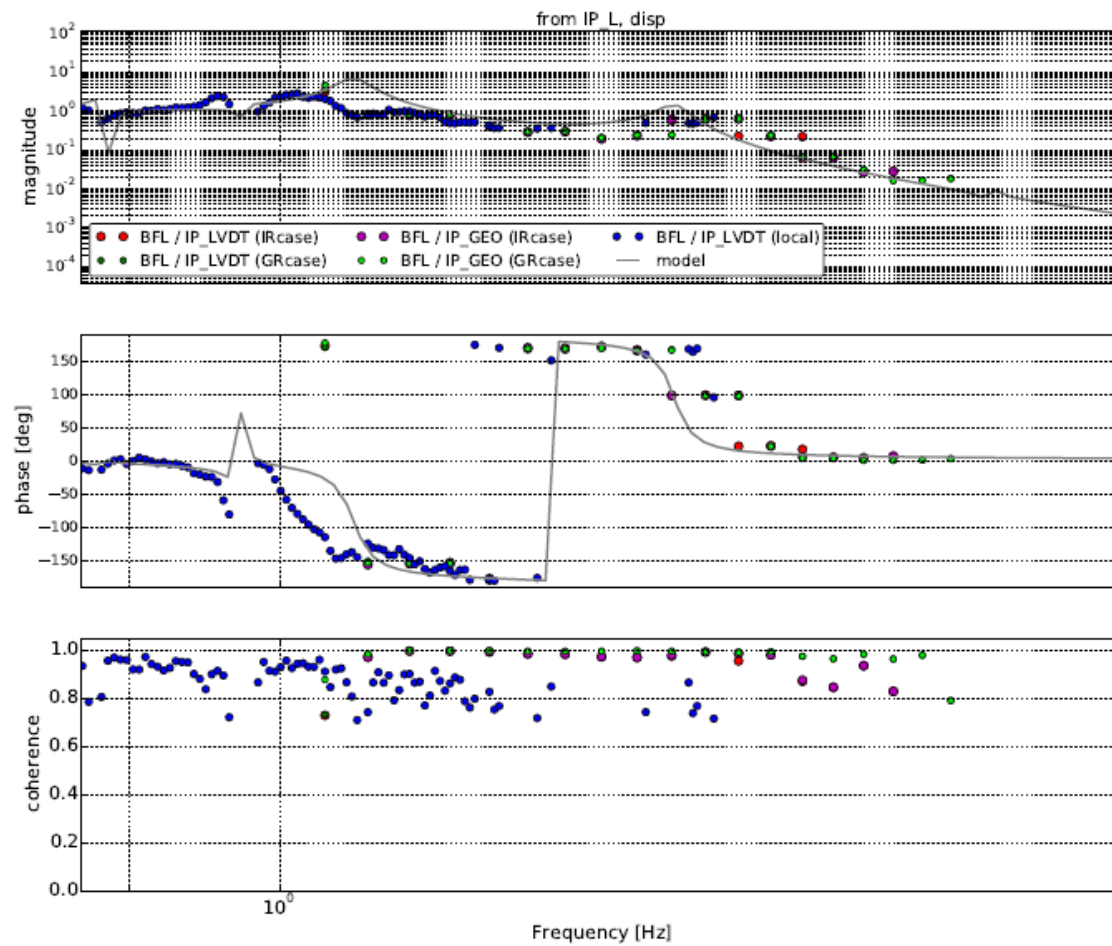
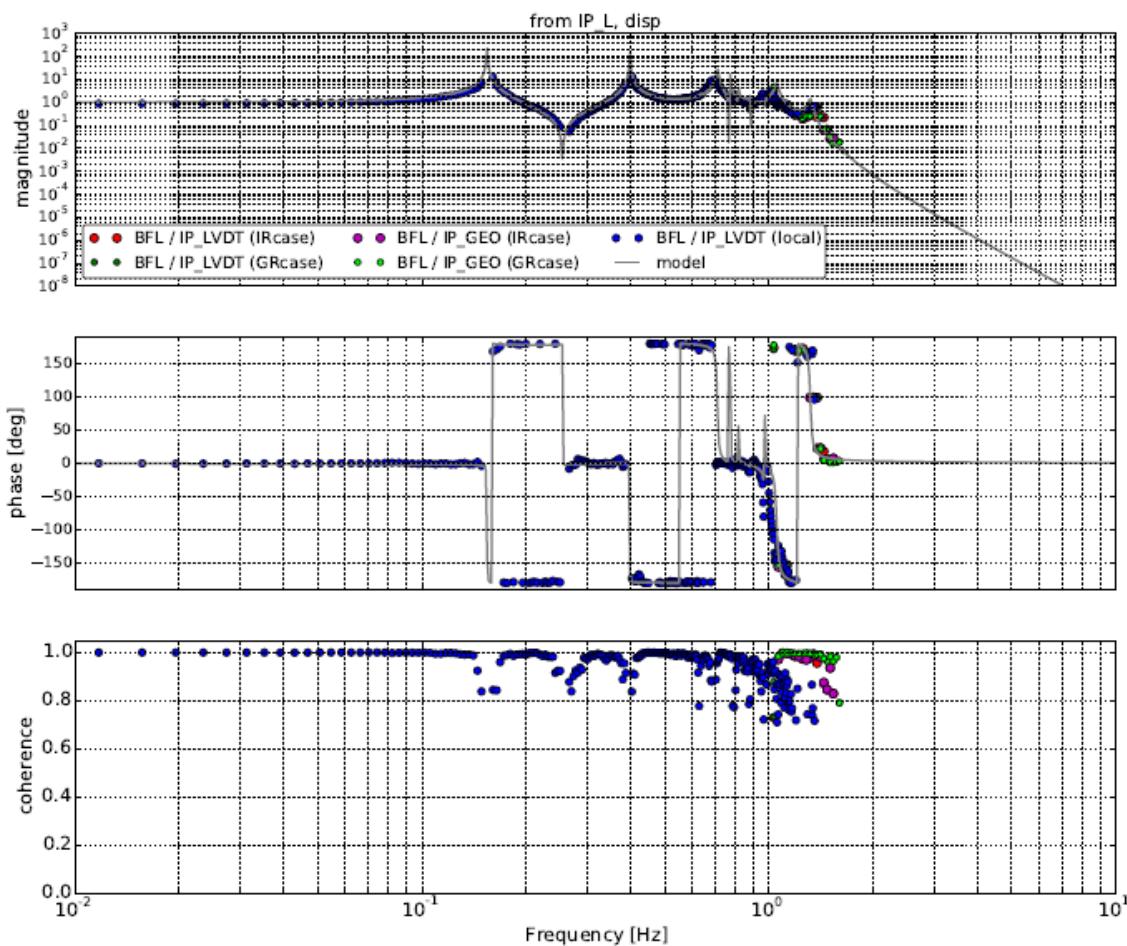
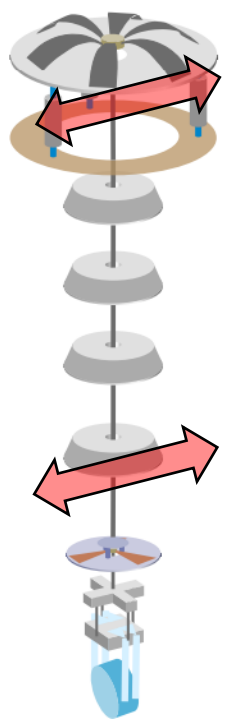
→ Not reliable.





# Results: displacement transfer functions, from IPL to BFL

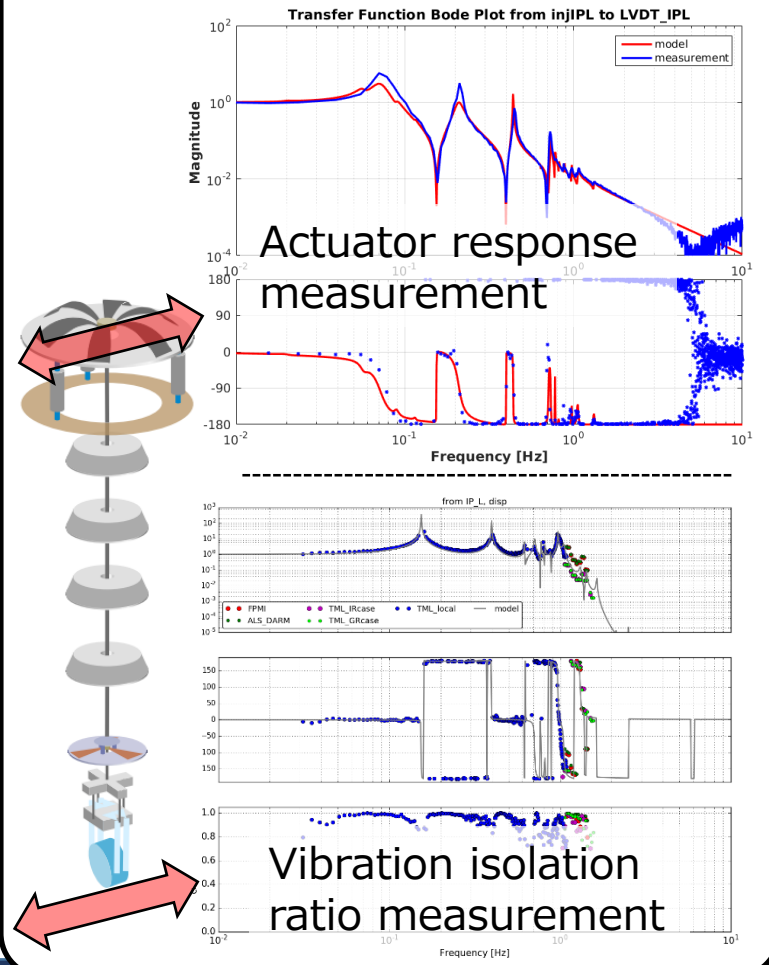
Including IP(geo) signal.



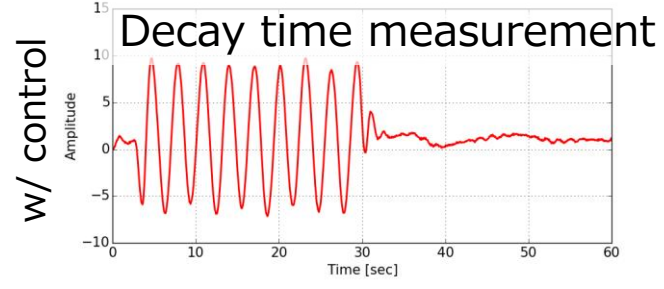
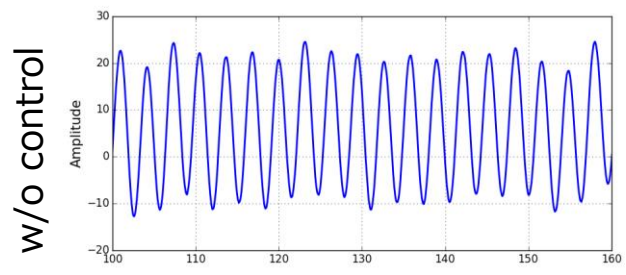
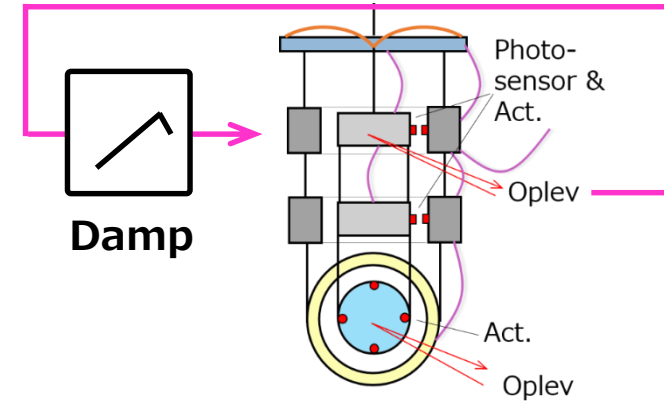
Notes: Resonance damping

# My work: Constructing controls toward interferometer lock

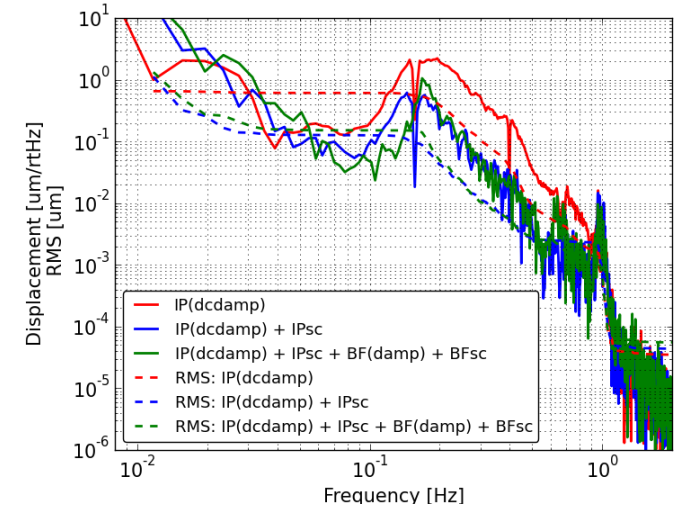
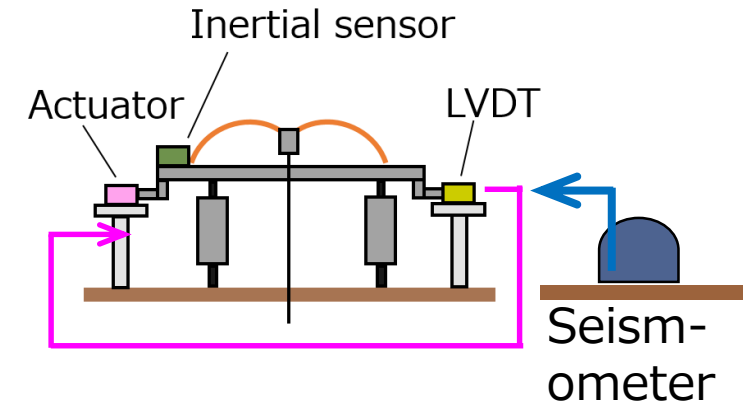
## 1. Mechanical system characterization



## 2. Resonance damping

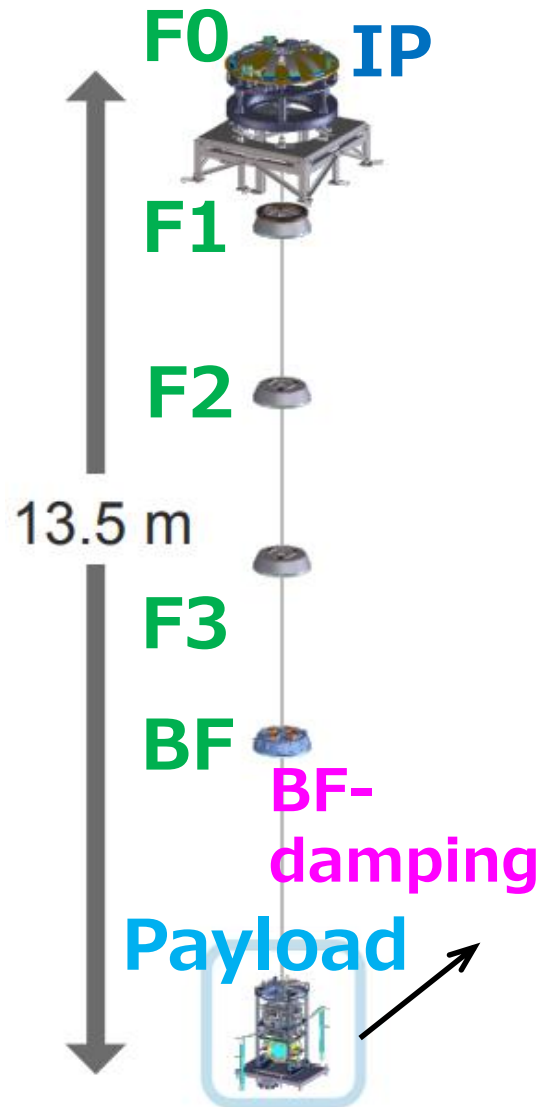


## 3. Mirror residual suppression



## 2. Resonance damping:

Control system with disp. sensors

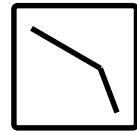


### Room-temperature part:



DC+Damp

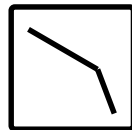
IP / Vertical filters / BF-Yaw



DC

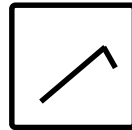
\* Pendulum mode damping  
\* drift compensation

### Cryogenic part:



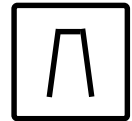
DC

Payload



Damp

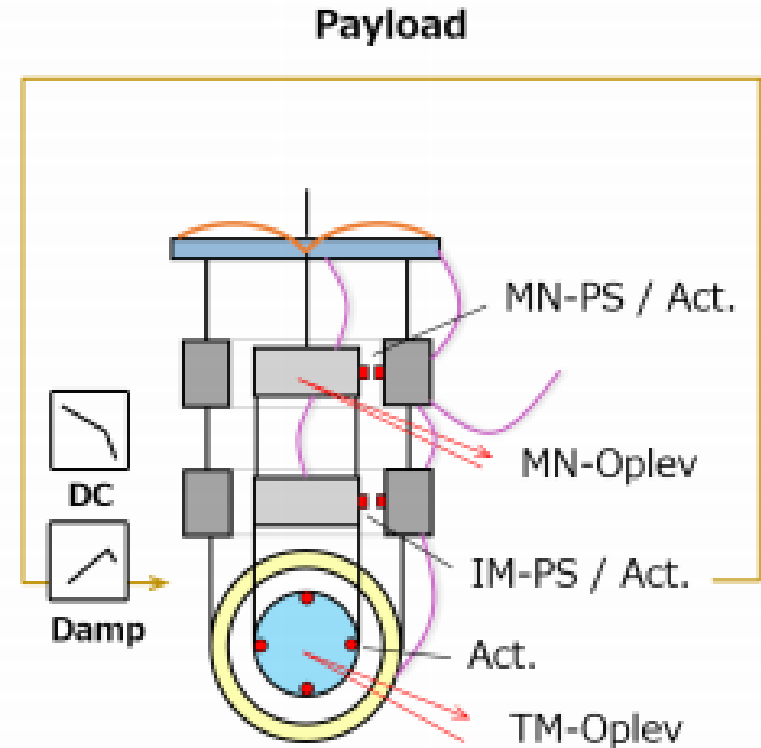
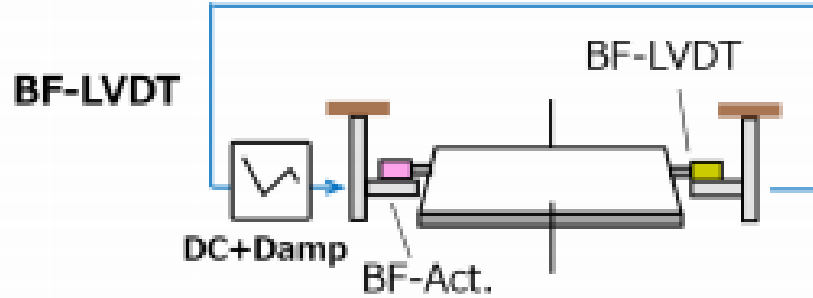
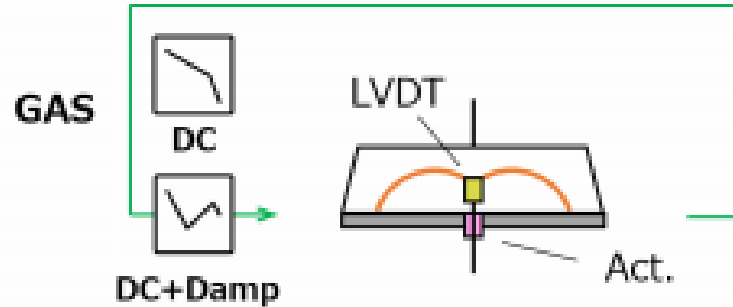
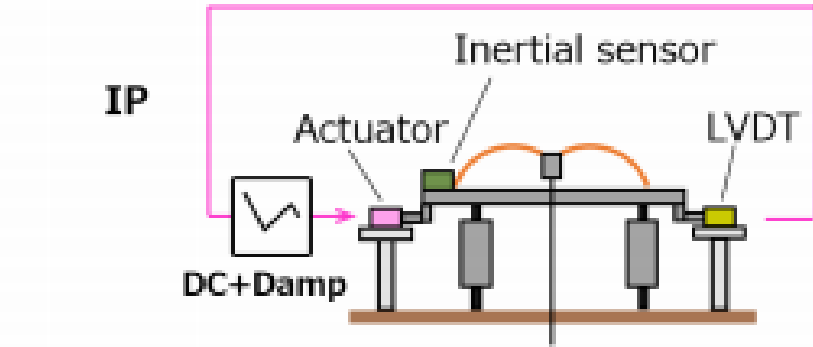
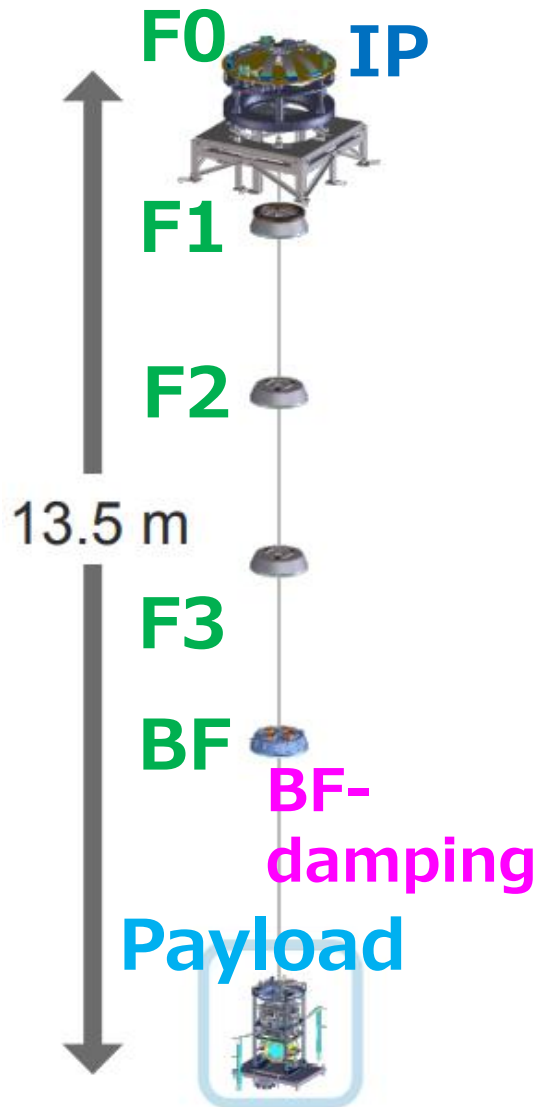
\* Internal mode damping  
\* Mirror alignment



Band-pass  
damping

# 2. Resonance damping:

Control system for damping with disp. sensors





## 2. Resonance damping:

Open loop transfer functions for Control system for damping with disp. sensors

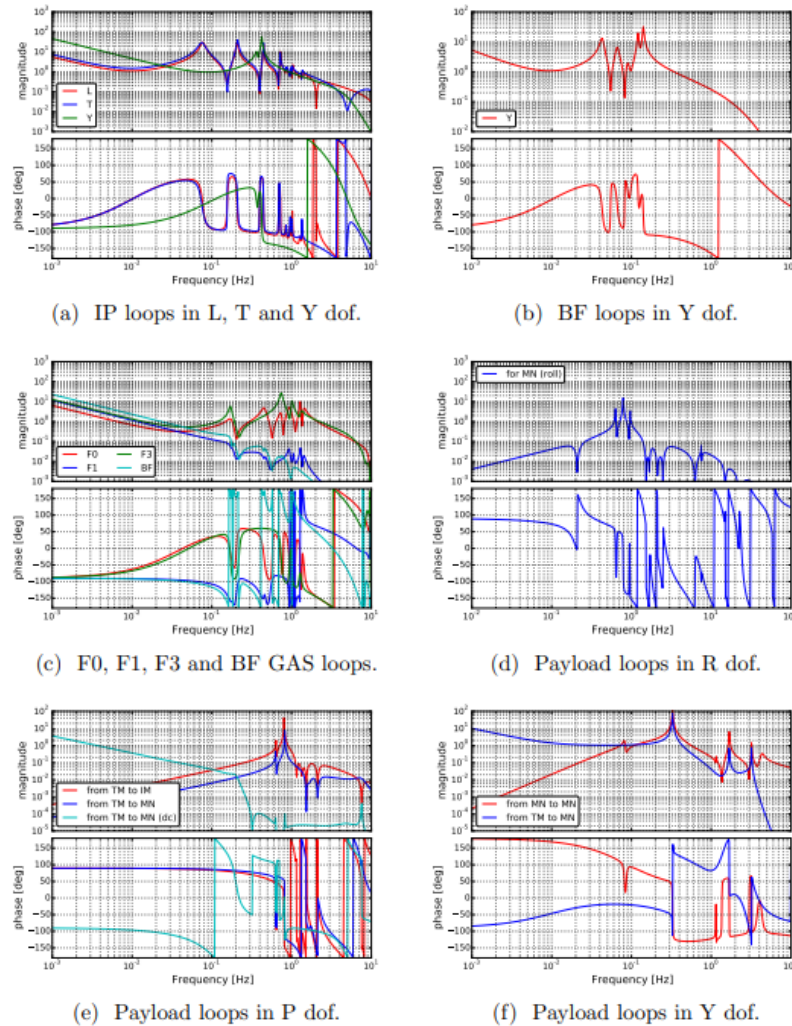


Figure 6.12: Open loop transfer functions of the implemented servo filters for the calm-down phase.

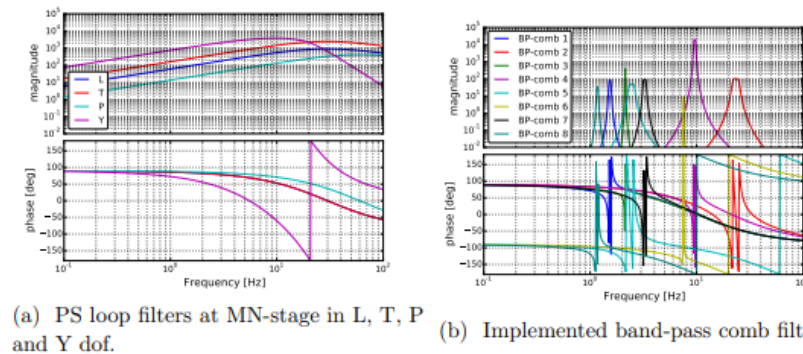
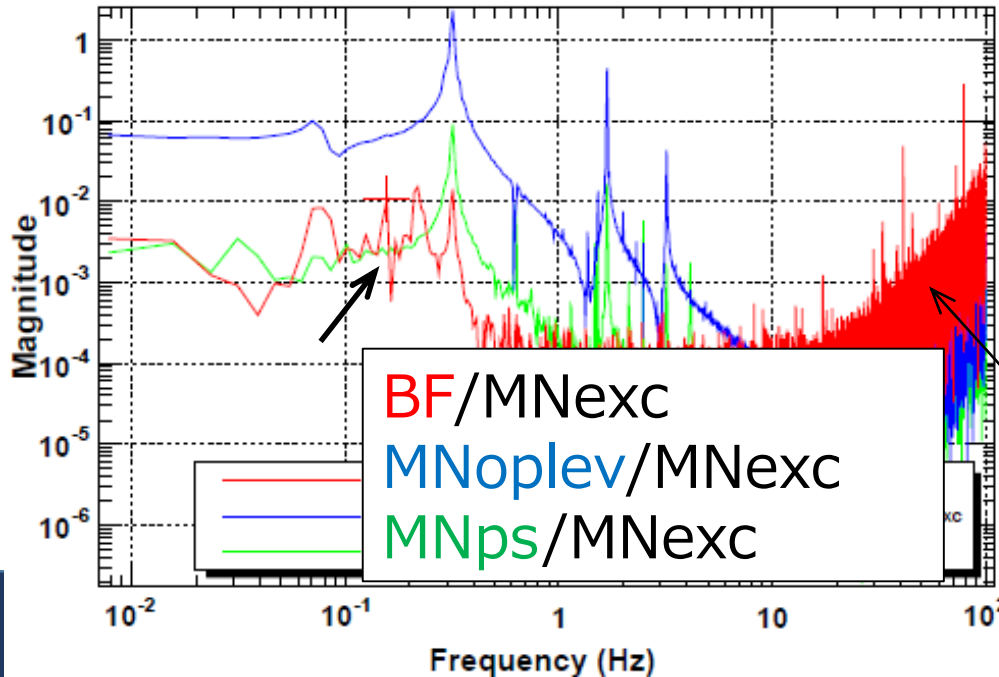
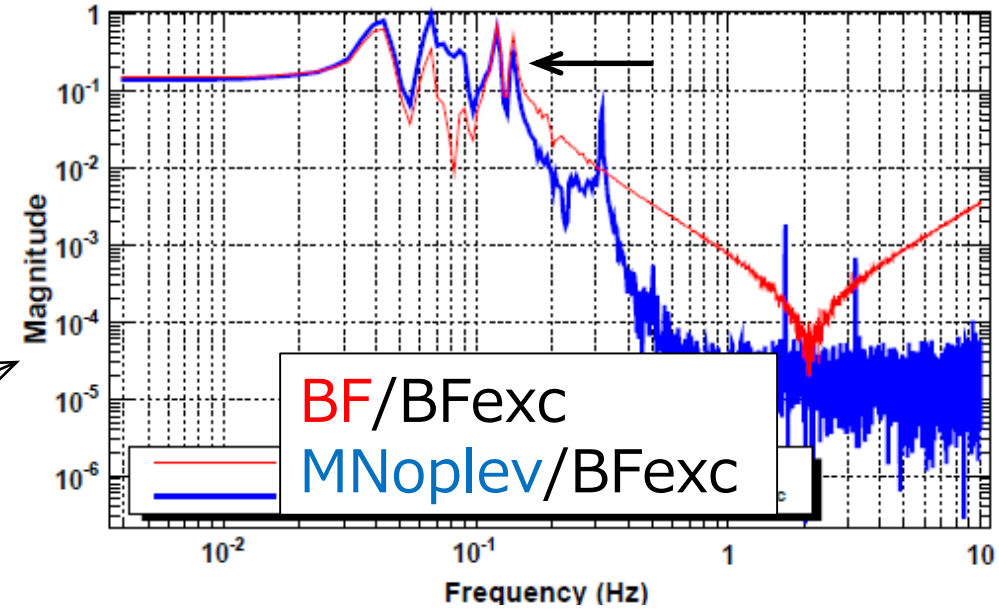
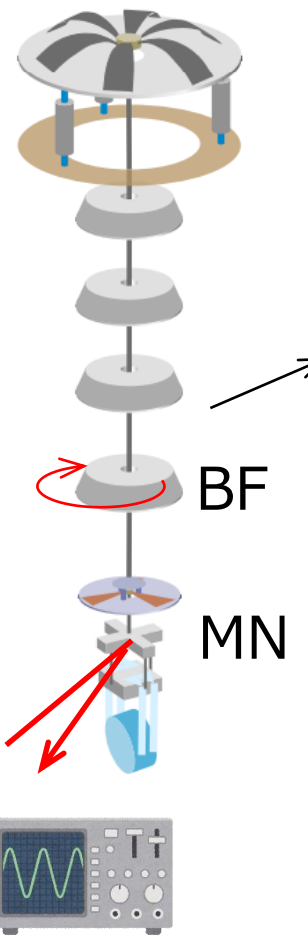


Figure 6.13: Implemented servo filters in addition to the ones in Table 6.1.



# So, is this unknown Yaw mode problematic for the target?

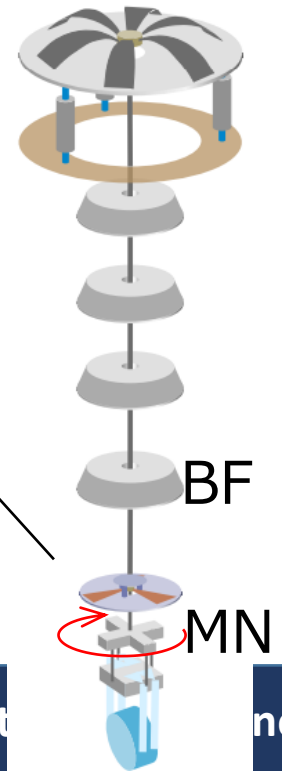


→ No for now, at least.  
for (current) lock-recovery.

\* When noise injected at **BF**-stage:  
→ The mode looks exited.

\* When noise injected at **MN**-stage:  
→ Not (clearly) exited in TM-chain.

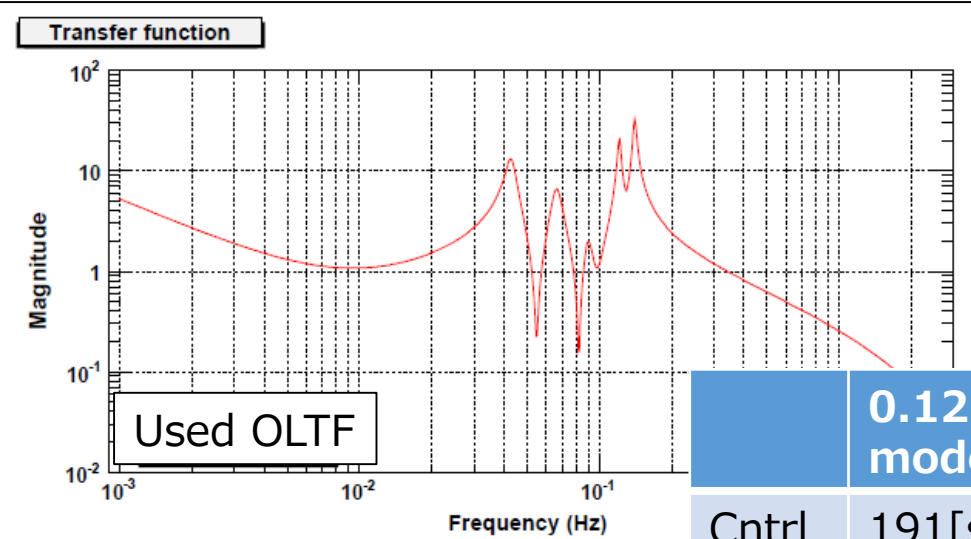
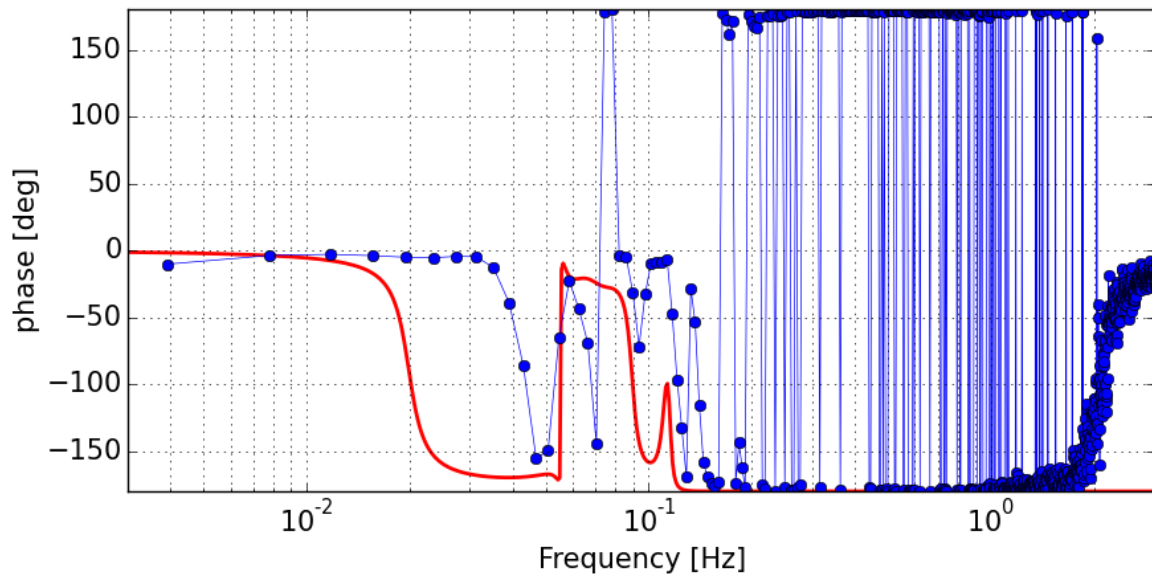
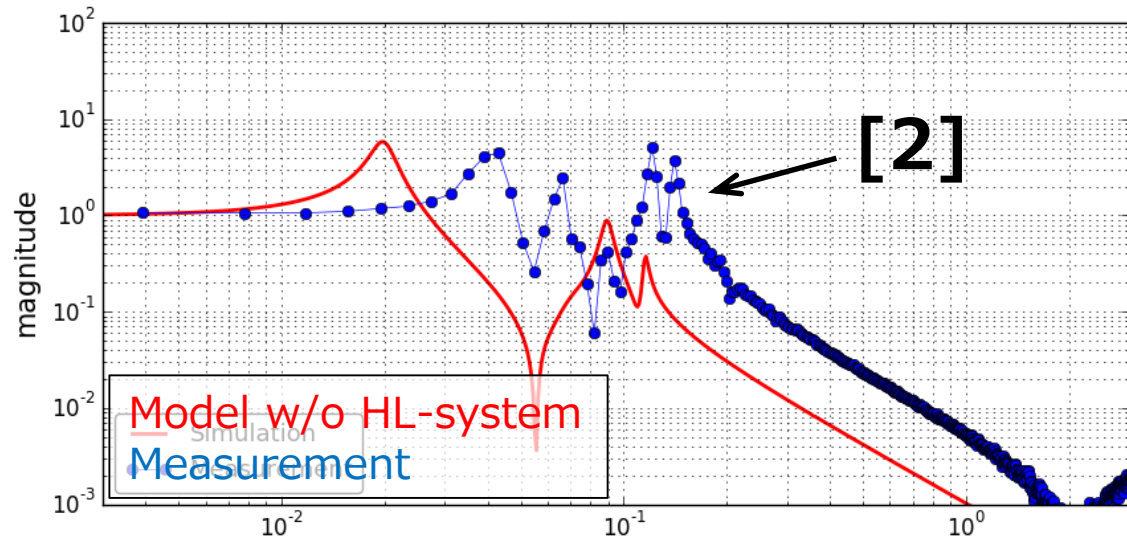
\* The decay time  $\sim 3$ min.



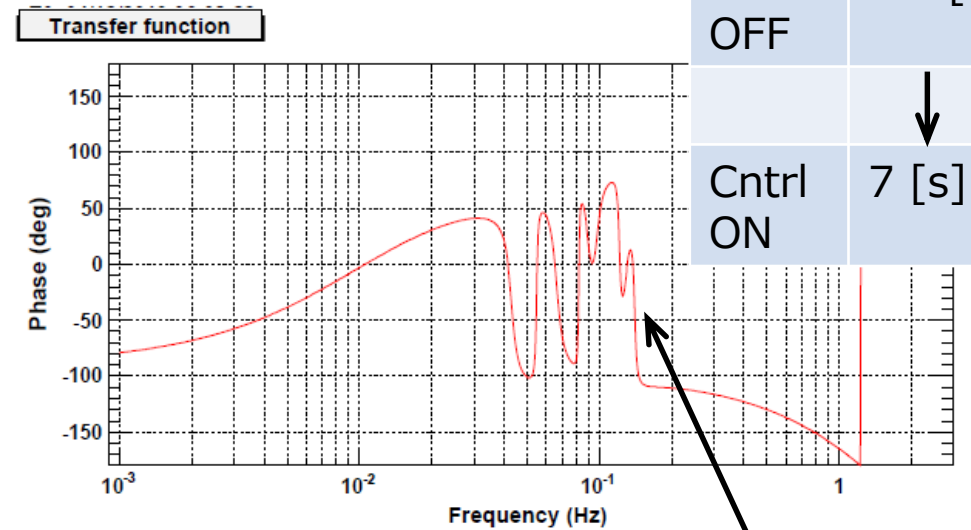
# Summary of this work:

- The installed damping control system damped all the resonances which disturbs the lock acquisition **for the lock-recovery mode.**
- exception: one mode
  - This mode looks from HL-system
  - This would be problematic when upper stages are used for the global controls. → Further improvement
- In this work, the payload damping system is constructed mainly with the optical levers (relatively small linear range).
  - better to utilize Photo-sensors more effectively.

# unknown Yaw mode [2]?



	0.12Hz mode	0.14Hz mode
Cntrl OFF	191 [s]	330 [s]
	↓	↓
Cntrl ON	7 [s]	180 [s]

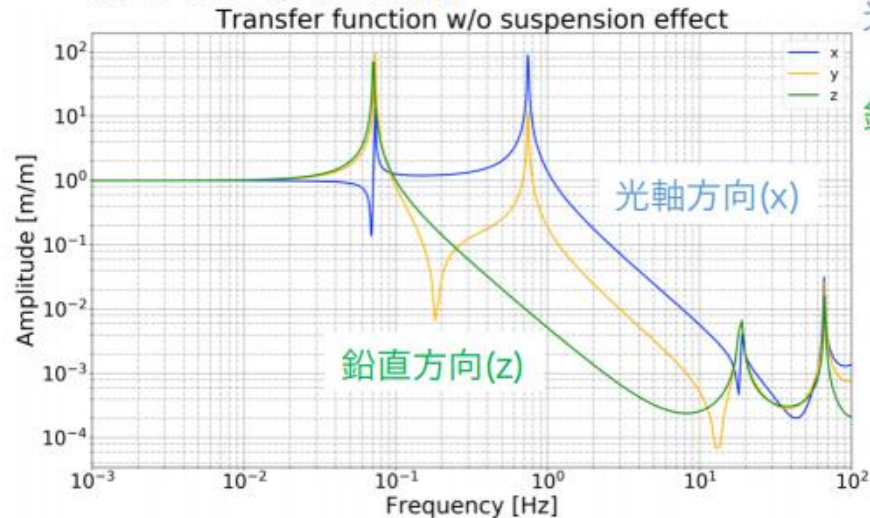


More finely tuned phase compensation might work

# Expected heat link frequency response

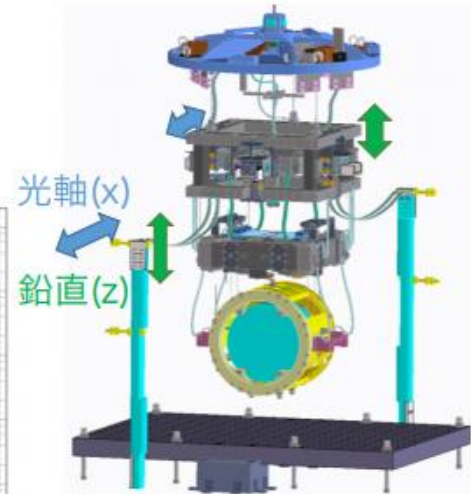
## 伝達関数とその補正

- 得られた伝達関数

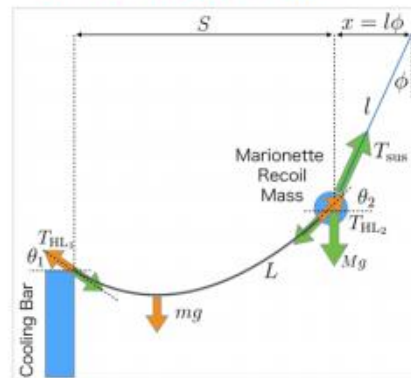


- 伝達関数の補正

上の解析結果では、MTRMが自由質点  
-> MTRMが懸架されている効果を入れる  
必要がある



1/300で鉛直方向の揺れが  
光軸方向とカップル

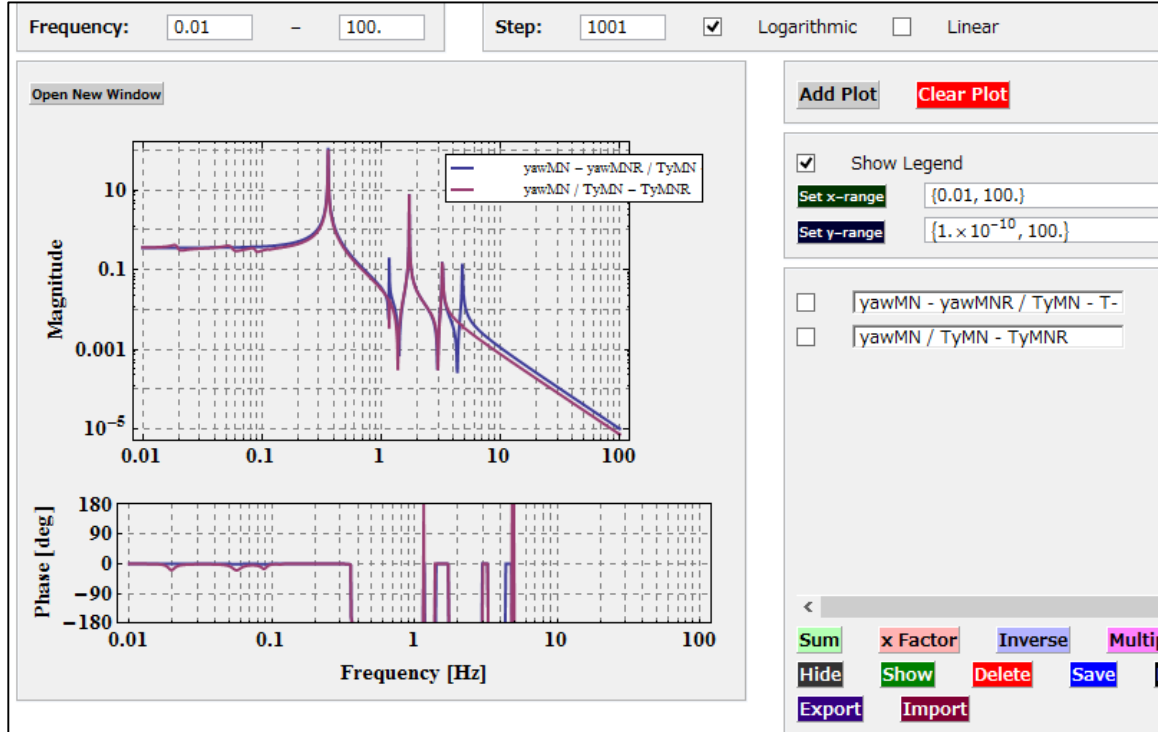


修士論文審査会 2018/01/11 理学部1号館414号室

42/48

JGW-P1807766

# Photo-sensor inter-calibration



\* According to a simulation, the following force TFs should have same DC gain (since RM-chain is still enough compared to TM-chain it seemed).

MN(Y)ps/MN(Y)exc and MN(Y)oplev/MN(Y)exc

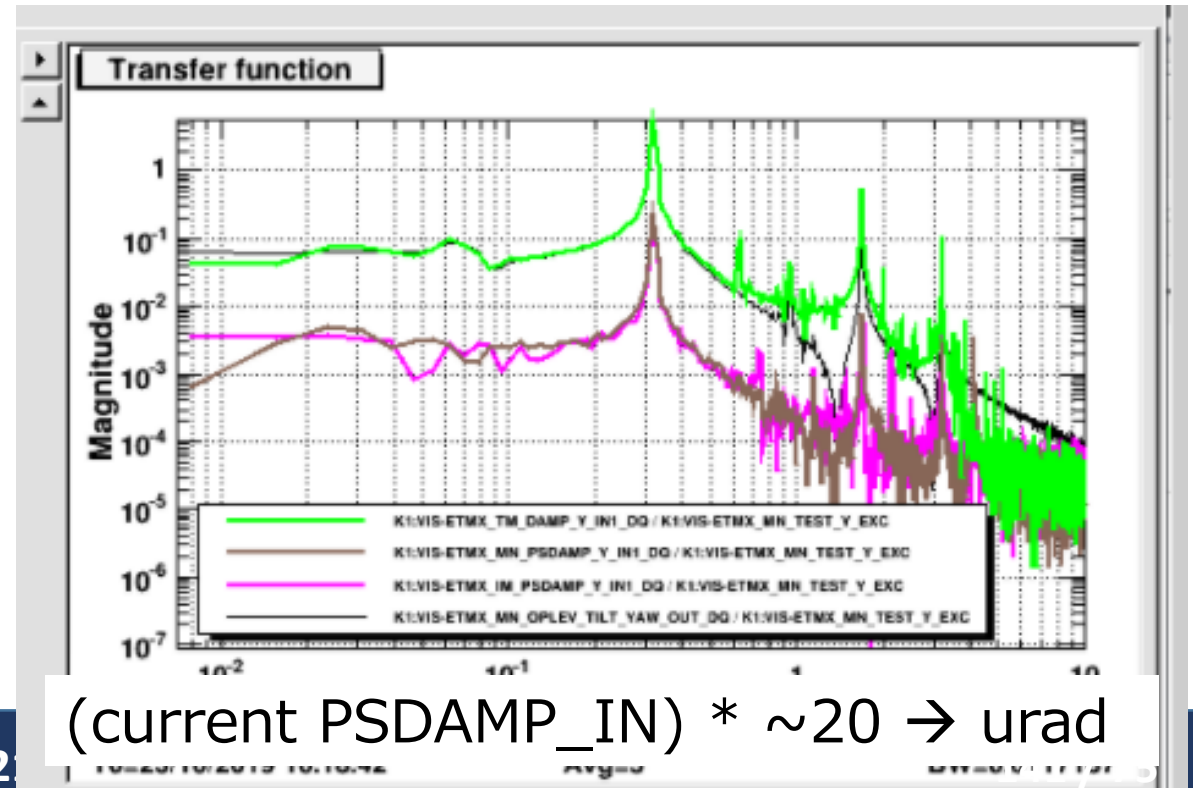
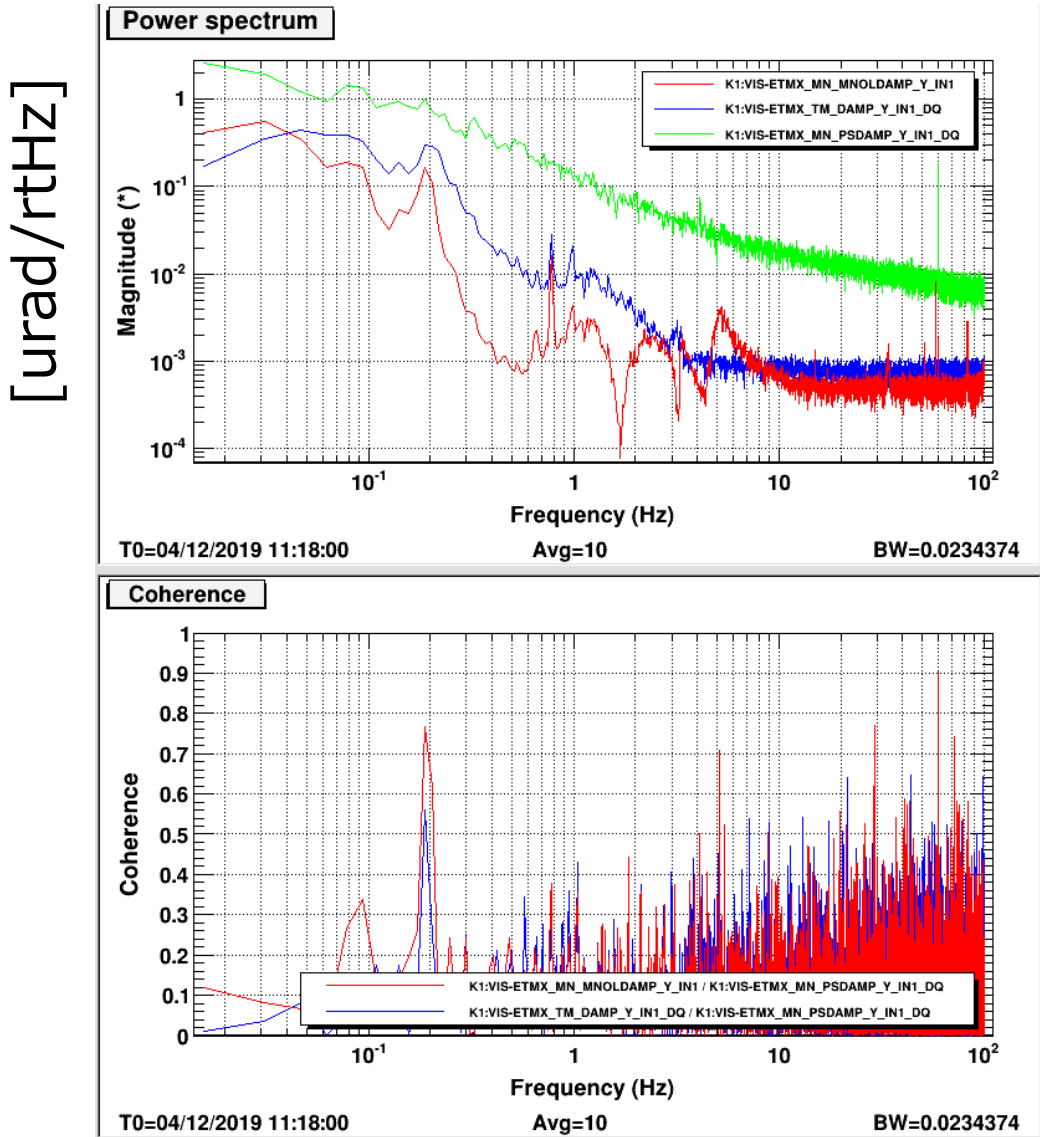


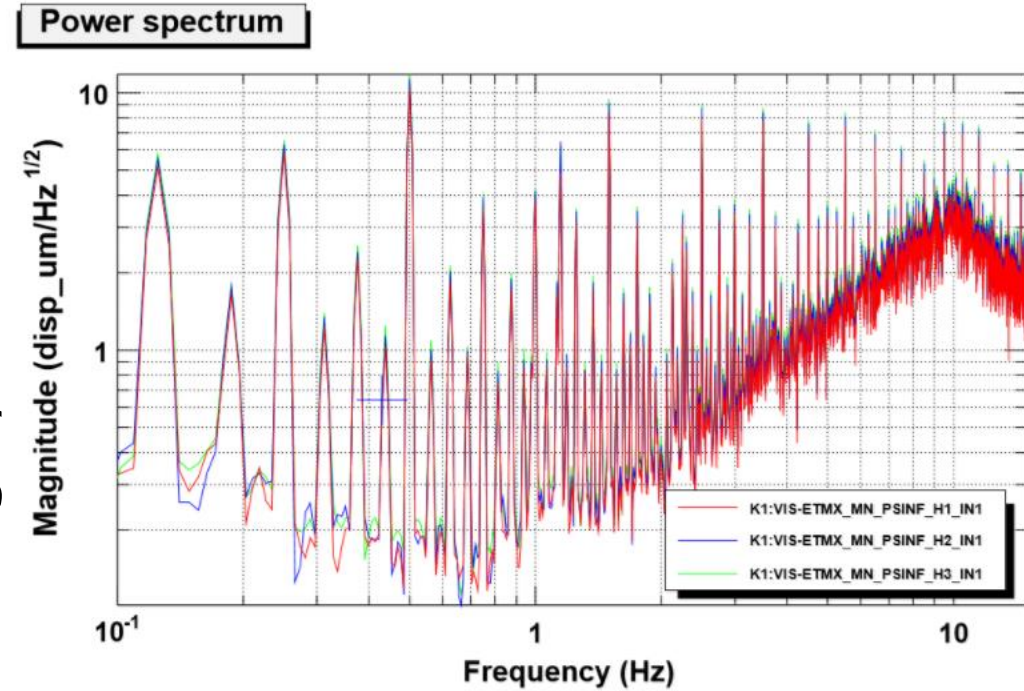


# Photo-sensor inter-calibration



- \* Spectra w/ the calibration factor.
- \* Might be too large (a bit) though, direction looks okay.

Roughly estimated



- \* We have to keep in mind that the PS in ETMX becomes sometimes crazy though.

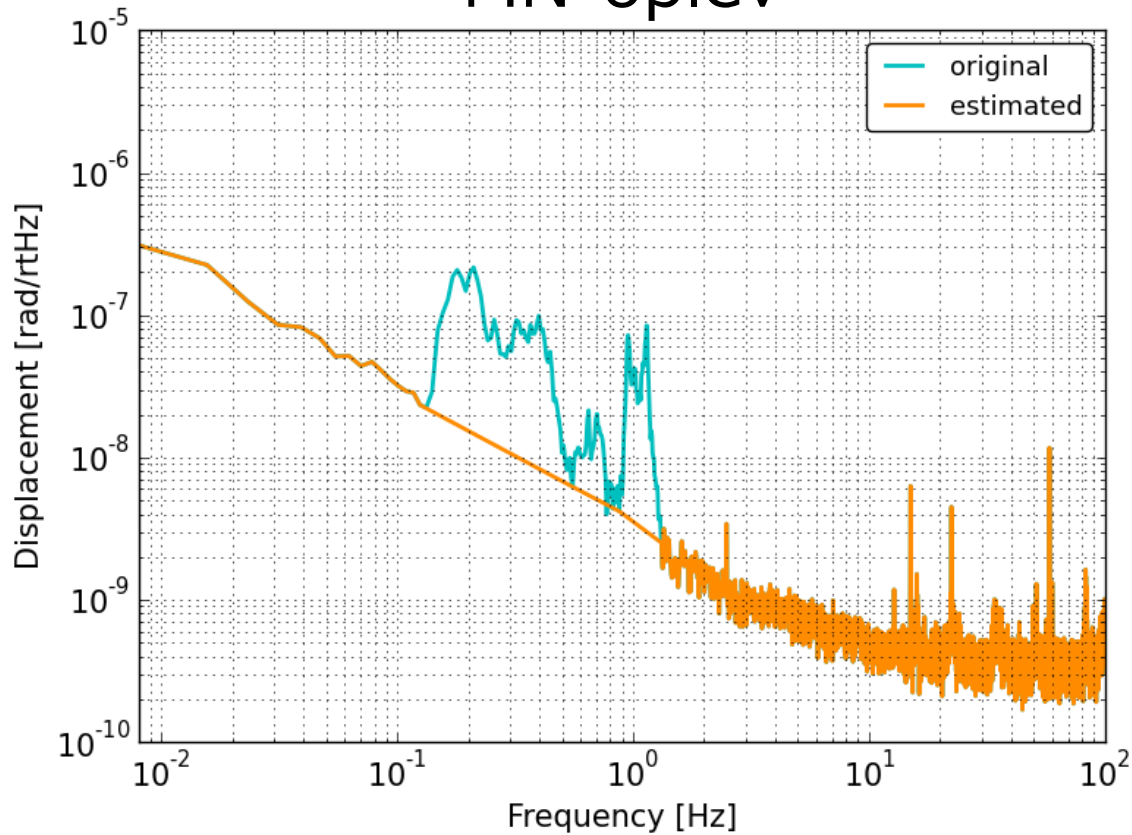


# Optical lever noise floor:

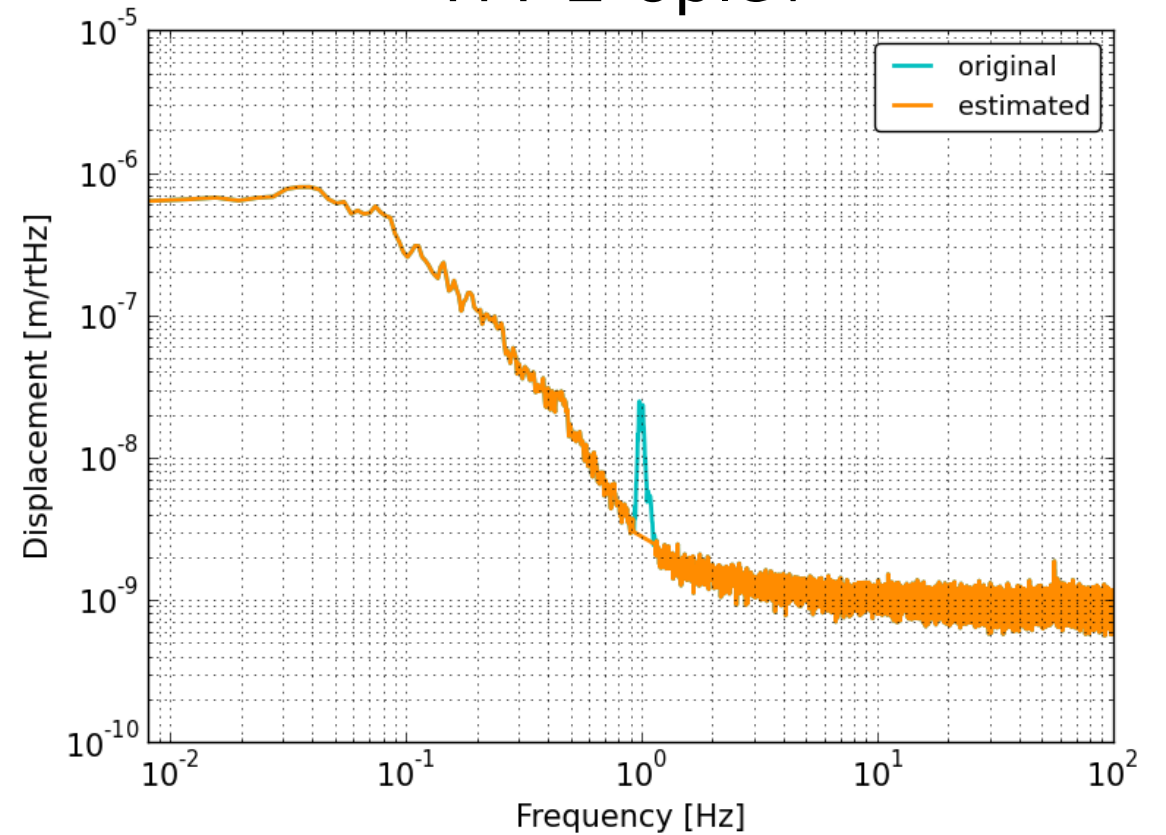
\* Obtained with interpolation:

( Estimated  $\rightarrow$  interpolated )

## MN-oplev

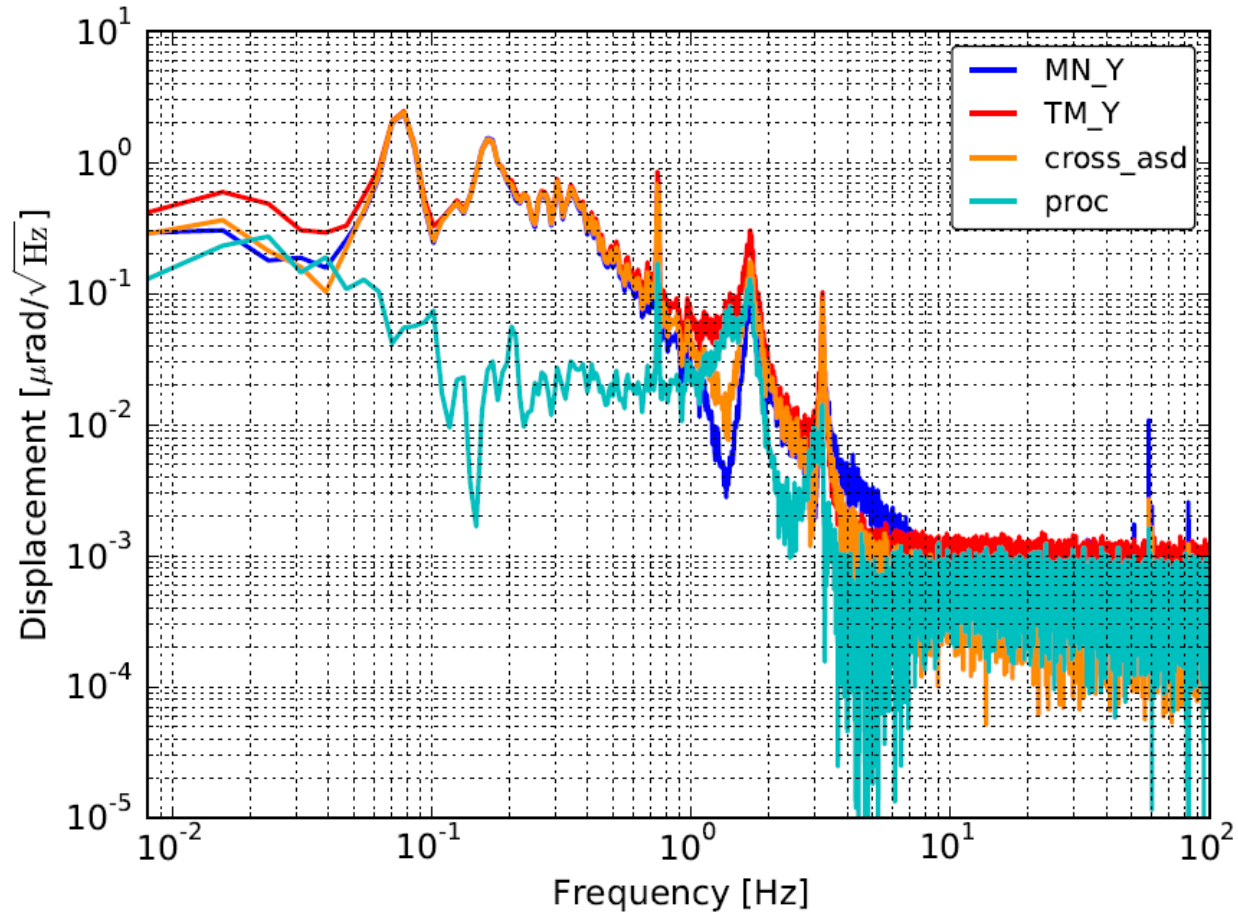


## TM-L-oplev



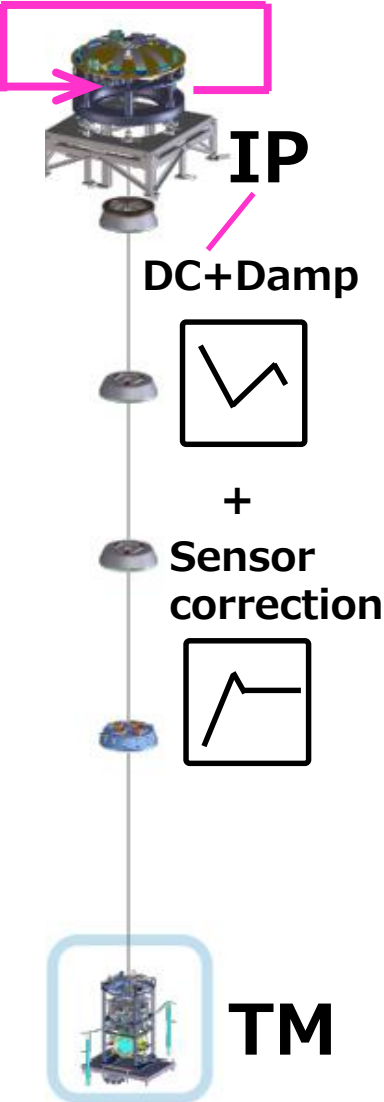
# Optical lever noise floor:

\* Obtained with correlation analysis (TMY\_ASD – MNY\_cross\_ASD):

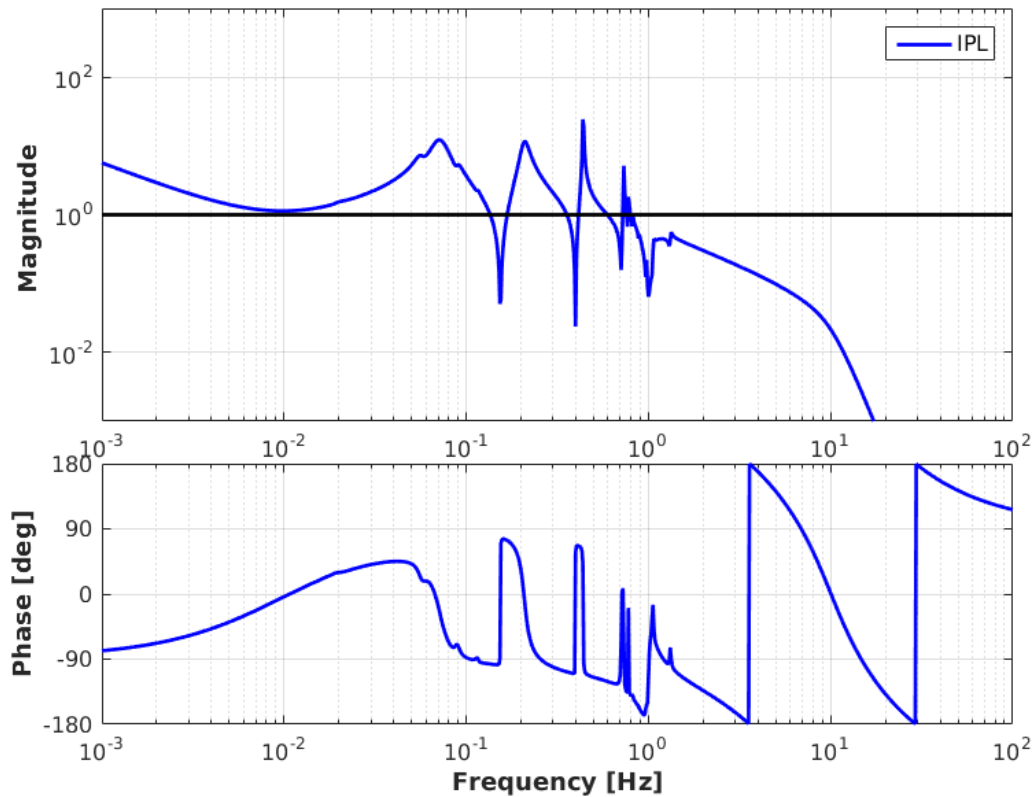


Notes: RMS suppression

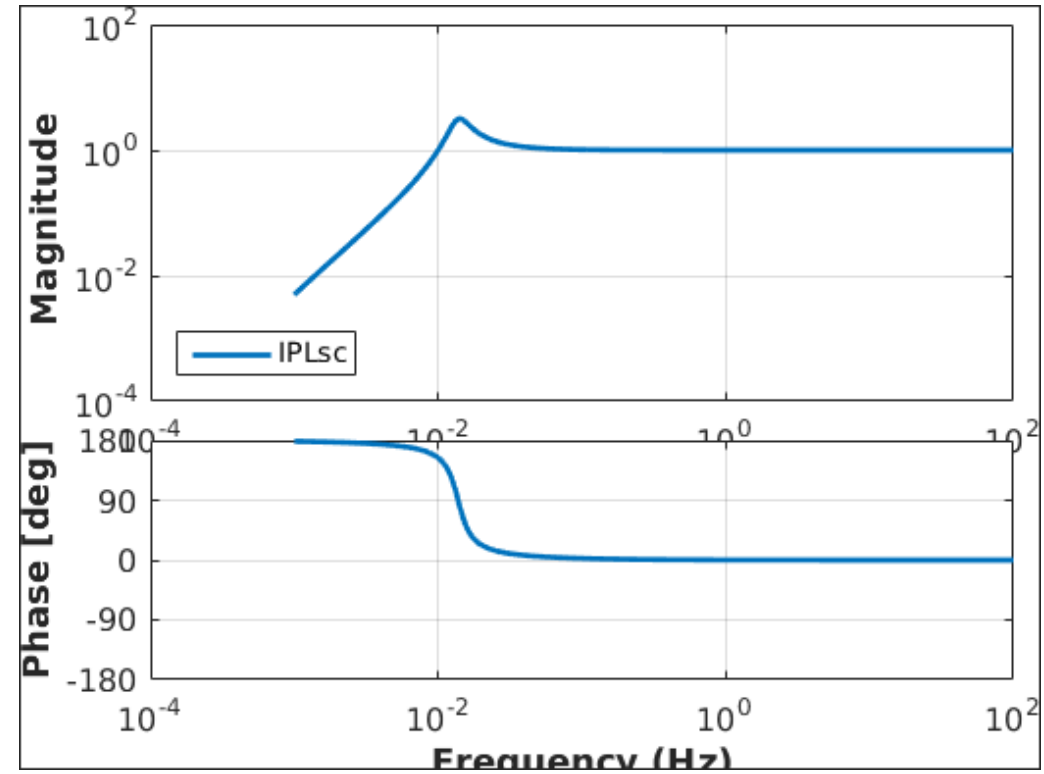
# 制御ループ° at IP-stage:



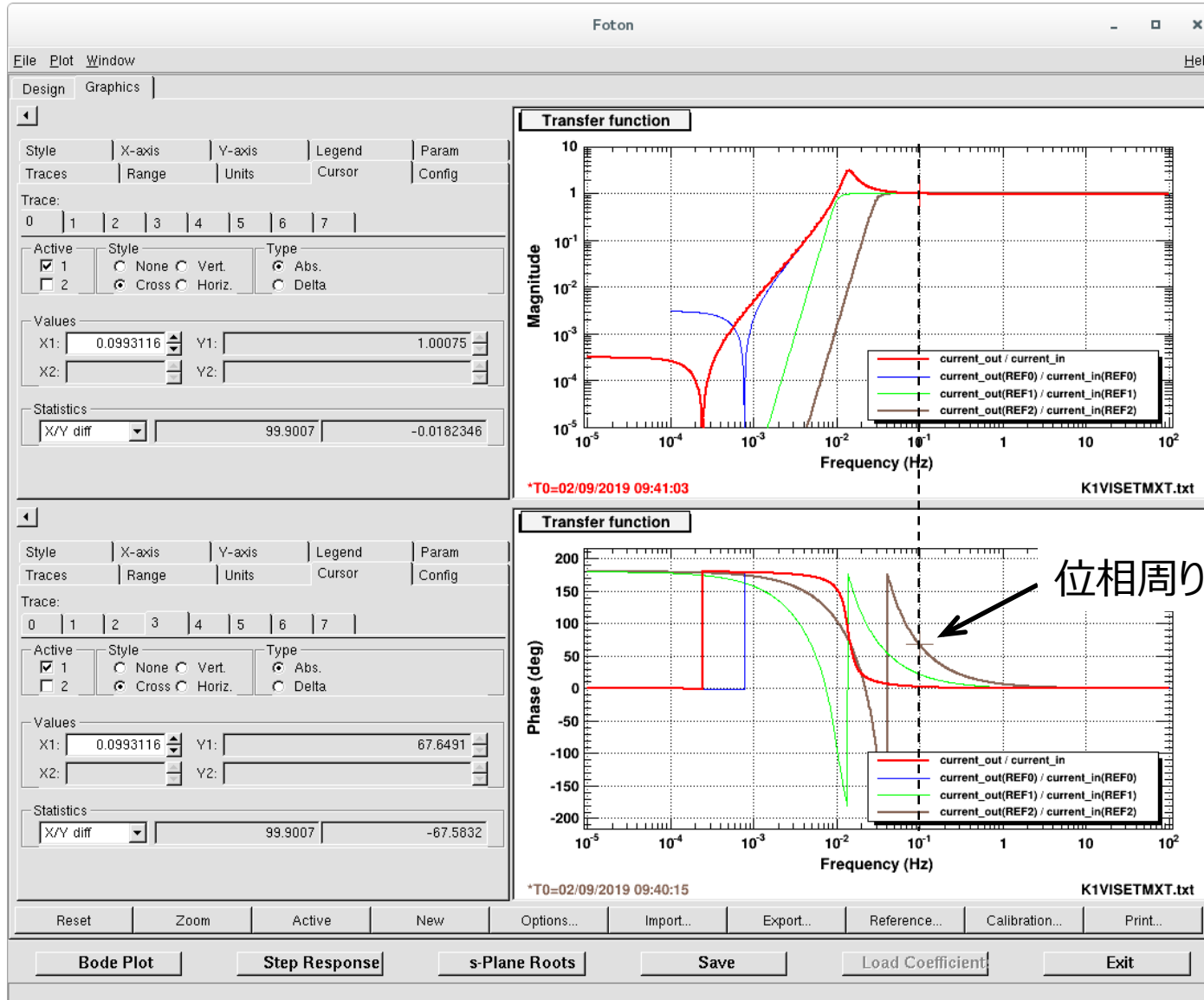
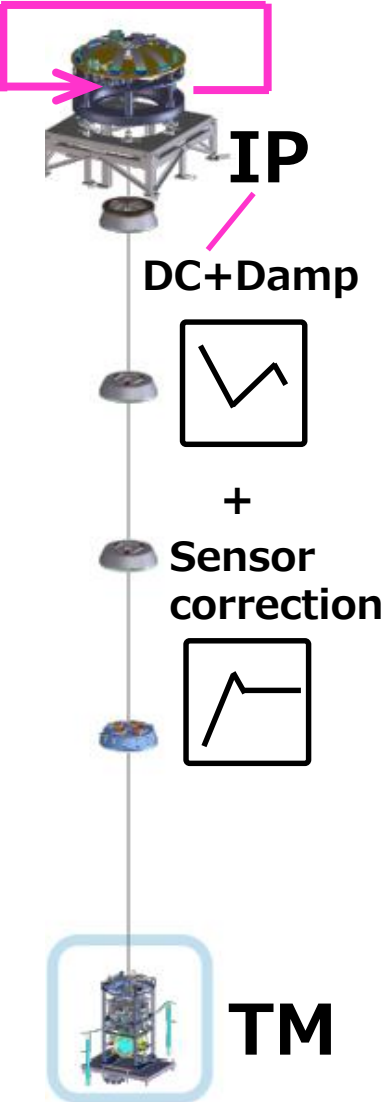
## 1. OLTF for IP-LVDT



## 2. Sensor correction filter

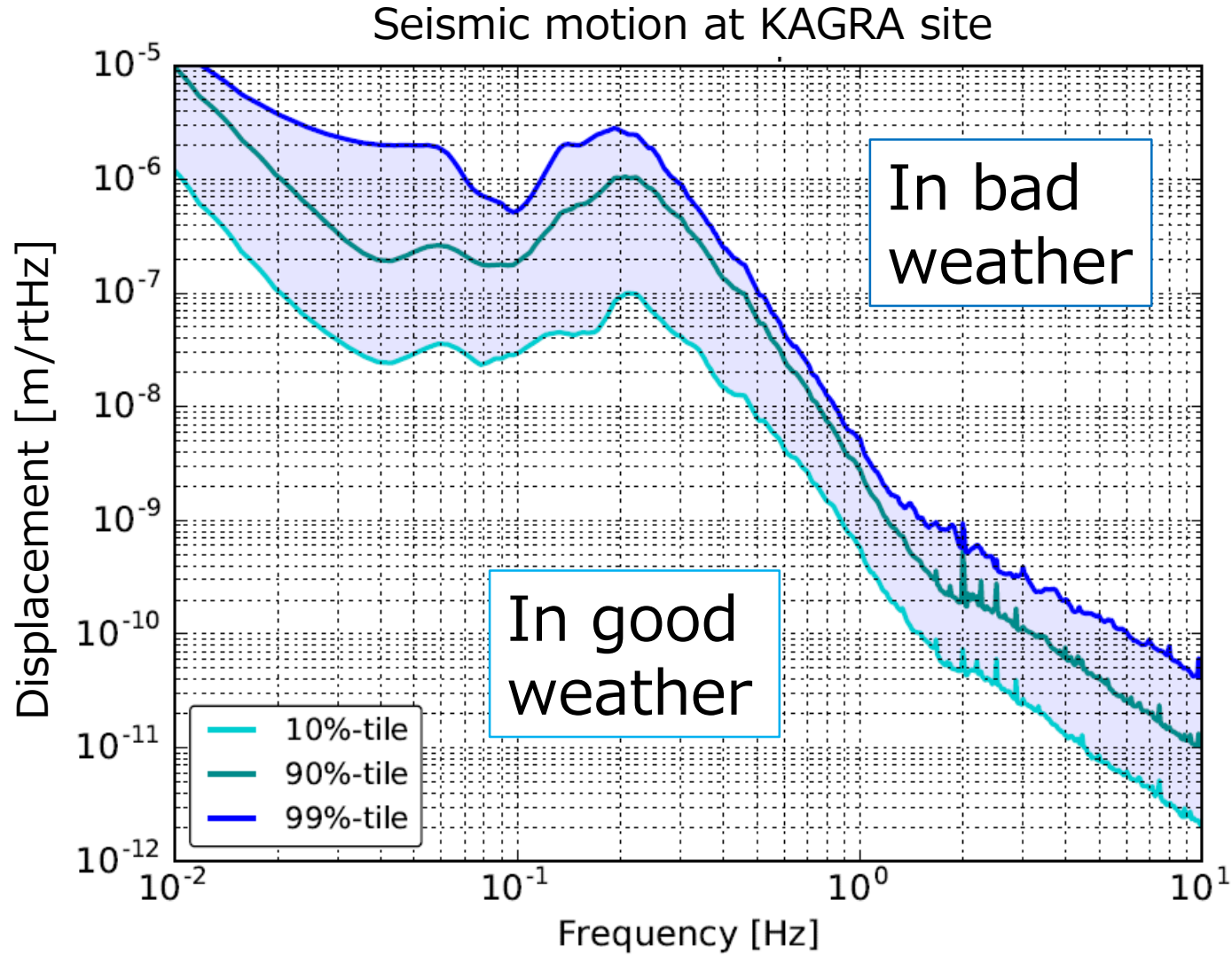


# Sensor correction filter の検討



位相周りがなるべく少ないものを採用した。

# Ground motion at KAGRA site

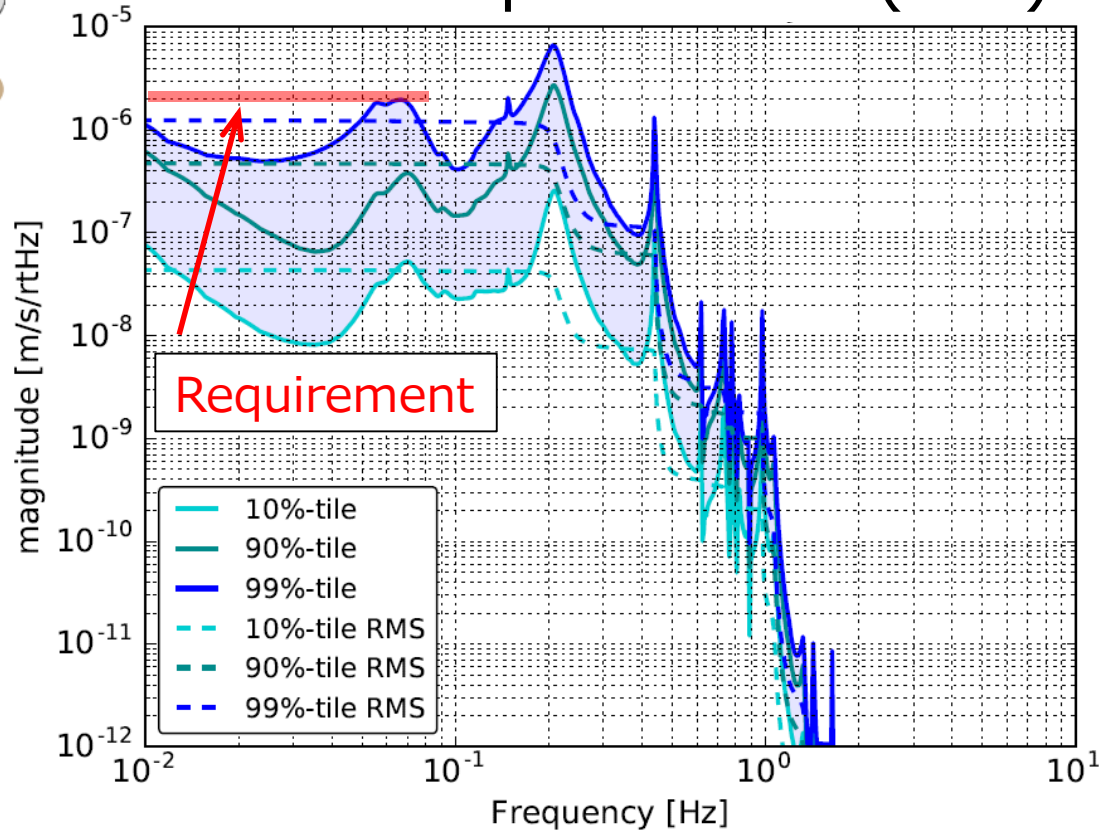




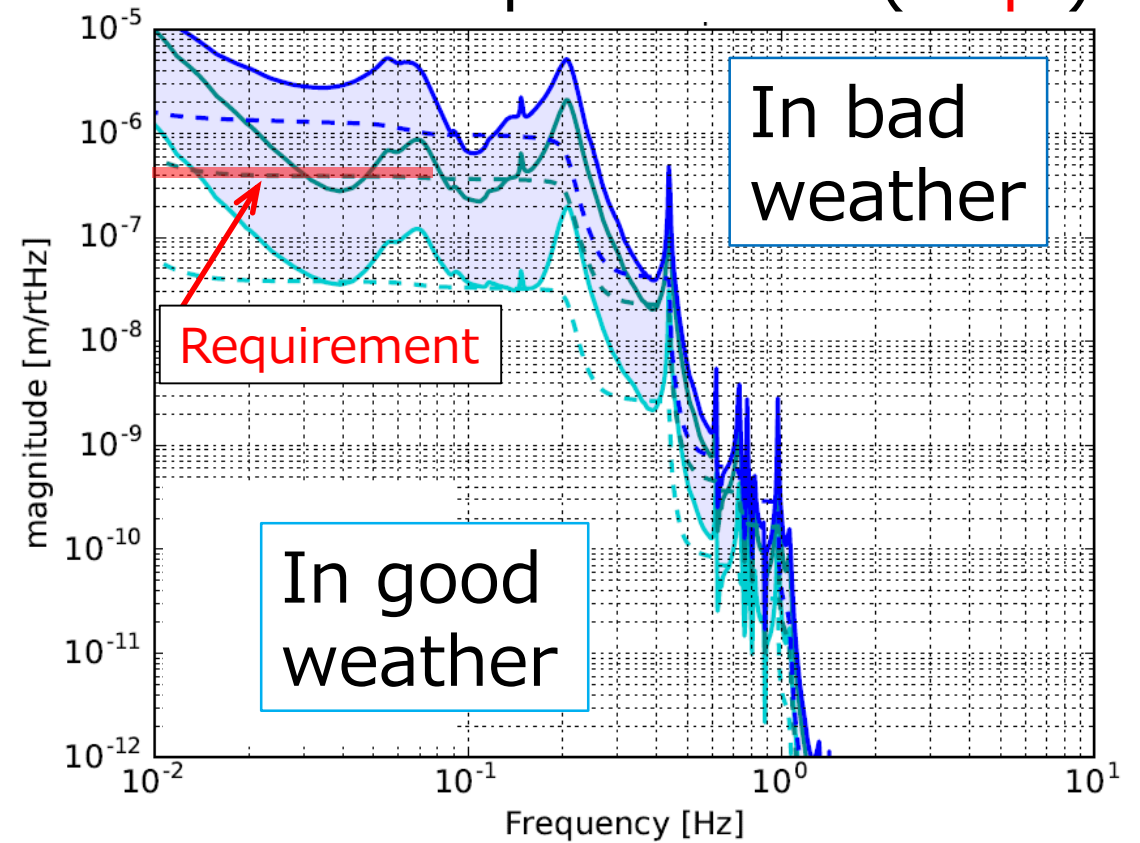
# Suspension response at KAGRA site w/o control

\* Simulated mirror residual motion:

## Mirror Displacement (vel.)



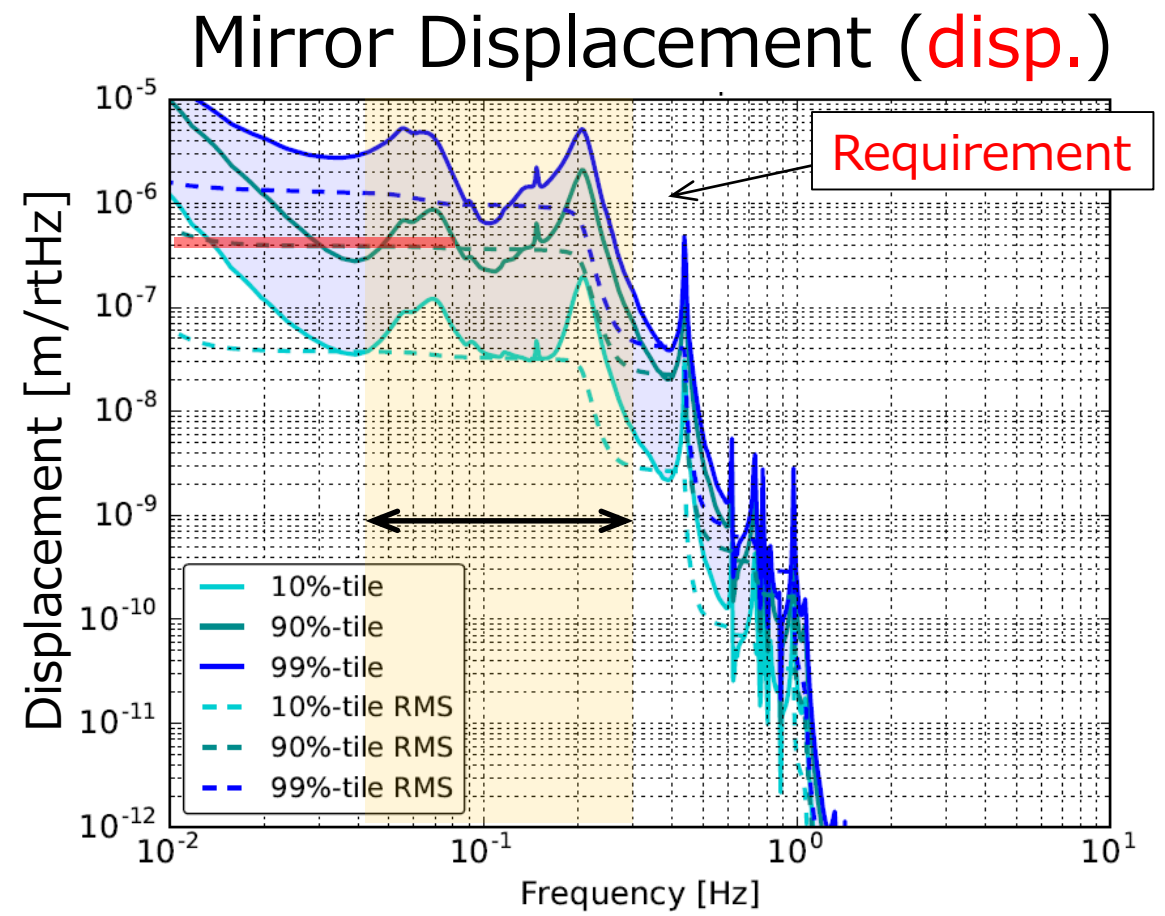
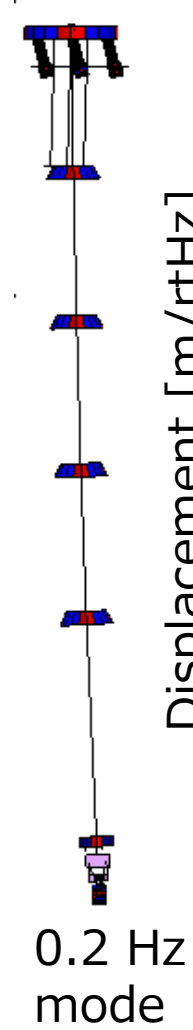
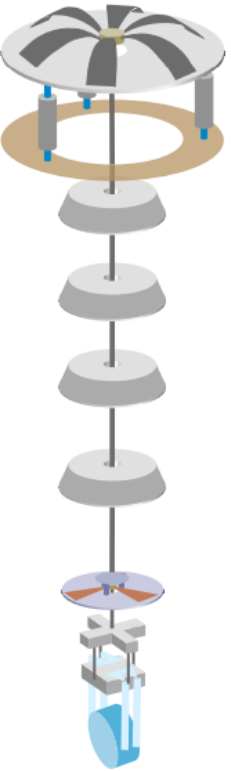
## Mirror Displacement (disp.)



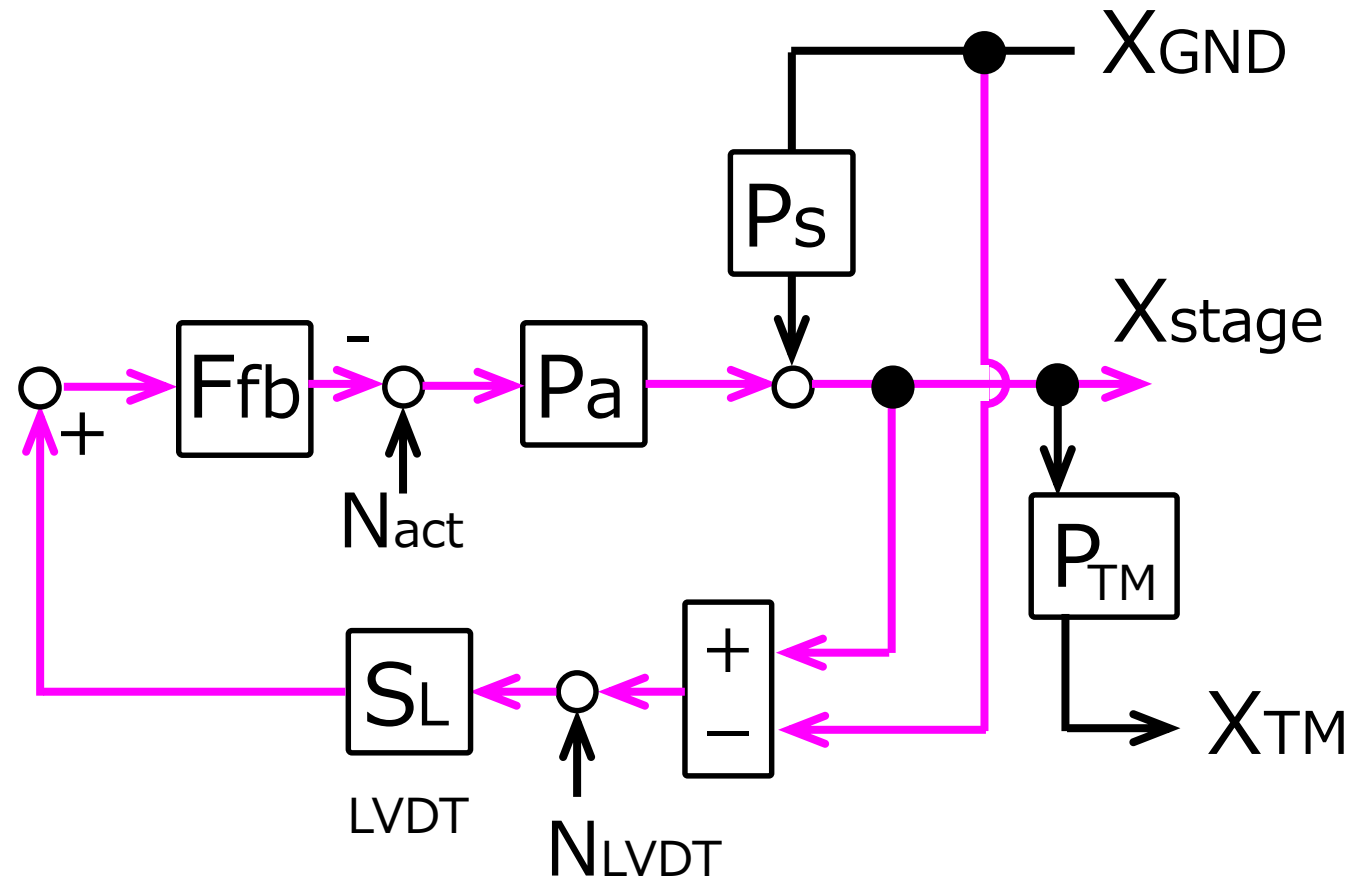
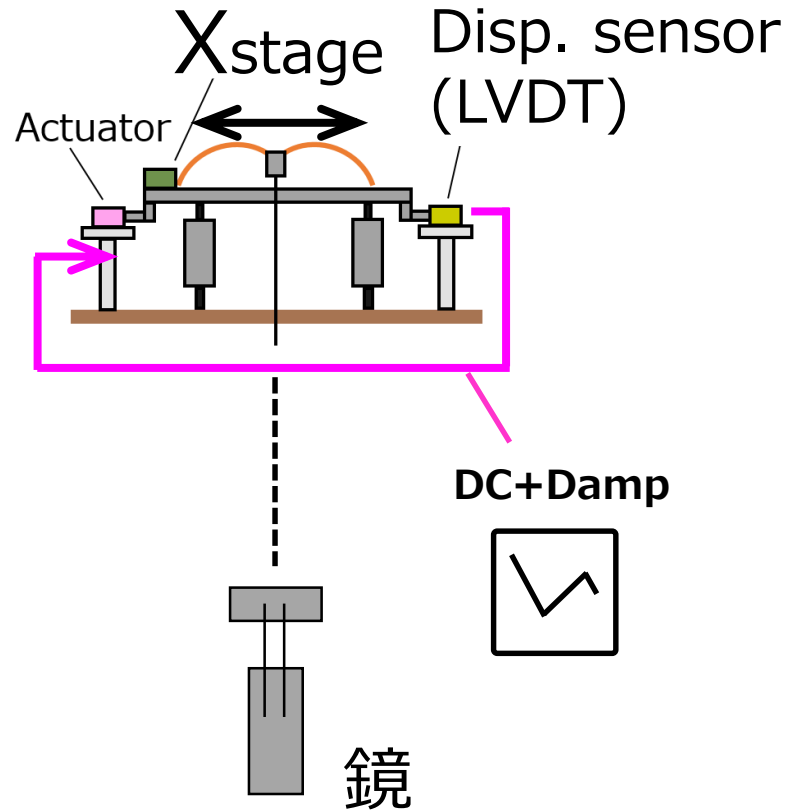
Ref: <https://gwdoc.icrr.u-tokyo.ac.jp/cgi-bin/private/DocDB/ShowDocument?docid=10436>

# Suspension response at KAGRA site w/o control

- \* In good weather  
→ req. will be satisfied.
- \* In bad weather (especially in winter)  
→ req. will not be satisfied
- \* Contribution to RMS is large in the band.  
→ To be suppressed  
→ at upper stage.



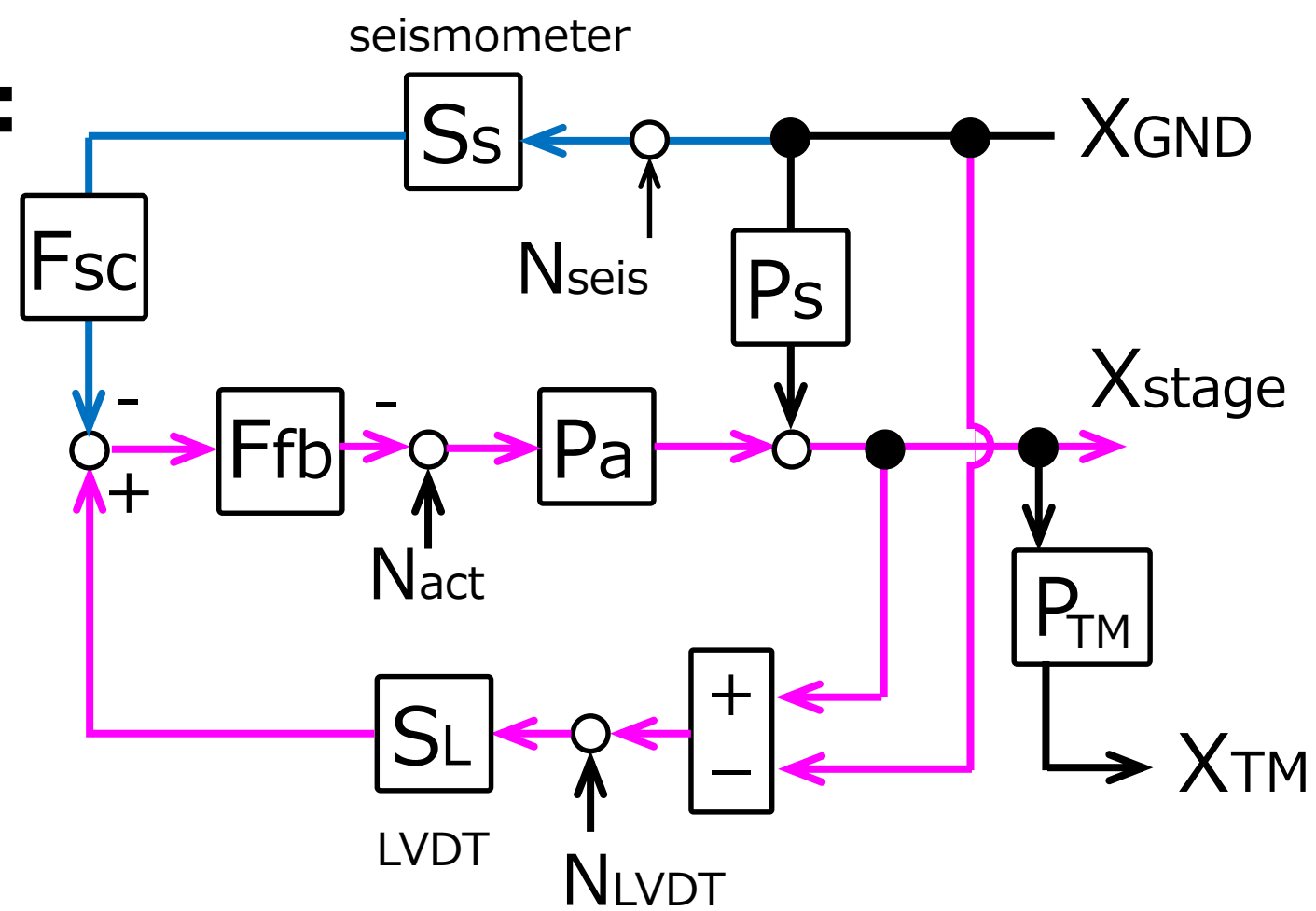
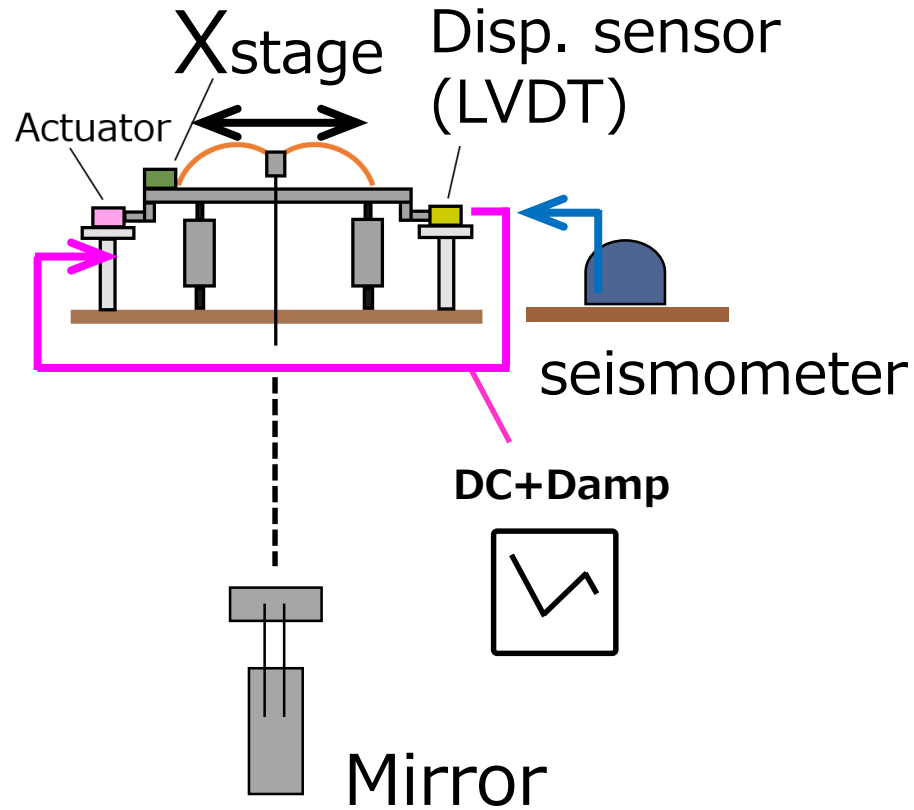
# Control overview (in L):



Disp. sensor uses:

$$(X_{stage} - X_{GND}) \longrightarrow X_{stage} \sim X_{GND}$$

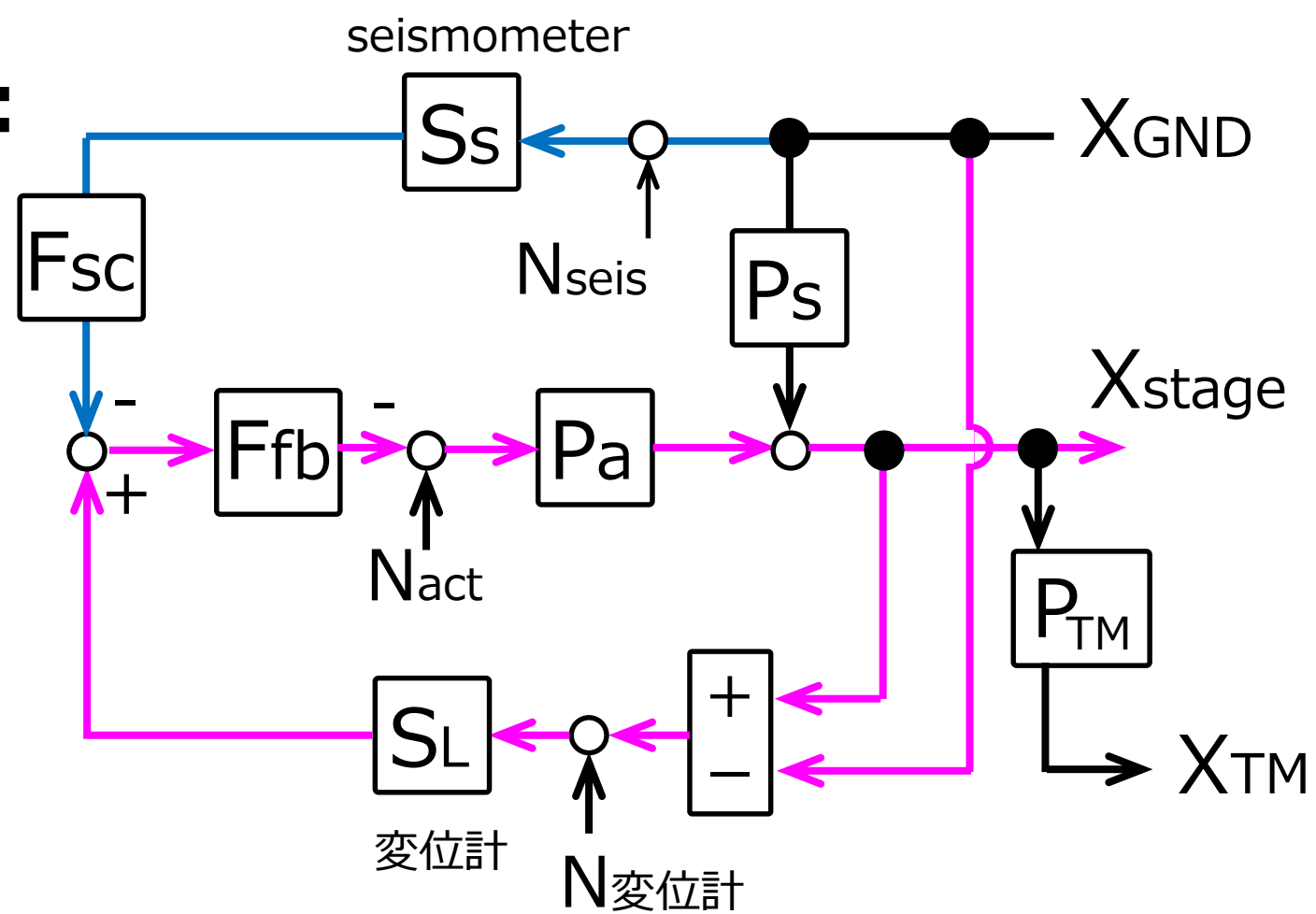
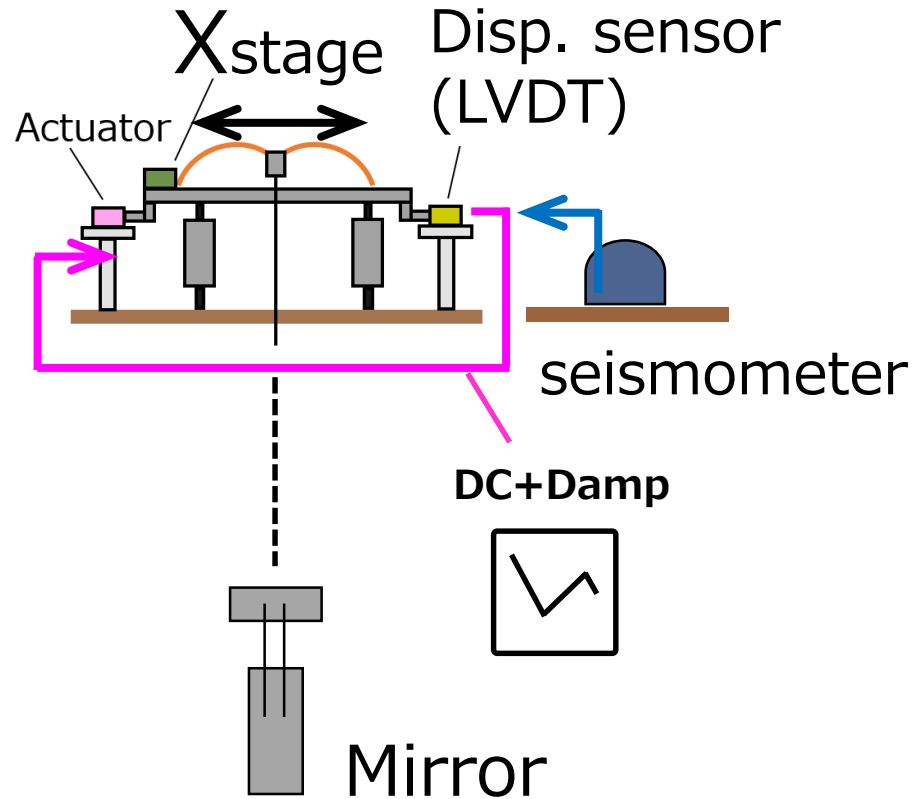
# Control overview (in L):



$$X_{stage} = \frac{1}{1 + G} \left[ G \left( 1 + F_{sc} \frac{S_s}{S_L} \right) + P_s \right] X_{GND}$$

$$( G = P_a F_{fb} S_L )$$

# Control overview (in L):



with  $F_{sc} = -S_L/S_s$ :

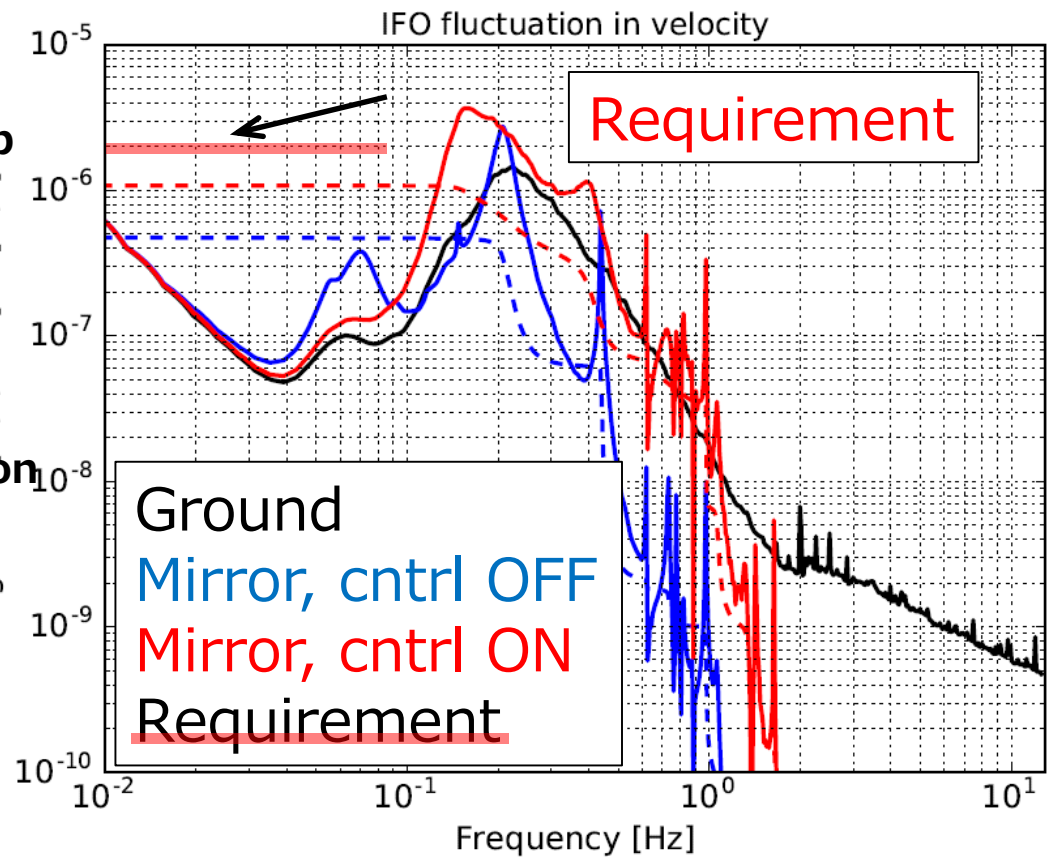
$$X_{stage} = \frac{1}{1 + G} \left[ G \left( 1 + F_{sc} \frac{S_s}{S_L} \right) + P_s \right] X_{GND}$$

**Cut the seismic noise injection via LVDT  
→ Sensor correction**

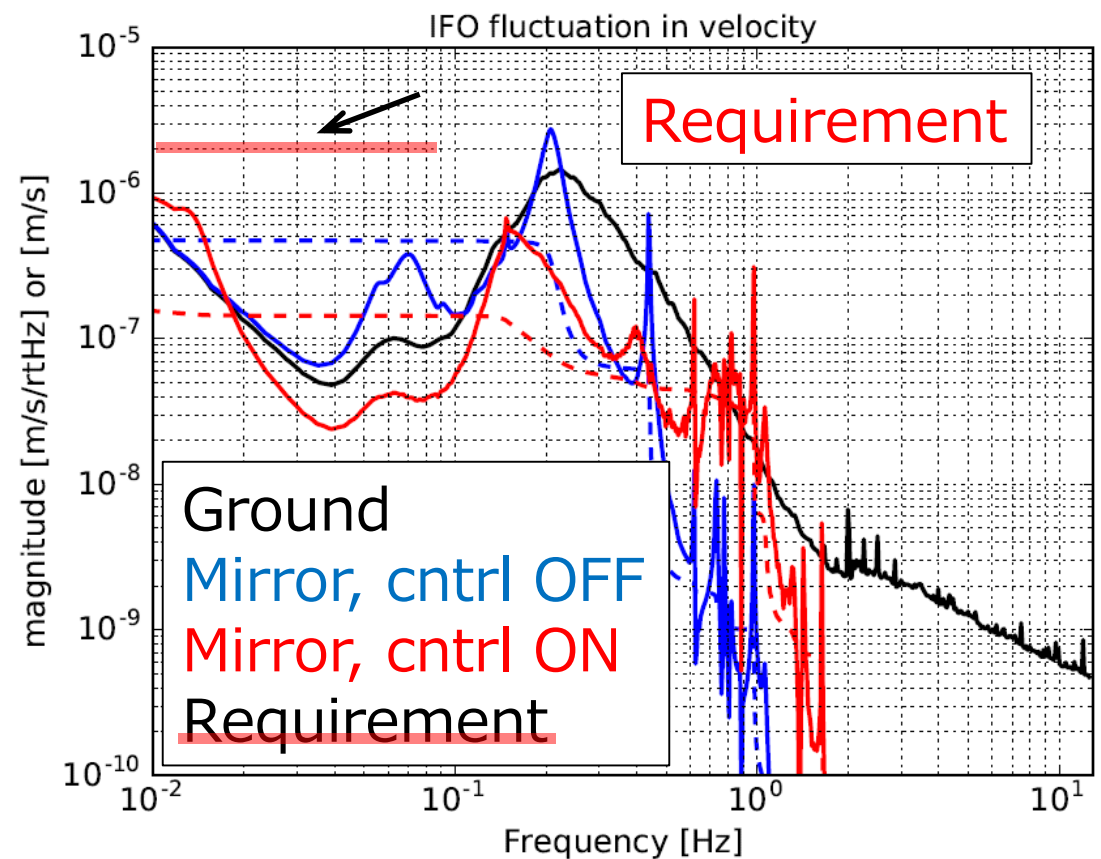
# Simulation: mirror **velocity** w/ 90%tile seismic motion



## Sensor correction **OFF**



## Sensor correction **ON**

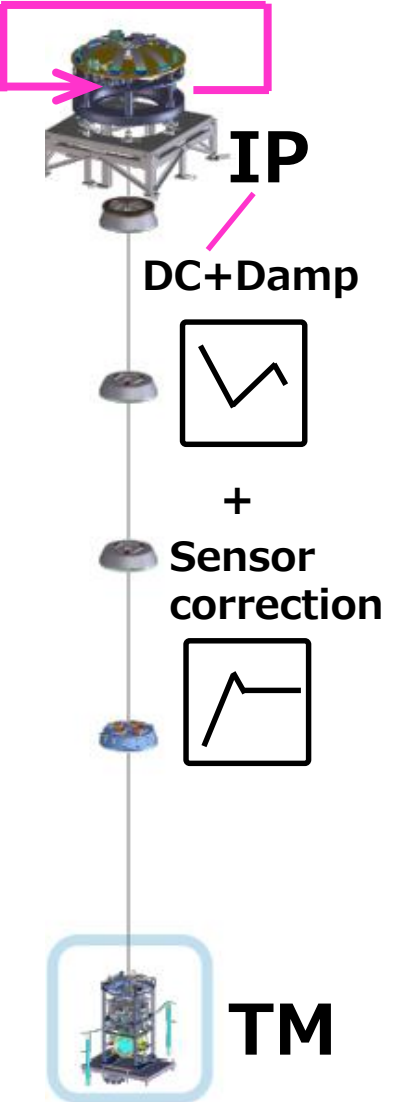


→ Sensor correction will satisfy requirement.

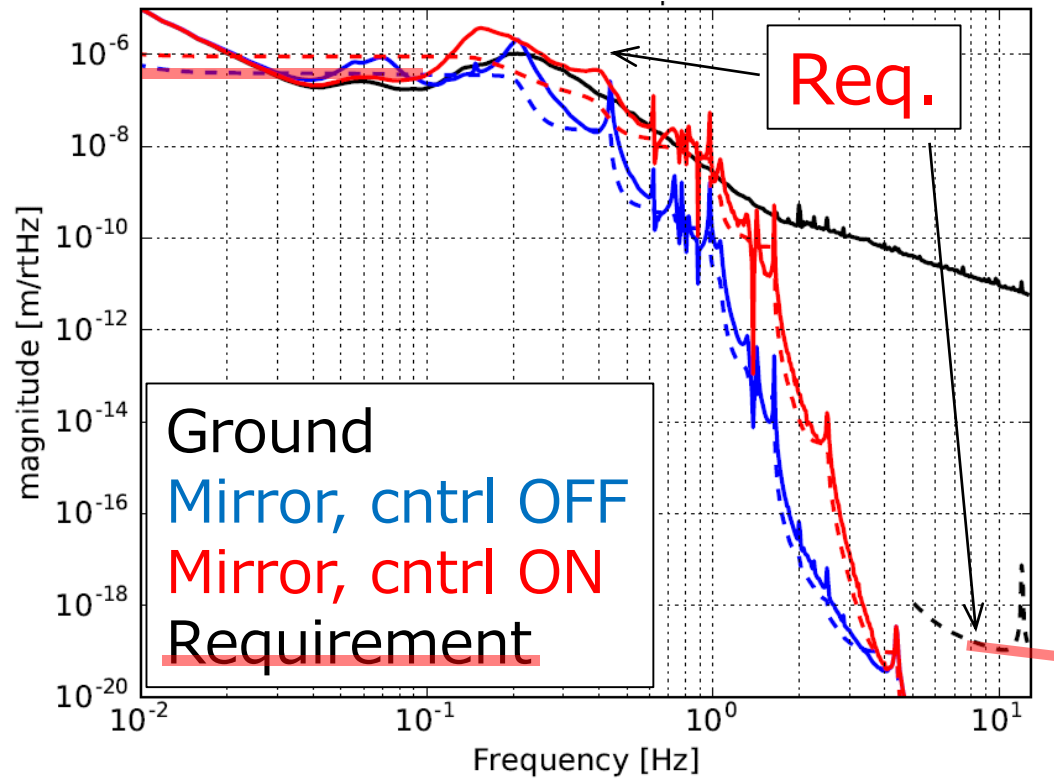




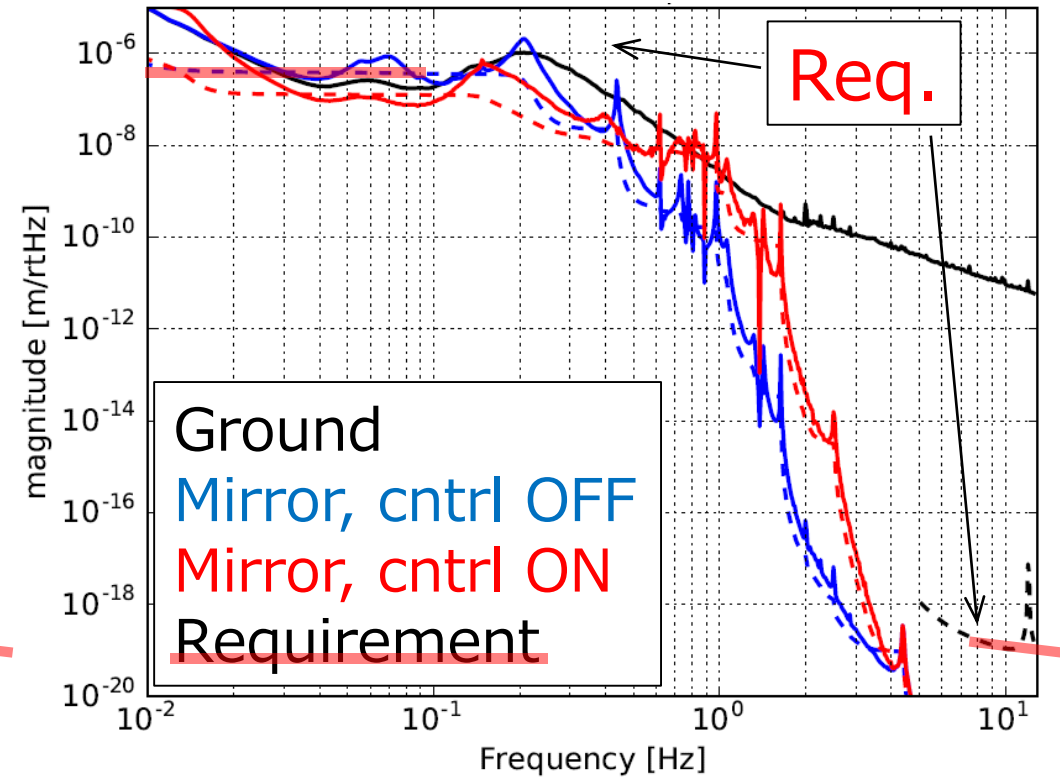
# Simulation: mirror **disp.** w/ 90%tile seismic motion



## Sensor correction **OFF**



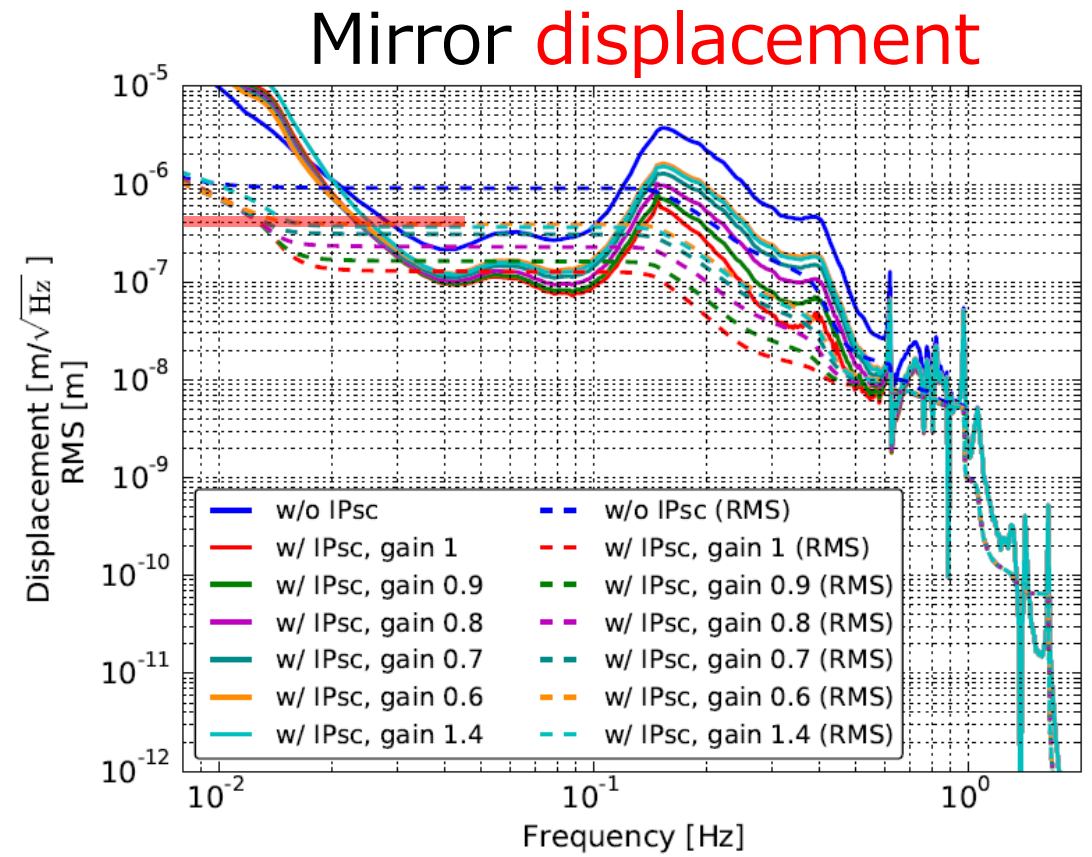
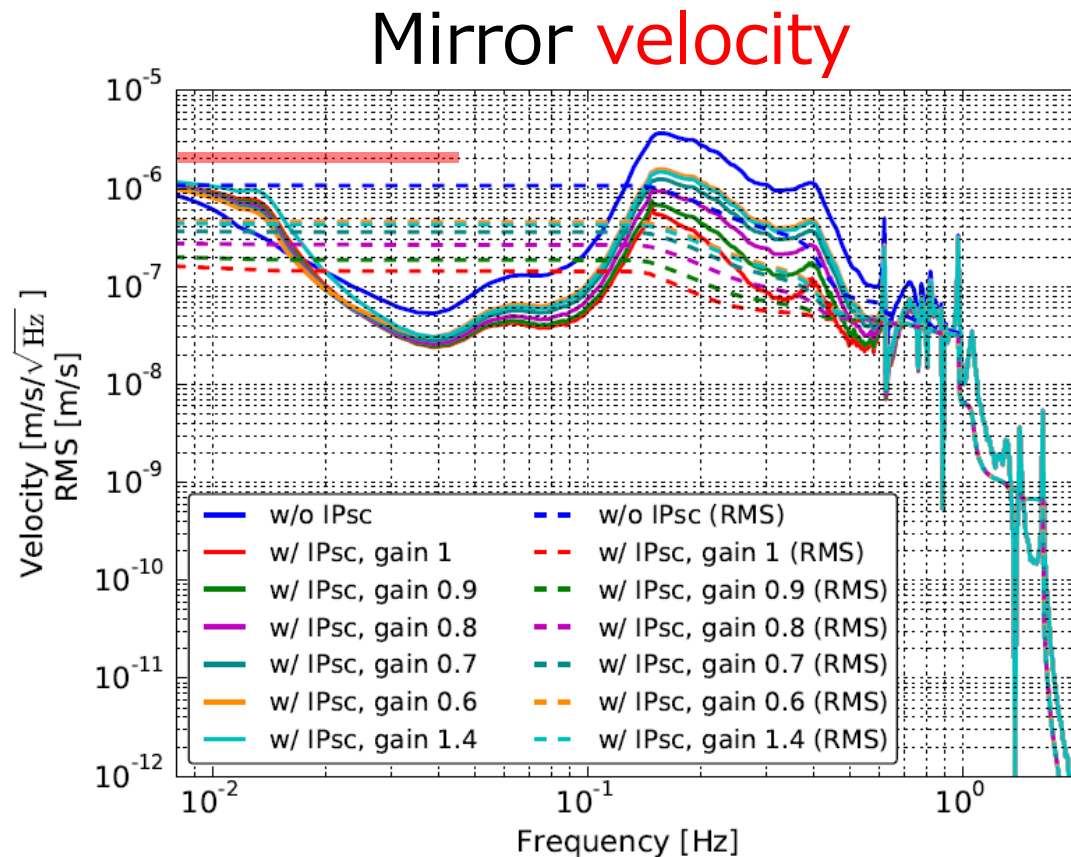
## Sensor correction **ON**



→ Sensor correction を用いて、要求値を満たせる。

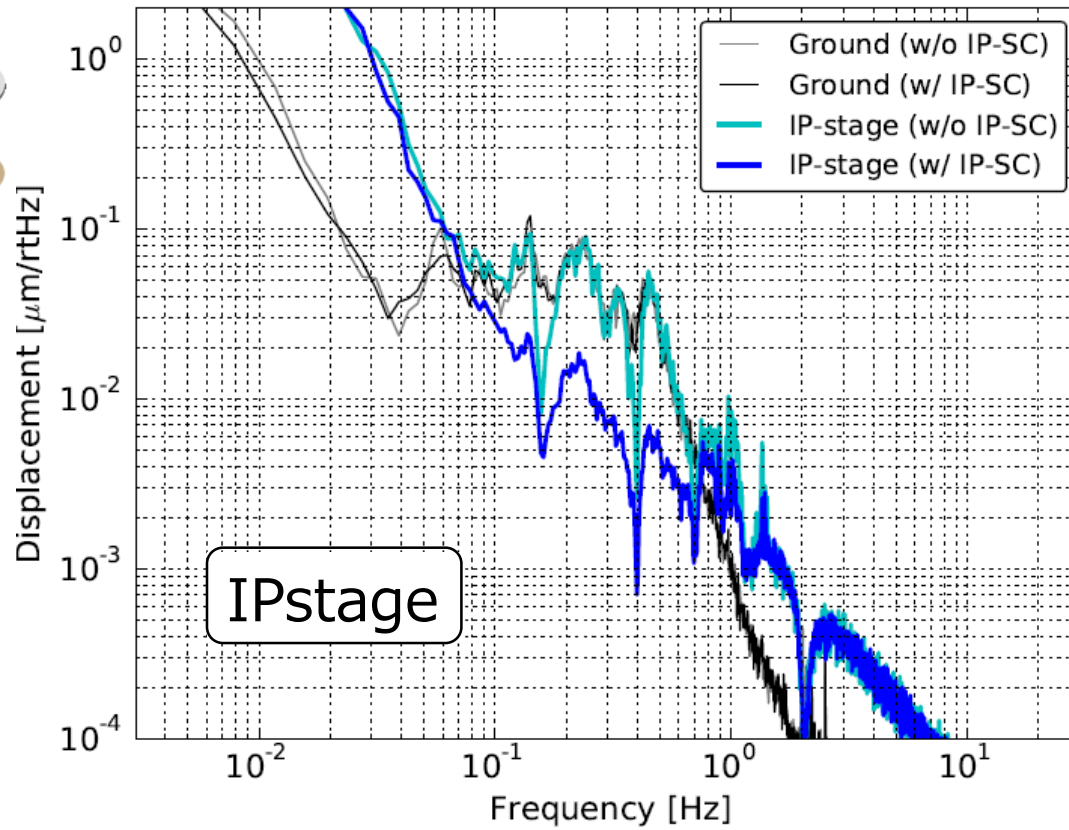
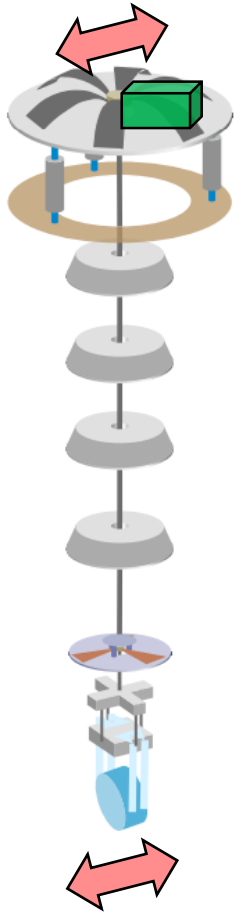
# Simulation: mirror motion w/ 90%tile seismic motion

\* Required precision of the inter-calibration:

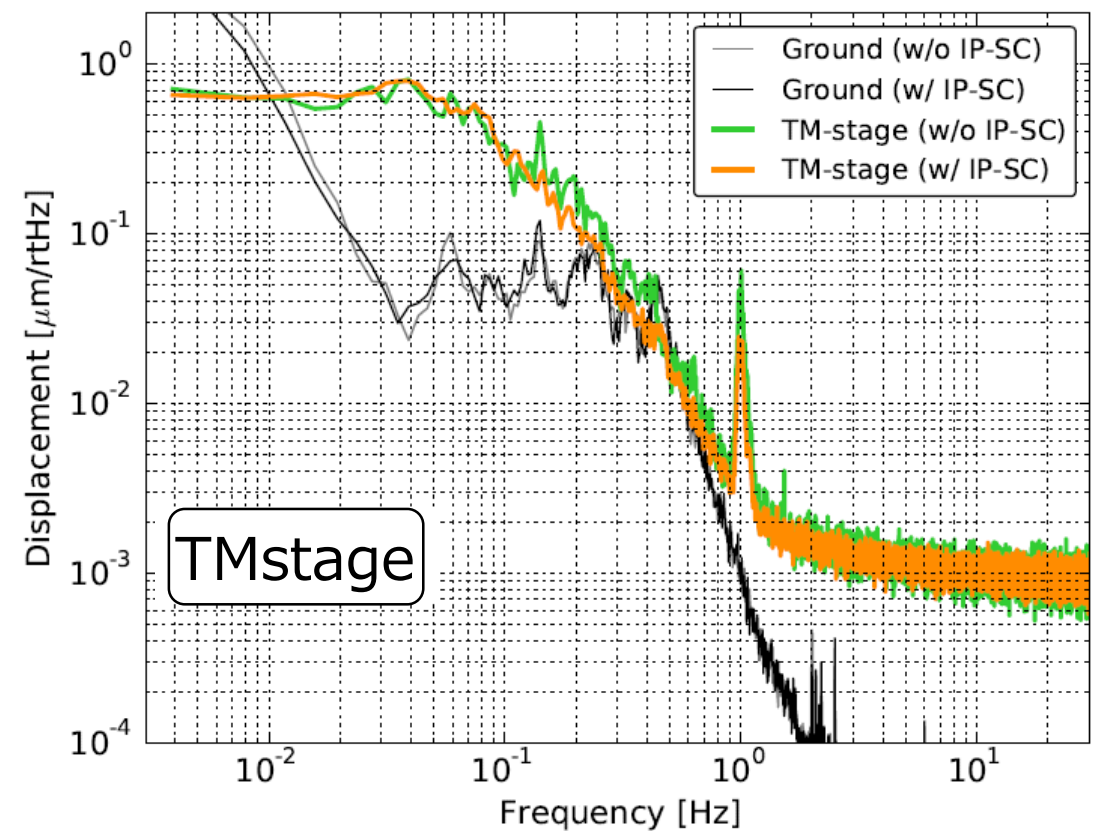


- Necessary: seis/LVDT < 40% difference
- Target: seis/LVDT < 10% difference

# Improvement at IP- & TM-stage

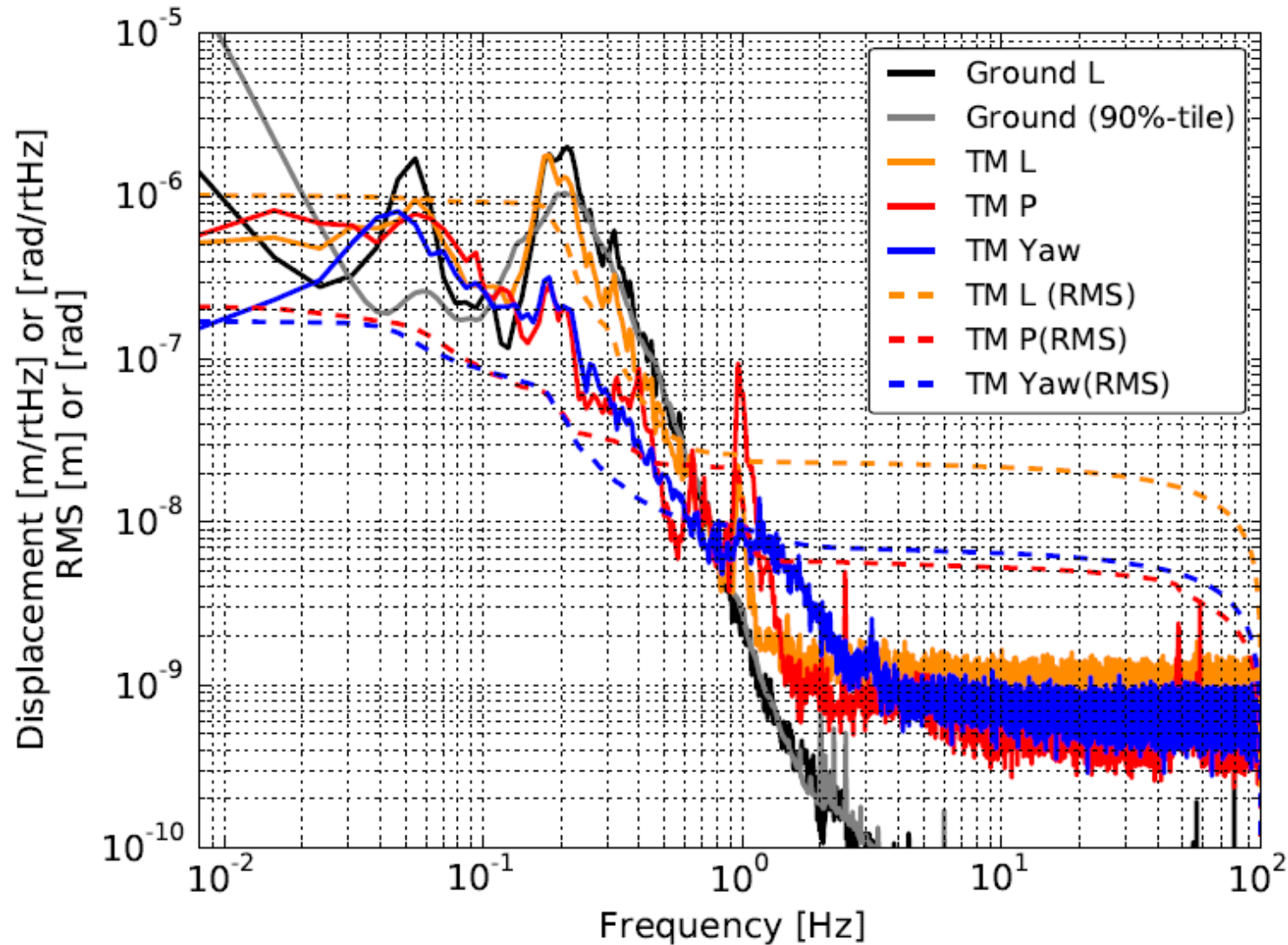


→ SC worked at 0.15 ~ 0.7Hz.



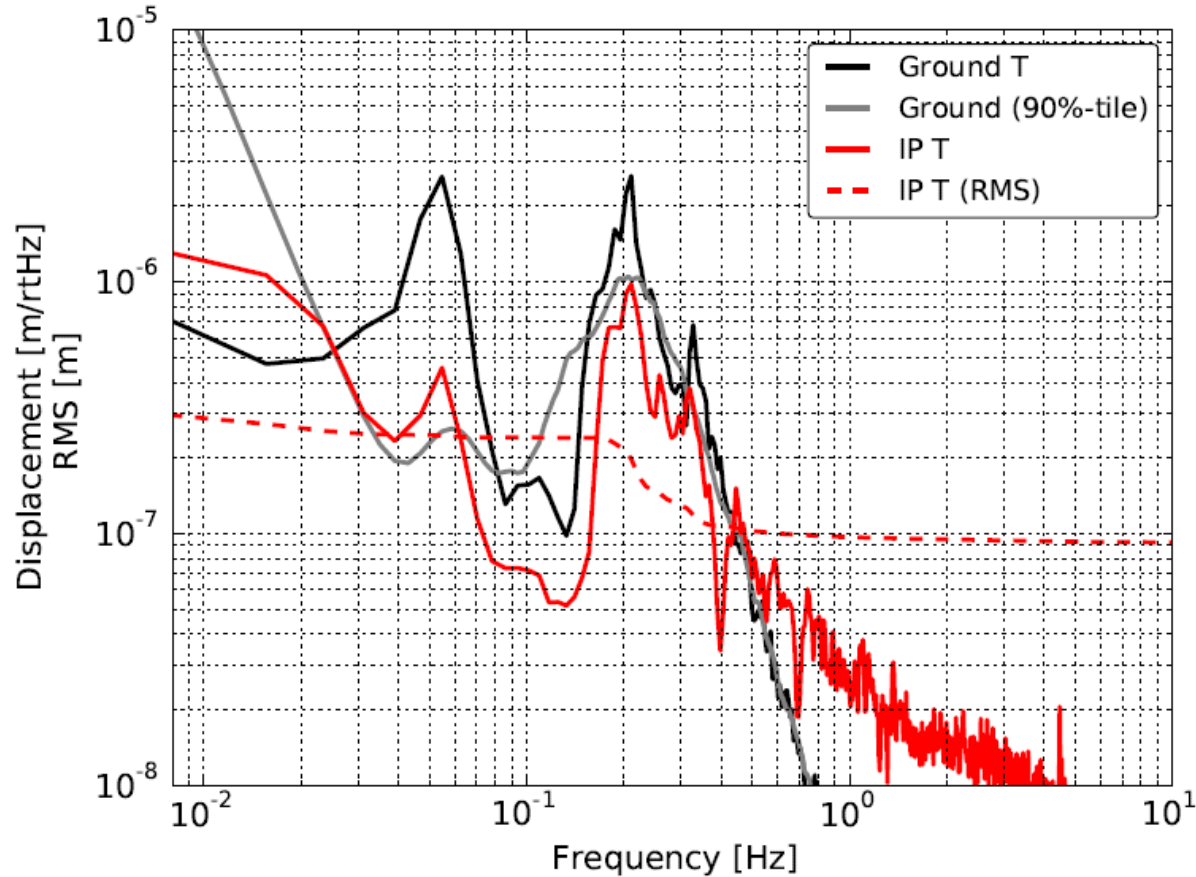
→ covered by TM oplev noise.

# Mirror angular motion (RMS) in Pitch & Yaw

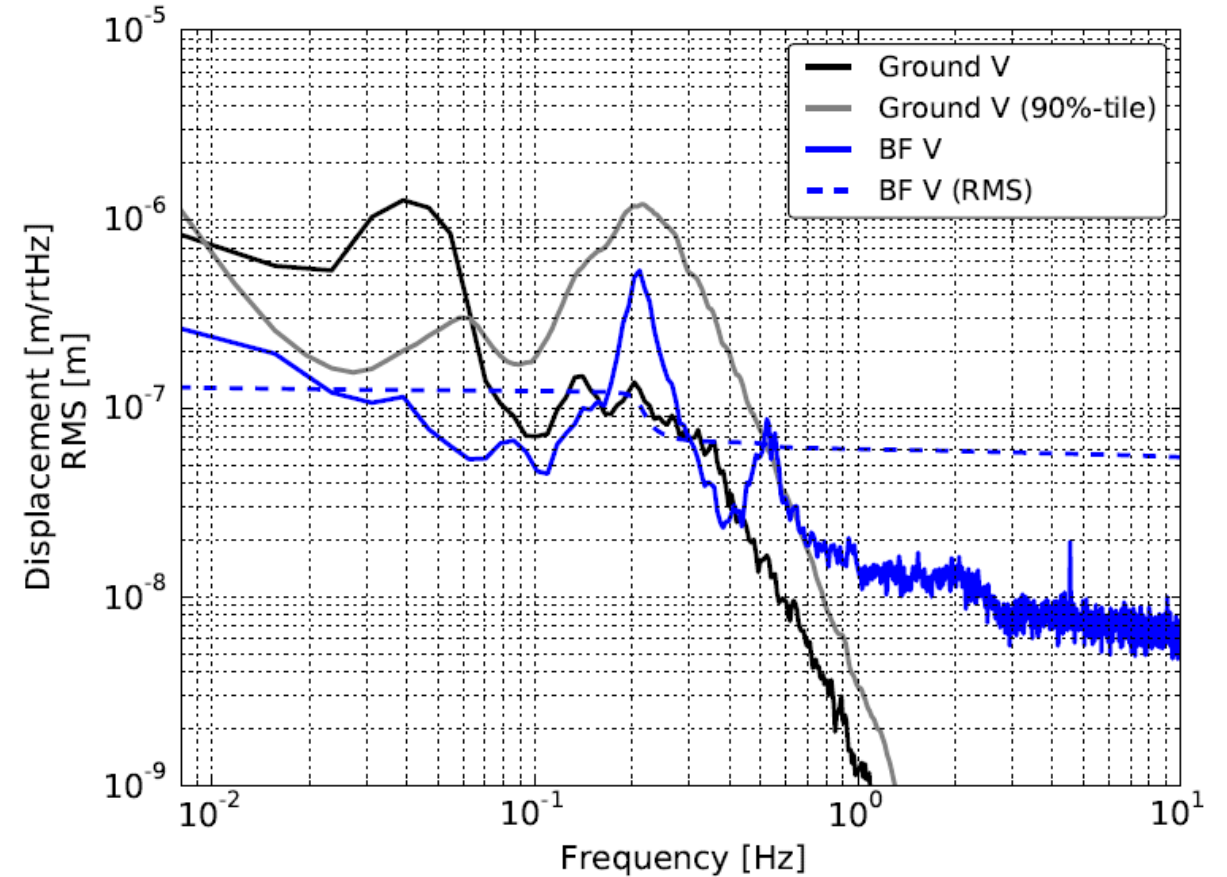




# Estimated mirror motion (RMS) in Transverse & Vertical

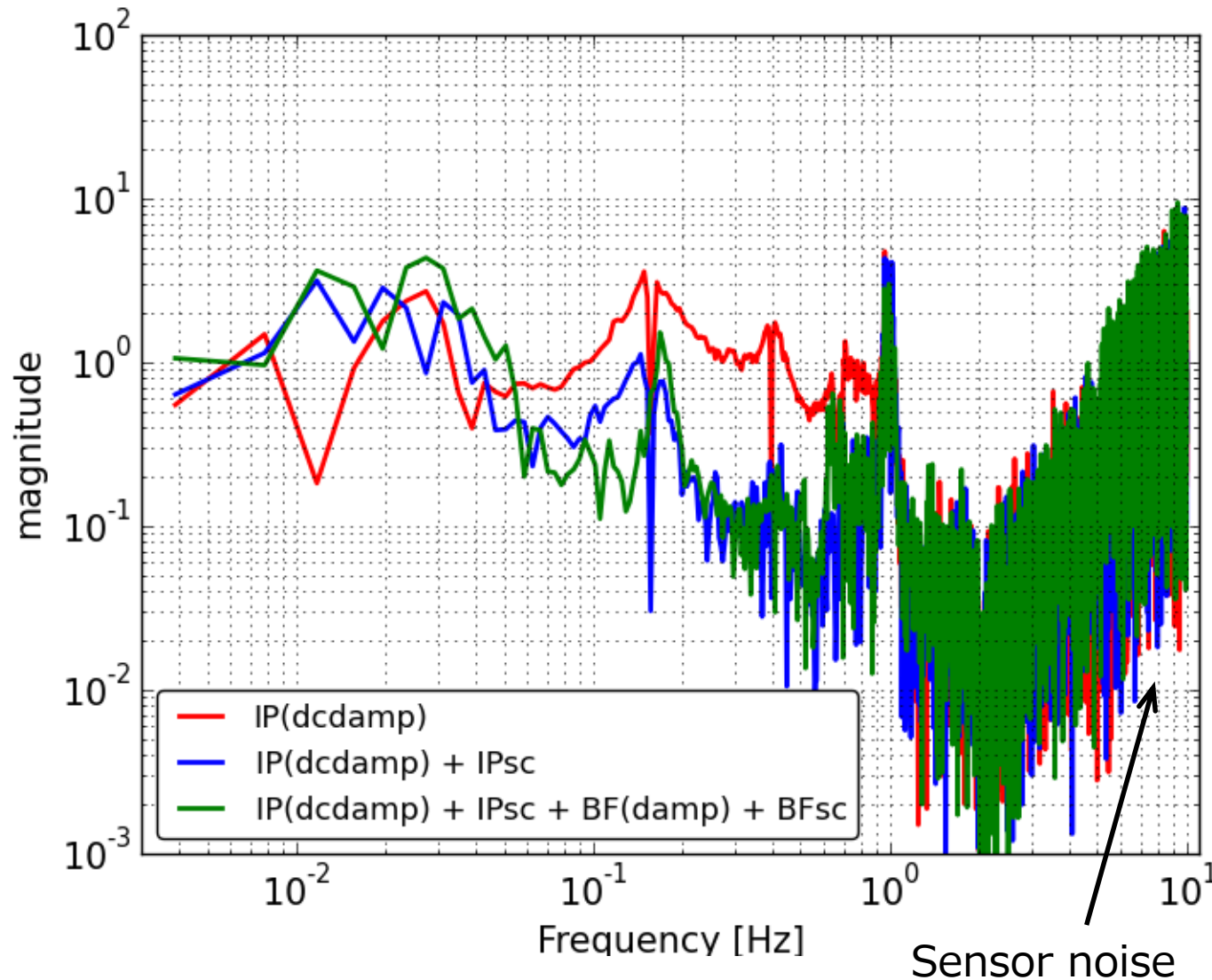


(Measured by geophone)



(Measured by BF-LVDT)

# By combining $(TML/IPL) * (IPL/GNDL)$



Displacement TF:  
From GND to TML

(measured at ETMX)

Is notch real?

→ Not sure.

→ tilt coupling from Geophone

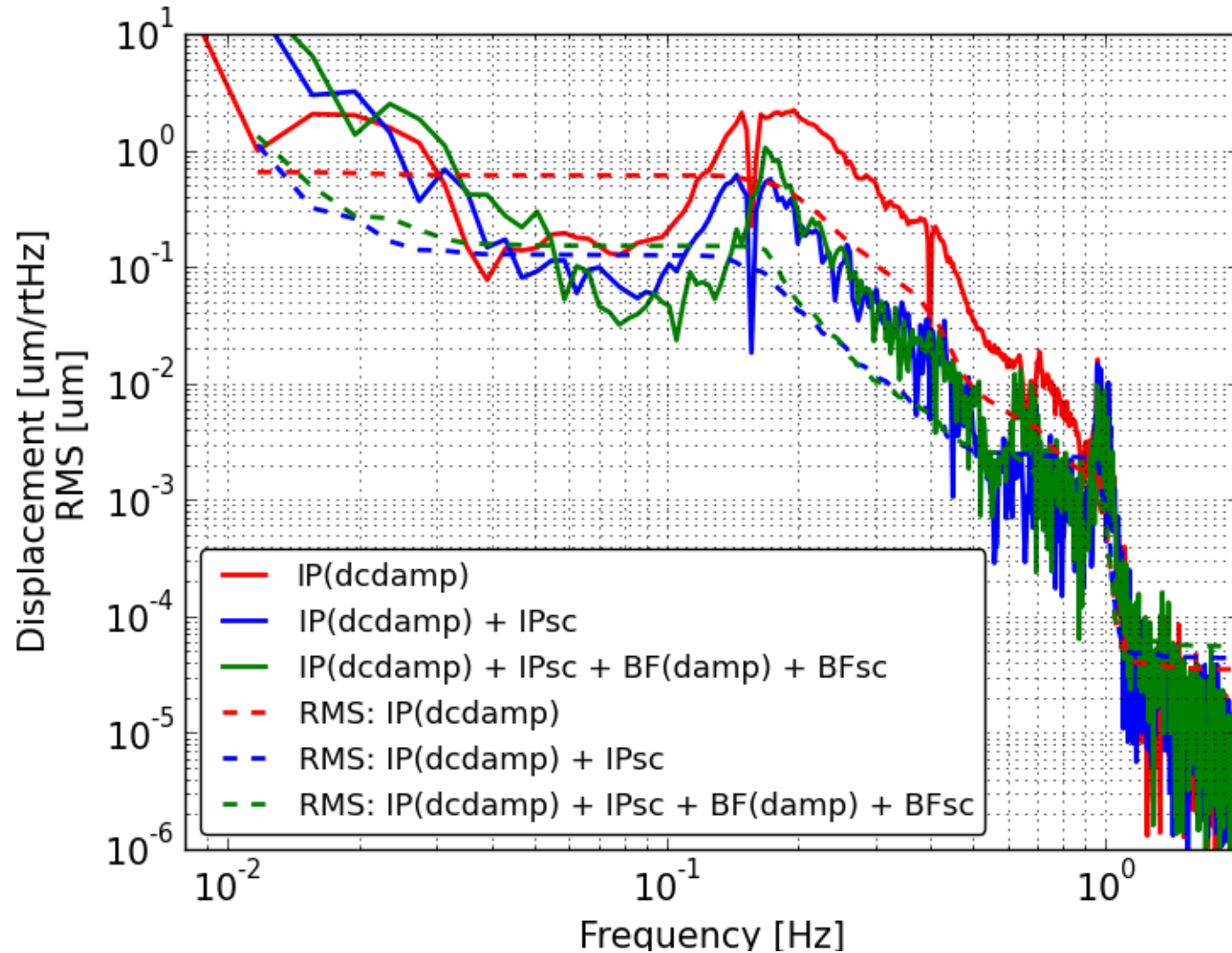
Or

→ Actual mechanical response

Whichever, the conclusion is same.



# By combining (TML/IPL)\*(IPL/GNDL)\*(GNDL\_model)

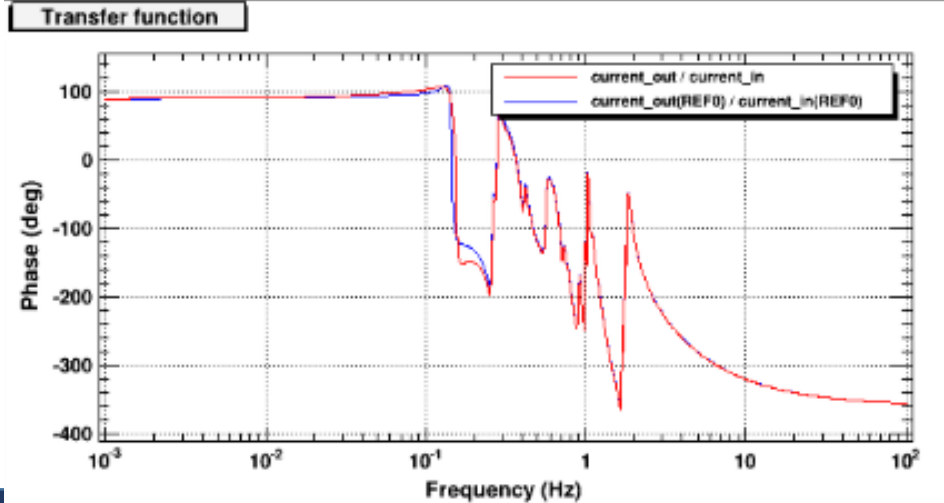
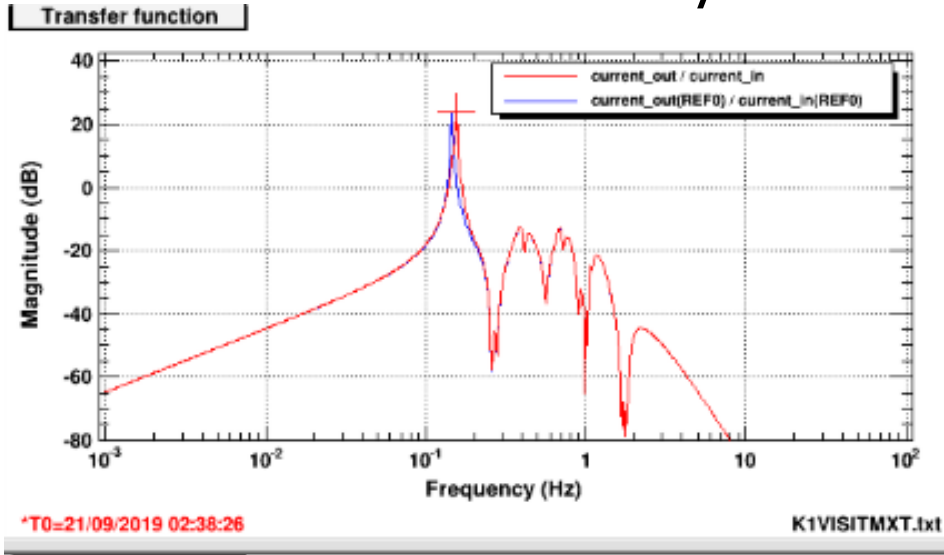


Disp. TF:

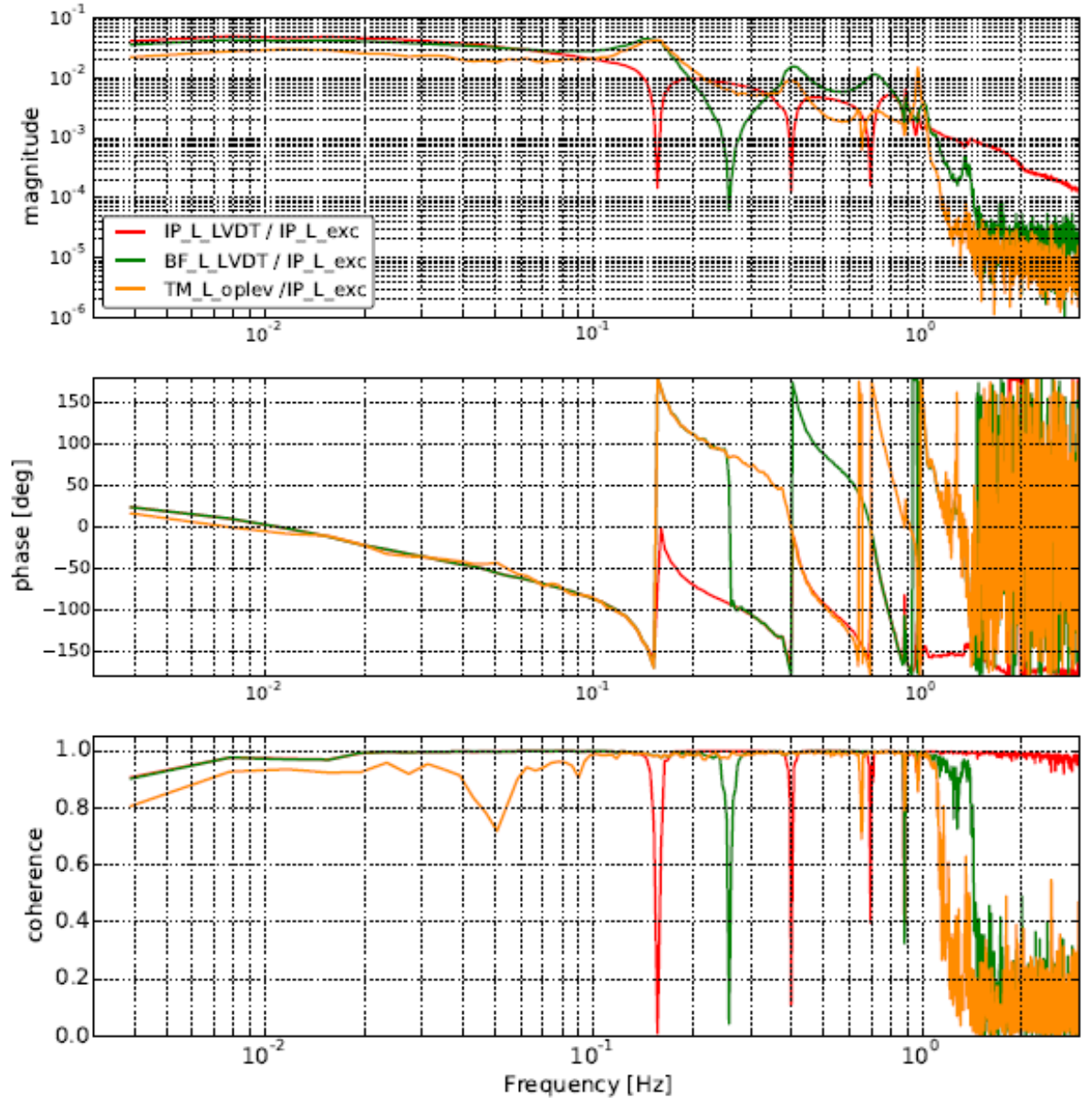
From GND to TML

# Control loop for BF-L/T

## OLTF for BF-L/T



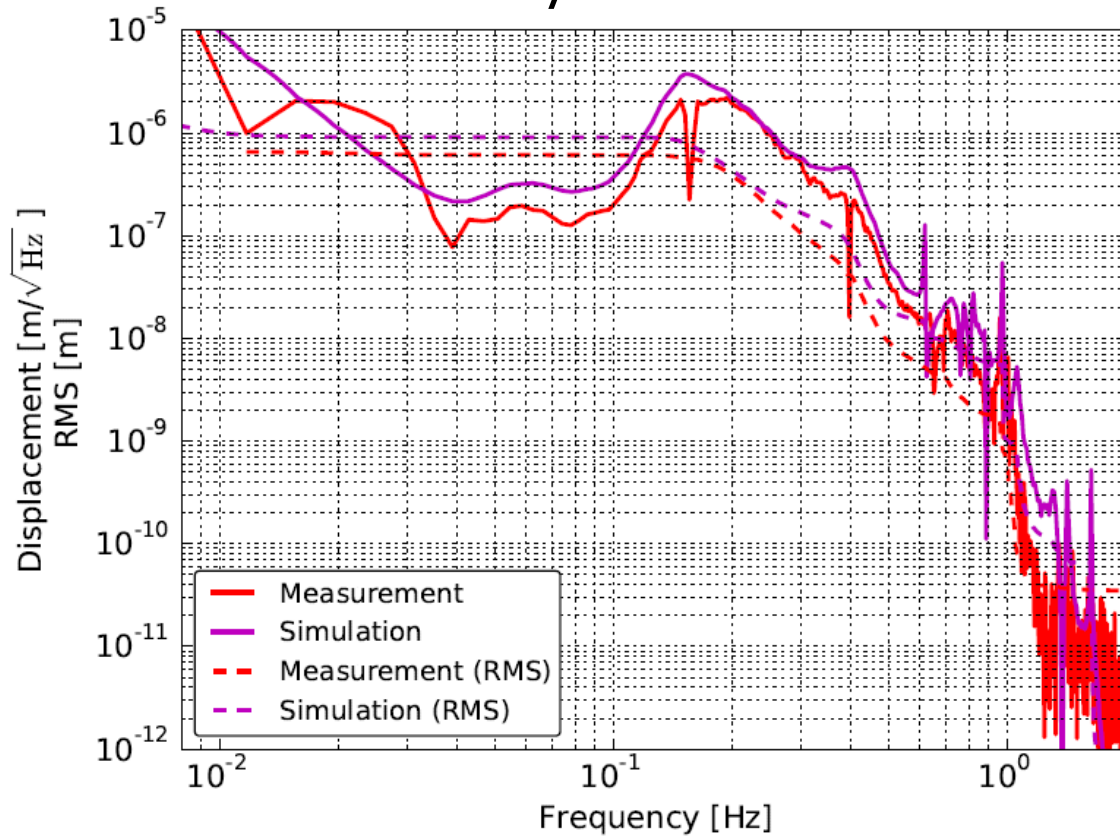
TFs when IP loops are closed.



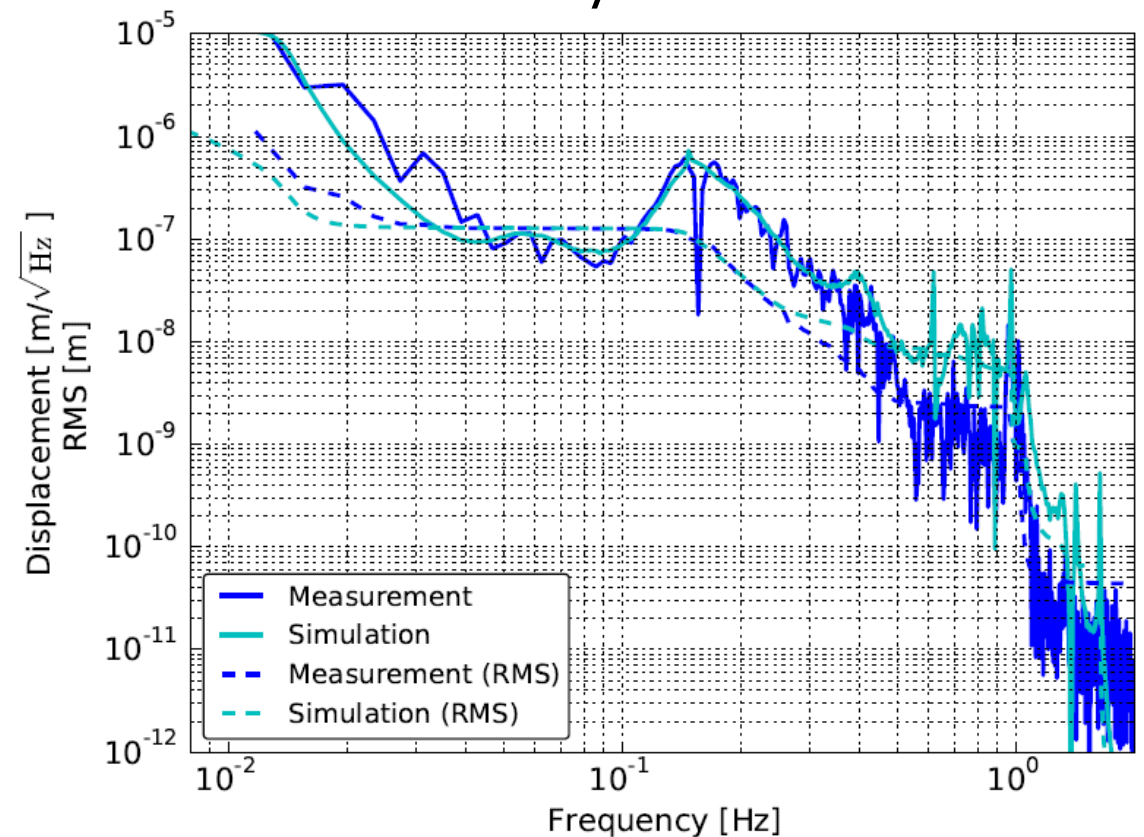
# Comparison: simulation vs. measurement

\* Mirror displacement w/ 90%tile seismic motion

w/o IPsc



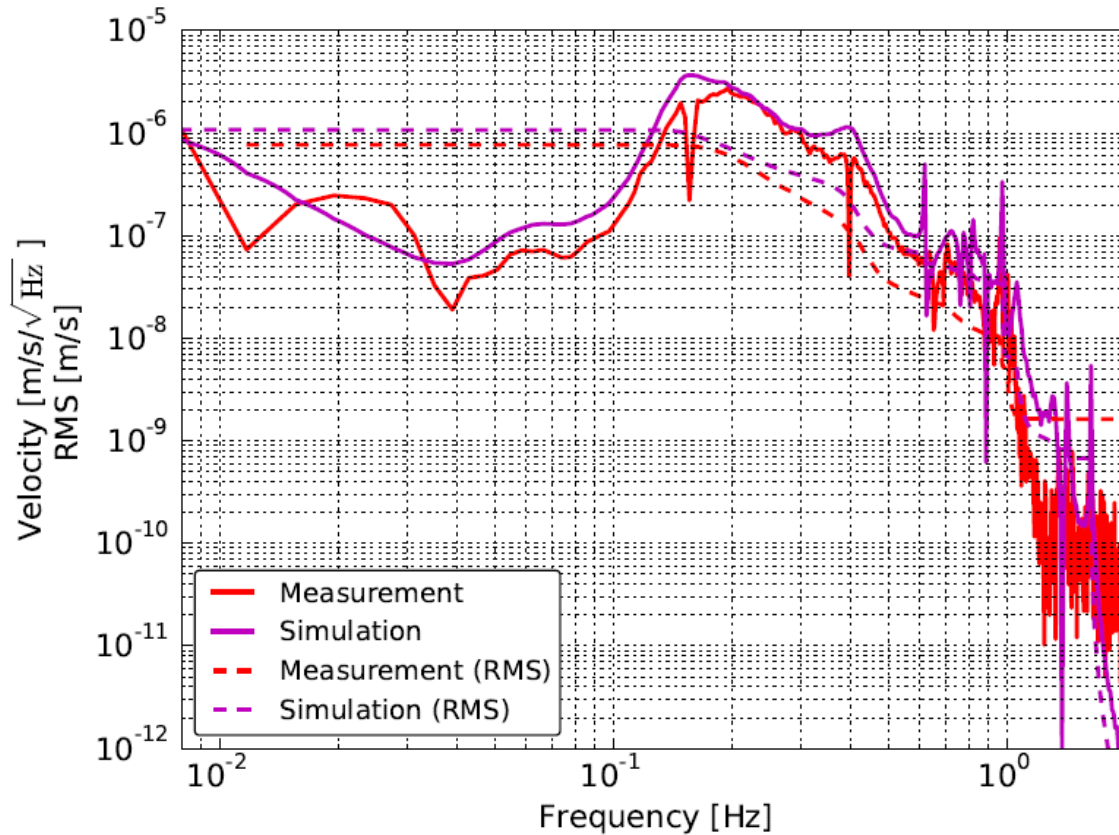
w/ IPsc



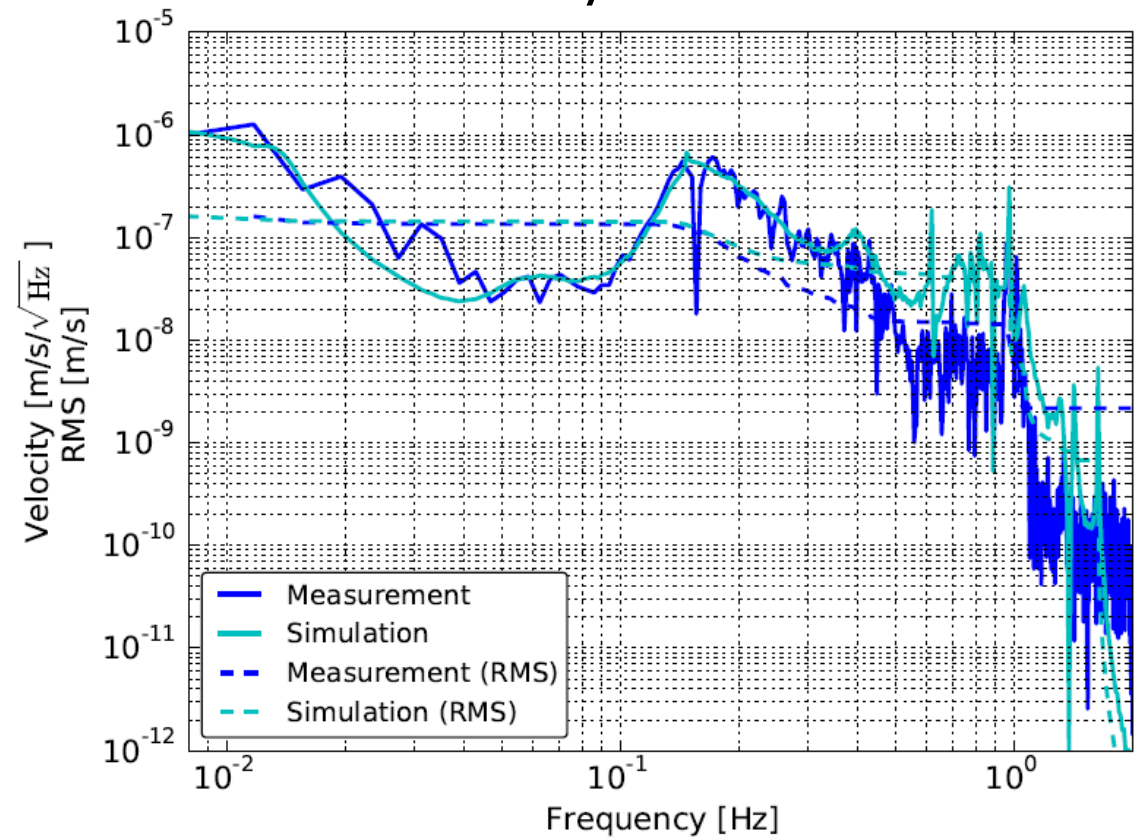
# Comparison: simulation vs. measurement

\* Mirror **velocity** w/ 90%tile seismic motion

w/o IPsc



w/ IPsc



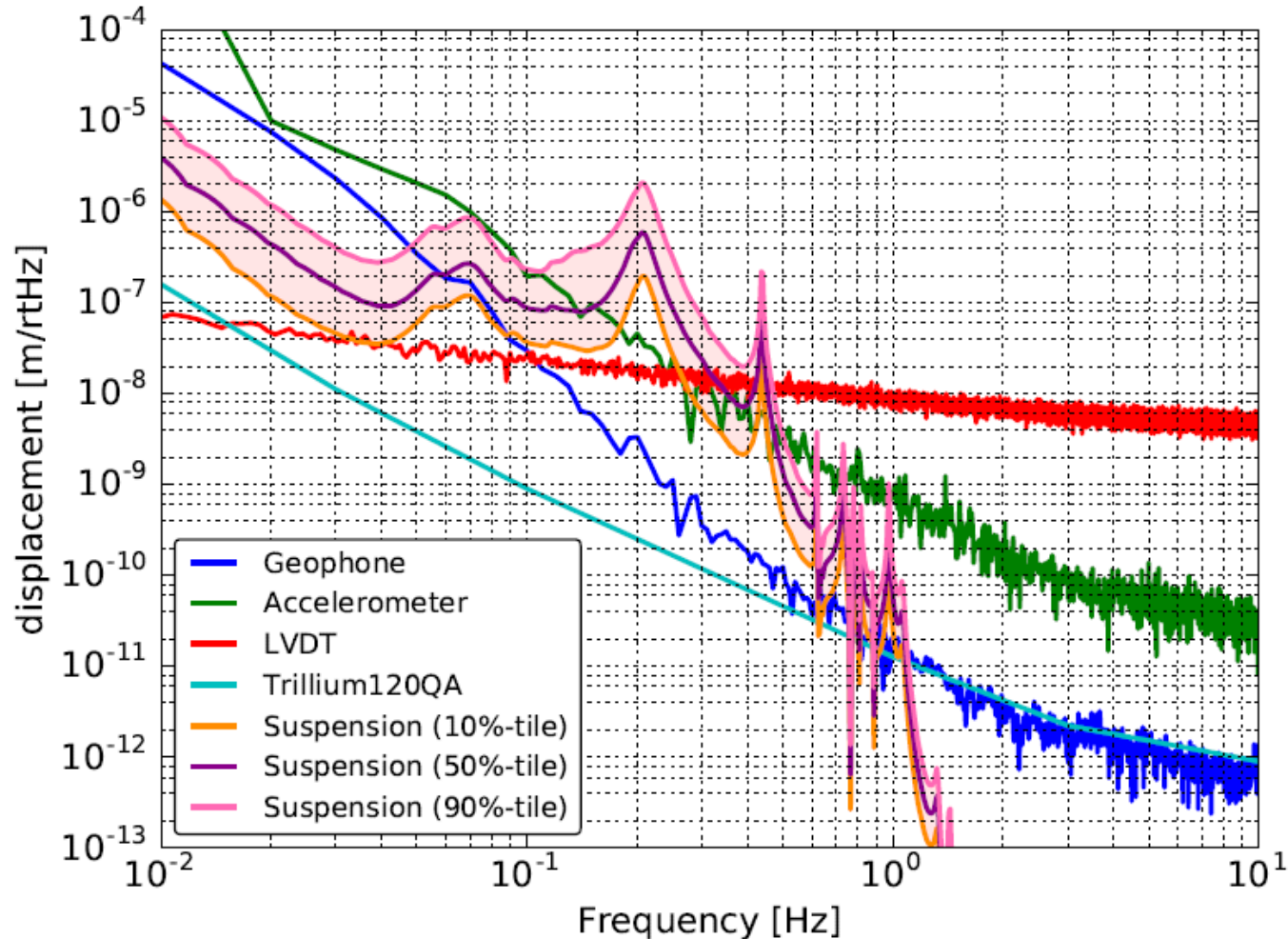
### 3. Mirror residual suppression

- \* Options for further stabilization:
  - \* implement inertial damping system with sensitive inertial sensors.
    - \* For this, subtract tilt-signal from the inertial sensors with tilt-meter might be necessary.
  - \* locally subtract tilt-signal from seismometer with tilt-meter.
  - \* actuate the ETMs so that their drifts follow that of ITMs with interferometer/cavity signal or strain-meter signal.



# Sensor self-noise vs. mechanical response

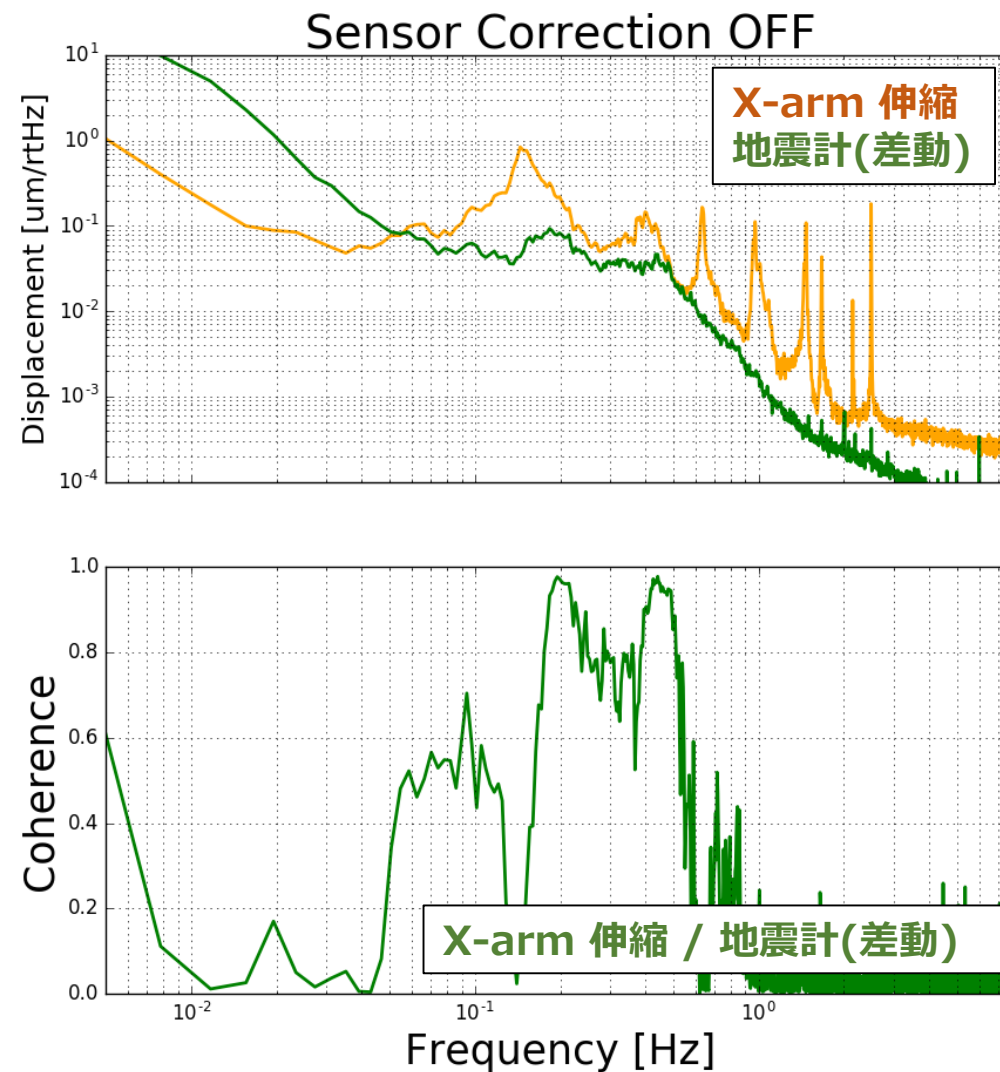
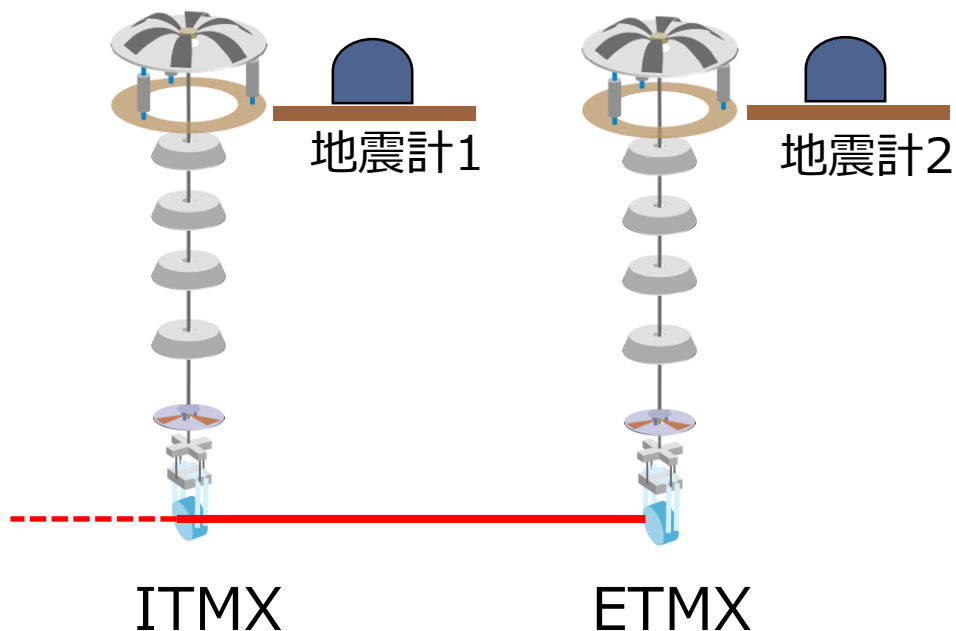
\* w/ 10%tile, 50%tile and 90%tile seismic motion:





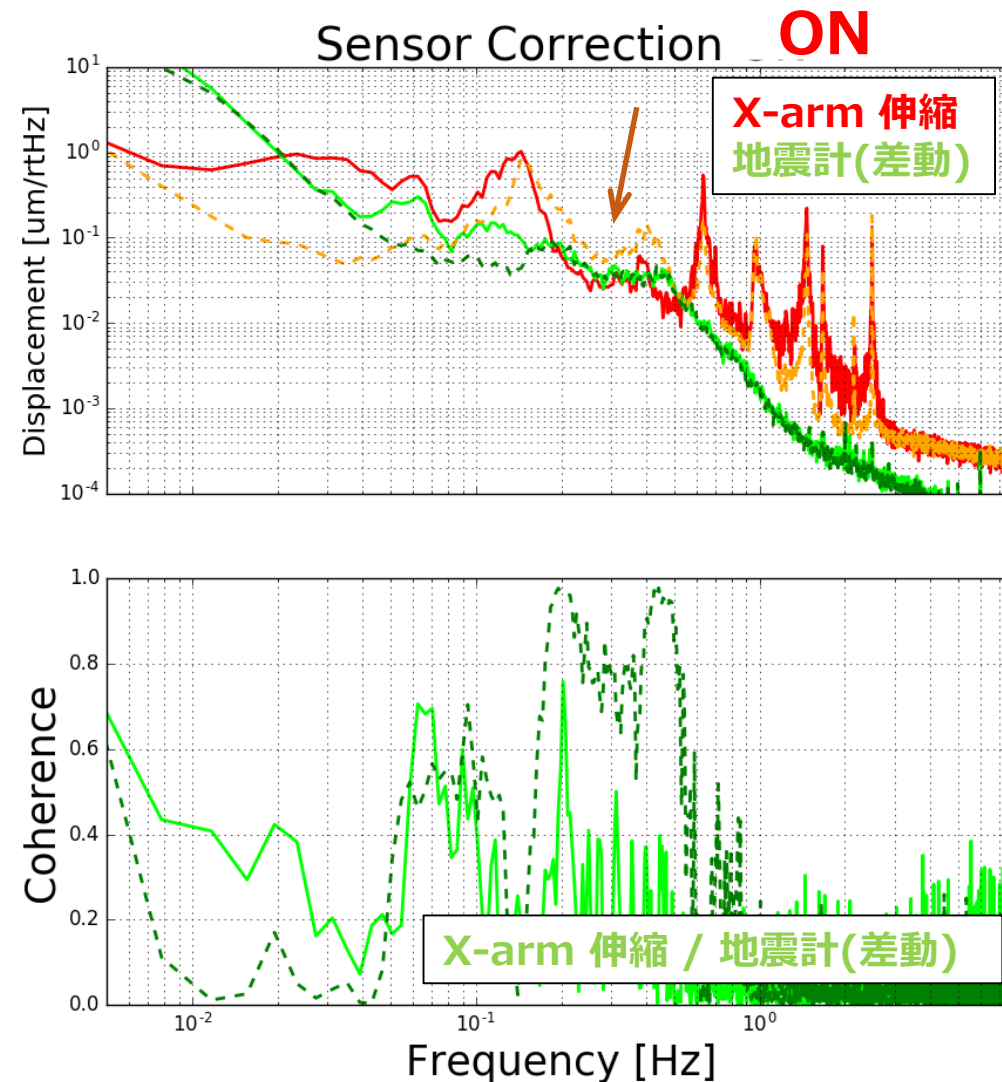
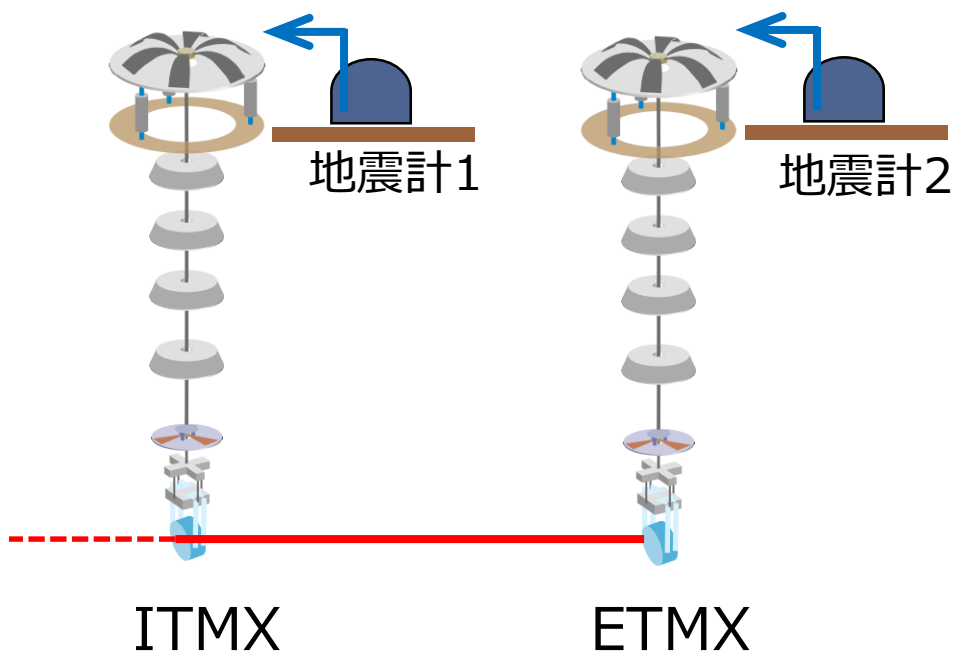
# テスト実装: 2つのサスペンションのIP-stageに実装、Xarm で見ると

- ETMX と ITMX に実装
- 0.15 ~ 0.7 Hzにて同様な改善あり
- X-arm (FP cavity) の共振器長の確認



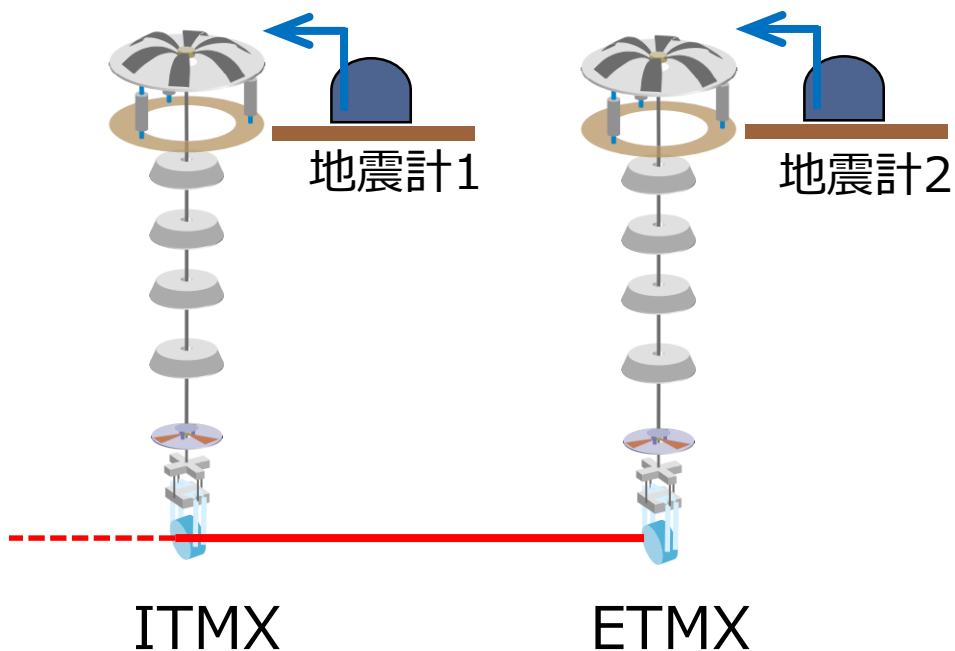
# テスト実装: 2つのサスペンションのIP-stageに実装、Xarm で見ると

→ X-arm (FP cavity) の共振器長では

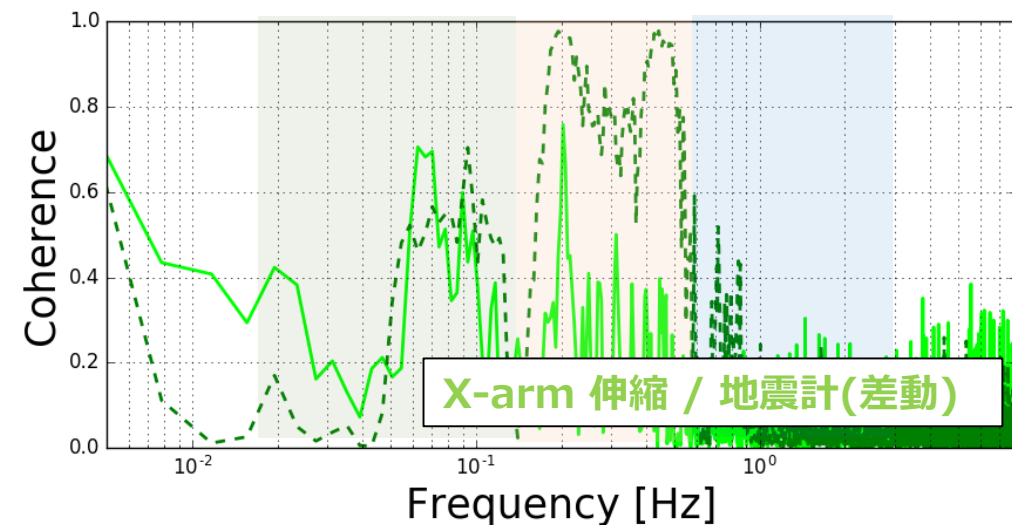
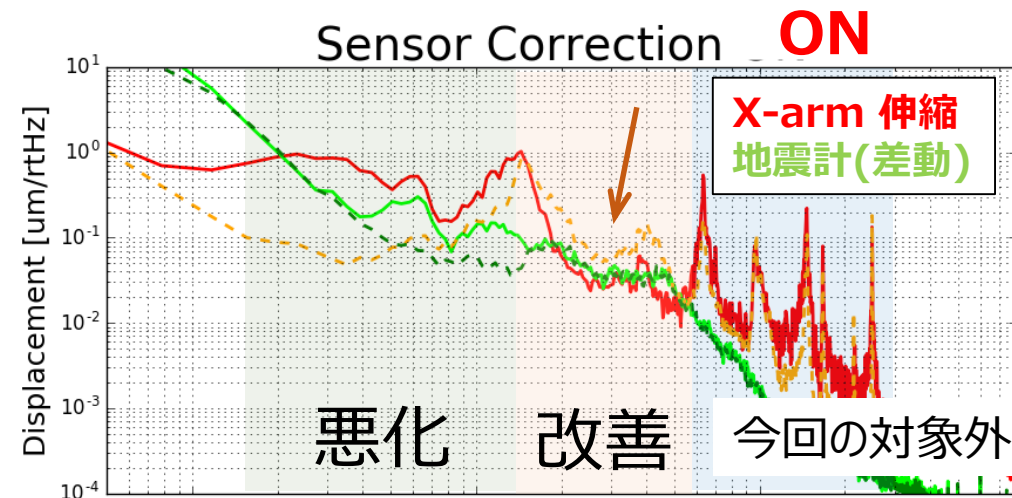


# テスト実装: 2つのサスペンションのIP-stageに実装、Xarm で見ると

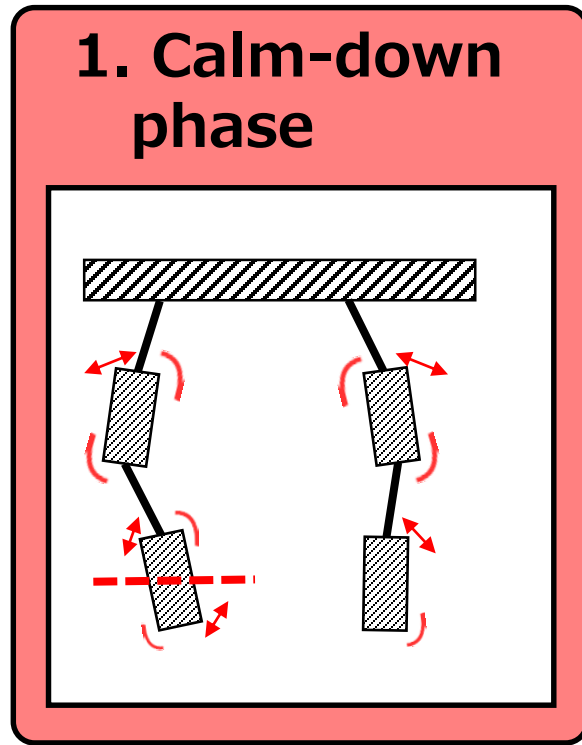
→ X-arm (FP cavity) の共振器長では



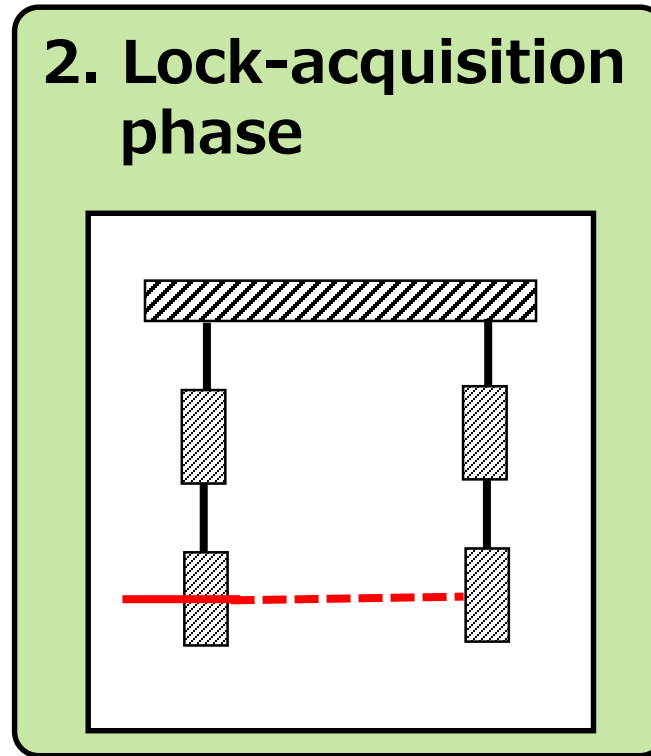
- SC worked at 0.15 ~ 0.6Hz.
- 低周波: 悪化
  - SC filterからの地震計の雑音の流入ほか
  - To be investigated.



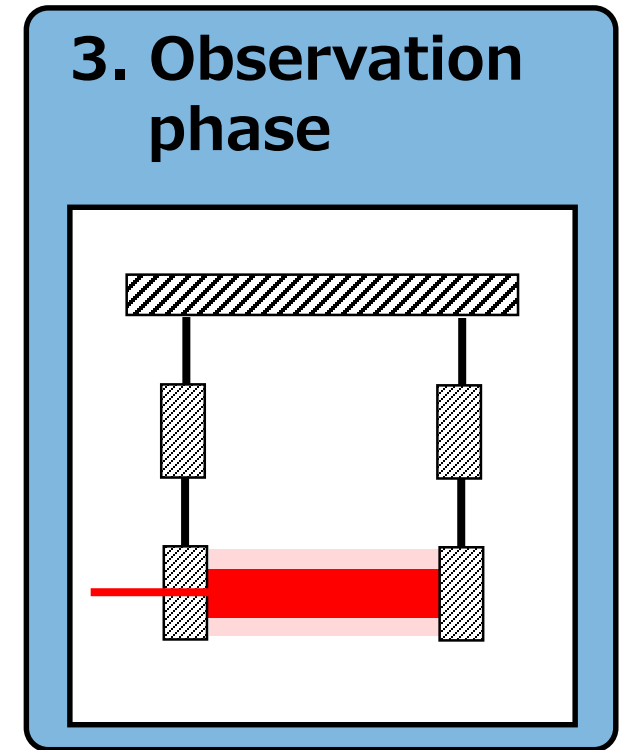
# Designing active control system / Control phase



Suppress  
large disturbance

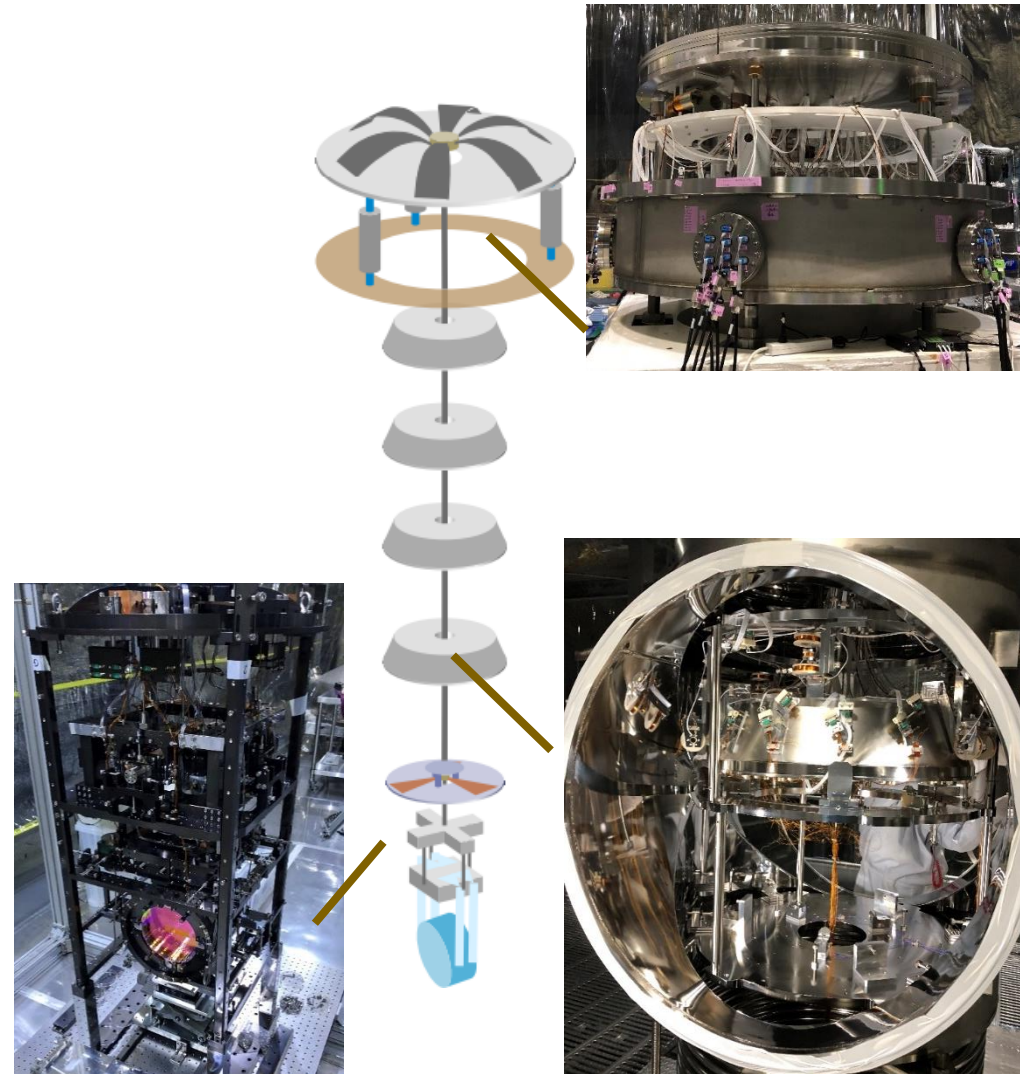


Reduce RMS velocity  
RMS angle  
(**R**oot-**M**ean-**S**quare)



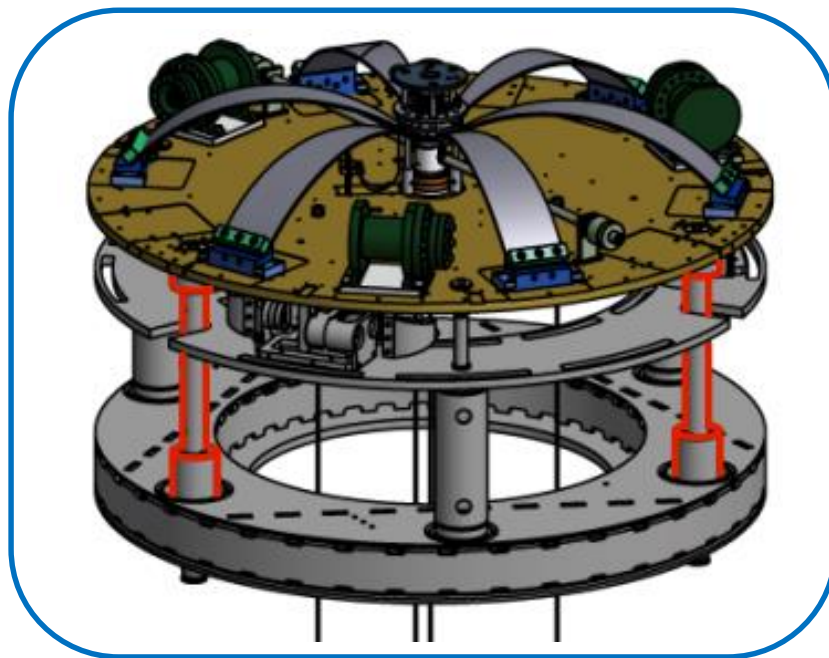
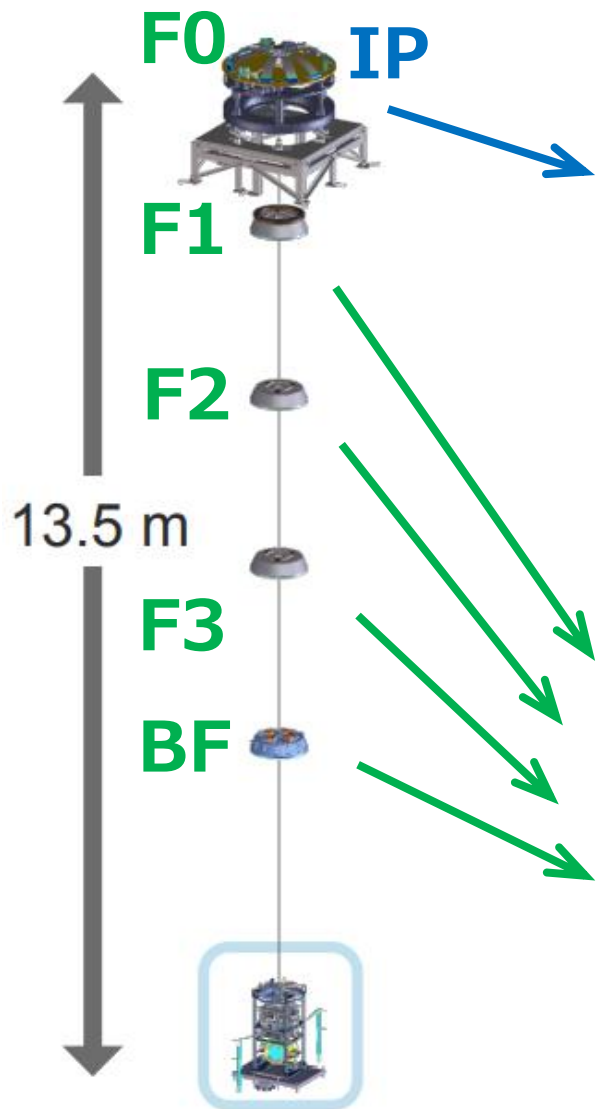
Keep position  
with low noise  
control

# Type-A suspension

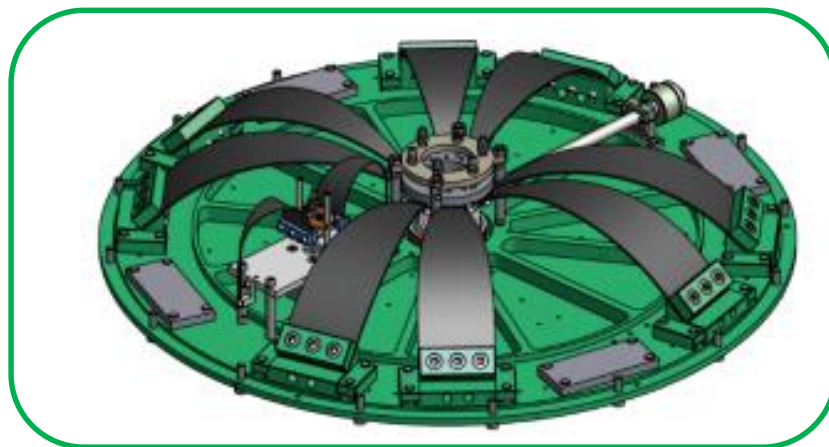




# メイン鏡用の防振装置



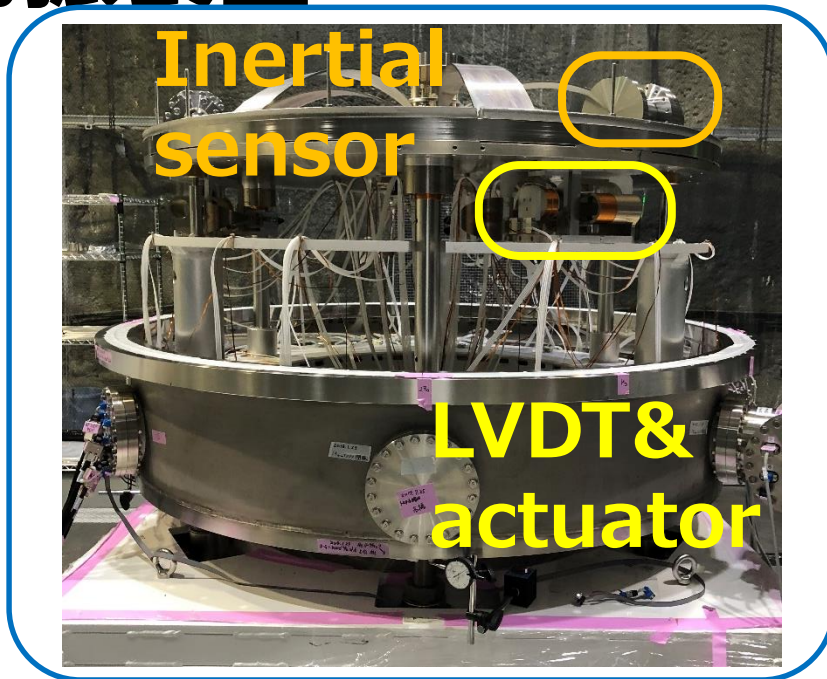
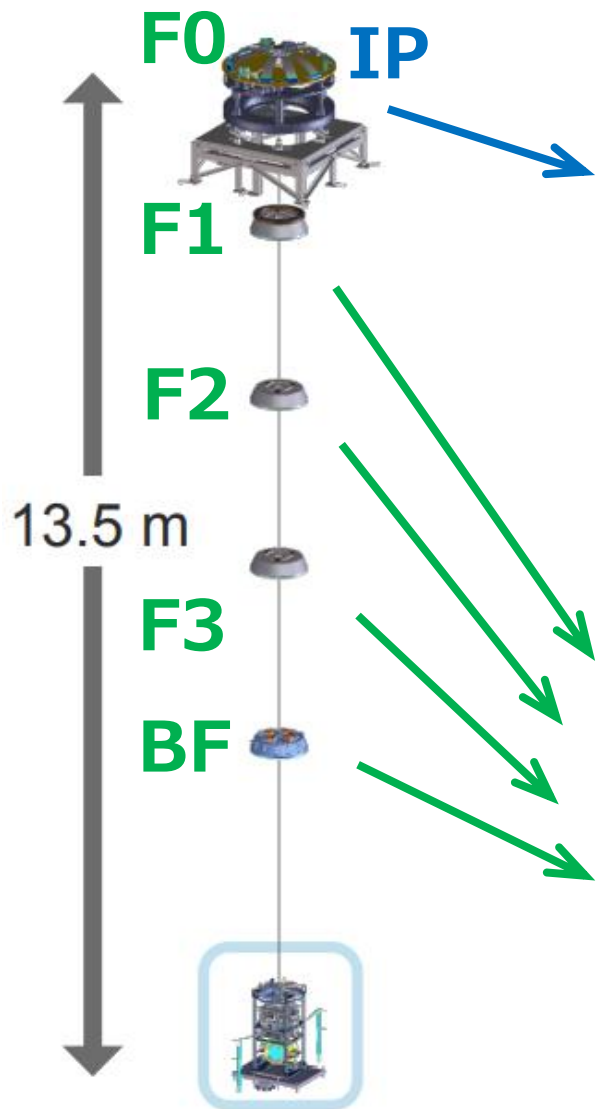
INVERTED PENDULUM  
( $\sim 70$  mHz)



GEOMETRIC-ANTI SPRING  
( $\sim 0.4$  Hz)



# メイン鏡用の防振装置



INVERTED PENDULUM  
with 3 horizontal  
-- LVDT & actuator units  
-- inertial sensors



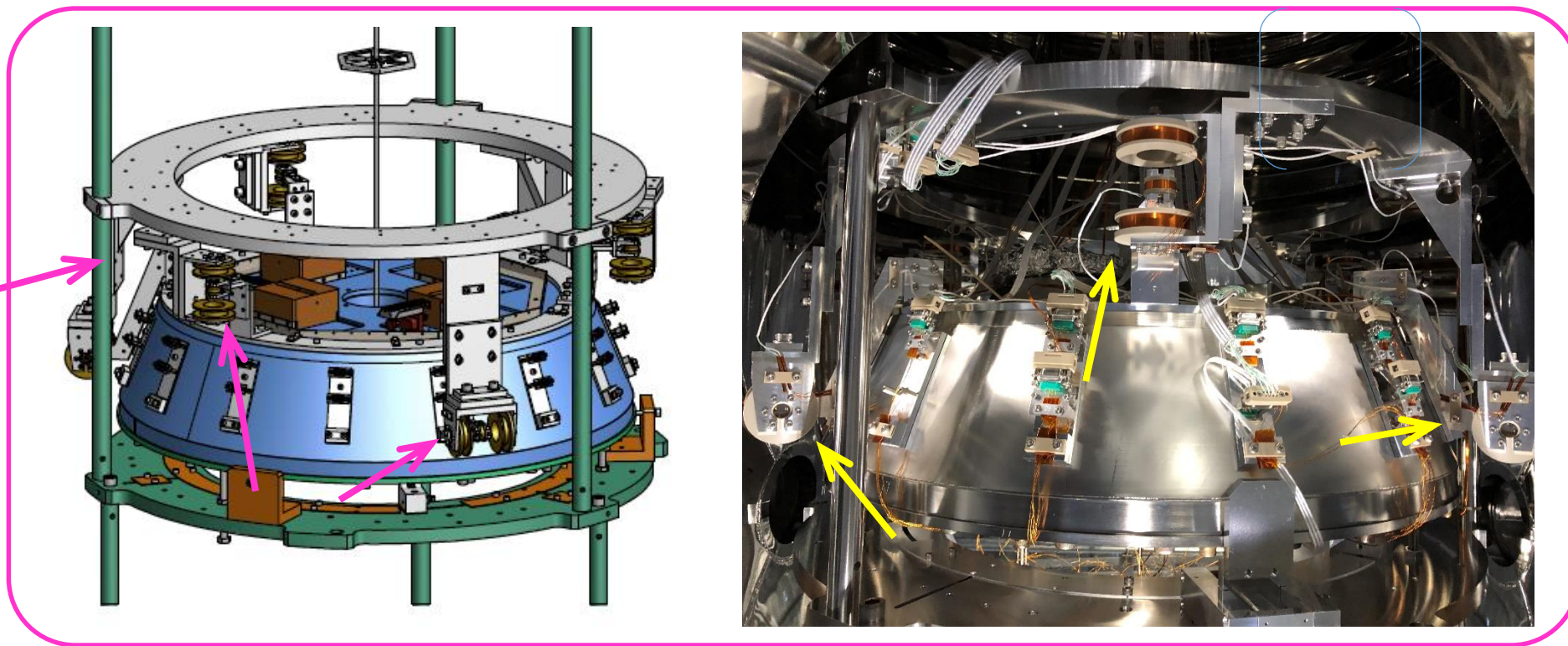
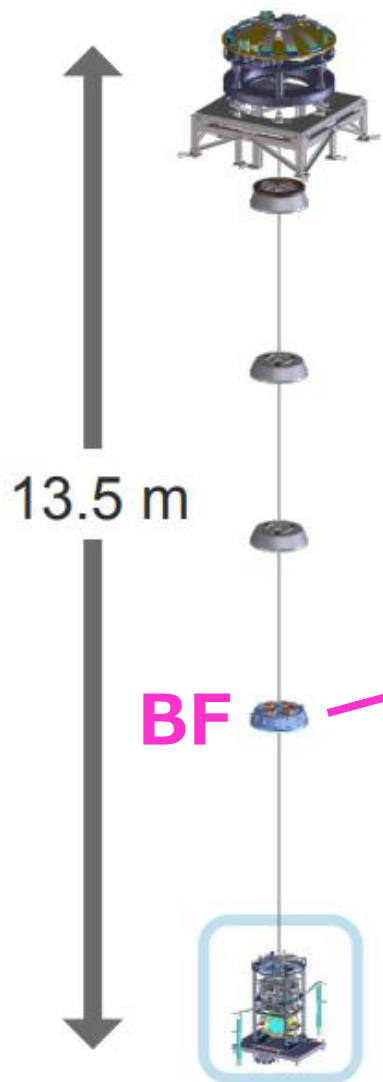
GEOMETRIC-ANTI SPRING  
with 1 vertical  
LVDT & actuator unit

# メイン鏡用の防振装置

(イタリアのグループの協力のもと開発)

## BOTTOM-FILTER DAMPER

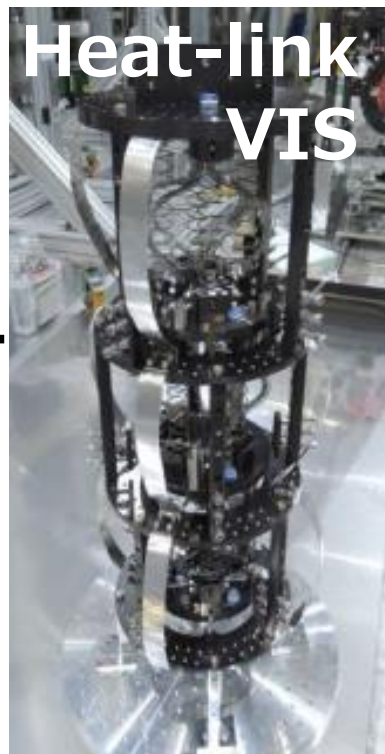
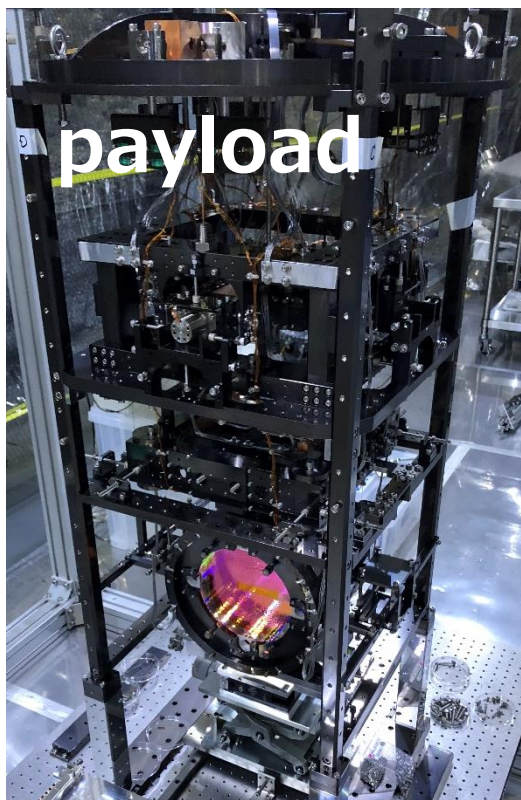
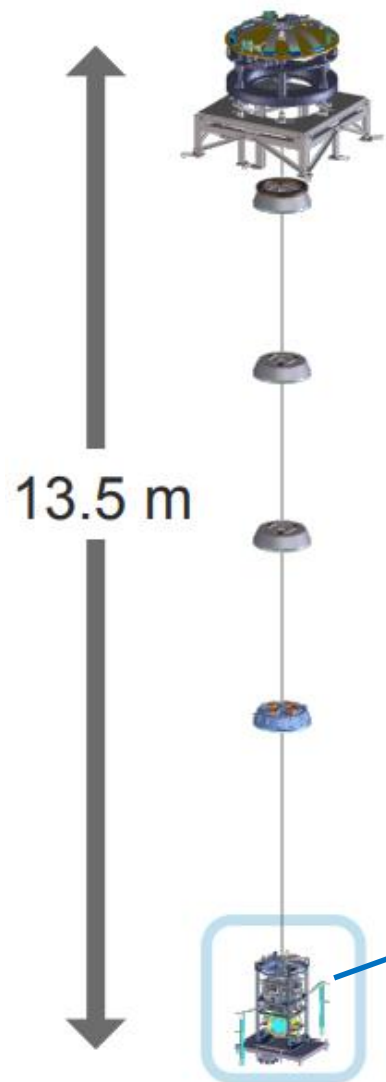
with 3 horizontal & 3 vertical LVDT & actuator units





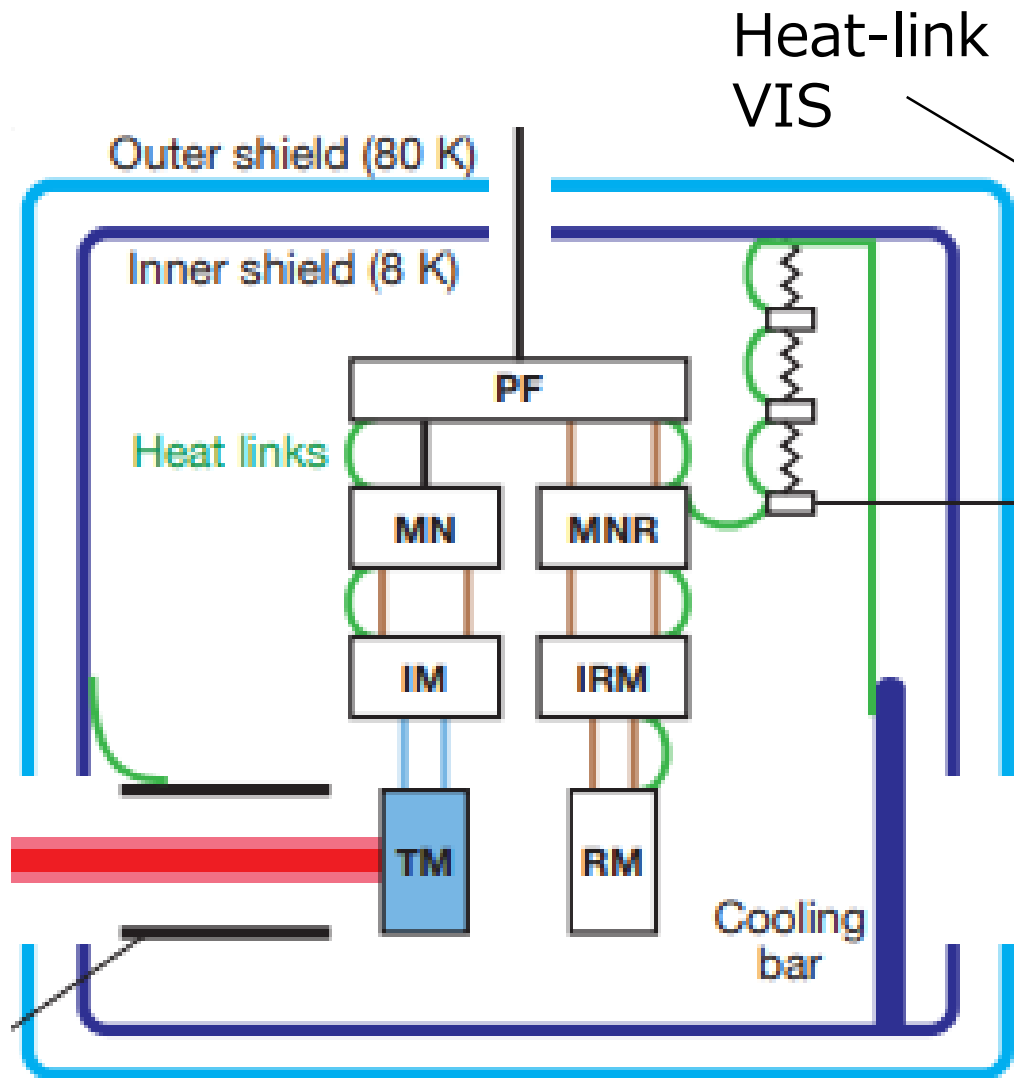
# And, the cryogenic part

Inside cryostat



+

(+ Wide-angle baffle)



JGW-P1809347

# Requirements, Type-A suspensions by YF

Table 5.2: Requirements on the Type-A suspension control. The column labeled as ref. describes the section which explains the reason of the requirements.

Items	Requirements	ref.
The calm-down phase		
1/e decay time	< 1 min.	§ 5.1.2
RMS displacement (transverse, vertical)	< 0.1 mm	§ 5.1.6
The lock acquisition phase		
RMS velocity (longitudinal)	< 2.0 $\mu\text{m}/\text{sec.}$	§ 5.1.3
RMS angle (pitch, yaw)	< 880 nrad	§ 5.1.4
RMS displacement (longitudinal)	< 0.39 $\mu\text{m}$	§ 5.1.5
RMS displacement (transverse, vertical)	< 0.1 mm	§ 5.1.6
The observation phase		
Control noise at 10 Hz (longitudinal)	< $8.0 \times 10^{-20} \text{ m}/\sqrt{\text{Hz}}$	§ 4.2
RMS displacement (longitudinal)	< 0.39 $\mu\text{m}$	§ 5.1.5
RMS displacement (transverse, vertical)	< 0.1 mm	§ 5.1.6
RMS angle (pitch, yaw)	< 200 nrad	§ 5.1.4
DC angle drift (pitch, yaw)	< 400 nrad	§ 5.1.4

# Requirements, Type-A suspensions by KO

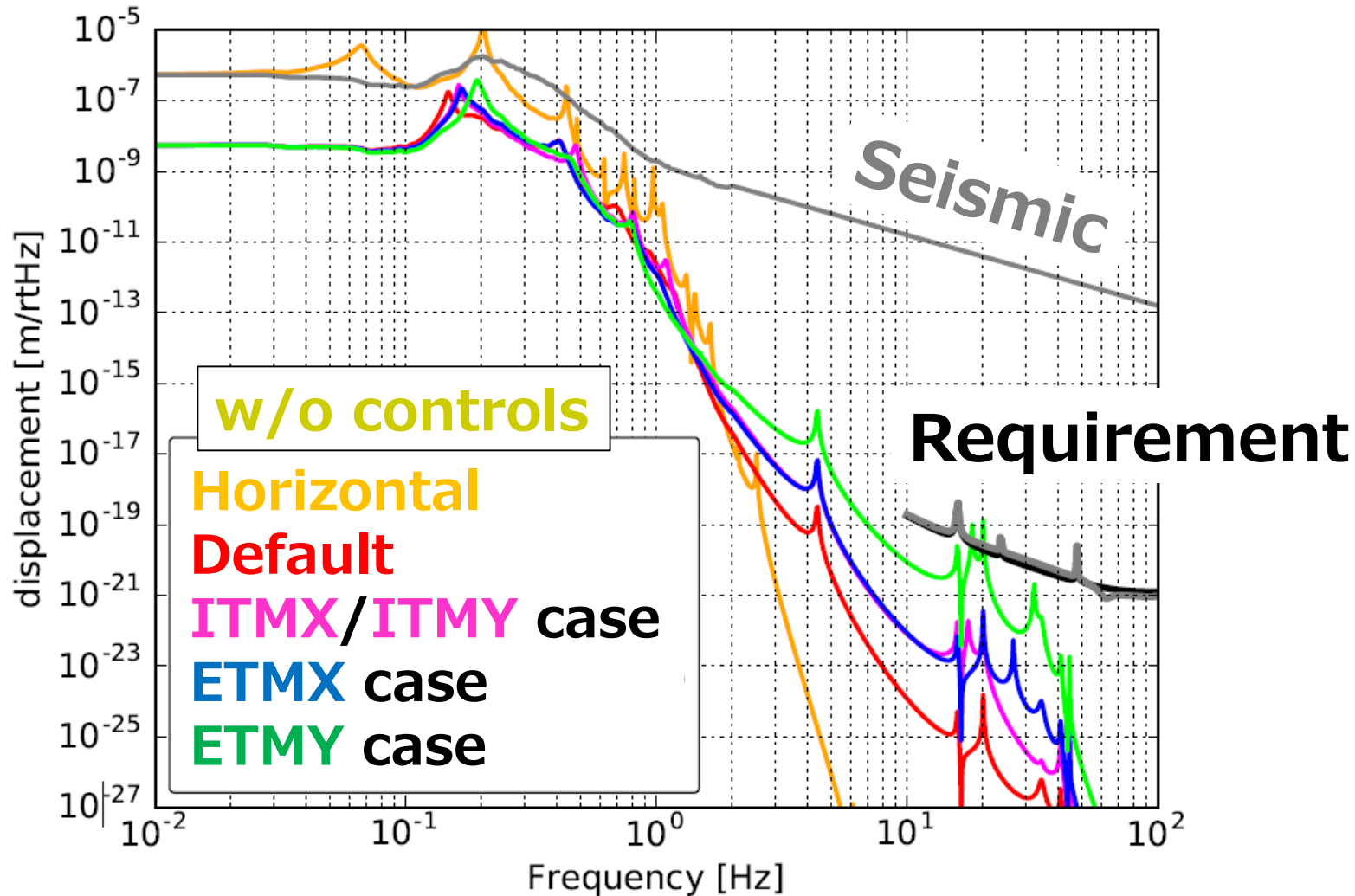
<b>Calm-down phase</b>		
Item	Requirement	For/Determined by
1/e modal decay time	< 1 min	Quick recovery
RMS displacement (L)	< 50 $\mu\text{m}$	Smooth transition to next phase
RMS displacement (T, V)	< 0.1 mm	Miscentering
RMS angle (P, Y)	< 50 $\mu\text{m}$	Smooth transition to next phase
<b>Lock acquisition phase</b>		
Item	Requirement	For/Determined by
RMS velocity (L)	< 240 $\mu\text{m/s}$	Auxiliary laser locking
RMS displacement (T, V)	< 0.1 mm	Miscentering
RMS angle (P, Y)	< 880 nrad	Optical gain degradation < 5%
<b>Observation phase</b>		
Item	Requirement	For/Determined by
Displacement noise (L) @ 10 Hz	< $8 \times 10^{-20} \text{ m/Hz}^{1/2}$	Sensitivity
Displacement noise (V) @ 10 Hz	< $8 \times 10^{-18} \text{ m/Hz}^{1/2}$	Sensitivity (1% coupling to L)
RMS displacement (T, V)	< 0.1 mm	Miscentering
RMS angle (P, Y)	< 200 nrad	Beam spot fluctuation < 1 mm
DC drift (P, Y)	< 400 nrad/h	Sustainable lock for 1 day left

(P, Y) are set as 50  $\mu\text{m}$  and 50  $\mu\text{rad}$ , respectively [28]. The RMS displacement for the other translational DoFs (T, V) are required for another reason which is mentioned shortly later.

[ref] K. Okutomi PhD

# Mechanical installation has done! **HOWEVER ..**

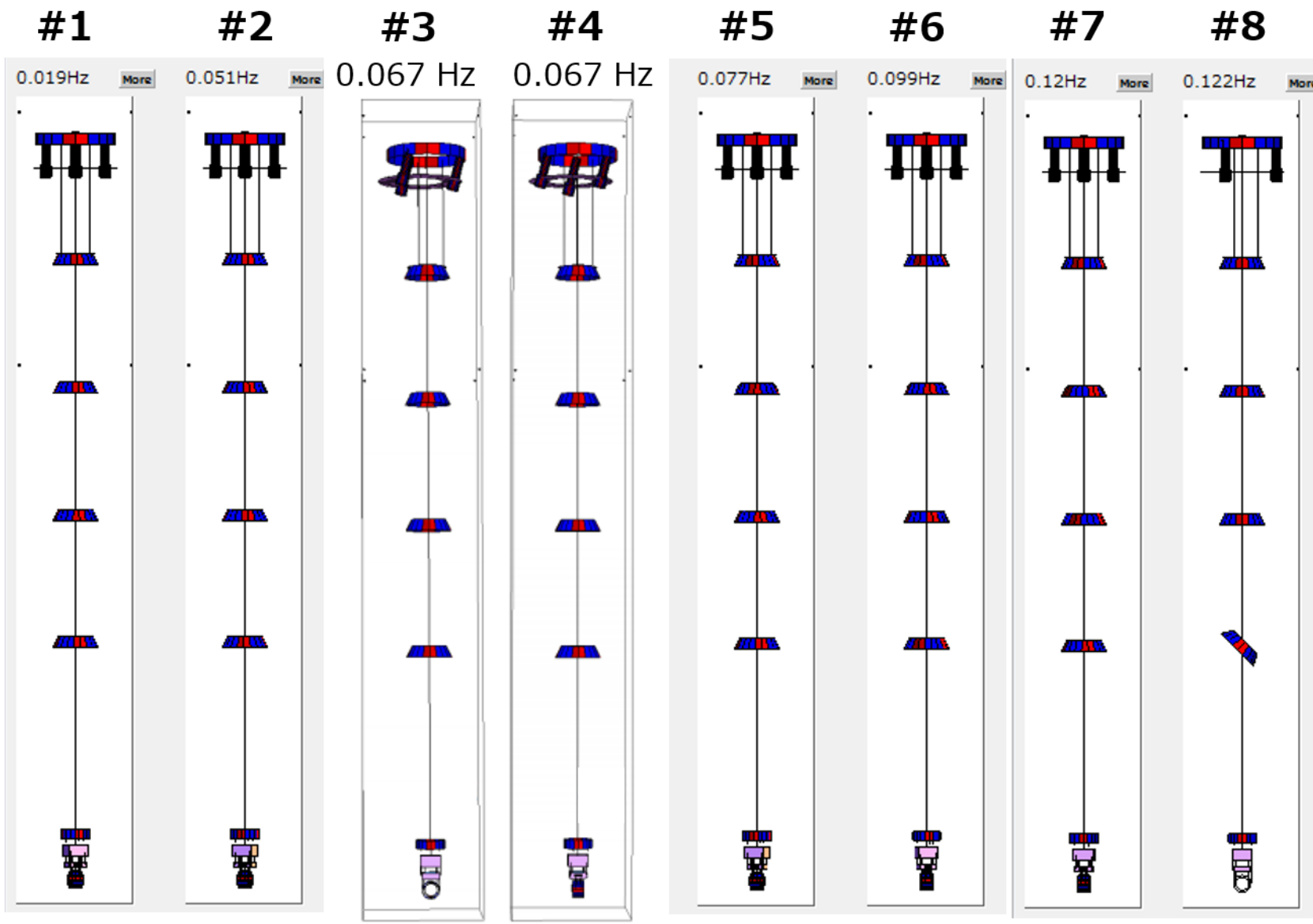
According to a simulation, assuming **1%** coupling,



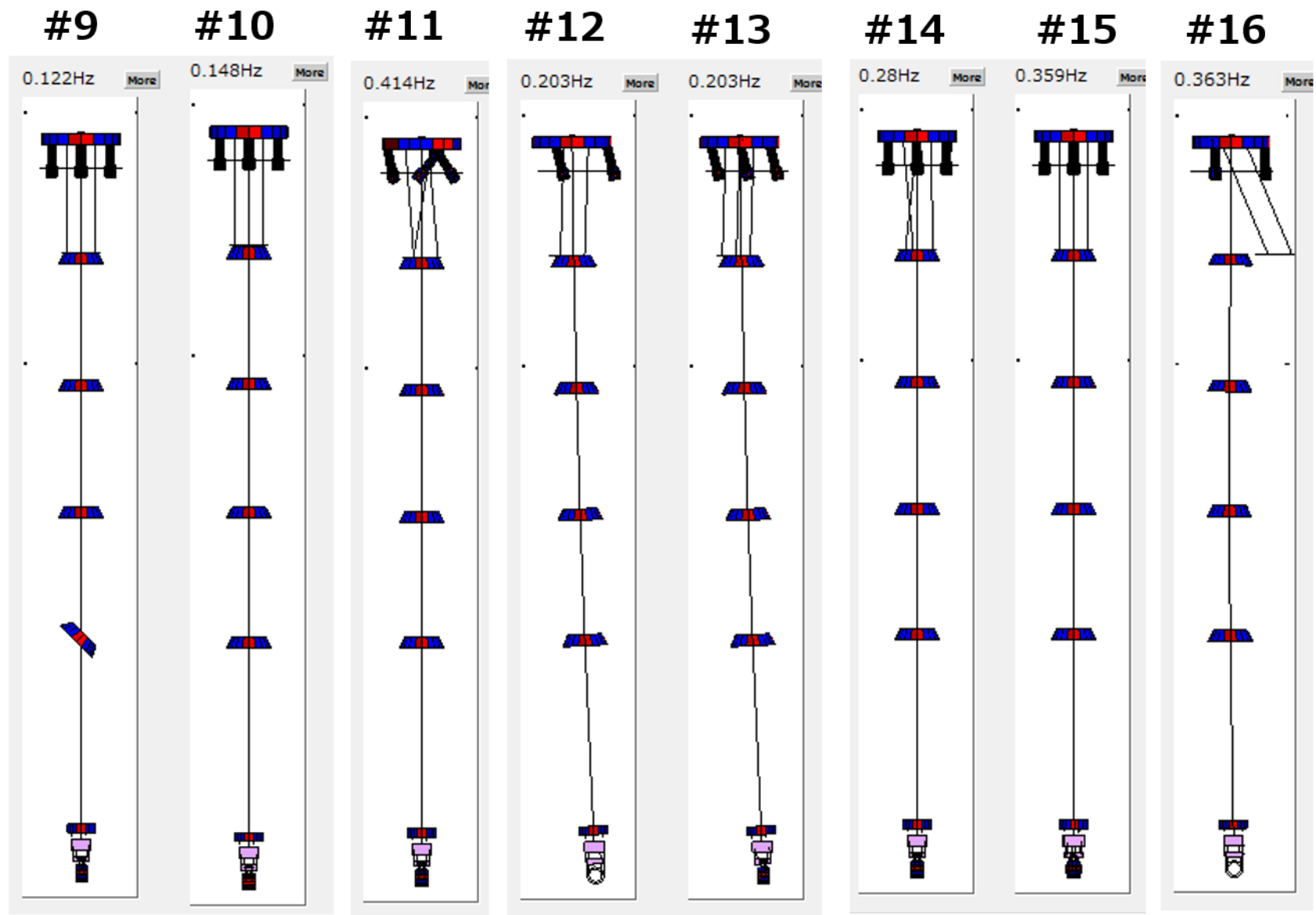
“acceptable for the O3-run”  
(should be)

Note:  
-- Modeled w/o Heat-links  
-- params are not tuned.

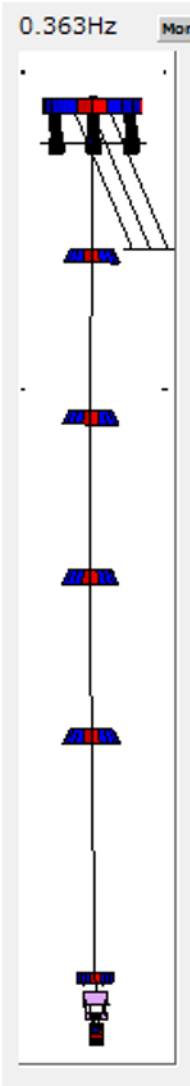




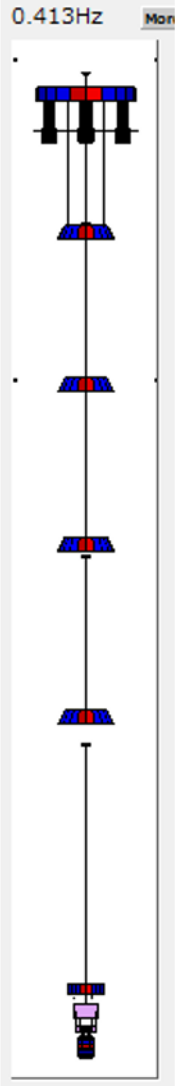
**Type-A SAS,**  
**'TypeA180429\_20K'**  
**Eigen mode: 75 modes**



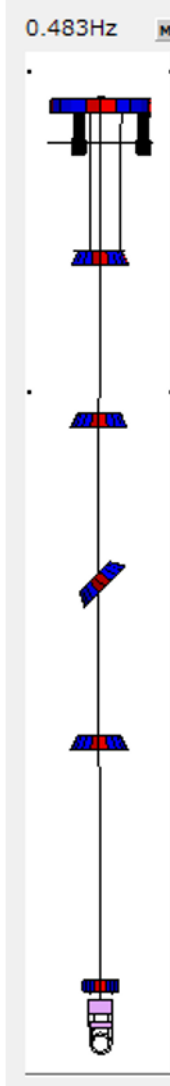
#17



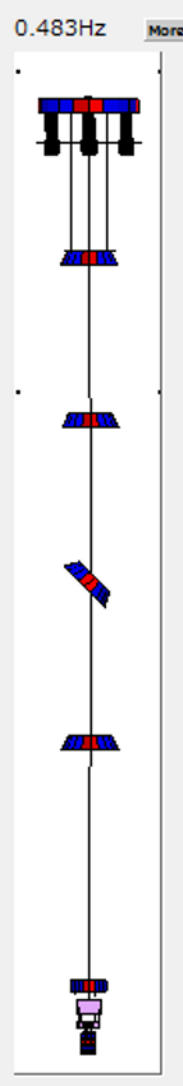
#18



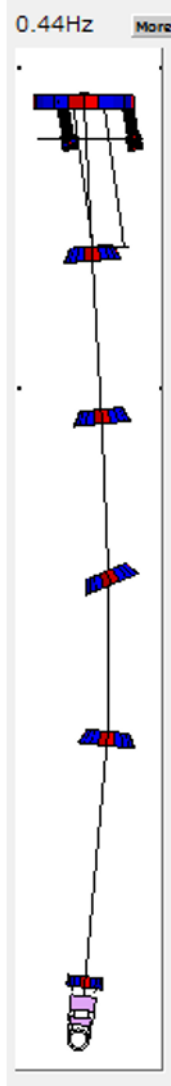
#19



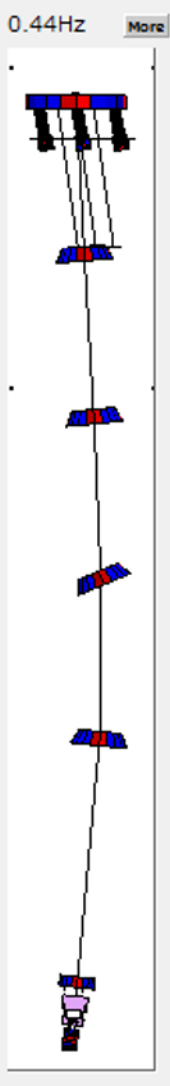
#20



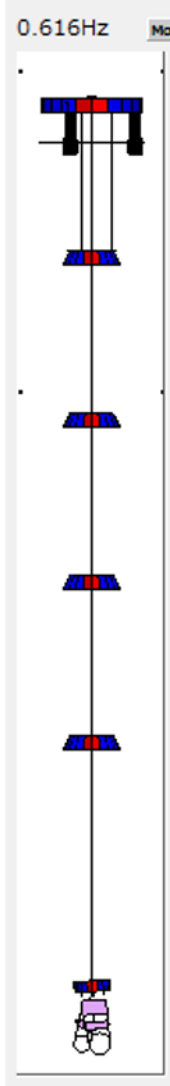
#21



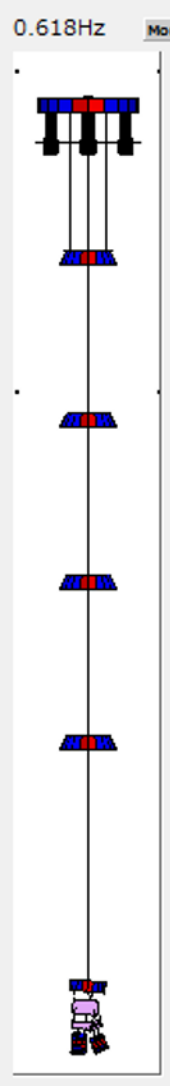
#22

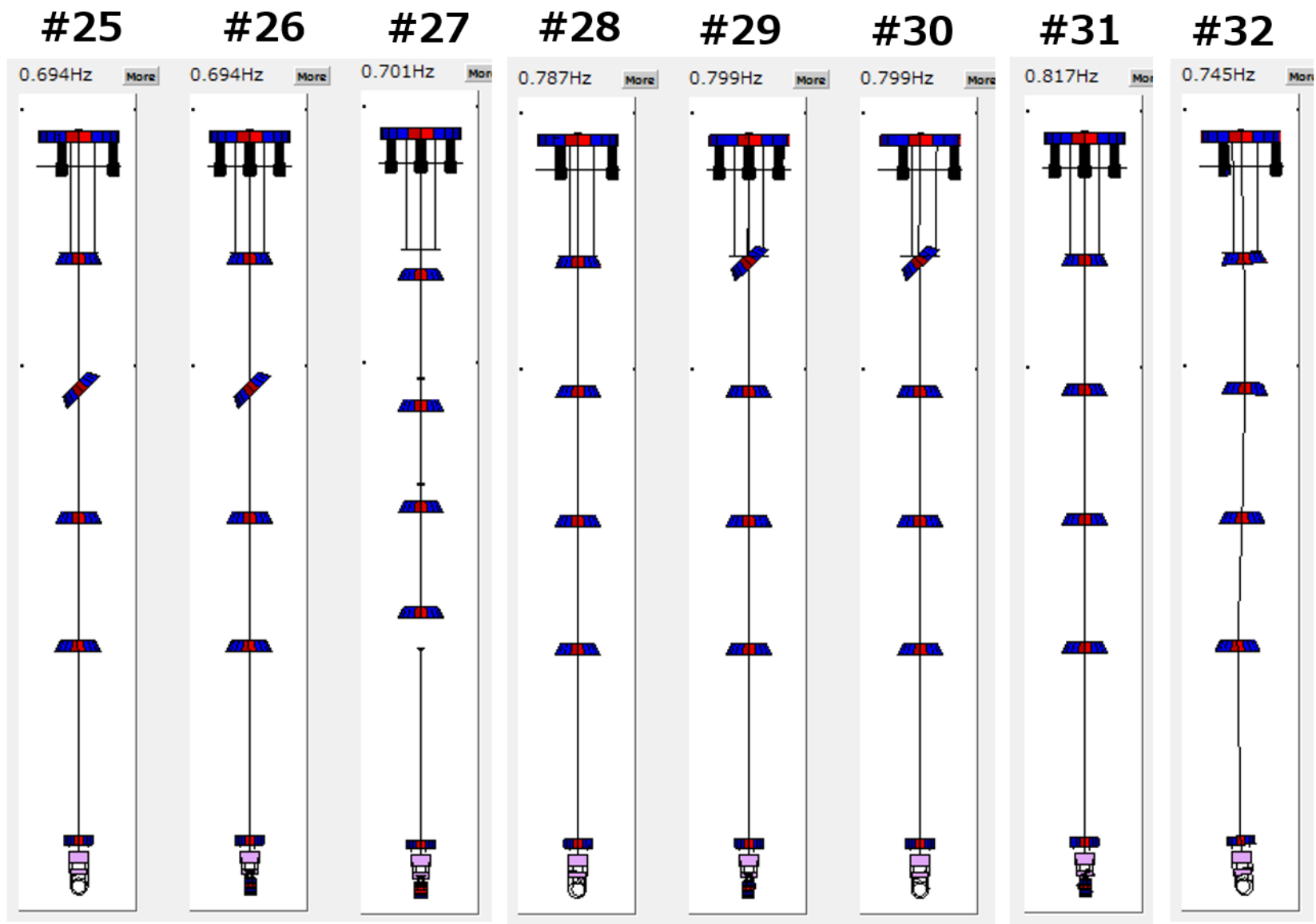


#23



#24





#33

#34

#35

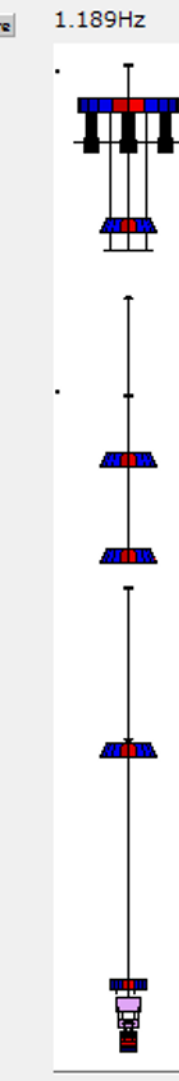
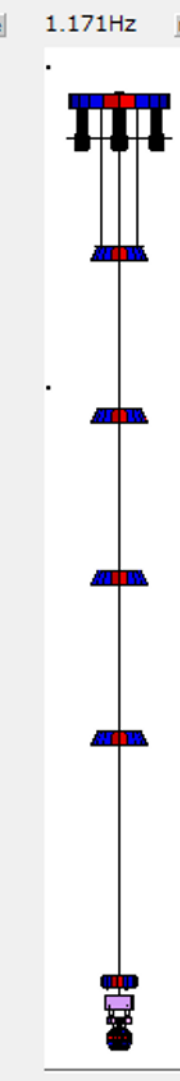
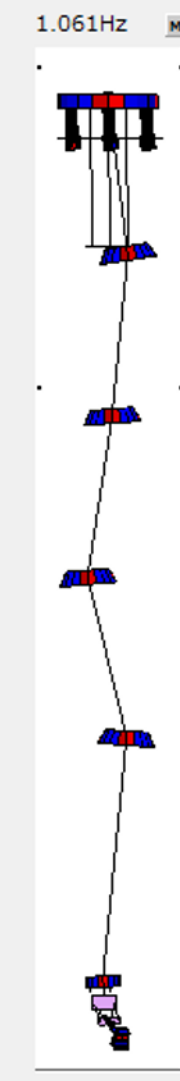
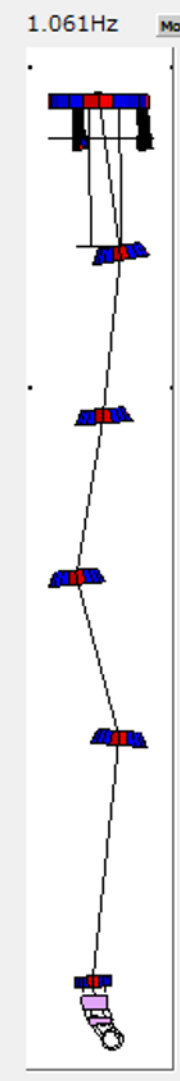
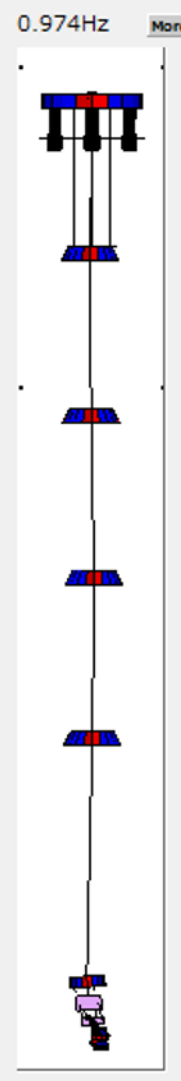
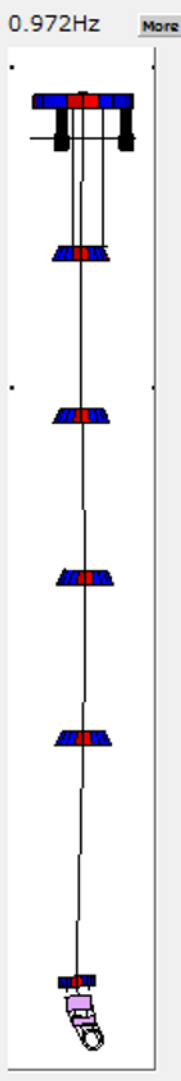
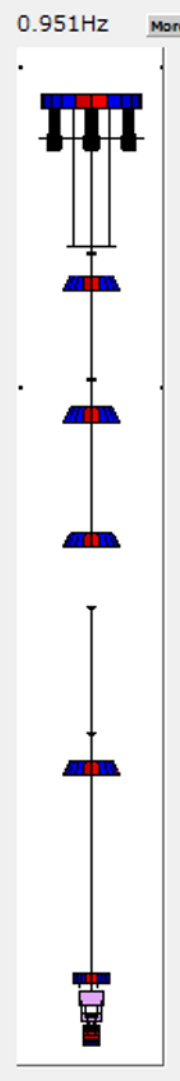
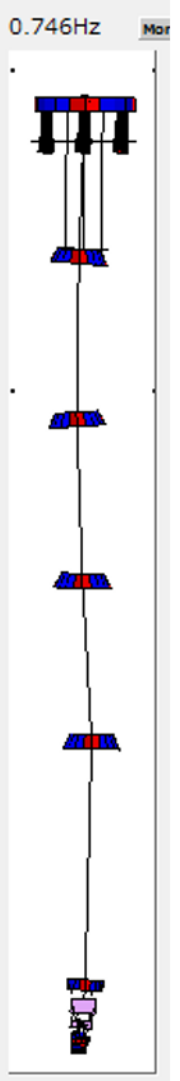
#36

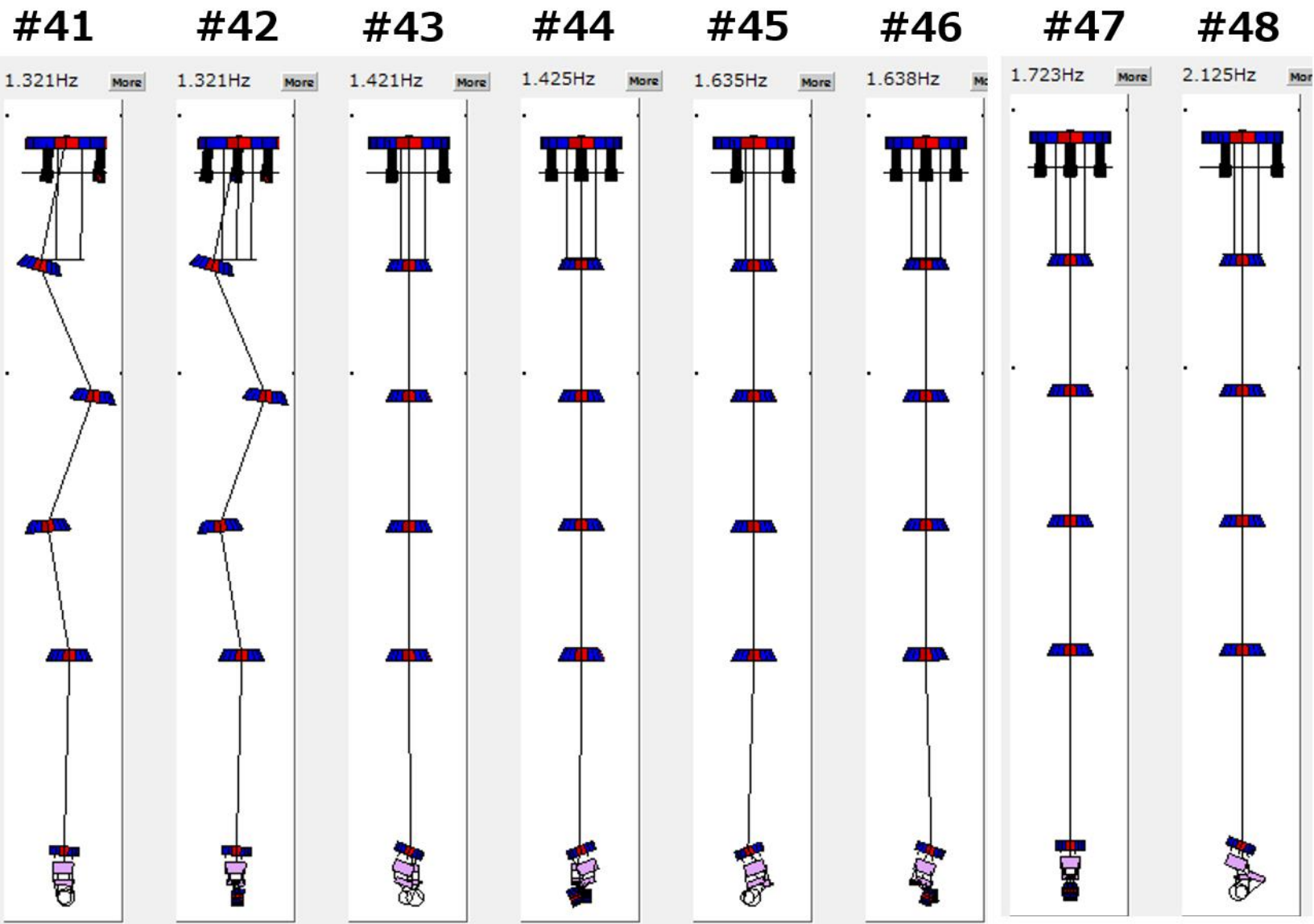
#37

#38

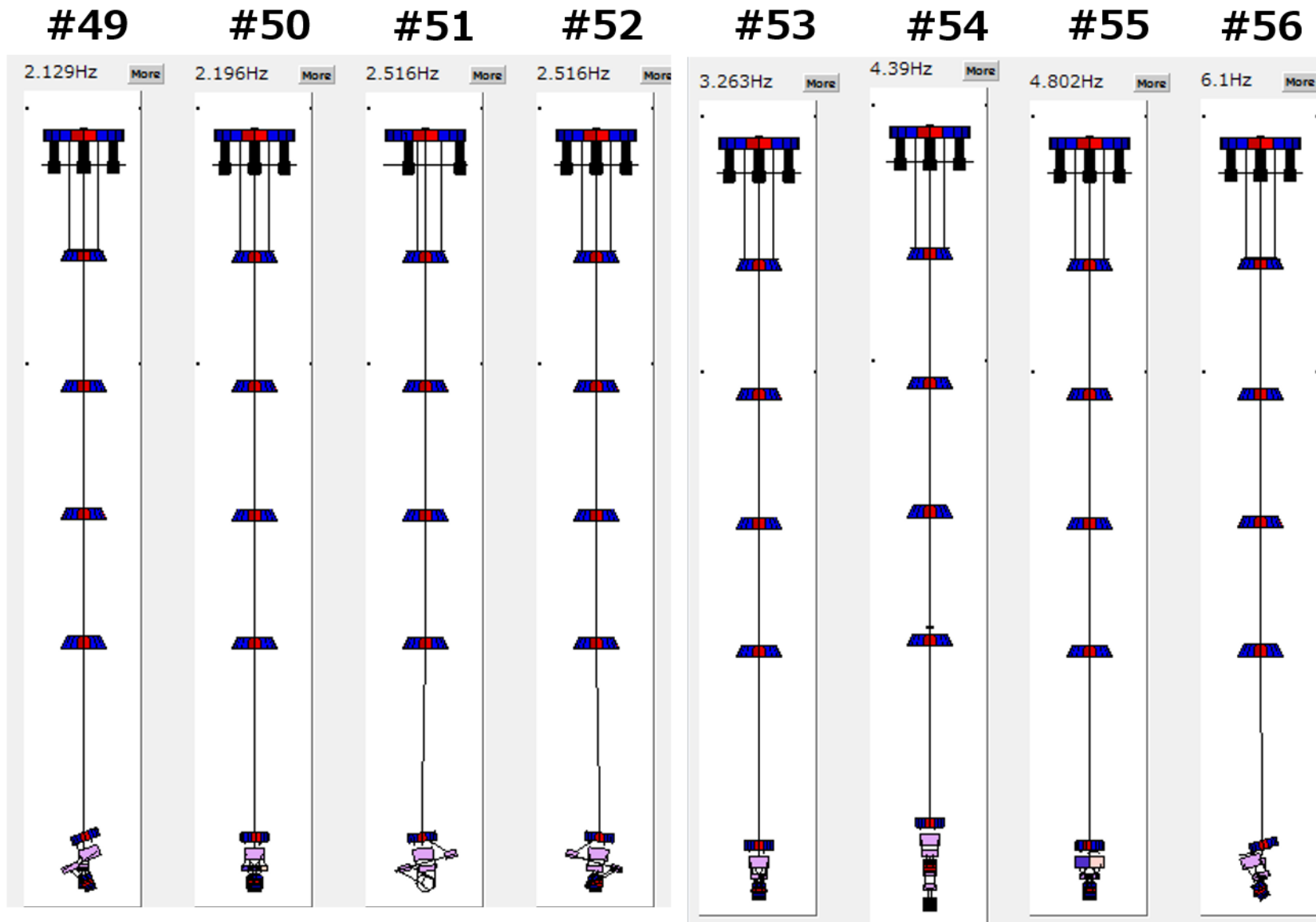
#39

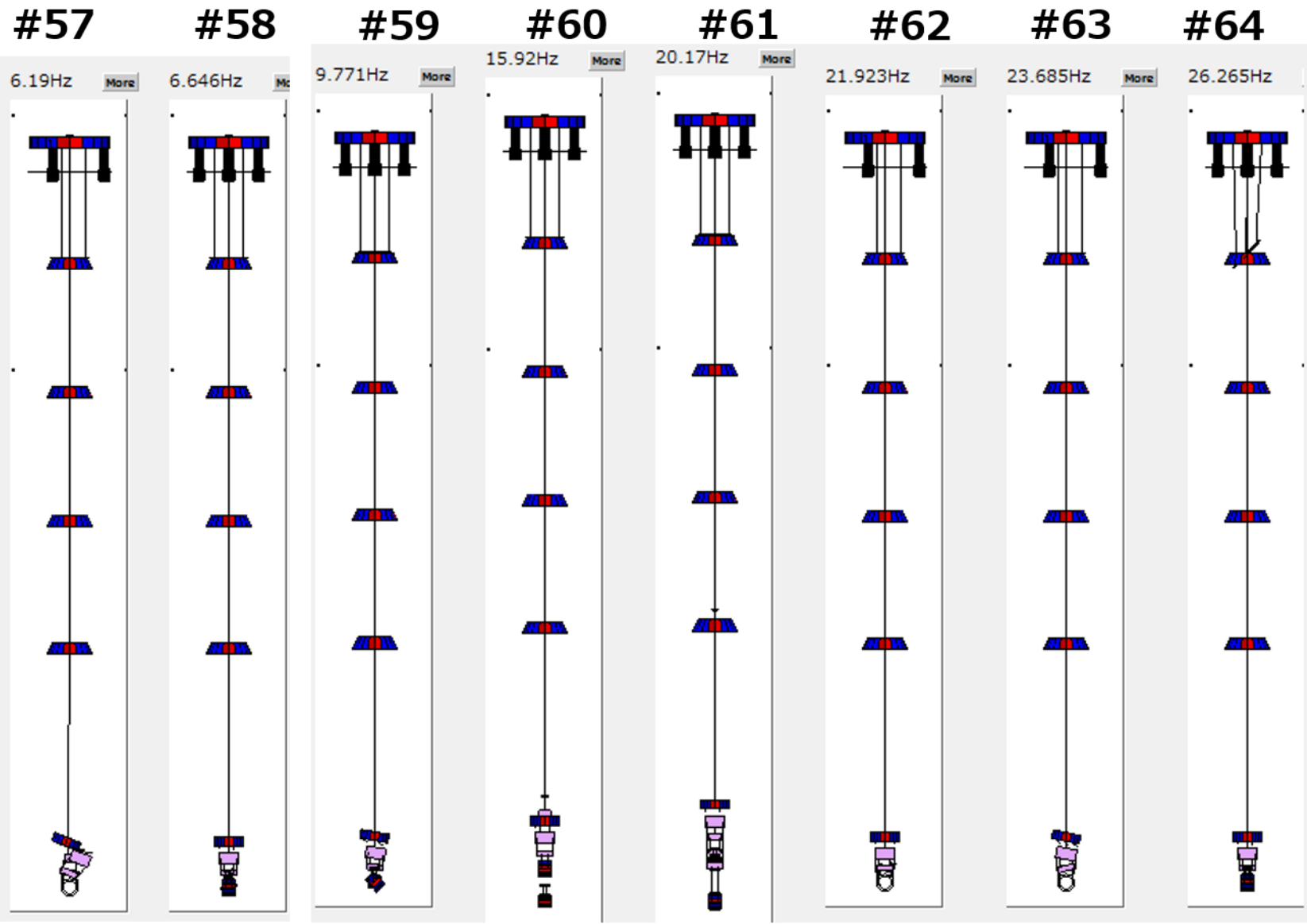
#40

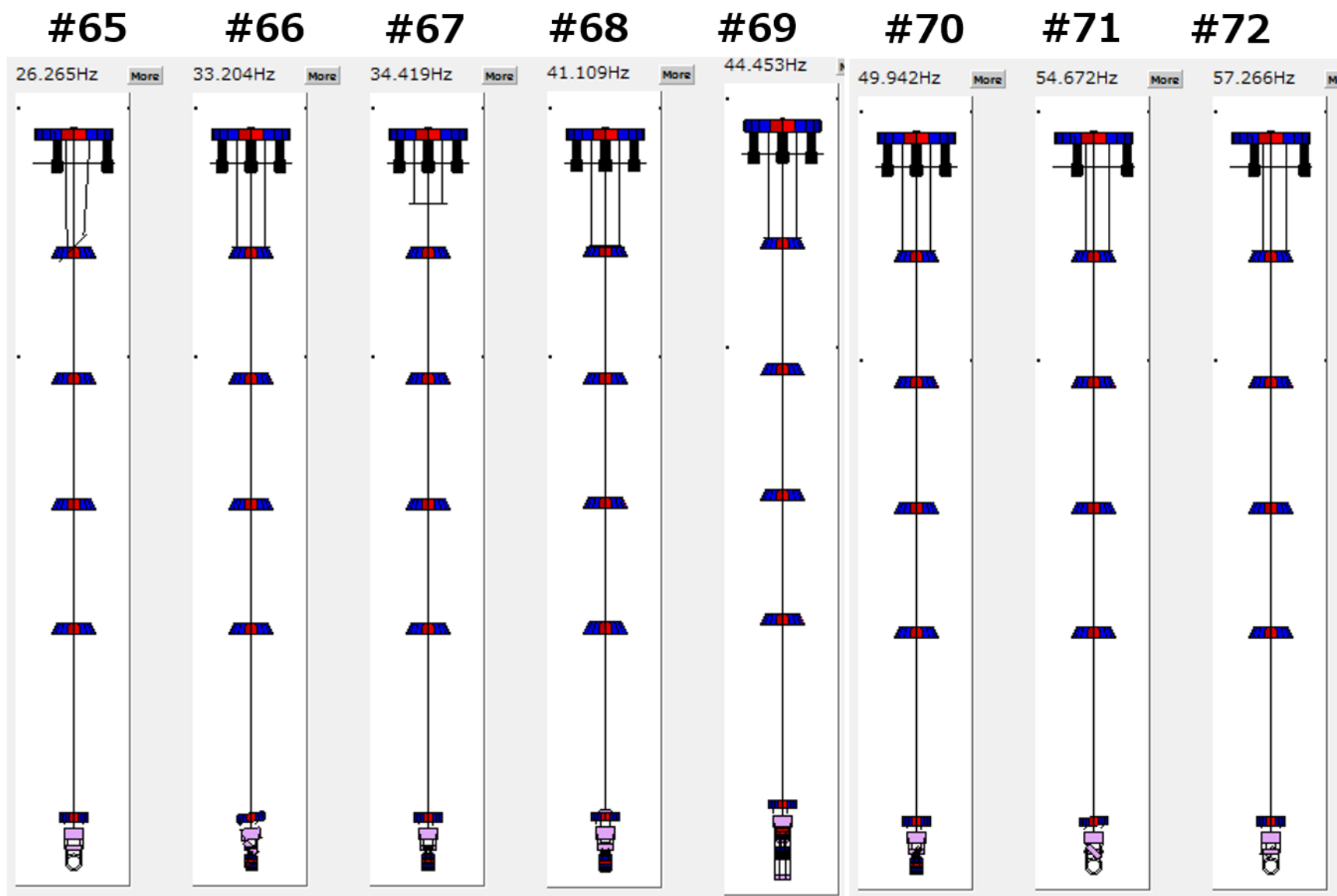












#73

#74

#75

